

Copyright

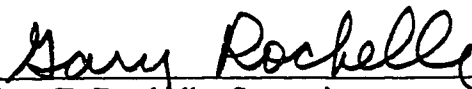
by

Lia Frieda Arthur

1998

Silicate Sorbents for Flue Gas Cleaning

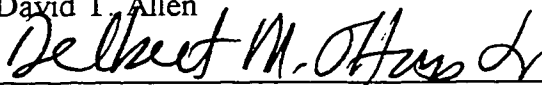
Approved by
Dissertation Committee:



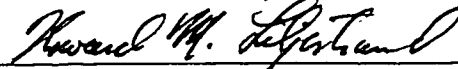
Gary T. Rochelle, Supervisor



David T. Allen



Delbert M. Ottmers, Jr



Howard M. Liljestrand



Ramon L. Carrasquillo

Silicate Sorbents for Flue Gas Cleaning

by

Lia Frieda Arthur, B.S., M.S.

Dissertation

Presented to the Faculty of the Graduate School of

The University of Texas at Austin

in Partial Fulfillment

of the Requirements

for the Degree of

Doctor of Philosophy

The University of Texas at Austin

December, 1998

To Noah Nathanael

Acknowledgments

I would like to thank and acknowledge Dr. Rochelle for his relentless enthusiasm during my work. His expertise, creativity, insight, and occasional song were both inspiring and necessary for the completion of this research.

Financial support was provided by the Texas Advanced Technology Program, The Separations Research Program, and the Environmental Solutions Program. Owens-Brockway graciously donated glass cullet for this work.

I thank my peers for their time, help, and patience in our many research related discussions. I also appreciate the camaraderie of our non-research related endeavors. To Kurt, Rajesh, Renae, Mshewa, Chris, Chen, Lingbing, Joe, Mark, Manuel, Paul, Sanjay, Shoichi, Mike, Norman, Nicole, and Sharmi; you will be my best memories of graduate school. I would also like to thank my undergraduate research assistants, Liany, Daniel, and Julie. I can't imagine how long it would have taken me without your help.

My infinite gratitude to my mentor and friend, Dr. Bruce Eldridge. God sends us few true door-openers, or boat-rowers, as it were. I'm glad that I recognized who you were.

I especially thank my wonderful husband for doing all of the chores while I worked on this dissertation and for lovingly tolerating my many, many mood swings. I am also deeply indebted to my family for their constant support of my schooling. Finally, but first and foremost, I thank God for always lighting the path before my feet and forgiving when I fall so short of His wishes.

Portions of this dissertation have been reprinted from "Preparation of Calcium Silicate Absorbent from Recycled Glass," by Lia F. Arthur and Gary T. Rochelle, *Environmental Progress*, Summer 1998, pp. 86-91. Reproduced with permission of the American Institute of Chemical Engineers. Copyright © 1998 AIChE. All rights reserved.

Silicate Sorbents for Flue Gas Cleaning

Publication No. _____

Lia Frieda Arthur, Ph.D.

The University of Texas at Austin, 1998

Supervisor: Gary T. Rochelle

Calcium silicate hydrates are effective alkaline sorbents for the removal of acid gases from humid flue gas streams. This work investigated the formation of calcium silicates from recycled consumer glass and iron blast furnace slag. The reaction between these high surface area solids and SO_2 in a humid gas stream was also studied.

The formation of high surface area solids was found to be highly dependent on both the pH and calcium concentration of the slurry. Even with a high concentration of lime intrinsic in slag, excess additional lime was required to maintain a sufficient pH. Gypsum was shown to be an effective additive for maintaining a high calcium concentration at 92°C . Increasing the temperature to 120°C , increased the surface area formation at short times, but produced a more crystalline product, with lower surface area at longer times. Neither agitation nor solids/water loading had any effect on the preparation of sorbents up to $80 \text{ m}^2/\text{g}$.

Above this surface area, only agitation had a clearly positive effect. The addition of CaCl_2 maintained a higher calcium concentration and high rate of surface area formation at 92°C , however the solids were less reactive with SO_2 than comparable solids prepared with gypsum. It is believed that the high chloride concentration may have resulted in a different solid phase that was visible on SEM but not with X-ray.

The SO_2 reactivity of high surface area glass sorbents was a strong function of the relative humidity of the gas, with temperature held constant. Sorbent surface area was also very important to the rate of SO_2 removal and maximum solids conversion. However, while surface area was necessary for high SO_2 reactivity, it was not sufficient, as seen with sorbents prepared with chloride.

An empirical model for the SO_2 / glass sorbent system showed that for a baghouse filter cycle time of one hour at 58% relative humidity, a stoichiometric ratio of 1.0 will achieve 62% removal from a 1000 ppm SO_2 gas stream. Increasing the stoichiometry to 2.0 increased the removal efficiency to 94%.

Table of Contents

Table of Contents.....	ix
List of Tables	xiv
List of Figures.....	xv
Chapter 1: Introduction.....	1
Chapter 2: A Comprehensive Literature Review	4
2.1 Overview	4
2.2 The ADVACATE Process	6
2.3 Preparation of Calcium Silicates.....	7
2.3.1 Absorbent Preparation from flyash.....	7
2.3.2 Effect of Temperature	10
2.3.3 Effect of Slurry Composition.....	12
2.3.4 Absorbent Preparation from Other Silica Sources	13
2.4 Reaction of SO ₂ with Hydrated Lime or Calcium Silicates.....	14
2.4.1 Effect of Relative Humidity	14
2.4.2 Effect of SO ₂ concentration.....	15
2.4.3 Effect of Additives	15
2.4.4 Reaction Modeling.....	15
2.5 Pilot-Scale Process Tests	16
Chapter 3: Experimental Methods and Procedures.....	17
3.1 Calcium Silicate Absorbent Preparation.....	17
3.1.1 Reagent Materials	17
3.1.2 Sorbent Preparation Reactors and Procedures	19
3.1.3 Solids Analysis	23
3.1.4 Liquid Analysis.....	26

3.2	SO ₂ Reaction with Solid Sorbents	27
3.2.1	Sandbed Reactor and Procedures	27
Chapter 4:	Calcium Silicate Production from Recycled Glass	31
4.1	Glass Dissolution	32
4.1.1	Effect of Hydroxide Concentration	32
4.1.2	Effect of Temperature	34
4.1.3	Combined Hydroxide and Temperature Effects.....	34
4.2	Effect of Reaction Variables on Sorbent Formation.....	37
4.2.2	Effect of Initial Surface Area	38
4.2.3	Effect of Gypsum at 92°C	40
4.2.4	Effect of Gypsum and CaCl ₂ at 120°C.....	44
4.2.5	Effect of Agitation.....	49
4.2.6	Effect of Solids/Water Ratio in Non-agitated Solids	51
4.2.7	Rinsing of Non-agitated Solids	51
4.3	Sorbent Characterization.....	52
4.3.1	X-Ray Diffraction.....	52
4.3.2	SEM	56
4.3.3	Surface Area Degradation	61
Chapter 5:	Calcium Silicate Production from Blast Furnace Slag	65
5.1	Effect of Reaction Recipe.....	65
5.1.1	Sulfide Control.....	66
5.1.2	Effect of Lime/Slag Ratio	69
5.1.3	Effect of Additives on Sorbent Formation.....	73
5.1.4	Release of Alkali from Slag	80
5.2	Sorbent Characterization - SEM.....	83
Chapter 6:	Reaction of SO ₂ with Glass and Slag Sorbents	87
6.1	Sandbed Gas Phase Analysis	87

6.1.1	Integration of SO ₂ Removal Data	88
6.2	Effect of Process Conditions on SO ₂ Reaction	89
6.2.1	Effect of SO ₂ Concentration.....	89
6.2.2	Effect of Temperature	91
6.2.3	Effect of Relative Humidity	93
6.2.4	Effect of Oxygen	94
6.3	Effect of Sorbent Characteristics on SO ₂ Reaction	95
6.3.1	Effect of Alkalinity / Surface Area.....	96
6.3.3	Reactivities of Other Silicate Sorbents	97
6.4	Characterization of Solids after Reaction With SO ₂	105
6.4.1	Verification of Final Conversions.....	105
6.4.2	Surface Area and Porosity Degradation	106
6.4.3	X-ray Pattern of Reacted Solids	107
6.5	Reaction Modeling.....	108
6.1.2	Experimental Reproducibility.....	108
6.5.1	Reactor Integration Model	110
6.5.2	Rate Model Derivation	111
6.5.3	Model Fit and Parameters.....	115
6.5.4	Predicted Baghouse Behavior.....	121
Chapter 7:	Conclusions and Recommendations.....	129
7.1	Sorbent Preparation from Glass.....	129
7.2	Sorbent Preparation from Slag	130
7.3	Sorbent Reaction with SO ₂	131
7.4	Recommendations.....	133
Appendix A:	Analytical Procedures	134
A.1	Atomic Absorption Standard Operating Instructions	134
A.2	BET Surface Area Standard Operating Instructions.....	135

Appendix B: Experimental Data	138
B.1 Raw Materials.....	138
B.2 Absorbent Preparation from Glass Experiments.....	139
B.2.1 Agitated Experiments	139
B.2.2 Non-agitated Experiments	142
B.3.1 Agitated Slag Preparation Experiments at 92°C	146
B.3.2 Non-agitated Slag Preparation Experiments at 92°C	150
B.4 X-Ray Diffraction Patterns for Solid Sorbents	151
B.5 Sandbed Experimental Data	152
Appendix C: Timelag Analysis of SO ₂ Analytical Train	175
C.1 Suspected Sources of Timelag.....	175
C.2 Timelag Model.....	176
Appendix D: Sample SO ₂ Removal Calculations.....	179
Appendix E: Fortran Code for Packed Bed and Baghouse Systems.....	181
E.1 Sandbed Reactor Model.....	181
E.2 Baghouse Prediction Model	184
References	187
Vita	193

List of Tables

Table 2.1:	Typical Composition of Flyashes (weight %)	8
Table 3.1:	Composition of Amber Container Glass	18
Table 3.2:	Composition of Iron Blast Furnace Slag	19
Table 3.3:	Reagent Grade Chemicals	20
Table 3.4:	Atomic Absorption Operating Parameters	27
Table 3.5:	Mass Flow Controller Parameters	29
Table 3.6:	Syringe Pump Calibrations	29
Table 4.1:	Curve Fits for Experimental Glass Dissolution Data	33
Table 4.1:	Rinsing of Non-agitated, Long-time Solids	52
Table 4.2:	Surface Area Degradation of Sorbents	63
Table 6.1:	Alkalinity Titrations of Reacted Sandbed Solids	106
Table 6.2:	Regressed Parameters for Individually Modeled Experiments	118
Table 6.3:	Simultaneous Model Regression Results	119
Table 6.4:	Baghouse Predictions of Average SO ₂ Removal	127
Table 6.5:	Baghouse Predictions Holding Solids Loading Constant	128
Table B.1:	Ground Recycled Glass	138
Table B.2:	Absorbent Preparation from Glass Experimental Results	139
Table B.3:	Absorbent Preparation from Slag Experimental Results	146
Table B.4:	Cross-Reference for X-ray Diffraction Patterns	151
Table B.5:	Sandbed Experimental Data	152
Table B.6:	Summary of Sandbed Experiments	174
Table C.1:	Timelag Regression Results	177

List of Figures

Figure 1.1: Small Source ADVACATE Process	3
Figure 2.1: Large Scale Flyash ADVACATE Process	7
Figure 2.2: Ternary Diagram for SiO_2 - CaO - H_2O System	10
Figure 2.3: Typical X-ray Diffraction Line Patterns for Tobermorites	11
Figure 2.4: Effect of Solution Ca^{+2} on CSH-I Solid	14
Figure 3.1: Glass Slurry Reactor for Atmospheric Reactions	21
Figure 3.2: Stainless Steel Autoclave for Pressurized Reactions	22
Figure 3.3: Sandbed Reactor System.....	28
Figure 3.4: Raw Data from a Typical Experiment.....	30
Figure 4.1: Effect of Hydroxide and Temperature on Glass Dissolution.....	33
Figure 4.2: Hydroxide Order of Glass Dissolution	34
Figure 4.3: Arrhenius Analysis of Glass Dissolution	35
Figure 4.4: Collapsed Glass Dissolution Data.....	37
Figure 4.5: Effect of Initial Surface Area of Glass	39
Figure 4.6: Collapse of Effect of Initial Surface Area of Glass	40
Figure: 4.7: Effect of Gypsum on Surface Area at 92°C	41
Figure 4.8: Effect of Gypsum on Calcium in Solution.....	43
Figure 4.9: Release of Sodium from Glass.....	44
Figure 4.10: Surface Area Formation at 120°C	45
Figure 4.11: Calcium Concentration in Slurry Solution at 120°C	46
Figure 4.12: X-ray Diffraction Patterns of Sorbents Prepared at 120°C	47
Figure 4.13: Release of Sodium from Glass.....	48

Figure 4.14: Effect of Non-agitation on Surface Area.....	49
Figure 4.15: X-ray Diffraction Pattern of Non-agitated, Long Time Solids	50
Figure 4.16: X-ray Diffraction Pattern: Fresh Reactants	53
Figure 4.17: X-ray Pattern: Disappearance of Gypsum and Lime.....	54
Figure 4.18: X-ray Pattern: Non-agitation and High Solids Loading	55
Figure 4.19: X-ray Pattern: Sorbents Prepared Without Gypsum.....	56
Figure 4.20: SEM: Unreacted Glass	57
Figure 4.21: SEM: Unreacted Lime/Glass/Gypsum Mixture	58
Figure 4.22: SEM: Reaction Product after 10 Hours	59
Figure 4.23: SEM: Reaction Product after 10 Hours - zoom	60
Figure 4.24: SEM: Reaction Product after 50 Hours	61
Figure 4.25: Surface Area Degradation	62
Figure 4.26: X-ray Pattern: Surface Area Degradation / Crystallinity.....	64
Figure 5.1: X-ray Pattern: Slag / Glass Comparison	66
Figure 5.2: Effect of Additives on Sulfide Concentration.....	67
Figure 5.3: Effect of Additives on Surface Area	68
Figure 5.4: Effect of Lime/Slag Ratio on Agitated Solids	70
Figure 5.5: Effect of Lime/Slag on Un-normalized Surface Area	71
Figure 5.6: Effect of Agitation on Slag Sorbents	72
Figure 5.7: Effect of Lime/Slag Ratio on Non-agitated Solids	73
Figure 5.8: Effect of Gypsum on Slag Sorbent Surface Area	74
Figure 5.9: Effect of Gypsum on Calcium Concentration.....	75
Figure 5.10: Effect of Gypsum on Normalized Slag Sorbent Surface Area.....	76

Figure 5.11: X-ray Pattern: Excess Lime in Slag Absorbents	77
Figure 5.12: X-ray Pattern: Surface Area Formation Without Excess Lime	78
Figure 5.13: Effect of CaCl_2 on Surface Area	79
Figure 5.14: Effect of CaCl_2 on Calcium Concentration	80
Figure 5.15: Release of Sodium from Slag During Preparation	81
Figure 5.16: Ratio of Sodium to Potassium Dissolution from Slag	82
Figure 5.17: SEM: Unreacted Ground Iron Blast Furnace Slag	83
Figure 5.18: SEM: Calcium Silicate Sorbents from Slag	84
Figure 5.19: SEM: Slag Sorbent Prepared with CaCl_2	85
Figure 5.20: X-ray Pattern: Slag Sorbent Prepared with CaCl_2	86
Figure 6.1: Effect of SO_2 Concentration	90
Figure 6.2: Effect of SO_2 Concentration at 29% RH	91
Figure 6.3: Effect of Temperature at Constant Relative Humidity	92
Figure 6.4: Effect of Relative Humidity at Constant Temperature	93
Figure 6.5: Effect of Oxygen on SO_2 Reactivity	95
Figure 6.6: Effect of Surface Area / Alkalinity	96
Figure 6.7: SO_2 Reactivity of Hydrated Lime and Glass ADVACATE	98
Figure 6.8: SO_2 Reactivity of Glass Sorbents Prepared at 120°C	99
Figure 6.9: SO_2 Reactivity of Non-agitated Glass Sorbents	100
Figure 6.10: Reactivity of Slag Sorbents	101
Figure 6.11: X-ray Pattern: Sorbents Prepared from Slag or Glass	102
Figure 6.12: Reactivity of Slag Sorbents Prepared with CaCl_2	103
Figure 6.13: Reactivity of Sorbents Prepared from Flyash or Silica Fume	104

Figure 6.14: Porosity of Unreacted and Reacted Solids	107
Figure 6.15: X-ray Pattern: Sorbent after SO ₂ Reaction	108
Figure 6.16: Precision of Sandbed Experimental Results	109
Figure 6.17: Physical System for SO ₂ / Solid Reaction Model	112
Figure 6.18: Effect of Timelag Correction on Model Prediction	115
Figure 6.19: Model Fit for Individually Regressed Experiments.....	116
Figure 6.20: Regressed Model Compared to Experimental Precision.....	120
Figure 6.21: Best and Worst Fit of Global Parameters at 50°C / 58% RH.....	121
Figure 6.22: Individual Bagfilter Performance	123
Figure 6.23: Overall Baghouse Filter Performance	124
Figure 6.24: Effect of Alkalinity Utilization.....	125
Figure 6.25: Effect of SO ₂ Concentration.....	126
Figure C.1: SO ₂ Analytical System	176
Figure C.2: Timelag Model: Step Change Regression	178

Chapter 1: Introduction

The Acid Rain Program (Title IV) of the Clean Air Act Amendments of 1990 required the reduction of SO₂ emissions throughout the utility power industry. Phase 1 of the program began January 1995, and affected 110 utility plants by limiting their average emissions to 2.5 lb./MMBTU. Beginning January 2000, Phase 2 of the Title IV legislation will tighten the restrictions on the original Phase 1 plants and will extend its reach to approximately 785 additional plants. Average emissions after the start of Phase 2 will be limited to 1.2 lb./MMBTU for all plants over 25 MW (Kuehn, 1993).

The uniqueness of Title IV was the creation of an overall emissions cap coupled with a market system for emission allowances. This allows the freedom to meet requirements by the best means for that plant. Some common options are: 1) switching to a low-sulfur fuel, 2) retrofitting with flue gas desulfurization control technology, or 3) purchasing of SO₂ allowances. The approach of Phase 2, along with the potential for future legislation regarding SO₂ emissions such as proposed revisions to the National Ambient Air Quality Standards concerning PM_{2.5}, leave the immediate future of flue gas desulfurization slightly uncertain (Platt, 1997). The long term future of SO₂ emissions will, no doubt, require further reductions from sources other than the major utilities, implemented in new and creative ways. The technology motivating this research is aimed at providing a gas cleaning option to smaller acid gas sources.

Currently there are several accepted control options for new plants or for retrofitting older plants. These include wet scrubbing, furnace injection, spray dryer absorption, and dry sorbent injection (Holzman and Atkins, 1988). The ADVACATE process was developed as a duct-injection flue gas cleaning alternative for coal-fired power plants (Rochelle, 1993). Its relatively small physical footprint and lower capital cost compared to wet desulfurization systems make it a viable alternative for retrofitting existing plants for more strict flue gas cleaning requirements.

The basis of the ADVACATE process is the cool-side duct-injection of ADVACATE solids to remove SO_2 , NO_x , and other contaminants from the flue gas stream. Removal occurs both in the gas duct and, more significantly, in the bag filter particulate control device. ADVACATE solids are formed by reacting hydrated lime with recycled fly ash from the power plant. A highly porous calcium silicate hydrate solid is formed that is capable of carrying a relatively large portion of water (~50 wt.%) while maintaining the handling characteristics of a powder. The large amount of water and exposed alkalinity enable high removal of acid gases along with high conversion of the solids.

The use of recycle fly-ash as the silica source for ADVACATE solids is probably the most economical when considering power plant applications. However, it is reasonable that other applications, such as smaller boilers, municipal waste incinerators, petroleum calciners, or clean-room operations, would not have an entire ADVACATE production facility on site and may or may not have access to usable flyash. These are the applications which this technology targets. ADVACATE solids could be produced centrally and distributed to various small-application sites that would have a variety of flue gas conditions. Figure 1.1 outlines a possible operational scheme.

Manufacturing ADVACATE solids apart from a coal-fired power plant presents the possibilities of other economical silica sources. It is known that the glassy silica particles in fly-ash react to form ADVACATE. It would be reasonable to expect that other amorphous silicas should react equally as well to form the silicate framework. Also, silica sources that carry with them a high concentration of alkalinity (i.e. CaO , or Na_2O) would be beneficial to the raw material economics, since that alkalinity will also be available for reaction with acid gases.

The preparation as outlined in Figure 1.1 begins with a possible grinding of the silica source, depending on the initial particle size. The silica is then reacted with lime and additives in an aqueous environment at elevated temperatures. The slurry must then be dewatered and dried before shipping to the source sites. The

gas could be contacted with the solids by a duct-injection / baghouse filter scheme as shown in Figure 1.1, or used as a fixed bed filter medium.

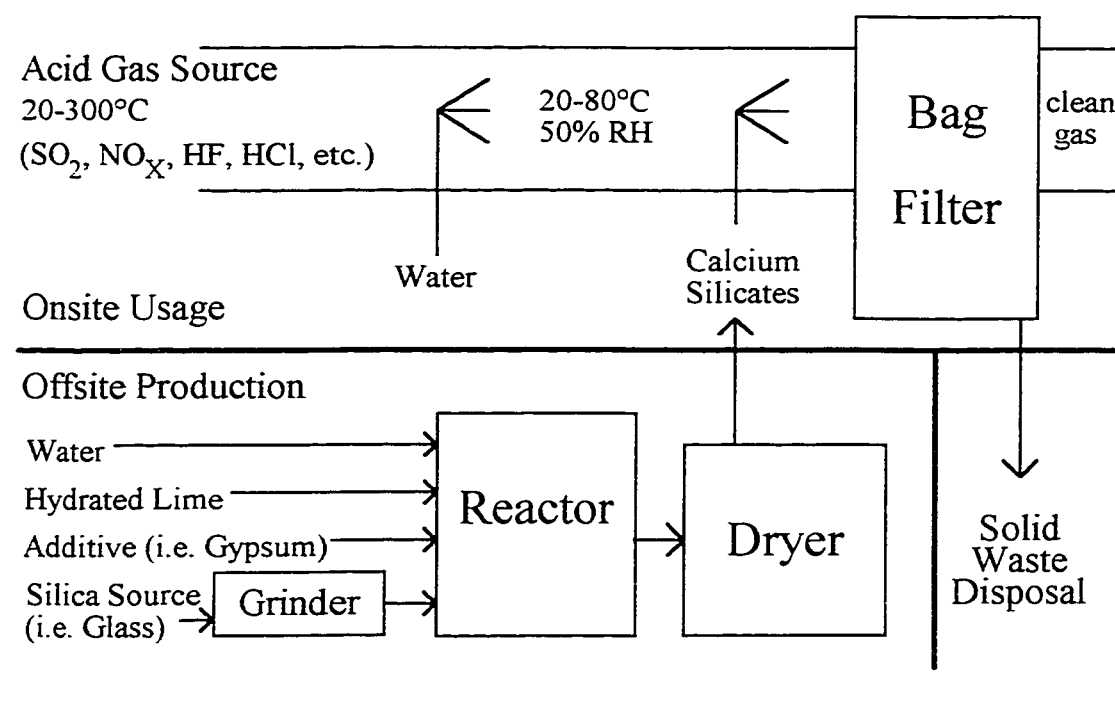


Figure 1.1: Small Source ADVACATE Process

This work explored the formation of calcium silicates from lime and recycled glass or iron blast-furnace slag, both of which contain intrinsically high alkalinity. Reaction variables such as temperature, agitation, solids content, and slurry composition were investigated. These variables were chosen for their possible impact on the economics of the process.

The reaction of these solids with SO_2 was also studied using a packed bed reactor to simulate bag filter conditions. Reaction variables studied in this system were SO_2 concentration, relative humidity, and temperature. The effects of solids characteristics, such as surface area, composition, and total alkalinity were also investigated. A semi-empirical model was constructed to match the data collected from the packed bed reactor and then was used to predict the performance of a baghouse filter.

Chapter 2: A Comprehensive Literature Review

This chapter is a review of previous research published on topics of interest to this research. Namely, this includes previous publications on the ADVACATE process, calcium silicate preparation from flyash and other silica sources, as well as the measurement and modeling of the reaction of SO₂ with hydrated lime or calcium silicates.

2.1 OVERVIEW

Cool-side duct injection processes for flue gas desulfurization (FGD) typically consist of the injection of a dry or semi-dry solid sorbent into the flue gas stream. The solids contact the gas and are separated along with the flyash in a particulate control system, i.e. a baghouse filter or electrostatic precipitator (ESP). SO₂ is removed by adsorption and reaction with the solids both in the duct and in the particulate removal system. In these processes, a bagfilter is normally beneficial for the FGD process by providing additional, forced gas/solid contact as the gas passes through the filter cake. The solids are then disposed of or recycled through the process.

Low temperature duct injection processes have generally used hydrated lime as an absorbent, accomplishing desulfurization by the reaction shown in Equation 2.1.



However, the solid/gas (Ca(OH)₂/SO₂) stoichiometric ratio needed for these processes is high since one-pass lime conversion is generally very low. Hydrated lime (Ca(OH)₂), the most reactive of common lime species, is known to only achieve ~30% (mol SO₂ / mol Ca⁺²) conversion, though this maximum can be increased with recycle. For this reason, much research has been done to increase the reactivity of the injection solids. One promising technique is the aqueous reaction of lime with an amorphous silica source, such as flyash, to produce high surface area calcium silicates. The high surface area and porosity of these solids make the alkalinity present more readily available for reaction with SO₂.

While numerous researchers have investigated the formation of reactive calcium silicates from flyash, this work focused on using high alkalinity silica sources, specifically container glass or blast furnace slag, in lieu of flyash. Though several publications discuss the use of silica sources other than glass, only Jozewicz et al. (1991a) has used bottle glass. Iron blast furnace slag has been studied in the context of cement formation. While the cement system is similar in chemical constituents present and the general pozzolanic reaction, the reaction conditions and kinetics are significantly different. Silicate absorbent is normally prepared under higher temperature and lower solids/water loading than cement. Therefore, this research represents an extrapolation from the previous research conducted with flyash and other silica sources.

Of particular importance to this research were the results presented by Peterson (1990) and Kind (1994) which showed the strongly positive impact of gypsum during slurry preparation on the surface area and SO_2 reactivity of the silicate solids. Peterson concluded that the gypsum served to bind the aluminum in the flyash, preventing the dilutary effect on the product solids. Kind concluded that the gypsum affected the rate of surface area growth by maintaining a sufficient calcium concentration for the silicate reaction to proceed. This was necessary to "buffer" the solution from the alkali being released from the flyash, and the subsequent pH increase. The presence of a gypsum solid phase in equilibrium moderated the pH of the solution and thereby also moderated the calcium concentration. Because of the high sodium content of glass, it was expected that this would also be apparent with the lime/glass system.

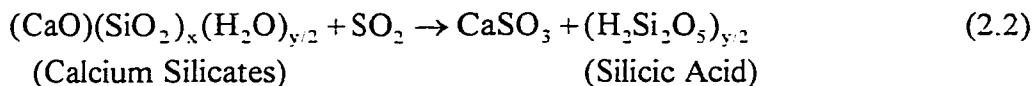
Also of interest to this research were previous investigations regarding the reaction between SO_2 and high surface area silicate sorbents. There is a significant body of research regarding the qualitative effects of reaction variables on the reaction between SO_2 and lime which was expected to extrapolate to this research. There have also been reactivity studies with silicate sorbents, though most were of lower surface area than those studied in this work. While several researchers have modeled the reaction between SO_2 and limestone, lime, or calcium silicate, they

have met with varying degrees of success (Klingspor et al., 1983; Ruiz-Alsop, 1986; Irabien et al., 1992; Garea et al., 1997).

The remainder of this chapter will give a more detailed summary of the previous research considered during this work. While most of the following references relate to the field in general, rather than specifically to this project, they provide the overall basis for this research.

2.2 THE ADVACATE PROCESS

The ADVACATE process was developed primarily as a flue gas desulfurization option for coal-fired power plants (Rochelle, 1993). Figure 2.1 shows a schematic of the process. High surface area calcium silicates are formed from the reaction between lime and recycled flyash in the presence of water. More recycled flyash is blended with the reacted slurry to lower the water content and form an injectable powder. The solids are then injected into the duct, where the water carried in the highly porous solids is evaporated, cooling and raising the humidity of the gas. The alkaline silicates react with SO_2 for a few seconds in the duct and for a longer period in the bag filter by the general reaction shown in Equation 2.2. It would also be possible to contact the solids with the gas in a spray dryer (Rochelle and Jozewicz, 1989; 1990).



The heart of the ADVACATE process is the solids preparation reaction. It is here that the amorphous silica combines with lime to form highly porous calcium silicate hydrates, thereby making the alkalinity present in the lime (and silica source) more available for reaction with SO_2 . Naturally, the required SO_2 removal can be always be achieved by the addition of excess solids or the recycle of unreacted solids. The advantage in increasing the solids reactivity is that the need for solids recycle or excess is reduced, and subsequently the overall solids loading in the system can be lowered.

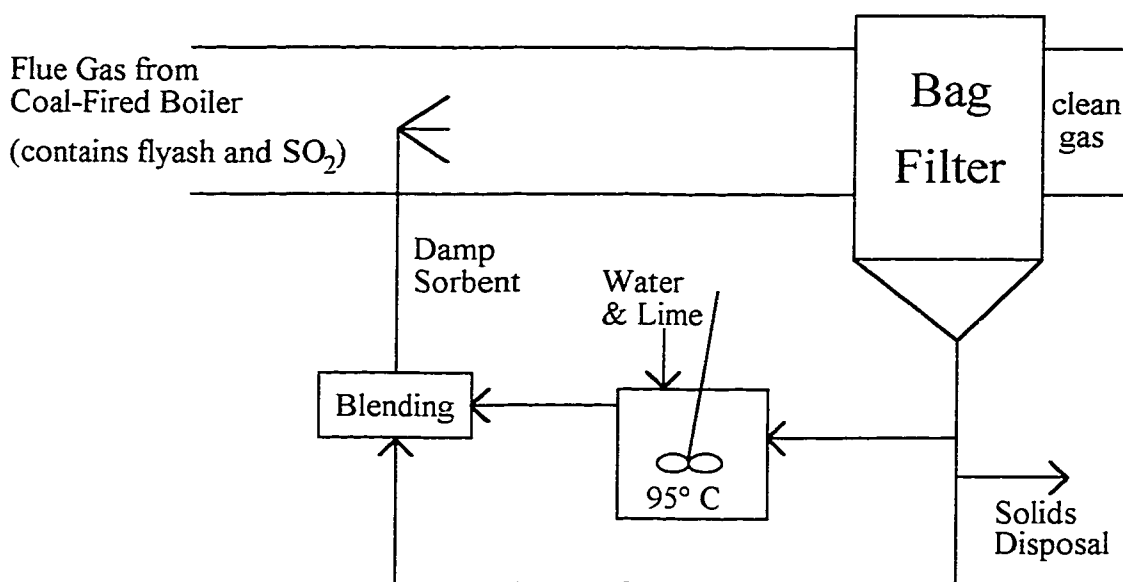


Figure 2.1: Large Scale Flyash ADVACATE Process

2.3 PREPARATION OF CALCIUM SILICATES

This section reviews the bench-scale research published on the pozzolanic reaction between lime and an amorphous silica source to create calcium silicate hydrates.

2.3.1 Absorbent Preparation from flyash

Since the ADVACATE and similar processes were originally designed for desulfurization of flue gas from coal fired power plants, most of the research on sorbent preparation has used flyash as the silica source. The chemical composition of flyash is directly related to the type of coal being used. Bituminous coal contains a lower calcium concentration than lignite or sub-bituminous coal. The flyash from plants firing bituminous coal has been termed "low-calcium" flyash. Sub-bituminous flyashes are commonly "high-calcium" flyashes. While some typical compositions are shown in Table 2.1, the silica/alumina ratio can vary widely within each of these groupings. Peterson found that while the alumina in flyash was incorporated into the product, it was the resulting silicates which were responsible for high surface area characteristics (Peterson, 1990).

Table 2.1: Typical Composition of Flyashes (weight %)

Oxide	SiO ₂	Al ₂ O ₃	CaO	MgO	Na ₂ O	K ₂ O	Fe ₂ O ₃	SO ₃
Low-Ca ¹	51.6	24.7	5.2	1.8	0.5	3.3	7.8	NR
High-Ca ²	32	19	28	5	1.3	NR	6	2

1: Low-Calcium Flyash (Jozewicz and Chang, 1989)

2: High-Calcium Flyash (JTM Industries, 1996)

NR: not reported

While the bulk of the research has been conducted with low-calcium flyash, Peterson (1987), Peterson and Rochelle (1988), and Izquierdo et al. (1992) reported that high-calcium flyash could be activated for reaction with SO₂ by slurrying in 85°C water without additional lime. Peterson (1987) and Peterson and Rochelle (1988) also observed that the addition of NaOH positively affected the formation of surface area and SO₂ reactivity under certain conditions. Stroud (1991) used a small amount of hydrated lime (0.1 g Ca(OH)₂/g flyash) to activate the high-calcium flyash in the presence of gypsum. This meant that the calcium intrinsic in the flyash could be made available for SO₂ reaction, and would imply that high-calcium flyash might be preferable to low-calcium flyash. However, Peterson's data (1990) showed that if the calcium intrinsic in the flyash was accounted for, low- and medium-calcium flyashes were in fact more reactive towards SO₂ when slurried with lime at 92°C for up to 8 hours. The ultimate specific surface area (m²/g) of the sorbent prepared from high-calcium ashes was also lower than that of low-calcium ashes. This was attributed to an effect of the different silica/aluminum concentrations between the flyashes.

Ca(OH)₂ conversion (mol SO₂ removed / mol Ca(OH)₂ added) was shown to increase from 0.2 to 0.8 when the flyash/lime ratio was increased from 1/1 to 20/1 for an 8 hour slurry time (Jozewicz et al., 1988b). While it might seem advantageous to maximize Ca(OH)₂ conversion by increasing the flyash/lime ratio, this also increases the solids loading in the system, including the bagfilter. Therefore, especially for low-calcium flyash with little intrinsic alkalinity, it would be best to maximize Ca(OH)₂ conversion by a means other than high flyash loading.

The aqueous reaction between lime and an amorphous silica source will produce a calcium silicate hydrate according to Equations 4.1-3. This is accomplished by the dissolution of the silica source in the high pH solution created by the lime. The dissolution of glass includes two primary phenomena, the extraction of alkali oxides from the silica matrix, and the breakdown of the silica matrix. Iler (1979) and El-Shamy et al. (1972) both present data showing the increased solubility of silica glass with increasing pH, especially above pH 11. Once the silica is dissolved, it re-precipitates with calcium in solution to form calcium silicates.

Figure 2.2 shows the ternary diagram of the better defined solid phases for the calcium silicate hydrate (CSH) system. Taylor (1964) states that the first products formed when calcium and silica are reacted in an aqueous environment will be of the tobermorite family having an approximate composition of $(\text{CaO})_5(\text{SiO}_2)_6(\text{H}_2\text{O})_5$. CSH-I and CSH-II, having Ca/Si ratios of 0.8-1.5 and 1.5-2.0, respectively, are considered tobermorites. There are also a plethora of more crystalline phases and one nearly-amorphous phase of the mineral. Taylor further states that at moderate temperatures, the non-crystalline tobermorites can persist indefinitely and that pressure hydration at high temperatures is normally required for crystallized calcium silicate hydrates to form. Figure 2.3 shows X-ray diffraction patterns for the generic groupings of tobermorites.

Peterson found that CSH-I, with a Ca/Si ratio of 1.3, was formed from the reaction of silica fume with lime. He also showed mainly non-crystalline products being formed from flyash and lime, with small amounts of $\text{Ca}_3\text{Al}_2(\text{SiO}_4)(\text{OH})_8$ in long time samples. The silicates created were almost completely amorphous with Ca/(Si+Al) ratio of 1.1 (Peterson, 1990). Tsuchiai et al. concluded that the low-calcium flyash/lime product used in the Tomato-Atsuma Power Station was mainly ettringite (Tsuchiai et al., 1995). Regourd (1987) details the morphology of CSH prepared from several different silica sources, including flyash, silica fume, and blast furnace slag. He gives a surface area for CSH at 200 m²/g. Ma et al. (1995) concludes that the porous structure of the calcium silicate hydrates consist of wedge-shaped pores.

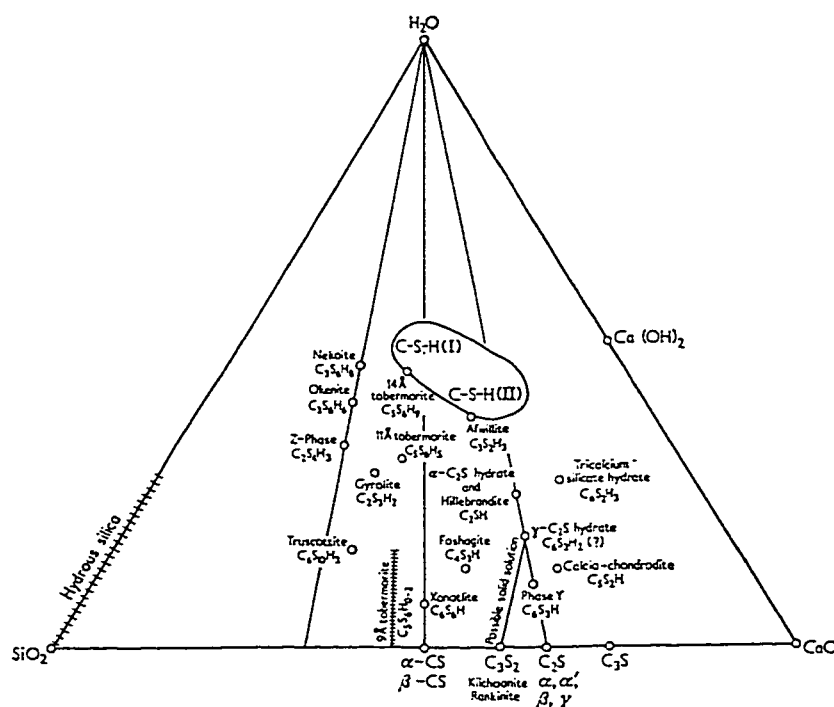


Figure 2.2: Ternary Diagram for SiO_2 - CaO - H_2O System

ref. Taylor (1964)

2.3.2 Effect of Temperature

For the reaction between flyash and lime, it was shown that for long slurry times (~12 hours) the SO_2 reactivity of the product increased with temperature up to 65°C . Above 65°C , the same ultimate SO_2 reactivity was achieved. For moderate slurry times, (<12 hours) the rate of reactive product formation increased with temperature up to 92°C (Jozewicz and Rochelle, 1986b). Peterson and Rochelle again showed that changing the temperature between 65° and 85°C did not effect solids SO_2 reactivity for 12 hour slurry times. For shorter reaction times, the SO_2 reactivity of solids slurried at 85°C was higher due to the increased silica dissolution rate at higher temperatures (Peterson and Rochelle, 1988).

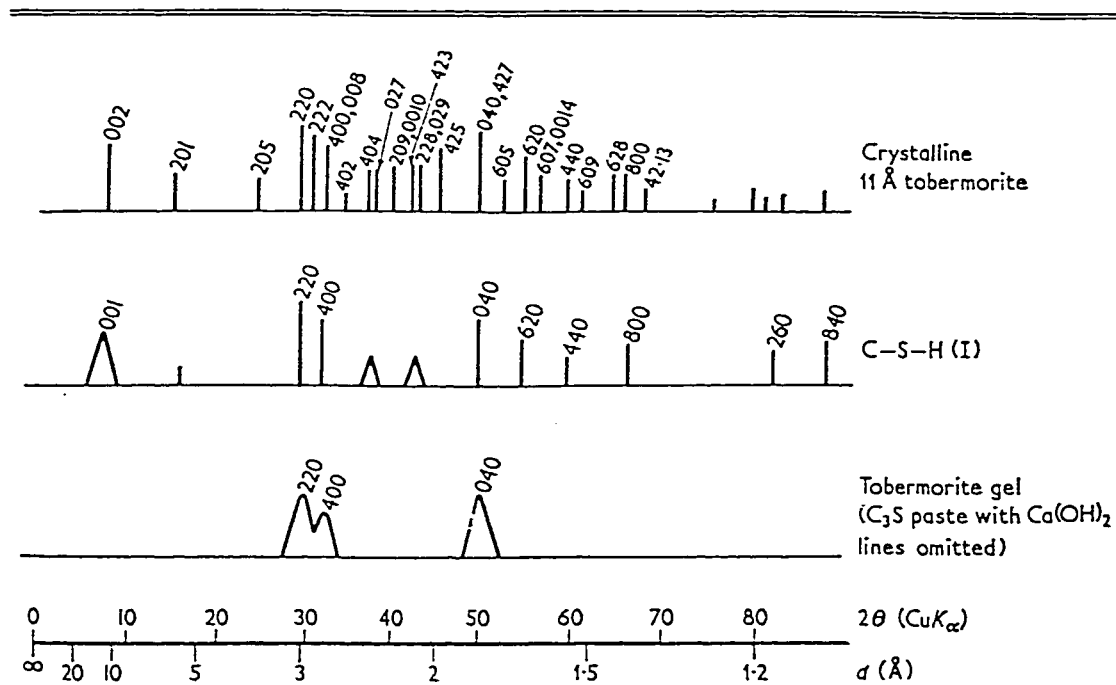


Figure 2.3: Typical X-ray Diffraction Line Patterns for Tobermorites

ref. Taylor (1964)

Pressure hydration, for reaction times less than 4 hours, produced product at a faster rate than atmospheric hydration at an optimum temperature of 150°C. The products were analyzed to have different morphologies depending on hydration conditions (Jozewicz et al., 1988a). It is unclear what the calcium silicate product should be when formed under high temperature conditions. Taylor (1964) states that pressure hydration will lead to crystalline materials, not the amorphous tobermorites created below 100°C that have been shown to be reactive with SO₂. Ma et al. (1995) showed surface area and porosity increased with temperature to 100°C when calcium silicates were prepared from flyash and lime. When the preparation temperature was increased to 180°C, the surface area and porosity of the product dropped.

2.3.3 Effect of Slurry Composition

The effect of NaOH on the formation of reactive silicates has been investigated extensively. It was hypothesized that the rate-limiting step was the dissolution of the flyash. Since it is known that the silica in flyash is glassy, and NaOH etches glass, it seemed reasonable that NaOH addition should increase the rate of reaction.

Peterson (1987) and Peterson and Rochelle (1988) showed the effects of NaOH on surface area formation and SO₂ reactivity. On one hand, the NaOH appeared to dissolve the flyash faster, resulting in a faster initial reaction rate. At higher NaOH concentrations, however, the NaOH suppressed the calcium concentration due to the common ion effect shown in Equations 2.3-4. As the sodium hydroxide concentration in solution rises, the concentration of calcium is reduced as determined by the solubility of the lime solid phase. This results in a lower rate of surface area formation. An optimum NaOH concentration was shown for the particular experimental conditions. NaOH was particularly helpful when activating the intrinsic alkalinity in solids prepared from high-calcium flyash.

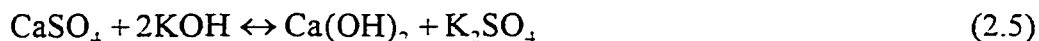


Phosphate appeared to increase the solids conversion, presumably by the increase in silica dissolution and possibly because of the dispersing properties of phosphates. An optimum concentration of several different phosphate sources was presented (Jozewicz et al., 1987).

Sulfite and sulfate species would be expected in the solids preparation slurry if a recycled flyash stream were being used. Peterson and Rochelle reported that the addition of calcium sulfite hemihydrate (CaSO₃•½H₂O) to slurries at 85°C, in the absence of NaOH, had little effect on the reactivity of the solids or the calcium solution concentration. In the presence of NaOH, however, calcium sulfite increased calcium concentration in solution and produced a more reactive product (Peterson and Rochelle, 1988). Gypsum (CaSO₄•2H₂O) was shown to have a strong positive effect on solids reactivity. Peterson and Rochelle looked at the reaction between lime and pure silica or alumina species with gypsum present.

They reported that gypsum may stop the formation of calcium aluminates, which have a low surface area and are unreactive (Peterson and Rochelle, 1990; Peterson, 1990).

Kind (1994) concludes that the presence of species such as gypsum or CaCl_2 maintains a dissolved calcium concentration, and limits the increase of pH over the course of the reaction. The hydroxide concentration, even without NaOH added, tends to rise as potassium and sodium is released from flyash. As shown in Equations 2.3-4, this rise in hydroxide will deplete the calcium in solution and slow the formation of reactive product. The presence of gypsum gives an additional supply of calcium as well as a supply of sulfate ion for the sodium or potassium to associate with as shown in Equation 2.5. This results in longer reaction times and higher surface area products (Kind et al., 1994b).



This supports the data presented by Taylor (1964) which shows that a calcium concentration between 1 mM and 20 mM in solution is necessary for a CSH solid phase with a Ca/Si ratio between 1 and 1.5 to be precipitated. This data is presented in Figure 2.4.

While adding certain salts undoubtedly increases the formation of reactive silicates, the presence of salts in the slurry solution may also precipitate on the surface of the sorbent and plug pores, reducing the available surface area (Wasserman, 1992).

2.3.4 Absorbent Preparation from Other Silica Sources

Calcium silicate hydrates have been formed from a number of amorphous silica sources. Peterson (1990) and Kind (1994) prepared high surface area solids from lime and silica fume. In screening tests, solids were prepared from a wide range of diatomaceous earths, tripolis, pumices, and several clays that were reactive towards SO_2 (Jozewicz et al., 1987; 1988b). The silicas were slurried at 90°C with CaO for 4 hours at a 1/1 ratio. Calcium conversions with SO_2 ranged from 0.24 to 0.84 (for a MIN-53 Natural Diatomaceous Earth) compared to 0.17 for unreacted $\text{Ca}(\text{OH})_2$. Natural diatomaceous earths made the more reactive sorbents (Jozewicz et al., 1987). Waste bottle glass was reacted with $\text{Ca}(\text{OH})_2$

and formed a sorbent that was more reactive towards HCl than unreacted $\text{Ca}(\text{OH})_2$. The glass was slurried at temperatures up to 90°C for up to 5 hours and then reacted with HCl for short times (3 sec) at $\sim 500^\circ\text{C}$ (Jozewicz et al., 1991a).

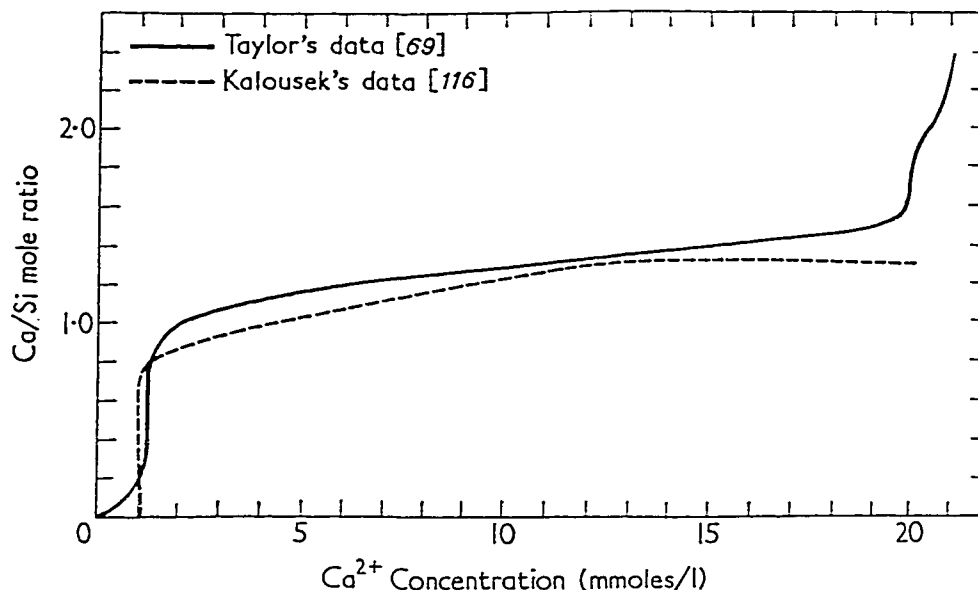


Figure 2.4: Effect of Solution Ca^{+2} on CSH-I Solid

Relationship of Ca/Si ratio in CSH-I solid to $[\text{Ca}^{+2}]$ in solution at room temperature. Ref. Taylor (1964)

2.4 REACTION OF SO_2 WITH HYDRATED LIME OR CALCIUM SILICATES

2.4.1 Effect of Relative Humidity

It has been shown qualitatively by a number of researchers that the reaction between alkaline sorbents, including lime and calcium silicates, is a strong function of relative humidity in the gas stream (Ruiz-Alsop, 1986; Jozewicz and Rochelle, 1986b; Chu and Rochelle, 1989; Martinez et al., 1991). Jozewicz et al. (1988b) showed that for solids prepared from diatomaceous earths and lime, the SO_2 capture increased up to a plateau at a relative humidity of 60%. Jozewicz et al. (1991b) presented a maximum short time conversion (<5 seconds) with an initial

free moisture of 30-50% for a given surface area. They thought that agglomeration of the solids at higher humidities may have decreased conversion, producing the maximum. Also, the positive correlation of critical moisture to pore volume was presented. Since pore volume naturally correlates with surface area, the relationship between critical moisture and surface area was also supported. Jozewicz et al. (1990) recommends that the relative humidity be held above 20% for SO₂ removal. In short, it is known that a substantial relative humidity is essential to high reaction conversion of alkaline sorbents with SO₂, whether the water originates in the gas stream or within the pores of the solid.

2.4.2 Effect of SO₂ concentration

The effect of SO₂ concentration was reported to be a function of relative humidity. At high relative humidity, or high SO₂ concentration, the solids conversion rate is kinetically controlled and is not a strong function of gas concentration. At low relative humidity, or low SO₂ concentration, the reaction rate appears to be mass transfer controlled, and therefore a function of concentration (Ruiz-Alsop, 1986; Rochelle et al., 1990).

2.4.3 Effect of Additives

The SO₂ reactivity of solids with moderate surface area typically correlated with BET surface area. The presence of deliquescent salts, during the slurry process, increased the moisture content on the solids beyond what was predicted by surface area, thereby increasing SO₂ reactivity (Kind et al., 1994b; Wasserman, 1992). Ruiz-Alsop (1986) also showed an increased reactivity when deliquescent salts were added to hydrated lime. Several hypothesis were proposed for the results: deliquescence, variable product layer porosity, or kinetic effects.

2.4.4 Reaction Modeling

Several researchers have modeled the low temperature, humid reaction between SO₂ and limestone, hydrated lime, or flyash/lime sorbents with varying degrees of success.

Klingspor et al. (1983) modeled the reaction between SO₂ and limestone, based on an unreacted, shrinking-core model with a reaction rate constant that

depended on solids conversion. While they tried other, more complicated models, this simple model achieved the best experimental fit.

Ruiz-Alsop (1986) modeled the reaction between SO_2 and $\text{Ca}(\text{OH})_2$ with a shrinking core model and zero order SO_2 concentration dependence. She correlated the solid diffusion coefficient and reaction rate constant with the relative humidity of the gas stream. The model also included a roughness parameter to account for inconsistencies in the porous structure of the solid.

The reactions of SO_2 with lime (Irabien et al., 1992) or with flyash/calcium sorbent (Garea et al., 1997) were modeled similarly. They used a model that was first order in SO_2 and was derived assuming the process was rate-limited by the adsorption of SO_2 onto the surface of the particle. The parameter representing SO_2 adsorption was found to be dependent on relative humidity.

2.5 PILOT-SCALE PROCESS TESTS

The development of the ADVACATE process has included both bench scale work as well as pilot scale tests. Sedman gives an outline of some of the process development (Sedman et al., 1990). Using a 100 m^3/h pilot plant, low-calcium flyash/lime and diatomaceous earth/lime sorbents were tested for SO_2 removal. For humid gas with 1000-2500 ppm SO_2 , removal ranged from 50% to 90% for solids loadings of 1 to 2 (moles SO_2 / mol Ca^{+2}). Recycling twice enabled 90% solids conversion of the solids (Jozewicz et al., 1986; 1988b).

Chapter 3: Experimental Methods and Procedures

This chapter summarizes the various experimental apparatuses and procedures used during the course of this work. Reaction materials, reactor systems, and analysis techniques for both the preparation of calcium silicate sorbents, as well as the reaction between these solids and SO_2 , will be described in detail.

3.1 CALCIUM SILICATE ABSORBENT PREPARATION

Calcium silicate sorbents were prepared by several methods described in these sections. All systems were aqueous slurries in nature and consisted nominally of a silica source and a lime source. In most cases, additives to affect slurry composition were also included. This section also summarizes the analysis techniques used to study these reaction systems.

3.1.1 Reagent Materials

3.1.1.1 *Recycled Glass*

The recycled glass used in this work was post-consumer container glass donated by Owens-Brockway in Waco, Texas. Samples of both amber and green "cullet" glass were obtained in the Fall of 1993. "Cullet" is the term for glass that has been crushed into pieces of approximately 1-2 cm.. While the samples were predominantly one color, contamination of one color batch with the other was evident. The cullet samples consisted of the crushed glass, mixed with debris from the consumer and recycling processes, including paper, dirt, and most likely dried beverage. The amber sample was used exclusively in this work, in lieu of the green. The brown color in container glass is normally produced by the addition of iron compounds, such as ferrous sulfide or iron pyrites, while the green glass is colored with chromium (Boyd and Thompson, 1980). It was decided to avoid any potential environmental impacts of working with chromium.

The cullet (~1-2 cm pieces of crushed glass) was ground in a disk attrition mill courtesy of the Department of Civil Engineering. The glass was then dry sieved into several fractions. The primary sample used in this work was the fraction passing through a 325 mesh sieve, with a measured BET surface area of

0.38 m²/g. A separate grinding / sieving batch provided samples of <325 mesh and 325-270 mesh, with BET surface areas of 0.51 and 0.27 m²/g, respectively. Table B.1 shows the measured surface areas of the various glass fractions.

The composition of the glass was measured by X-ray Fluorescence, courtesy of Acurex Environmental, Corp. The measured values compare well with those published by Kirk-Othmer as seen in Table 3.1.

Table 3.1: Composition of Amber Container Glass

Oxide	Elemental wt.% (Acurex, 1996)	Oxide wt.% (Acurex, 1996)	Oxide wt.% (Boyd et al., 1980)
SiO ₂	37.0	79.2	72.48
Al ₂ O ₃	1.23	2.32	1.87
CaO	8.32	11.6	10.79
MgO	0.623	1.03	0.02
Na ₂ O	11.24	15.1	14.17
K ₂ O	0.0103	0.012	0.45
FeO	0.392	0.50	0.21
S	0.0341		
Total		109.76	99.99

3.1.1.2 Iron Blast Furnace Slag

The sample of ground granulated iron blast furnace slag used in this work was donated courtesy of Koch Industries. The primary function of the iron blast furnace is to reduce iron ore (iron oxides) into molten iron metal. Calcium oxide and magnesium oxide, otherwise known as flux, are added to the blast furnace to remove silica, alumina, sodium, potassium, and sulfur. The flux and impurities are removed from the furnace as a molten slag, solidified, and ground (Peacey and Davenport, 1979; Virgalitte et al., 1997).

The measured BET surface area of the slag was 3.62 m²/g. An approximate composition of the slag was provided via Material Safety Data Sheet information provided by Koch. Table 3.2 shows the nominal weight percentages for this particular sample compared to published average values.

3.1.1.3 Hydrated Lime

The lime ($\text{Ca}(\text{OH})_2$) used was a rotary mill hydrate (Code MR200) donated by the Mississippi Lime Company in April 1995, and also used by Chisholm and Rochelle (1998). It had a measured BET surface area of $21.6 \text{ m}^2/\text{g}$, and an alkalinity of 13.09 mmol/g as determined by the procedure outlined in Section 3.1.3.4. The theoretical alkalinity of $\text{Ca}(\text{OH})_2$ is 13.496 mmol/g , indicating that this sample was essentially 97% pure. It is assumed that the most likely impurity would be CaCO_3 formed from contact with atmospheric CO_2 . For experiments conducted prior to April 1995, a rotary mill hydrate (Code MR200), also donated by the Mississippi Lime Company was used. This was the same sample used by Kind (1994).

Table 3.2: Composition of Iron Blast Furnace Slag

Oxide	Oxide wt.% (Koch, 1980)	Oxide wt.% (Virgalitte et al., 1997)
SiO_2	30-45	32-42
CaO	30-45	32-45
MgO	8-15	5-15
Al_2O_3	5-14	7-16
S	0-3.5	0.7-2.2
MnO	0-1	0.2-1.0
K_2O	0-1	not reported
Na_2O	0-1	not reported
TiO_2	0-1.5	not reported
Fe_2O_3	0-0.75	0.1-1.5
Other	0-5	not reported

3.1.1.4 Reagent Grade Chemicals

Several reagent grade chemicals were utilized during the course of this work. Table 3.3 outlines the sources of these chemicals.

3.1.2 Sorbent Preparation Reactors and Procedures

3.1.2.1 Glass Dissolution Measurements

The rate of glass dissolution was measured by agitating ground glass ($0.38 \text{ m}^2/\text{g}$) in KOH at a solids loading of $2.00 \text{ g glass} / \text{L solution}$.

Ethylenediaminetetraacetic Acid (1.25 g EDTA / g glass) was also included in the solution to complex any calcium that would be released from the glass and to prevent any precipitation of calcium silicates. Experiments were conducted at several temperatures and hydroxide concentrations.

The experiments below 100°C were conducted in a polypropylene bottle submerged in water and placed in the atmospheric reactor described in 3.1.2.2. The experiments at 120°C were conducted in the stainless steel pressurized reactor described in 3.1.2.3. Samples were withdrawn from the reactors at various points in the experiment, and filtered through a 0.45 μm syringe filter. The liquid filtrate was analyzed by atomic absorption spectroscopy for silicon, calcium, and sodium.

Table 3.3: Reagent Grade Chemicals

Formula	CAS	Source	Assay (%)
AgNO_3	7761-88-8	Mallinckrodt	not available
$\text{CaSO}_4 \cdot 2\text{H}_2\text{O}^*$	10101-41-4	Sigma	100.7
CaCl_2	10043-52-4	EM Scientific	90.0 min.
CsCl	7647-17-8	Spectrum	99.0 min.
$\text{FeSO}_4 \cdot 7\text{H}_2\text{O}$	7782-63-0	Spectrum	99.0 min.
KOH	1310-58-3	EM Scientific	95.0 min.
KCl	7447-40-7	EM Scientific	99.0-100.5
NaOH	1310-73-2	Spectrum	95.0-100.5
Na_2SO_3	7757-83-7	EM Scientific	98.0 min.
$\text{Na}_2\text{S}_2\text{O}_3 \cdot 5\text{H}_2\text{O}$	10102-17-7	Spectrum	99.5-100.5
HCl (aq)	7647-01-0	Fisher	1.995-2.005 N
$\text{H}_2\text{O}_2 \text{ (aq)}$	7722-84-1	EM Scientific	29.0-32.0
$\text{NH}_4\text{OH (aq)}$	1336-21-6	EM Scientific	28.0-30.0

*Lot # 102H1067

3.1.2.2 Atmospheric Sorbent Preparation

Sorbents were prepared from slurries at 92°C in an atmospheric reactor pictured in Figure 3.1. The 500 mL jacketed pyrex reactor was connected to an water/ethylene glycol temperature control bath (Lauda M3) which controlled to $\pm 0.1^\circ\text{C}$. The slurry was stirred at 350 rpm with a mechanical agitator (Stedfast Stirrer, Model SL600, Fisher Scientific) placed through a plexi-glass lid on the

reactor. Though the reactor was covered to minimize water loss, it was not airtight.

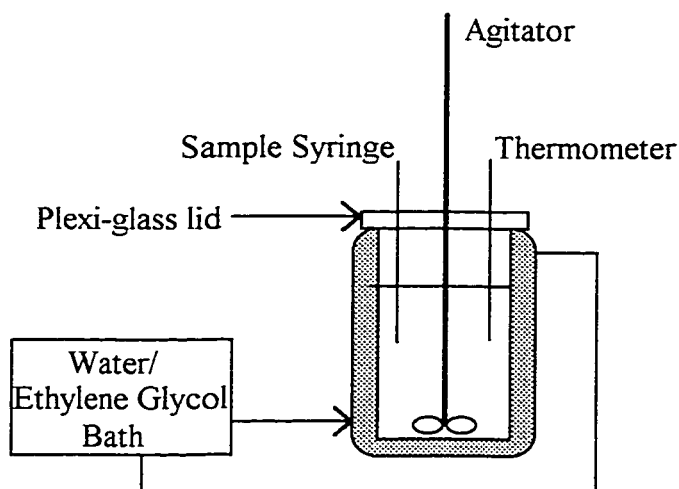


Figure 3.1: Glass Slurry Reactor for Atmospheric Reactions

A typical slurry reaction began by first heating the water to the experimental temperature. The solids, including lime, silica, and gypsum, were then added to the hot water at time zero. For reactions conducted with soluble additives, such as CaCl_2 or $\text{NaSO}_3/\text{Na}_2\text{S}_2\text{O}_3$, the additives were added to the water before heating. For slag slurries with H_2O_2 addition, 3-5 mL peroxide were added whenever Lead Acetate paper gave a positive brown reading indicating H_2S release. Samples of about 55 mL were withdrawn via a plastic syringe at various reaction times with the agitator running. The samples were filtered with the help of a water aspirator through a medium porosity filter paper. The liquid filtrate was filtered again through a $0.45\ \mu\text{m}$ syringe filter and stored in polypropylene bottles for later analysis. The solids were vacuum dried at 90°C and $>30\ \text{inHg}$ vacuum for 6-24 hours and then sieved through an 80 mesh screen sieve to break up the powder. The solid samples were also stored in polypropylene bottles.

3.1.2.3 *Pressurized Sorbent Preparation*

Experiments at 120°C were conducted in a 500 mL pressurized stainless steel autoclave as shown in Figure 3.2. The autoclave was a MagneDrive II, Packless Zipperclave, built by Autoclave Engineers, Inc. The pressure in the reaction vessel was determined solely by the vapor pressure of the slurry at that temperature. Agitation was accomplished by a magnetically rotated impeller providing for a theoretically sealed reaction environment. The speed of agitation was approximately 500 rpm, but was poorly controlled with a motor driven by house air. The temperature was controlled with a ceramic band heater attached to a temperature controller. It is estimated that the system controlled to $\pm 5^\circ\text{C}$, as measured by the single controller thermocouple. Since the thermocouple could not be simultaneously connected to a meter and the controller, the temperature behavior is an estimate.

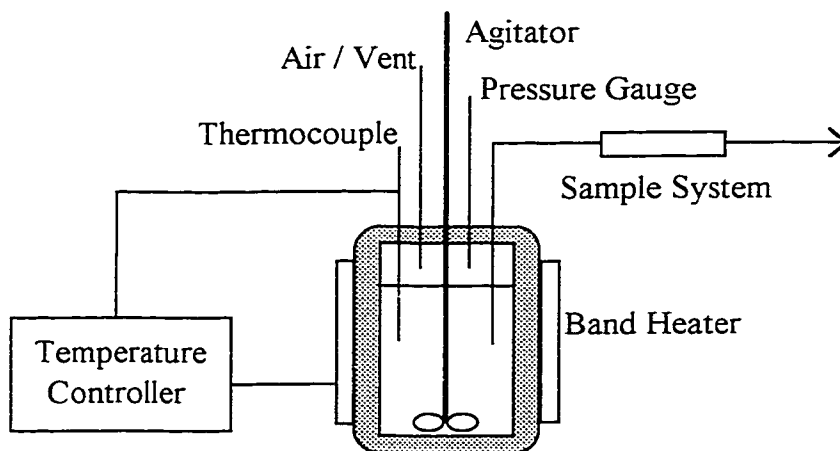


Figure 3.2: Stainless Steel Autoclave for Pressurized Reactions

Typically, experiments began by heating the water to $\sim 85^\circ\text{C}$. The solids were then added, and the reaction chamber sealed. Reaction temperature was normally reached in less than 15 minutes. Samples were taken over the course of the experiment through a submerged sample tube by pressurizing the vessel with air to ~ 70 psig and allowing the pressure to force the sample into a holding tube.

The sample was allowed to cool slightly, usually for 5-10 minutes, in the holding tube prior to filtering, in order to avoid water flashing. The sample was then filtered and dried as described in 3.1.2.2. After sampling, the reactor was vented to its previous operating pressure.

3.1.2.4 *Non-agitated Sorbent Preparation*

Solids were prepared without agitation in single sample vials. These vials were 8 mL glass vials with wax paper lined plastic screw-caps. The unreacted solids and water were mixed and weighed in the vial, which was then capped. Sets of vials were placed in a Blue M temperature controlled convection oven and individual samples removed at the appropriate reaction time. They were weighed for water loss (<5%) and vacuum dried without caps, as previously described in 3.1.2.2. If the water loss during the reaction exceeded 5%, that particular sample was thrown out. It is important to note that the samples were not filtered prior to drying, so the precipitation of any solution salts may pose another difference from solids prepared with agitation.

3.1.3 Solids Analysis

3.1.3.1 *BET Surface Area and Porosity*

All solids were measured for BET (Brunauer-Emmett-Teller) surface area, with selected samples further analyzed for porosity and pore size distribution. For experiments prior to January 1996, surface area was measured with a Micromeritics AccuSorb 2100E Physical Adsorption Analyzer. After January 1996, a new Micromeritics Accelerated Surface Area and Porosimetry System, ASAP 2010, was used.

Samples were degassed for at least 12 hours under vacuum and at ambient temperature. Degassing is necessary to remove any adsorbed gases, particularly water. However, higher than ambient temperatures were not used to avoid the desorption of hydrated waters from the solids. High purity helium was used to measure the free space of the sample. The adsorption measurements were conducted with ultra high purity nitrogen adsorption at 77.35 °K, the temperature of liquid nitrogen at the normal atmospheric barometric pressure.

BET surface area calculations assume that multi-layer adsorption is possible, however at very low partial pressures, monolayer adsorption occurs. Equation 3.1 relates the total volume adsorbed to the equilibrium partial pressure and is commonly known as the "BET equation." (Brunauer et al., 1938; Micromeritics, 1995)

$$\frac{p}{v(p_0 - p)} = \frac{1}{v_m c} + \frac{(c - 1)p}{v_m c p_0} \quad (3.1)$$

where: p = pressure
 p_s = saturation pressure
 v = volume of nitrogen adsorbed at pressure p
 v_m = volume of nitrogen monolayer
 c = constant

At low partial pressures, the adsorption isotherm is linear as the initial monolayer is adsorbed. The BET equation can be fit to this range of data using v_m and c as parameters. Knowing the volume of a monolayer of nitrogen, v_m , and the size of a nitrogen molecule allows for the calculation of the surface area of the solid.

3.1.3.2 *X-ray Diffractometry*

Powdered X-ray diffraction patterns were obtained for some samples using diffractometers maintained by the Materials Science Division in the Department of Mechanical Engineering. One system consisted of Philips PW 1729 generator and Philips APD 3520 data collection system. The other system was powered by a Philips PW 1720 generator coupled with a Philips Ortec Counter/Timer. Both generators were operated at 40 mV and 30 mA, and both systems were PC controlled. The powder samples were packed into aluminum sample holders. Diffraction patterns were normally taken at 2-theta range of 5 to 70 degrees using a Cu K_α source. Patterns were sometimes analyzed using the software JADE, available with one of the PC control systems. This software had built-in access to patterns published in JCPDS (1997).

3.1.3.3 SEM

A JEOL JSM35C Scanning Electron Microscope was used to look at selected solid samples. The samples were first mounted on aluminum disks using a special double-sided tape. They were then sputtered using a Pelco Model 3, sputter coater. In practice, a 1000x magnification provided the best balance between focus and surface detail.

3.1.3.4 Alkalinity

The alkalinity of the solids was measured using a simple acid dissolution and pH titration. The solids (~0.1 - 0.2 g) were weighed and mixed with 50 mL 0.1 M HCl in a beaker, covered with parafilm, and stirred for 10 min. with a magnetic stir bar. The entire mixture was then titrated with ~0.2 M NaOH to the phenolphthalein endpoint. The HCl was diluted from standardized solution, while the NaOH was made from NaOH pellets and standardized against the HCl. The divalent alkalinity of the solids were therefore determined by equation 3.2.

$$\text{divalent_alk(mmol)} = \frac{(50\text{mL})(0.1\text{MHCl}) - (x\text{mL})(y\text{MNaOH})}{(g\text{solid})(2\text{ mmol} / \text{mmol_divalent})} \quad (3.2)$$

where: x = mL NaOH used to reach phenolphthalein end
 y = molarity of NaOH, standardized to HCl
 g = measured weight of solids

3.1.3.5 Selective Dissolution

Product composition of the solids was measured by a technique known as Selective Dissolution by previous researchers (Kind, 1994a). The premise of the technique is that calcium silicate solids will be soluble in moderate acid, while the unreacted silica source, i.e. flyash or glass, will be insoluble. The technique was modified slightly from what was done previously by lowering the solids to water acid ratio to prevent what appeared to be the gelling of the silica.

For this research, the solids (~0.02g) were weighed into a beaker, mixed with 50 mL 0.1 M HCl as measured with pipette, covered with parafilm, and stirred for 10 min. with a magnetic stir bar. The solution was then filtered through

a 0.45 μm syringe filter and the filtrate stored in a polypropylene bottle. It was later analyzed for Si, Ca^{+2} , and Na^{+} with atomic absorption spectrophotometry.

3.1.4 Liquid Analysis

3.1.4.1 *pH*

The pH of liquid samples was measured at ambient temperatures using a Corning pH meter 130. Two Corning General Purpose Combination probes were used over the course of this research, Cat. Nos. 476531 and 476182. Both were equipped with replaceable ceramic junctions and a refillable outer shell. This compartment was rinsed with de-ionized water and filled with saturated KCl solution about once a week. The pH system was calibrated between 7.0 and 10.0 with standard buffer solution.

3.1.4.2 *Atomic Absorption Spectrophotometry*

A Varian model AA-1475 atomic absorption spectrophotometer was used to measure calcium, sodium, potassium, and silicon concentrations in solution. This method is based on the premise that atoms, when excited, will absorb light at a defined wavelength. The sample is aspirated through a capillary tube into an acetylene/air or acetylene/nitrous oxide flame operating at 2500 - 3000 $^{\circ}\text{C}$. A hollow cathode lamp containing the specific element intended for measurement emits light at the needed wavelengths. The light beam is split into a reference beam and a measurement beam, which passes through the flame. A photomultiplier tube measures the light intensity at the set wavelength. The attached computer calculates the decrease in light intensity, or absorbance. The machine is capable of a linear calibration of up to three standards, as well as a built-in integration routine to smooth out signal noise. Appendix A.2. outlines the standard operating procedures for this apparatus.

For this research, standards were diluted from 1000 ppm AA standards purchased from Fisher and Aldrich Chemicals. The ranges and wavelengths used were those suggested by Varian (1979) and are presented in Table 3.4. Ion suppressants were added to all standards and samples in the concentrations listed in Table 3.4. These are used to increase the sensitivity of the measurement by suppressing the ionization of the element measured.

Table 3.4: Atomic Absorption Operating Parameters

Element	Range (ppm)	Wavelength (nm)	Spectral Band Pass (nm)	Suppressant
Calcium	0.5 - 4.0	422.7	0.5	50 mM KCl
Sodium	0.5 - 2.0	589.6	1.0	50 mM KCl
Silicon	10 - 100	251.6	0.2	none
Potassium	0.5 - 2.0	766.5	1.0	1000 ppm CsCl

3.1.4.3 *Sulfide Potentiometric Titration*

Sulfide concentration was measured by a potentiometric method derived from those published (Tamele, 1960; Shen, 1997). The sample containing sulfide (5 mL) was pipetted below the surface of 50 mL anti-oxidation solution (~1.0 M NaOH ; 0.05 M NH_3OH) to inhibit the air oxidation of the sulfide. The solution was then titrated with 0.01 M AgNO_3 to the potentiometric endpoint as measured with an Orion silver / silver sulfide electrode, 941600, compared to the reference electrode in the Corning pH combination electrode.

3.2 SO_2 REACTION WITH SOLID SORBENTS

3.2.1 Sandbed Reactor and Procedures

3.2.1.1 *Sandbed Reactor System*

The reaction between SO_2 and solid sorbents was studied in a packed bed reactor system also used by Nelli (1997) and shown in Figure 3.3. A simplified flue gas was synthesized from compressed SO_2/N_2 (~0.5%) diluted with nitrogen or air, depending on the desired oxygen content. All flows were metered by Brooks model 5850C mass flow meters controlled with a Brooks model 5878 Controller box. Flow controller details are outlined in Table 3.5. A Harvard Apparatus Infusion Pump supplied water to a helical Pyrex evaporator supported within a Tracor Stone F1-D Furnace to humidify the flue gas. The temperature in the furnace was controlled by a Cole-Parmer model 2603 Voltage Controller. The flowrate of water from the syringe pump was measured by weighing the water output over time. Results are shown in Table 3.6.

The sandbed reactor was a glass reactor, 7.5 in. long and 1.5 in. in diameter. A 2 mm course glass frit was installed in the bottom portion of the reactor to support the sand / sorbent mixture. The reactor was sealed by a ground

glass fitting, held by a metal clamp and several rubber bands. The reactor was then suspended upright in a water bath which was controlled by a Lauda MS temperature controller.

The SO_2 concentration was measured with a Thermo Electron Pulsed Fluorescent SO_2 Analyzer, Series 43. A Taurus digitizer and PC were used for automatic data collection of the analyzer output. Since this analyzer was designed primarily for steady state measurements, there was a significant timelag associated with the analyzer. The analysis and modeling of this timelag are described in Appendix C.

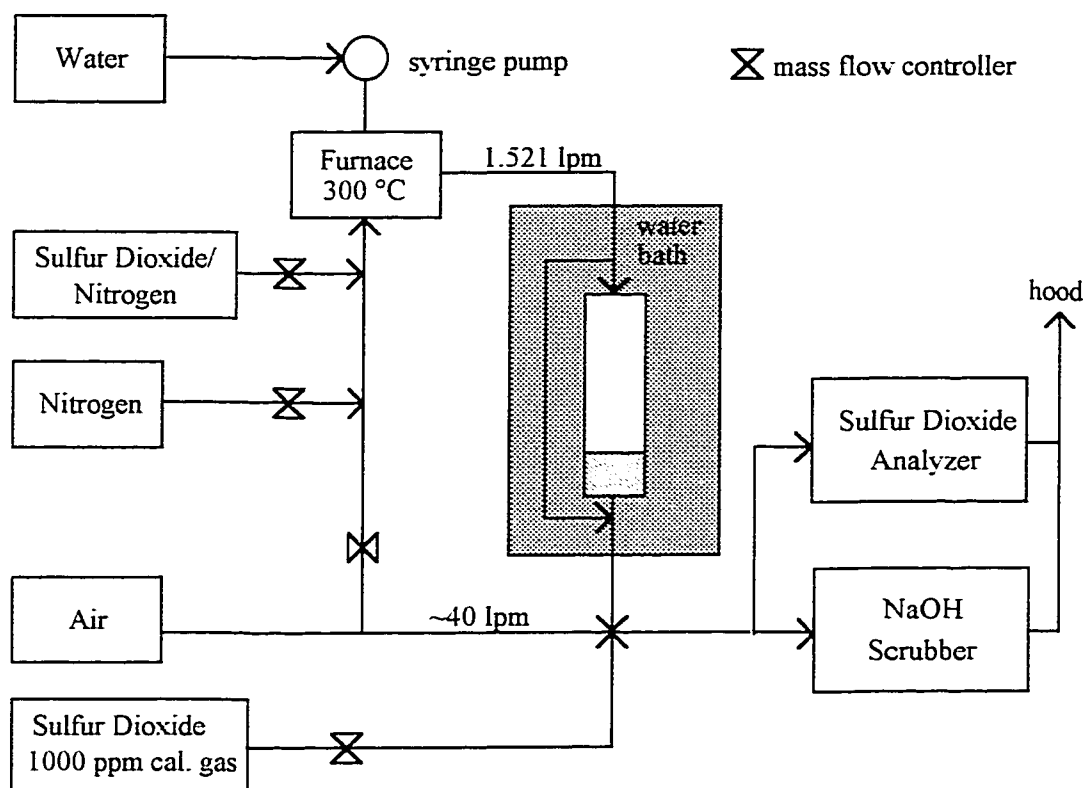


Figure 3.3: Sandbed Reactor System

There was a bypass line within the temperature controlled water bath to allow the synthesized flue gas and analytical system to reach steady state prior to

reaction. The flue gas, with concentrations ranging from 0-2000 ppm was diluted heavily with house air to bring the concentration into the 0-50 ppm range of the analyzer. This also eliminated condensation problems in the analytical system by reducing the relative humidity of the gas. The majority of the outlet flow was sent through a NaOH sparging system, normally operating at pH 13. A small portion of the gas was pulled off by a small vacuum pump in the SO₂ analyzer.

Table 3.5: Mass Flow Controller Parameters

Gas	Controller Serial No.	Nominal Range (slpm)	Calibration (actual lpm)	R ²
N ₂	8507HC027521/010-1	0-2.5	0.030923+ 0.024526x	0.9997
SO ₂	8507HC027528/010-1	0-1	-0.0042248+ 0.012625x	0.99992
SO ₂ calibration.	9103HC037044/1	0-2	-0.085391+ 0.022412x	0.99816
Air	9310HC038405	0-0.5	0.00097317+ 0.004899x	0.99998

Table 3.6: Syringe Pump Calibrations

Setting	60cc plastic: Flowrate (g/min)	30cc ground glass Flowrate (g/min)	30cc plastic Flowrate (g/min)
6	0.74		
7	0.39	0.193	0.224
8	0.18	0.094	0.110
9	0.072	0.033	0.043
10	0.036		0.024
11	0.0168		0.012
12	0.0067		

3.2.1.2 Typical SO₂ Reaction Experimental Procedures

A typical experiment began with a calibration using only air and SO₂ calibration (1000 ppm) gas. This allowed for the setting of the air dilution rate, which was not measured, but remained constant over the course of the experiment. After adjusting the air flowrate to give an SO₂ signal of ~45 ppm, thereby giving a

two point calibration of 0 and 1000 ppm, the system was purged of all SO_2 . The sorbent to be tested was weighed into a small beaker and mixed with quartz sand at a ratio of 0.1 g sorbent / 30 g sand. A ratio of 30x was shown to be sufficient for sandbed studies using CaCO_3 (Klingspor et al., 1983). The solids were placed on the glass frit and exposed to a nitrogen stream at the experimental humidity for 20 minutes. The SO_2 flue gas was then made and allowed to pass around the reactor through the bypass line until the flows stabilized and the analytical train reached steady state. This step normally took <30 minutes. At time zero, the flow was diverted from bypass into the reactor. Most experiments were conducted for 1 hour, even if the SO_2 removal after an hour was still greater than zero. Figure 3.4 shows the raw data collected after time zero from a typical experiment.

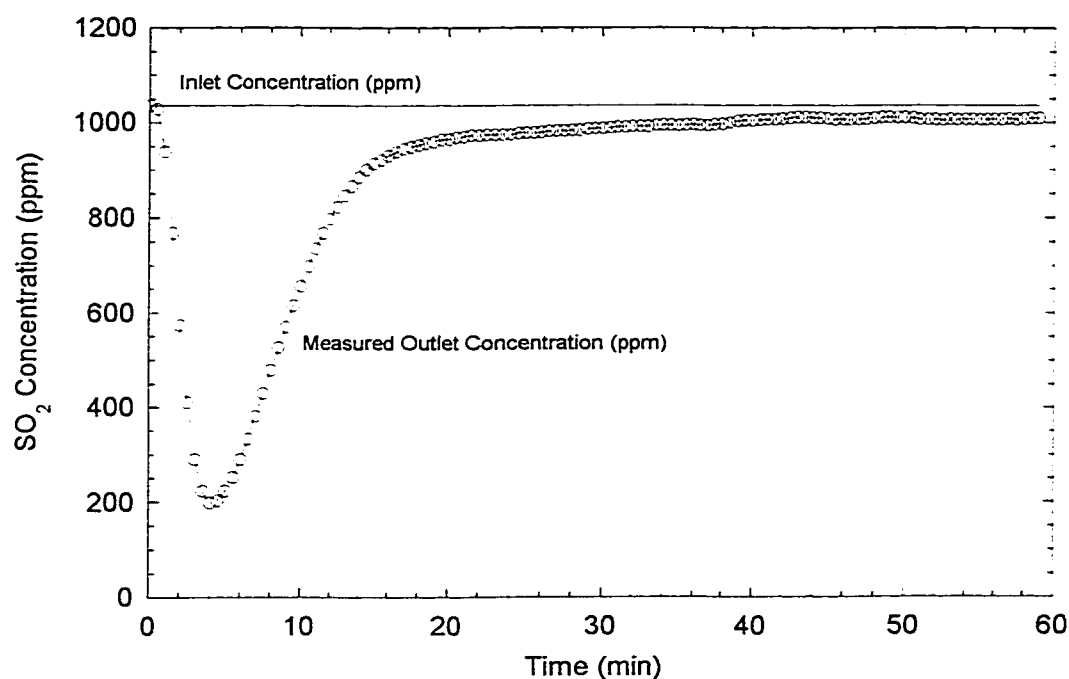


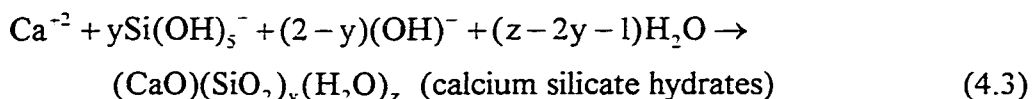
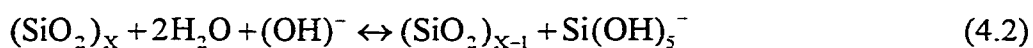
Figure 3.4: Raw Data from a Typical Experiment

Run #51; ~1000 ppm SO_2 inlet; 50°C; 58 %RH;
1.52 lpm; 0.1 g glass ADVACATE (4/28/97-50)

Chapter 4: Calcium Silicate Production from Recycled Glass

This chapter presents results and discussion regarding the preparation of calcium silicates from lime and post-consumer glass. Reaction variables that are of potential economic importance have been investigated over the course of this research. These variables include initial surface area of the silica, agitation, temperature, slurry composition, and solids loading. In addition, investigation of glass dissolution rates and sorbent characteristics was done to further the understanding of this system.

The aqueous reaction between lime and silica is believed to proceed according to Equations 4.1-3. The mechanism begins with the dissolution of the lime into calcium and hydroxide in solution. The increased pH of the solution instigates the breakdown of the silica framework, releasing silica into solution. The calcium ion and silica then precipitate as calcium silicate hydrates. It is believed that Equation 4.2 is chemical rate-limiting at times prior to the precipitation of a product layer. The mechanism shows the dependence of the overall reaction on the pH and calcium concentration.



The primary goal of this research was to prepare alkaline sorbents which are reactive with SO_2 . Because SO_2 reactivity has been correlated with the amount of moisture the solids can hold within the pore structure (Jozewicz et al., 1991b), and this has been shown to correlate with surface area (Stroud, 1991), surface area was used as the convenient measure of the reactivity of the product solids. This simplification should hold true as long as the sorbent composition / phase remains constant. Therefore, while the bulk of the solids preparation results are presented in the form of maximizing surface area, the most promising sorbents

were also tested for actual SO_2 reactivity. Those experimental results are presented in Chapter 6.

4.1 GLASS DISSOLUTION

As stated previously, the dissolution of the glass by Equation 4.2 is thought to be the chemical rate-limiting step at early times in the reaction system to form calcium silicates. To quantify this system better, glass dissolution experiments were conducted at several different temperatures and hydroxide levels. The total concentration of silica in this sample of glass was determined to be 0.37 g Si / g glass by X-ray fluorescence courtesy of Acurex Environmental (1996). The dissolution data were normalized by this amount and presented in Figures 4.1.

4.1.1 Effect of Hydroxide Concentration

Figure 4.1 shows the rate of silica dissolution as a function of hydroxide concentration at 92°C. The nominal hydroxide levels were corrected for the effect of EDTA acid, assuming that all four EDTA acidic groups reacted with hydroxide. In other words, solutions which contained 0.05 M, 0.1 M, and 0.2 M potassium hydroxide before the addition of 8.55 mM EDTA, are labeled as 0.016 M, 0.066 M, and 0.166 M, respectively. It is evident in Figure 4.1 that the rate of dissolution increases with both time and hydroxide concentration, as expected from Equation 4.2. The crossing of the 0.016 M and 0.066 M data after ~10 hours was unexpected and is attributed to experimental error.

Table 4.1 contains the regressed curve fits for the data shown in Figure 4.1. These equations were used for extrapolation of the data.

The order of reaction with respect to hydroxide concentration can be obtained by plotting the hydroxide concentration versus the inverse of the time required to reach a given silica dissolution level. Figure 4.2 shows the reaction order with respect to hydroxide concentration at 30% and 40% silica conversion to be 0.75 and 0.61 respectively. Peterson (1990) found the dissolution of silica from low-calcium flyash was approximately first order in hydroxide concentration under similar conditions. The discrepancy is most likely due to the inconsistent experimental data shown in Figure 4.1. If the reaction order is determined at 40%

using only the 0.166M and 0.066M experiments, the slope is 0.94, which is closer to the expected first order dependence.

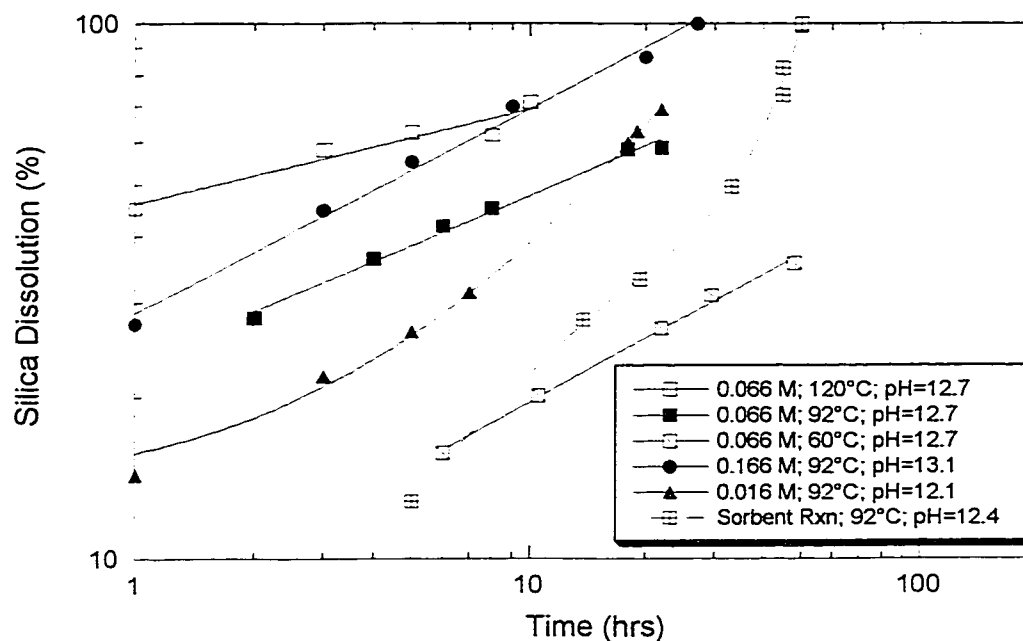


Figure 4.1: Effect of Hydroxide and Temperature on Glass Dissolution

400 mL KOH; 0.8 g glass; 1.0 g EDTA acid

Labeled KOH concentration was corrected for neutralization by EDTA acid. Measured pH values listed.

Total Silica = 0.37 g/g glass (Acurex, 1996).

Sorbent Rxn: lime/glass/gypsum - 1/1/0.5; 20% solids; 92°C.

Table 4.1: Curve Fits for Experimental Glass Dissolution Data

[OH ⁻]	Temperature	Curve Fit	R ²
0.016M	92°C	$y=13.2+2.59x$	0.999
0.066M	92°C	$y=18.3+30.6\log(x)$	0.994
0.166M	92°C	$y=23.5+50.0\log(x)$	0.983
0.066M	60°C	$y=-2.11+22.3\log(x)$	0.993
0.066M	120°C	$y=45.8+22.9\log(x)$	0.912

4.1.2 Effect of Temperature

The dissolution rate as a function of temperature is also presented in Figure 4.1. As expected from most dissolution processes, the silica dissolution increased with time and temperature. The temperature dependence was determined by fitting data at a specified silica dissolution to an Arrhenius equation. The Arrhenius analysis of the data at 40% silica conversion is shown in Figure 4.3. This arbitrary conversion (40%) was chosen to minimize the extrapolation of the data regressions shown in Figure 4.1. The regressed parameter gave an activation energy of $(10564)(1.9873 \times 10^{-3} \text{ kcal/mol/}^\circ\text{K}) = 21.0 \text{ kcal/mol}$. This was in good agreement with Peterson (1990), who reported an activation energy of 20.8 kcal/mol for flyash. Peterson also gives a good overview of the mechanism for silica dissolution (1990).

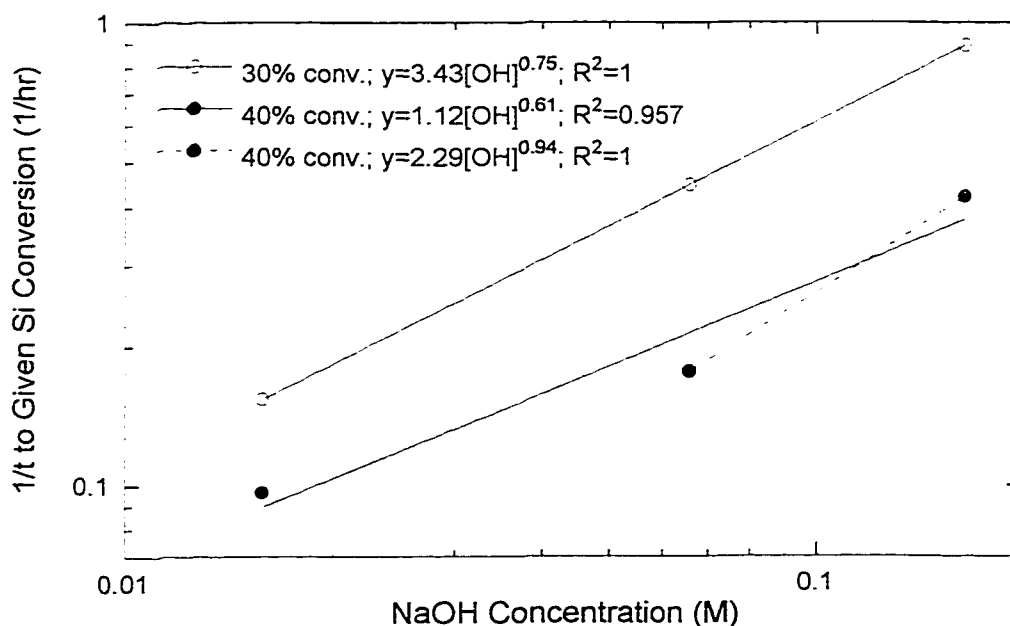


Figure 4.2: Hydroxide Order of Glass Dissolution

4.1.3 Combined Hydroxide and Temperature Effects

If it is assumed that 1) the effects of hydroxide and temperature on the rate of silica dissolution are independent and separable, and 2) that the temperature

dependence follows an Arrhenius form, then it holds that Equation 4.4 represents the system.

$$\frac{d(\text{Conv}_{\text{Si}})}{dt} = [\text{OH}^-]^a * b \exp(-E_a/RT) \quad (4.4)$$

Furthermore, by normalizing the experimental time by the right hand side of Equation 4.4, the dissolution data should collapse. Figure 4.4 presents the experimental data with time normalized to the hydroxide and temperature rate effects, causing the data to collapse reasonably well.

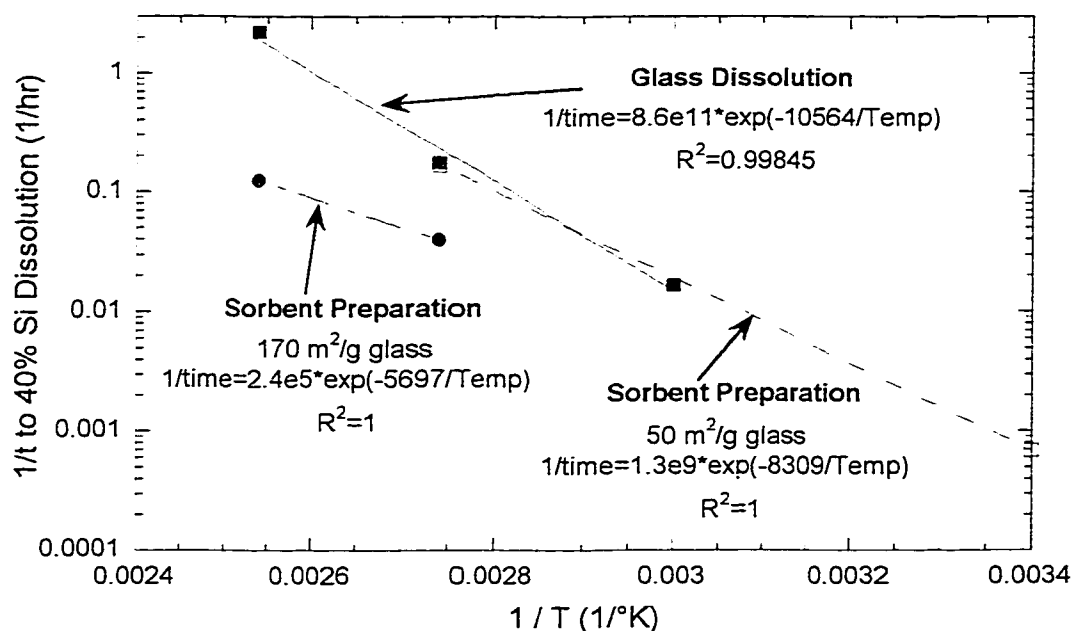


Figure 4.3: Arrhenius Analysis of Glass Dissolution

Sorbent Preparation: lime/glass/gypsum-1/1/0.5; 20% solids
 Selective Dissolution Analysis on solids of 170 m²/g.

The rate of silica dissolution during sorbent preparation was determined by selective dissolution of solids prepared at 92 °C and 120 °C. The results are shown, along with pH results, in comparison to glass dissolution experiments in Figure 4.1.

An activation energy of 11.3 kcal/mol was regressed in Figure 4.3 for the preparation of sorbent having an area of 170 m²/g glass. This conversion (surface area) was chosen because it was prior to the sharp decrease in the rate of surface area formation that occurs at 120°C shown in Section 4.2.4, and it also corresponds to approximately 40% silica conversion for comparison with glass dissolution data. If glass dissolution were rate-limiting, it would most likely be rate-limiting at the beginning of the reaction, prior to any significant product layer formation. Yet, even at what appears to be the initial rate of reaction for sorbent preparation, the activation energy is different than that of glass dissolution. Furthermore, it is clear from Figure 4.1 that the rate of silica dissolution is significantly slower during sorbent preparation at similar temperatures and hydroxide levels. The overall limiting step, therefore, is most likely a diffusion step through a calcium silicate product layer, even at relatively early times.

For the preparation of sorbent having a lower surface area of 50 m²/g glass, an activation energy of 16.5 kcal/mol from experiments at 92°C and 21°C. It appeared that perhaps at this low surface area (20 m²/g solid) the preparation system approached the glass dissolution limit.

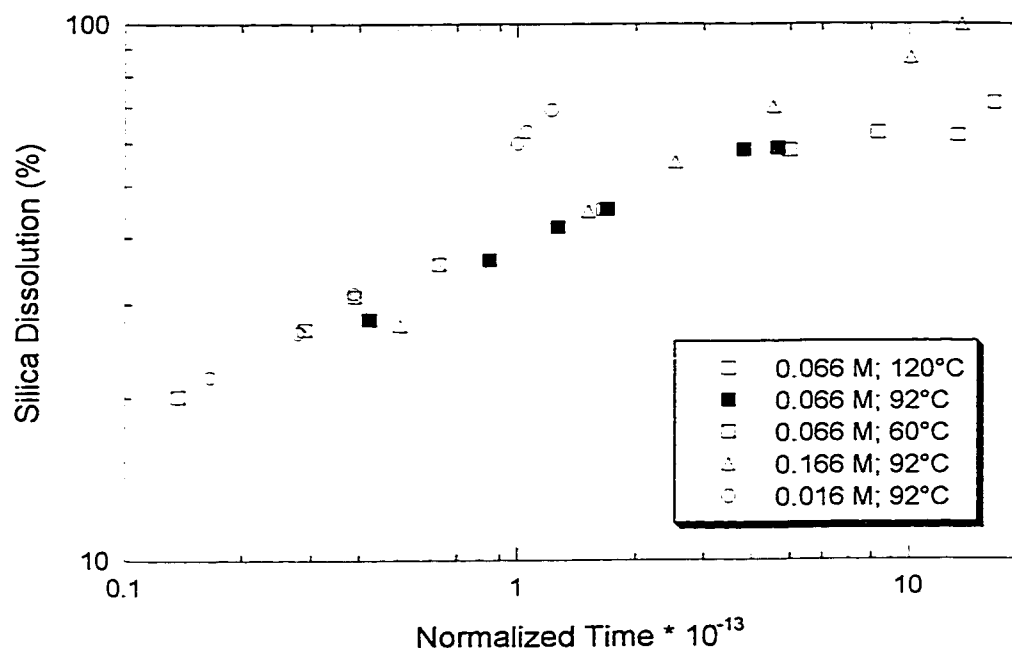


Figure 4.4: Collapsed Glass Dissolution Data

Normalized Time = time (hr.) * $[\text{OH}^-(\text{M})]^{0.94} * \exp(-21.0/\text{R}(\text{kcal/mol})/T(^{\circ}\text{K}))$

Labels indicate KOH concentration corrected for EDTA.

Experiments contained 400 mL KOH; 0.8 g glass; 1.0 g EDTA acid.

4.2 EFFECT OF REACTION VARIABLES ON SORBENT FORMATION

This section presents results from experiments investigating the effects of reaction conditions on the formation of calcium silicate from lime and recycled glass. Reaction variables included initial surface area of the glass, addition of gypsum at 92°C, addition of gypsum or CaCl_2 at 120°C, and therefore also the effect of temperature, agitation, and solids / water ratio under non-agitated conditions. Each of these variables is of potential economical importance to the overall process shown in Figure 1.1. The initial surface area is a direct function of the extent of glass grinding, a relatively costly process. The other conditions of interest affect the size and complexity of the reactor and/or drying operations.

4.2.2 Effect of Initial Surface Area

Calcium silicates were prepared from three different glass samples having measured BET surface areas of 0.273, 0.381, and 0.532 m²/g, respectively. The experiments were conducted at 92°C under agitated conditions with gypsum as an additive. Figure 4.5 shows that the rate of surface area formation increased with initial surface area of the glass.

There are several options for the rate-limiting step in the formation of calcium silicate solids. One possibility is the dissolution of the silica source. However, as shown in the previous section, this most likely is not the rate-limiting process except at extremely short times. It is also known that calcium and silica cannot both maintain significant concentrations in solution before calcium silicate will precipitate. It is possible that in systems with a sufficient calcium concentration in solution (>2mM), the silica never reaches bulk solution. Instead, the silica is precipitated at the point of dissolution, on the surface of the glass. In this instance, the rate limiting step would be a diffusion process through a calcium silicate product layer covering the glass. Whether that process is the diffusion of the calcium hydroxide from solution into an unreacted core, or the diffusion of the silica oxide out through the product layer is yet undetermined. Either way, the rate of the process would be proportional to the surface area of the silica source.

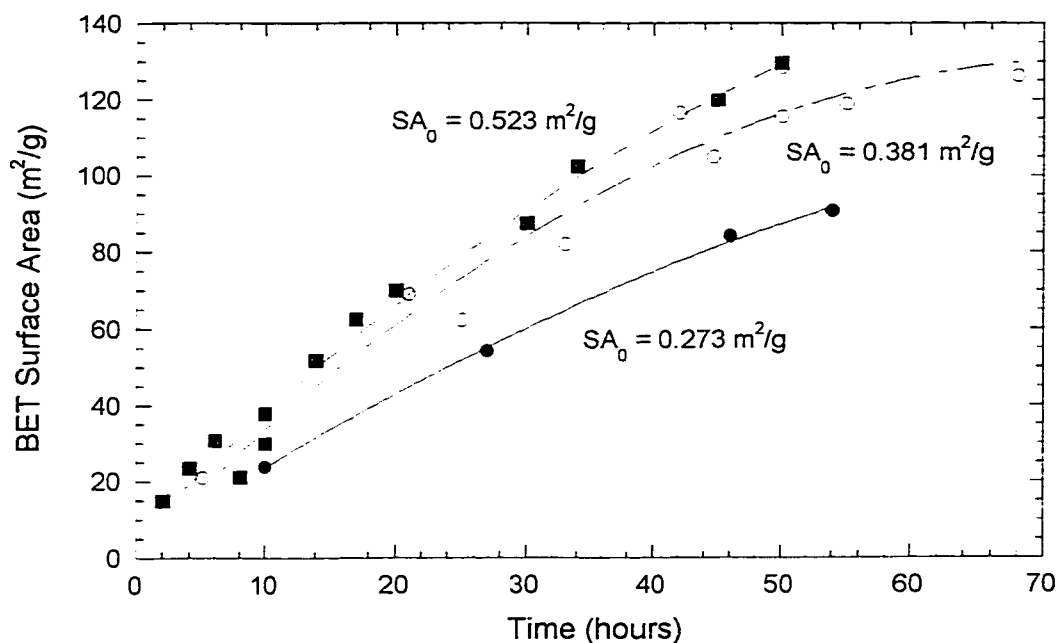


Figure 4.5: Effect of Initial Surface Area of Glass

92°C; agitated

400 mL H₂O; 40 g lime; 40 g glass; 20 g gypsum

experiments: 3/2/94; 3/5/94; 4/4/94; 11/21/94; 4/28/97; 8/22/94

By normalizing the time to a reference surface area, Figure 4.6 shows that the data presented in Figure 4.5 collapse relatively well. This supports the hypothesis that the rate of surface area formation is directly proportional to the initial surface area of the glass.

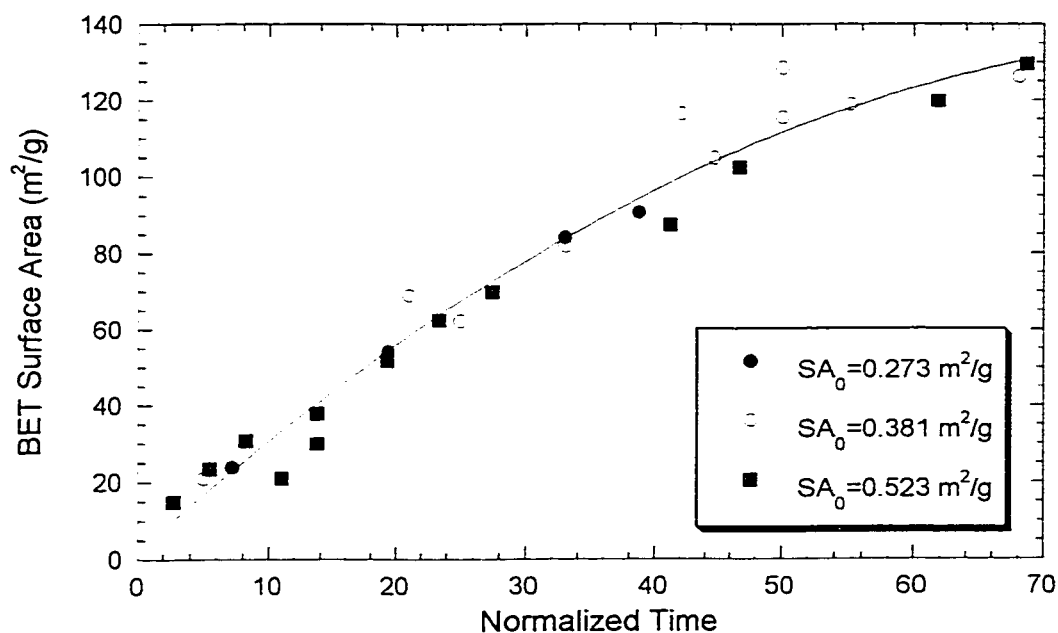


Figure 4.6: Collapse of Effect of Initial Surface Area of Glass

92°C; agitated

1/1/0.5 lime/glass/gypsum wt. ratio; 20% solids

Normalized Time = time * (SA_0/SA_{0ref}); $SA_{0ref} = 0.381 \text{ m}^2/\text{g}$.

experiments: 3/2/94; 3/5/94; 4/4/94; 11/21/94; 4/28/97; 8/22/94

4.2.3 Effect of Gypsum at 92°C

While hydrated lime and silica are the primary reactants of interest, it has been shown that adding other compounds to the reaction slurry, such as gypsum or calcium chloride, produced sorbents from flyash with increased surface area and SO_2 reactivity (Kind, 1994; Kind et al., 1994; Peterson, 1990). In order to have a baseline without gypsum for comparison, agitated experiments with 1.00 g lime / 1.00 g glass / 0 g gypsum and 20% solids were run at 92°C. Figure 4.7 shows that the rate of surface area formation decreased by 10 hours of reaction time, when the concentration of calcium in solution decreased below 1 mM as shown in Figure 4.8. The calcium concentration change was also accompanied by a pH change from 12.3 to 13.0.

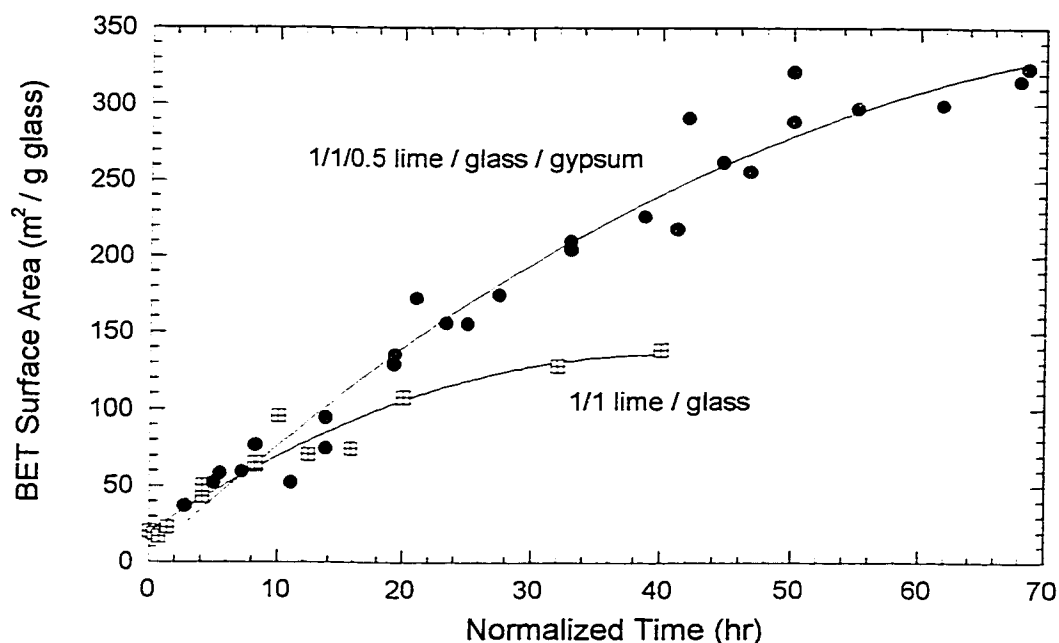


Figure: 4.7: Effect of Gypsum on Surface Area at 92°C

agitated; 20% solids; Labels indicate weight ratios.

Normalized Time = time * (SA₀/SA_{0ref}); SA_{0ref} = 0.381 m²/g.

The results seen in this experiment are similar to those found from experiments with fly ash. The drop in the rate of product formation was attributed to the "calcium effect" seen by Kind (1994). It was concluded that potassium released during the dissolution of the fly-ash associated with available hydroxide. As the potassium hydroxide concentration increased, the pH increased, and the equilibrium concentration of calcium, as determined by the solubility of Ca(OH)₂, decreased below the amount necessary for the formation of high surface area CSH to proceed at an appreciable rate.

Glass does not contain a significant amount of potassium (Table 3.1), however, the portion of sodium is appreciable. As sodium is released from the glass, the sodium hydroxide concentration in the solution increases, and the dissolved calcium concentration decreases. This common-ion effect is represented

by Equations 4.5-6. This solution effect was also observed in the fly ash system with the addition of NaOH (Peterson and Rochelle, 1988).



Gypsum ($\text{CaSO}_4 \cdot \text{H}_2\text{O}$) has been added to the reaction mixture to counter the "calcium effect" caused by the release of sodium. Kind (1994) showed gypsum to be an effective additive in the case of flyash/lime systems at 92°C. The presence of a gypsum solid phase produced an increased calcium concentration over the duration of the experiment, in addition to providing sulfate ion for potassium to associate with. It is thought that this allowed for a higher reaction rate, producing solids with much higher surface area than systems without gypsum.

The same effect was seen in glass/lime systems. Equation 4.7 shows how gypsum diminishes the impact of the sodium on solution pH and calcium concentration. Figure 4.8 shows that the concentration of calcium in solution remained between 8 and 20 mM over 50 hours when gypsum phase was added to the reaction. Taylor (1964) stated that a calcium concentration between 1 and 20 mM is necessary to produce the CSH solid phase with a Ca/Si ratio of ~1.0 - 1.5 (Figure 2.3), believed to be one of the desired, high surface area phases. A product prepared after 50 hours with gypsum present was analyzed by selective dissolution and found to have a Ca/Si ratio of 1.5 (Appendix B). The pH in solution also remained below 13 for the system with a gypsum phase, even though the sodium concentration increased over the course of the reaction as shown in Figure 4.9. It is evident from Figure 4.9 that the release of sodium, within the scatter of the data, is not affected by the presence of gypsum.

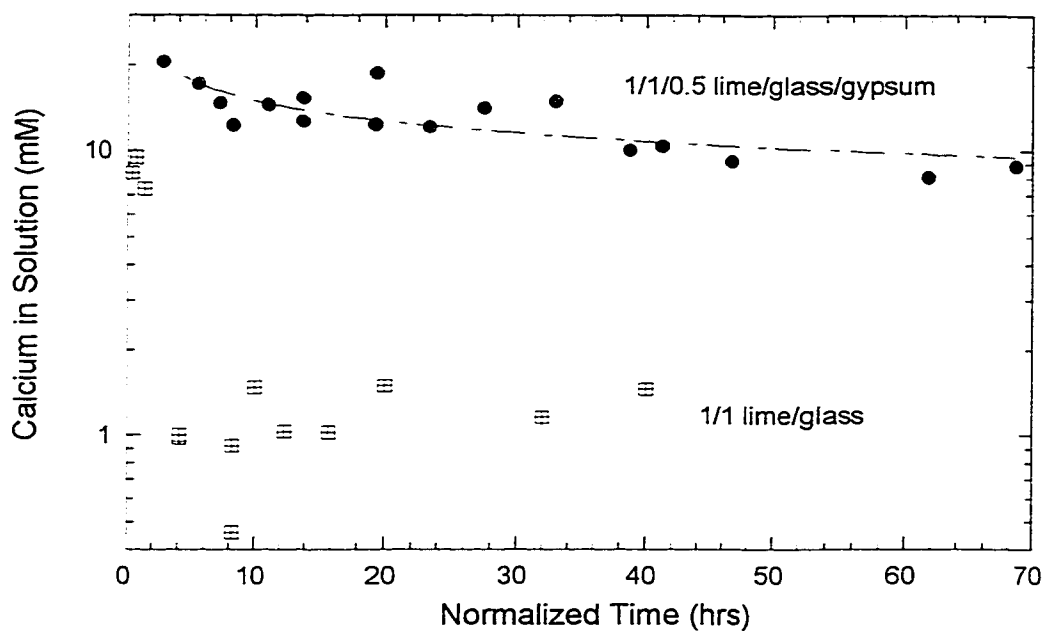


Figure 4.8: Effect of Gypsum on Calcium in Solution

92°C; agitated; 20% solids; Labels indicate weight ratios.

Normalized Time = time * (SA_0/SA_{0ref}); $SA_{0ref} = 0.381 \text{ m}^2/\text{g}$.

While it might seem counterproductive to buffer the solution pH, the results clearly indicate that this was beneficial. A certain hydroxide level was required for the dissolution of silica, however, a pH above ~13 depressed the solubility of Ca^{+2} . A balance between pH 12 and 13 seemed to work best.

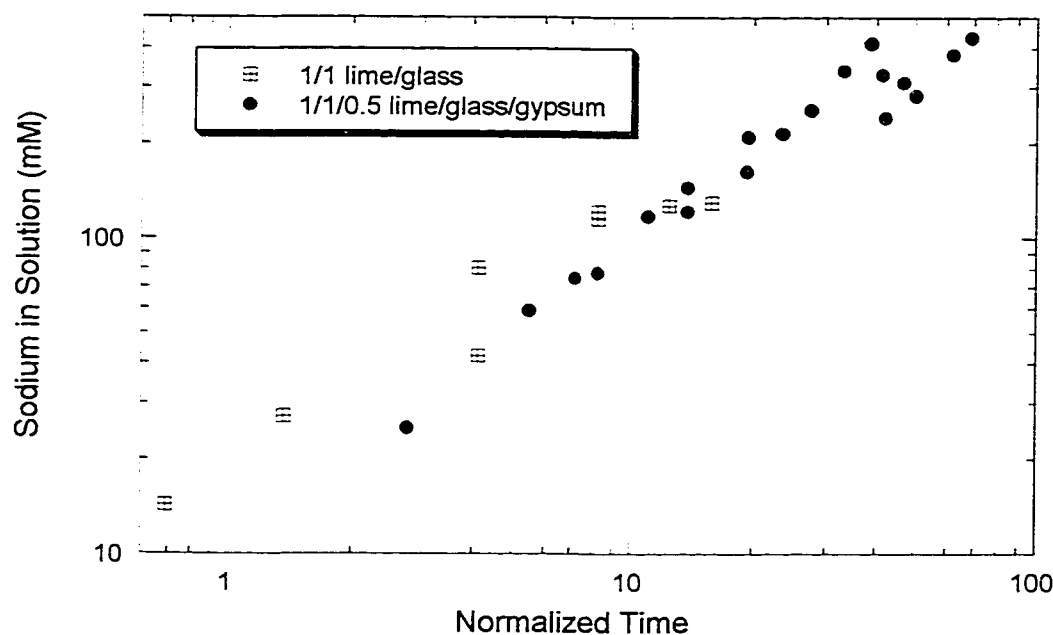


Figure 4.9: Release of Sodium from Glass

92°C; agitated; 20% solids; Labels indicate weight ratios.

Normalized Time = time * (SA_0/SA_{0ref}); $SA_{0ref} = 0.381 \text{ m}^2/\text{g}$.

4.2.4 Effect of Gypsum and CaCl_2 at 120°C

Experiments were conducted at 120°C without any additives (lime and glass alone), with gypsum, and with calcium chloride. Since the additives were intended to buffer any solution effects of sodium released from the glass, the total solids content of each experiment was altered to maintain a constant glass/water ratio. The formation of surface area is shown in Figure 4.10.

It is evident from Figure 4.10 that the initial rate of surface area formation increased with temperature regardless of the presence of additives. This was expected, as the reaction was presumed to be rate-limited by either the dissolution of the glass or diffusion through a precipitated product layer as discussed in Section 4.1.3. Both of these rates would increase with temperature. However, the formation of surface area slowed dramatically after 8 hours. The addition of gypsum or calcium chloride additives appeared to increase the ultimate surface

area over the reaction without any additives, though these reactions also slowed significantly. Furthermore, the reaction at 92°C with gypsum present continued to form surface area past 300 m²/g, far beyond the reactions at 120°C.

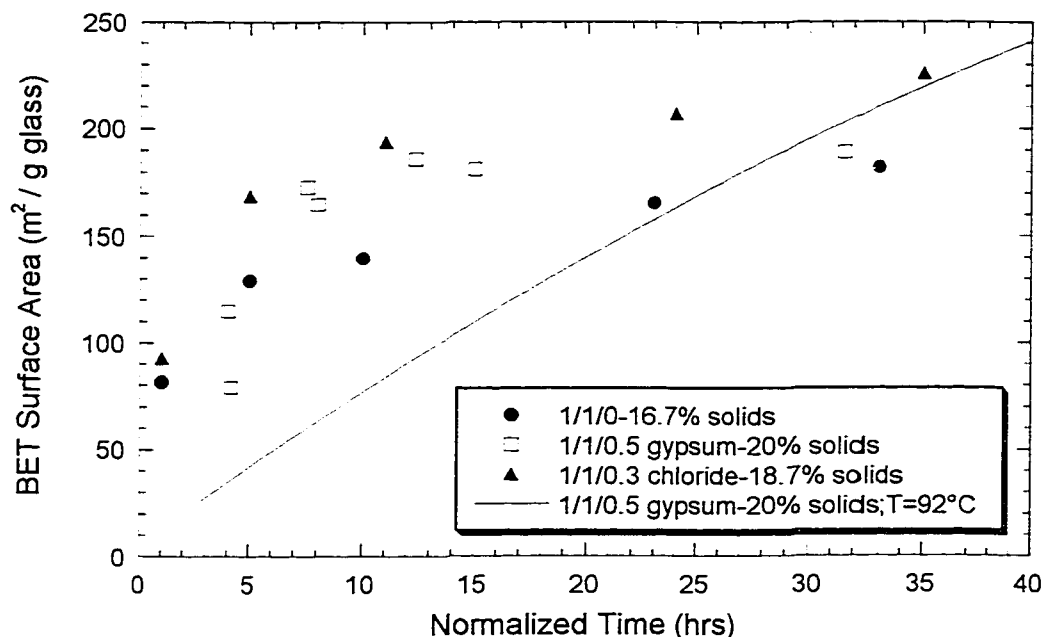


Figure 4.10: Surface Area Formation at 120°C

agitated; 400 mL water;

1/1 lime/glass: 40 g lime / 40 g glass

1/1/0.5 lime/glass/gypsum: 40 g lime / 40 g glass / 20 g gypsum

1/1/0.3 lime/glass/chloride: 40 g lime / 40 g glass / 12 g CaCl₂

Normalized Time = time * (SA₀/SA_{0ref}); SA_{0ref} = 0.381 m²/g.

The surface area behavior of the three systems at 120°C were not directly correlated with the calcium concentration (Figure 4.11). The calcium concentration for the system without additives decreased to ~1 mM within the first 10 hours of reaction. The addition of gypsum maintained a slightly higher concentration at early times, but also decreased within 8 hours. This drop can be explained, in hindsight, by the low solubility of calcium sulfate at 120°C. Though gypsum (CaSO₄·2H₂O) was added, above 42°C the anhydrous form of calcium

sulfate is less soluble and therefore preferred (Hill, 1937). Unfortunately, the solubilities of both phases also decrease with increasing temperature. The system with calcium chloride added maintained a relatively large calcium concentration over the period tested, yet the rate of surface area formation decreased substantially.

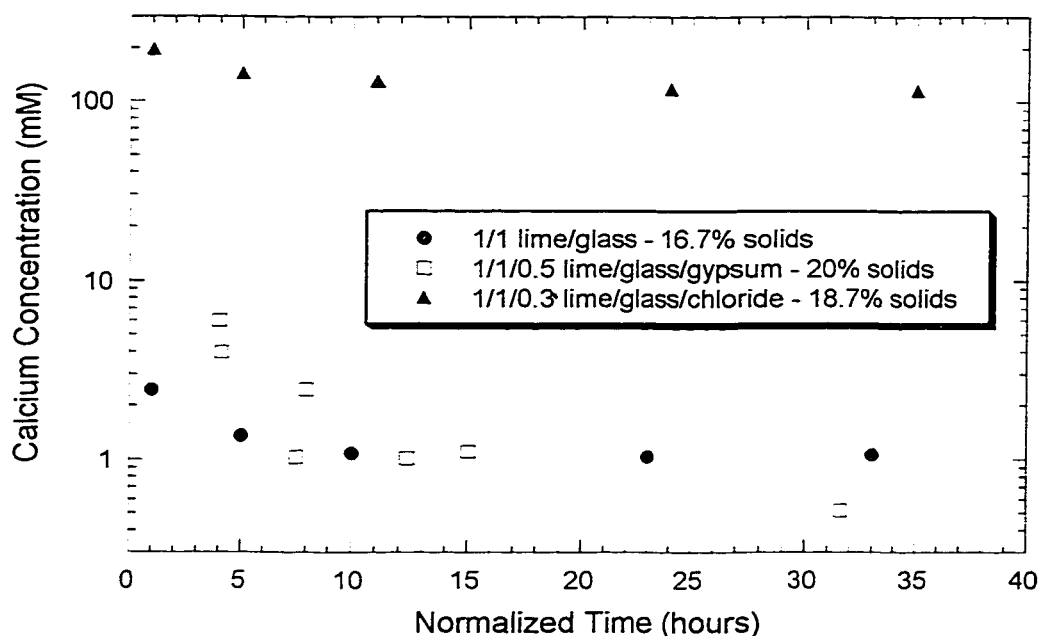


Figure 4.11: Calcium Concentration in Slurry Solution at 120°C

agitated; 400 mL water;

1/1 lime/glass: 40 g lime / 40 g glass

1/1/0.5 lime/glass/gypsum: 40 g lime / 40 g glass / 20 g gypsum

1/1/0.3 lime/glass/chloride: 40 g lime / 40 g glass / 12 g CaCl_2

Normalized Time = time * ($\text{SA}_0/\text{SA}_{0\text{ref}}$); $\text{SA}_{0\text{ref}} = 0.381 \text{ m}^2/\text{g}$.

A possible explanation is that a calcium silicate hydrate solid phase with a lower specific surface area than CSH-I is being formed at the higher temperature. According to Taylor (1964), the desired CSH-I phase is formed when the calcium concentration is between 1 and 20 mM, and the temperature is below 100°C. Above 100°C it is more likely to form more crystalline species.

Figure 4.12 shows X-ray diffraction patterns for solids formed at 92°C with gypsum, and at 120°C with either gypsum or calcium chloride added. The two sorbents produced at 120°C exhibited the characteristic CSH humps, however the patterns also appeared to be more crystalline in nature, especially the sorbent prepared with gypsum. This supports the hypothesis that a phase other than near amorphous CSH-I was also being produced at 120°C. Though a different solid phase may explain a lower than expected surface area, a lower reactivity with SO₂ or other acid gases should not be assumed. The aluminum peaks are caused by the X-ray diffractometer sample holder, not the sorbent.

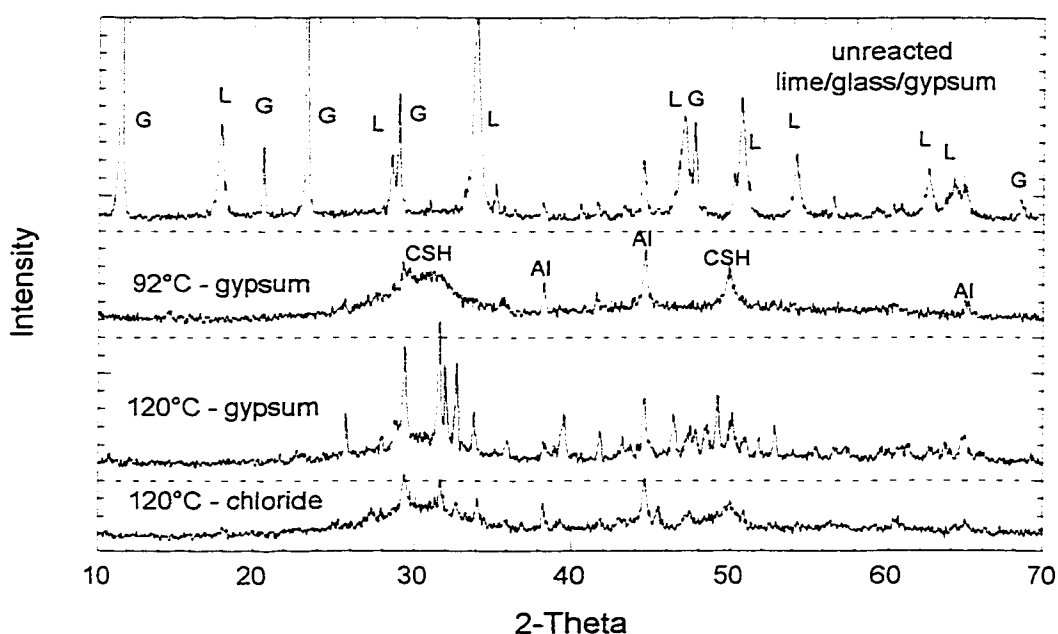


Figure 4.12: X-ray Diffraction Patterns of Sorbents Prepared at 120°C

unreacted sample: 1/1/0.5 lime/glass/gypsum

92°C-gypsum: 11/21/94-25; SA=62 m²/g

120°C-gypsum: 12/6/94-15; SA=72 m²/g

120°C-chloride: 9/19/96-24; SA=90 m²/g

for details regarding samples, see Appendix B

L: hydrated lime (portlandite) peaks; G: gypsum peaks

Figure 4.13 shows the release of sodium as product surface area is formed for agitated samples at all conditions. As the glass is dissolved over time to form calcium silicates, the sodium present in the glass is released. This fact should be independent of the conditions of the reaction slurry. While there is substantial scatter in the longer time data, the general trend follows as expected.

The sodium from the glass provided non-trivial amounts of alkalinity. The sample prepared with gypsum present at a recipe of 1/1/0.5 (4/28/97-50) had a measured alkalinity of 6.6 mmol/g compared to hydrated lime with 13.09 mmol/g. In this case, the sodium from the glass accounted for 21% of the alkalinity. In other words, each gram of glass contributed alkalinity equivalent to 0.26 g Ca(OH)_2 .

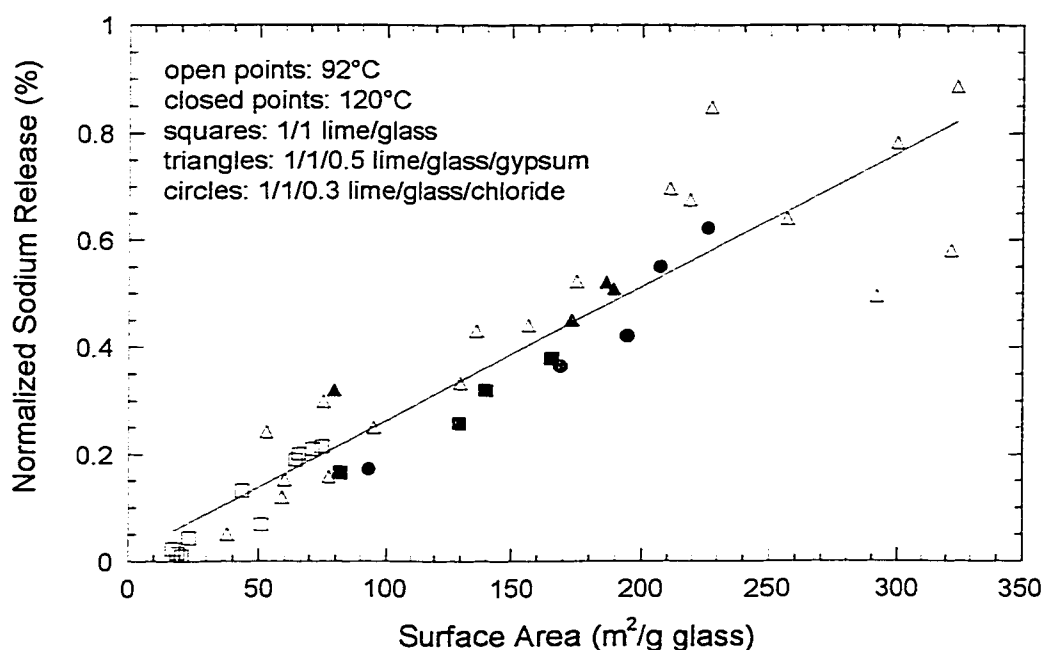


Figure 4.13: Release of Sodium from Glass

Normalized Sodium: measured solution concentration / total sodium in glass.

Total sodium = 0.1124 g Na / g glass (Acurex, 1996).

Normalized Time = time * ($\text{SA}_0/\text{SA}_{0\text{ref}}$); $\text{SA}_{0\text{ref}} = 0.381 \text{ m}^2/\text{g}$.

4.2.5 Effect of Agitation

The effect of agitation was measured with sorbents prepared from lime and glass with gypsum present. Figure 4.14 presents the surface area formation of solids prepared with and without agitation. It was shown that for surface areas below $\sim 200 \text{ m}^2/\text{g}$ glass ($80 \text{ m}^2/\text{g}$), agitation did not affect the rate of surface area formation. Above that surface area, agitation provides a significant positive effect.

The ability to prepare sorbents without mechanical agitation would be economically beneficial to the ADVACATE process shown in Figure 1.1. A non-agitated reactor would be both cheaper and easier to maintain. The results clearly indicate that if sorbent of $80 \text{ m}^2/\text{g}$ is sufficient for the particular application, then non-agitated preparation is adequate.

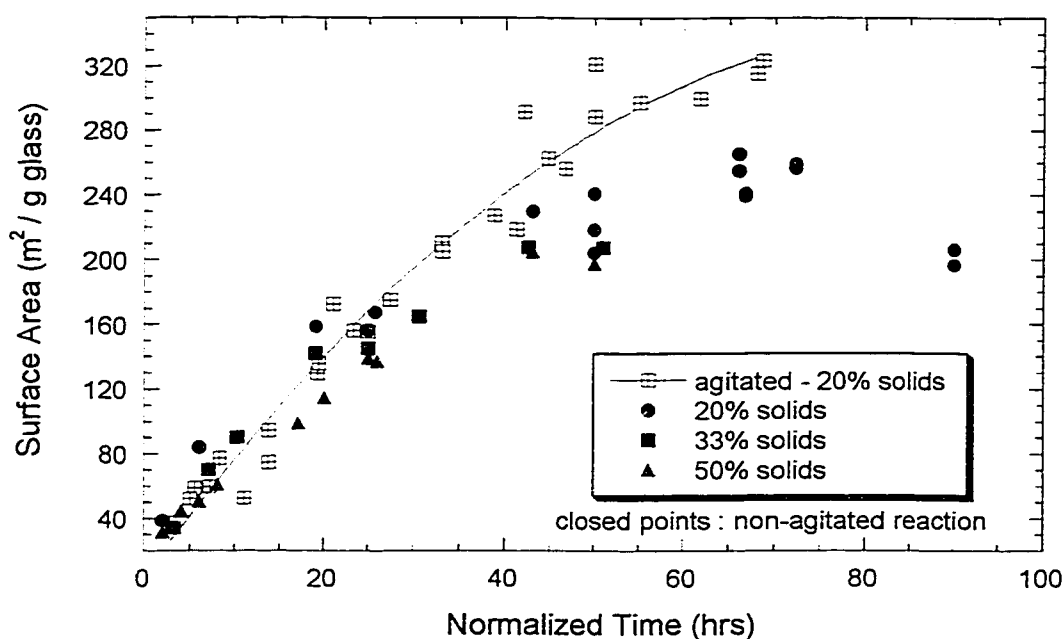


Figure 4.14: Effect of Non-agitation on Surface Area

92°C; 1/1/0.5 lime/glass/gypsum weight ratio

% solids = solids / (water+solids) * 100

Normalized Time = time * (SA₀/SA_{0ref}); SA_{0ref} = 0.381 m²/g.

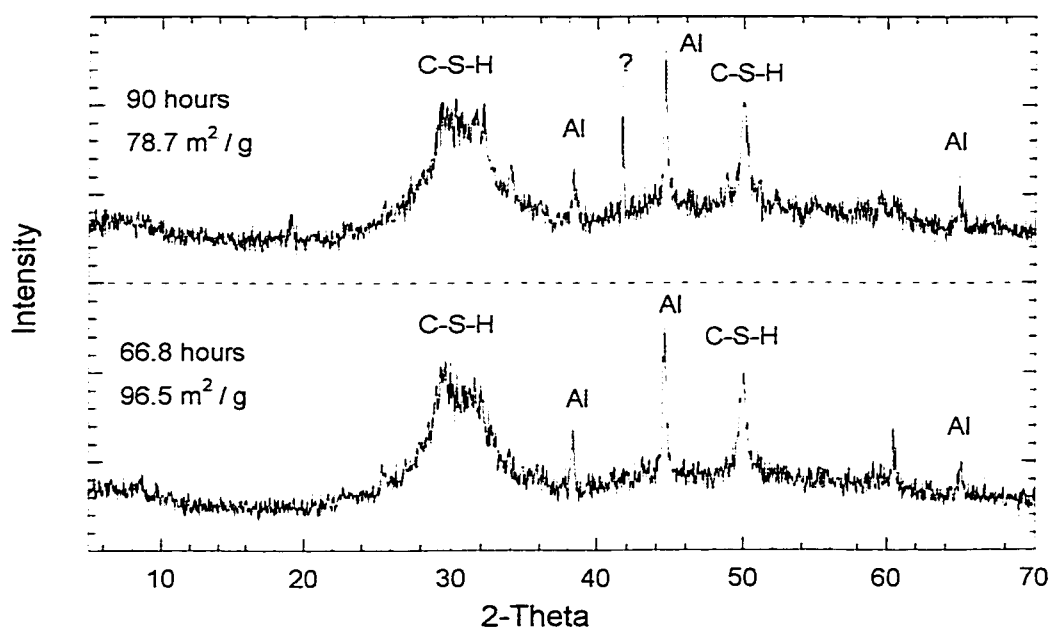


Figure 4.15: X-ray Diffraction Pattern of Non-agitated, Long Time Solids

non-agitated; 92 °C; 4 mL water; 0.4 g lime; 0.4 g glass; 0.2 g
gypsum
samples: 4/7/97-66.7a; 4/7/97-90a

The decrease in surface area noticed at very long times under non-agitated conditions is not fully understood. It is possible that this was an experimental anomaly, as both samples came from the same experiment (4/7/97-90a and 90b). Kind (1994) also observed occasions where solids prepared at long CSTR residence times (>16 hours) were lower than those prepared with shorter residence times. He attributed that loss of surface area to the nucleation and precipitation of a different, lower surface area, solid phase. X-ray diffraction patterns were measured for the non-agitated, long time sample. It was expected that if a solid phase with a lower specific surface area was forming, that it would most likely also be more crystalline. Figure 4.15 shows the X-ray diffraction patterns for non-agitated samples with 67 and 90 hours of reaction time. While there was an

unidentified peak at 90 hours, it is not evident from the patterns that there considerable crystallinity formed.

4.2.6 Effect of Solids/Water Ratio in Non-agitated Solids

The ability to increase the solids/water ratio also would be extremely beneficial to the overall economics of the ADVACATE process by reducing the amount of dewatering and drying necessary to form a free-flowing powder. Difficulty with a high solids/water ratio arises when agitation is used. Above ~20% solids, the slurry quickly becomes viscous and paste-like. Simple agitation is not feasible. While paste agitation is available, non-agitated paste formation would be most ideal.

Figure 4.14 also shows the effect of solids/water ratio on the rate of surface area formation. Between 20% (slurry) and 50% (paste), within the scatter of the experimental data, the solids loading did not affect the surface area formation prior to 80 m²/g. After 80 m²/g, it appears that solids loading may have a small effect. But again, with the experimental scatter taken into consideration, the effect is not notable. In other words, sorbent with 80 m²/g of surface area can be prepared with agitation at 20% solids loading, or without agitation at 50% solids loading. The later situation is clearly the more economic, both from the impact on the preparation reactor, as well as the reduced drying requirements.

4.2.7 Rinsing of Non-agitated Solids

It was hypothesized that the positive effect of agitation at longer times might be a function of pore plugging by the solution salts. Because non-agitated samples were not filtered prior to vacuum drying, any salts in solution would be precipitated on the surface of the solid. Wasserman (1992) reported that for solids made from flyash with gypsum and chloride as additives, the surface area increased moderately with rinsing.

Table 4.1 shows the BET surface area of long-time, non-agitated solids before and after rinsing with water. The solids were prepared at 92°C, with 1/1/0.5 lime/glass/gypsum by weight, and 20% solids loading. For rinsing, 0.5-2.0 g of the sample was mixed with 50 mL deionized water and stirred for 10 minutes. The slurry was then filtered through a buchner filter fitted with medium porosity

paper, and rinsed with another 50 mL of water. The solids collected on the filter paper were then vacuum dried at 90°C and 30 inHg vacuum.

Table 4.1: Rinsing of Non-agitated, Long-time Solids

Sample ID	Unrinsed SA (m ² /g)	Rinsed SA (m ² /g)	% Change
10/3/97-66a	106.2	72.46	-31.8
4/7/97-67	57.9	71.9	24.2
4/7/97-90	55	68.9	25.3
8/7/97-50	81.7	108.1	32.3
8/7/97-50	81.4	107.9	32.6
9/17/97-72.25a	103.7	106.9	3.1
9/17/97-72.25c	102.7	68.52	-33.3

It is evident from Table 4.1 that clear results regarding the effect of rinsing were not obtained. It is possible that the procedure for re-wetting and re-drying of the solids caused unknown structural changes to the solids.

4.3 SORBENT CHARACTERIZATION

This section covers measurements made on silicate solids prepared from recycled glass in an effort to better understand the effects of the preparation system on the final sorbent characteristics.

4.3.1 X-Ray Diffraction

Powder X-ray diffraction patterns of a variety of sorbents at different stages of preparation were measured. The objective was to qualitatively observe changes in the solids, and any effects caused by reaction conditions.

Figure 4.16 shows the diffraction patterns for unreacted glass, lime, and gypsum. The crystallinity of the lime and gypsum were clearly in contrast with the amorphous 'hump' of the glass. When these three compounds were mixed, the glass hump all but disappeared under the strong peaks of the lime and gypsum. This can be seen in the first (bottom) pattern in Figure 4.17.

Figure 4.17 presents the evolution of the 1/1/0.5 lime/glass/gypsum product through the course of the agitated aqueous reaction. The diffraction patterns were of solid products from increasing reaction times, and therefore increasing surface area.

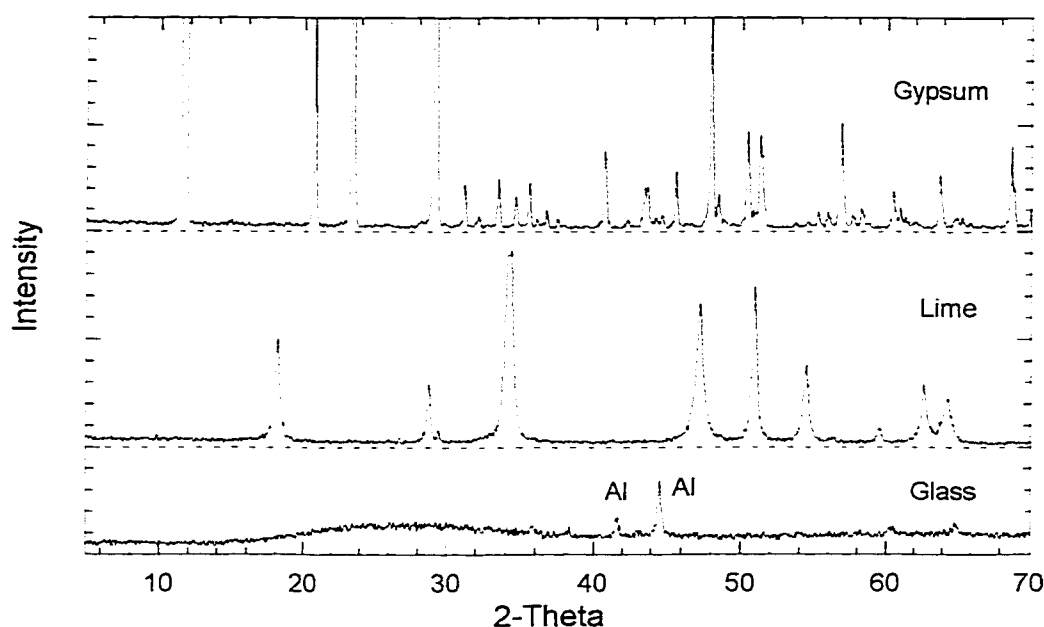


Figure 4.16: X-ray Diffraction Pattern: Fresh Reactants

glass: ground recycled glass (0.381 m²/g)

lime: Ca(OH)₂ - Mississippi Rotary Hydrate

gypsum: CaSO₄•2H₂O - Sigma Chemicals

Aluminum peaks are caused by diffractometer, not sample.

Lime and gypsum peaks have been truncated.

The amount of gypsum used in the experiment was determined to be in excess of the amount of sodium present in the glass. However, it is clear from Figure 4.17 that the gypsum solid phase was no longer present at very low surface areas, or reaction times. This was unexpected as the solution composition results presented in Section 4.2.3 indicated that gypsum was positively affecting the calcium concentration throughout the reaction. It was assumed that the benefit of gypsum over another calcium source was due to the buffering capabilities from moderate dissolution of a solid phase in equilibrium. The peaks at ~15, 26, 32, and 49 2-Theta are indicative of both an anhydrous form (PDF# 43-606) and a hemi-hydrated form (PDF# 45-848) of calcium sulfate (JCPDS, 1997). Hill (1937)

states that the anhydrous is the more stable form above 42°C. Therefore, it is clear that the gypsum converted to a hemi-hydrate or anhydrous phase, though which of the two was not clear.

Figure 4.17 also shows the depletion of the lime solid phase at ~54 m²/g. However, even without a lime solid phase, the system continued to react to produce a higher surface area product.

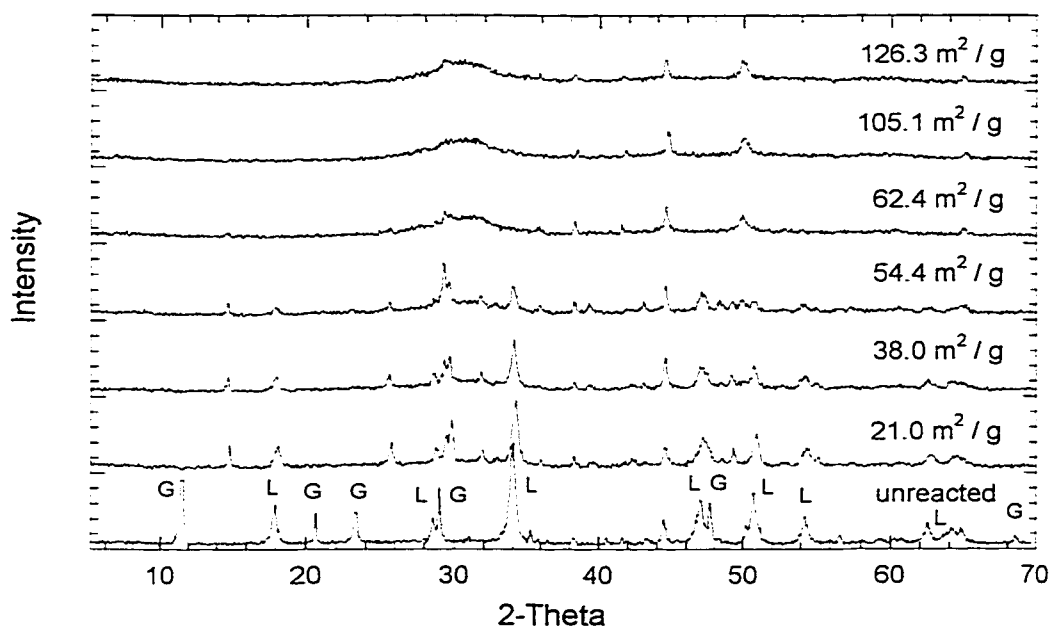


Figure 4.17: X-ray Pattern: Disappearance of Gypsum and Lime

agitated; 92 °C; 400 mL water; 40 g lime; 40 g glass; 20 g gypsum
 21.0 m²/g: 11/21/94-5; 38.0 m²/g: 3/5/94-10;
 54.4 m²/g: 8/22/94-10; 62.4 m²/g: 11/21/94-25;
 105.1 m²/g: 4/28/97-44.7; 126.3 m²/g: 4/28/97-68
 unreacted: 1/1/0.5 lime/glass/gypsum; 8.8 m²/g (calculated).
 Aluminum peaks are caused by diffractometer, not sample.
 Lime and gypsum peaks have been truncated.

Figure 4.18 presents the diffraction patterns from solids prepared with and without agitation, and at 20% and 50% solids loading. All of the samples were prepared at 92°C with gypsum present as an additive. It is evident from Figure

4.18 that these reaction conditions did not significantly affect the solid phase formed.

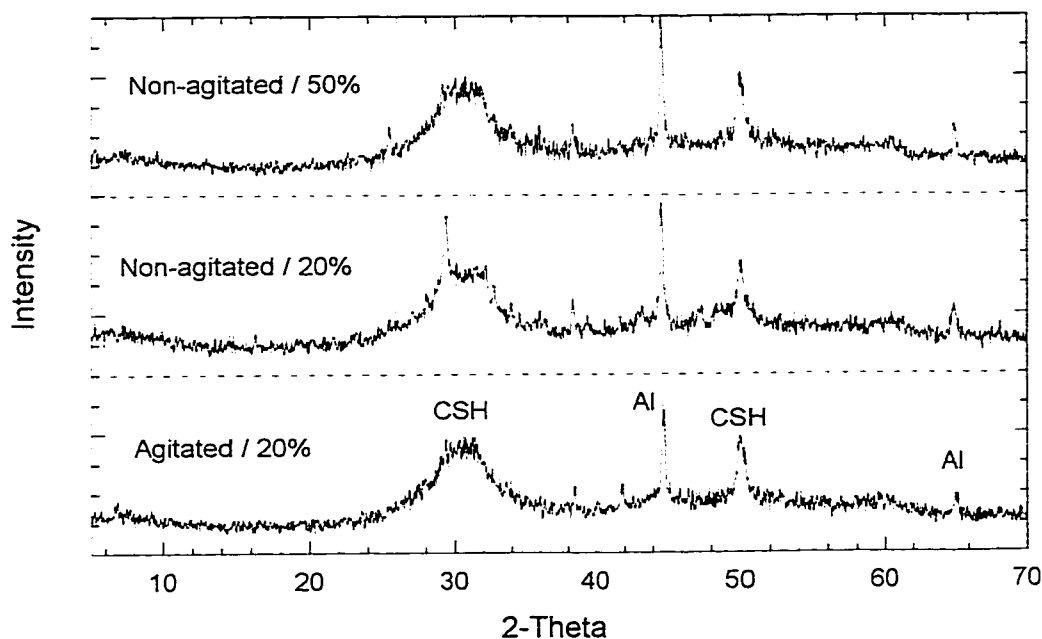


Figure 4.18: X-ray Pattern: Non-agitation and High Solids Loading

92 °C; 1/1/0.5 lime/glass/gypsum wt. ratio

agitated / 20%: 4/28/97-44.7; SA=105.1 m²/g

non-agitated / 20%: 1/22/97-43-20%; SA=92.0 m²/g

non-agitated / 50%: 1/22/97-43-50%; SA=82.0 m²/g

Figure 4.19 presents the diffraction patterns from solids prepared without any additives present, at 92°C and 120°C. The last (top) pattern presented is of a sample with a similar surface area prepared with gypsum for comparison. While not predominant, a few of the patterns showed slightly more crystallinity than that of the sample prepared with gypsum. According to the data presented in Figure 2.3 (Taylor, 1964), it might be expected that if the calcium concentration in solution dropped below 1 mM, a more crystalline phase would form. The calcium measured in solution for these particular samples ranged from 1.0-1.5 mM. Because the increased crystallinity is apparent in only some of the samples, it is

possible that a transition region between amorphous and crystalline regimes was observed. Perhaps a mixture of crystalline and amorphous phases was created.

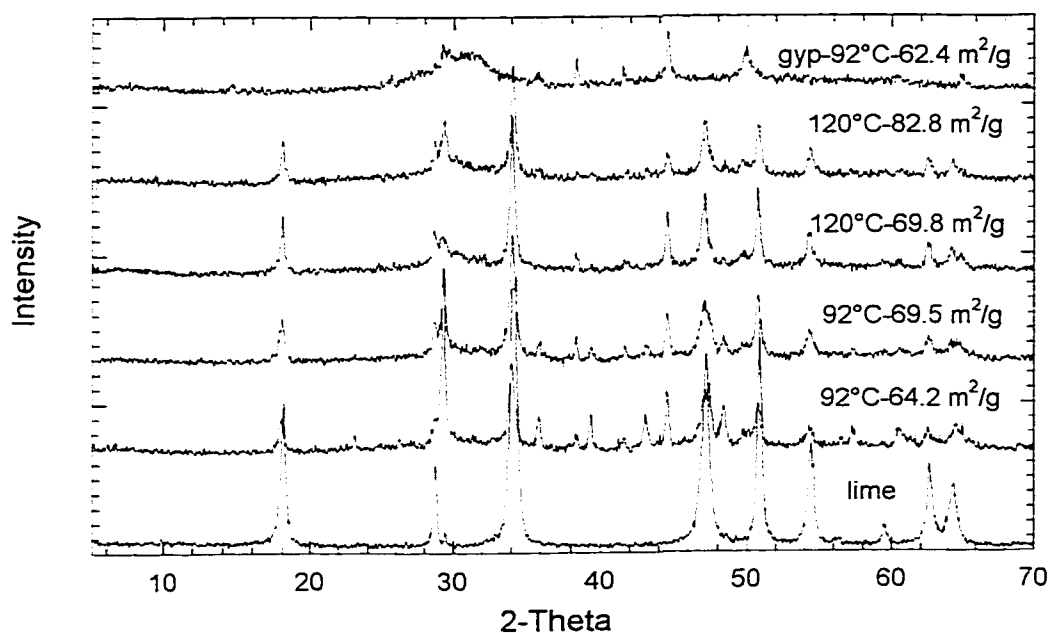


Figure 4.19: X-ray Pattern: Sorbents Prepared Without Gypsum

92°C: 64.2 m²/g: 11/28/94-32; 69.5 m²/g: 11/28/94-40
 120°C: 69.8 m²/g: 9/25/96-10; 82.8 m²/g: 9/25/96-23
 gyp/92°C: 62.4 m²/g: 11/21/94-25
 Lime and gypsum peaks have not been truncated.

4.3.2 SEM

Scanning electron micrography was also used to observe the reaction to form calcium silicate hydrates. This tool provided qualitative, visual evidence of the gross changes taking place in the solids.

The SEM picture of unreacted glass (0.381 m²/g) is shown in Figure 4.20. This sample was the fraction of glass passing through a 325 mesh sieve, and was not bounded on the smaller side. The wide particle size distribution was evident from the photo. The smooth surfaces and random edge fractures also resembled crushed glass on a larger, more familiar, scale.

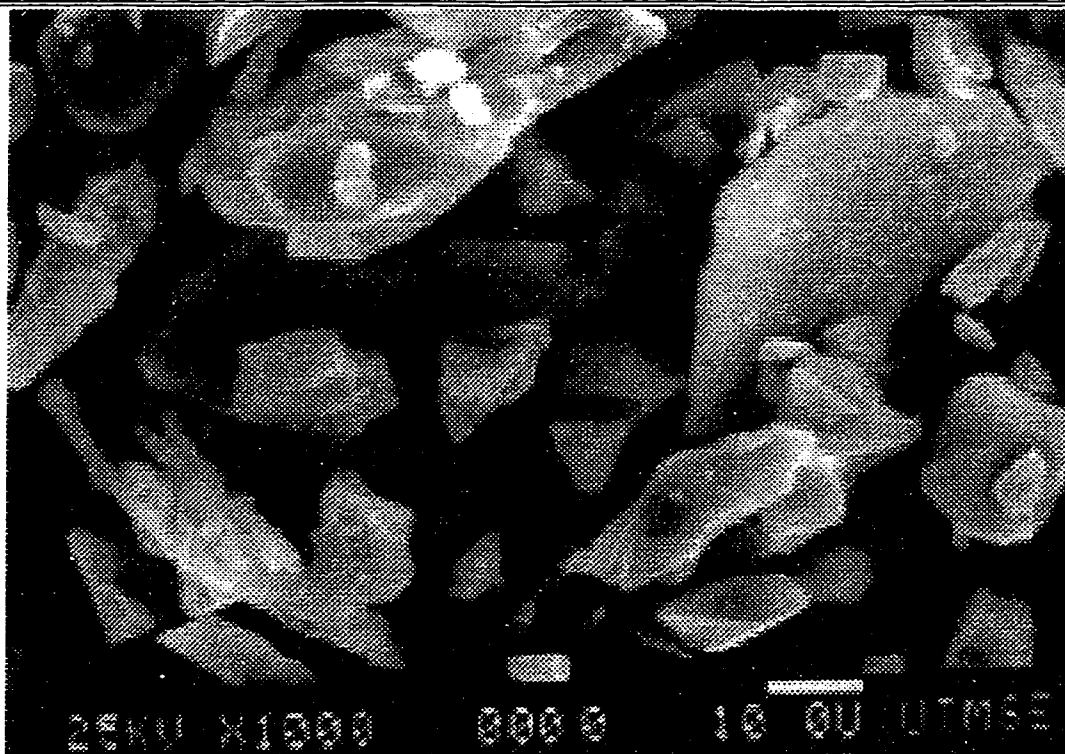


Figure 4.20: SEM: Unreacted Glass

Ground Unreacted Recycled Glass; SA=0.381 m²/g

Figure 4.21 shows a micrograph of an unreacted mixture (1/1/0.5) of lime, glass, and gypsum. The jagged glass can be seen in the central left portion of the image. The large crystal in the lower central portion of the photo was gypsum. On this scale, gypsum appeared very crystalline, while the glass had random fracture patterns. The feathery substance throughout the image was agglomerations of small lime crystals.

After 10 hours of reaction, the sorbent, now with 48 m²/g of surface area, is shown in Figure 4.22. While glass and lime are still quite visible, no gypsum crystals are apparent. Figure 4.23 shows a zoom image of a piece of glass from this sample, and the increased surface detail. It is not clear whether the surface texture is from an etched glass surface, precipitated product, or both.

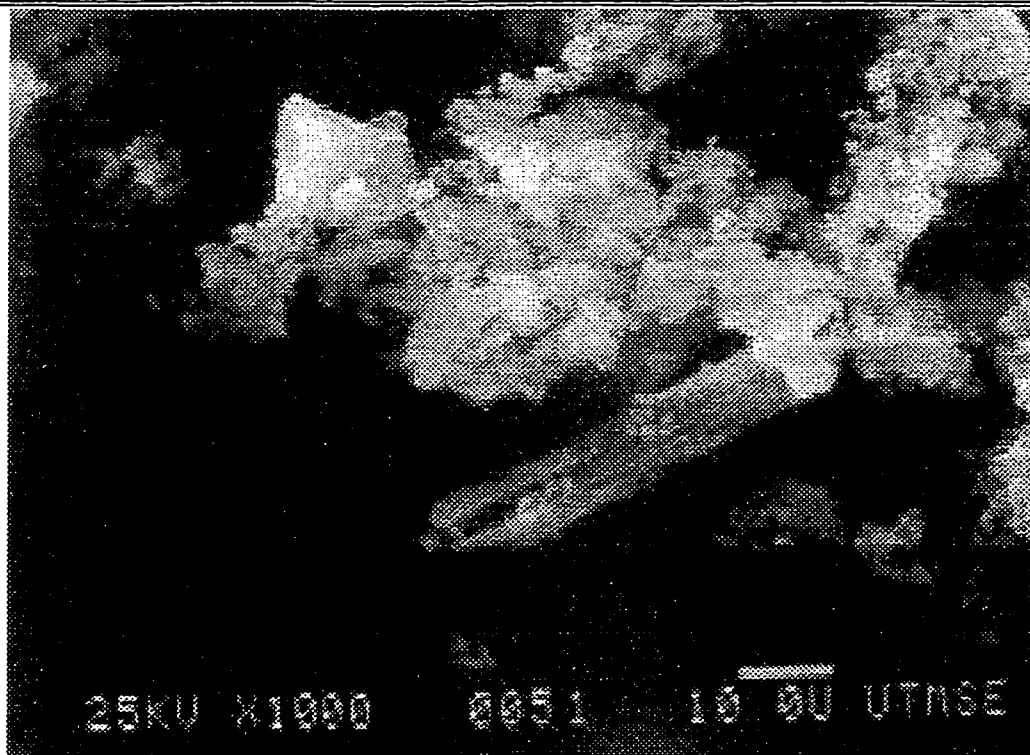


Figure 4.21: SEM: Unreacted Lime/Glass/Gypsum Mixture

1/1/0.5 weight ratio

Figure 4.24 shows the SEM photo of the reaction product after 50 hours of reaction. The solid then had a surface area of $130 \text{ m}^2/\text{g}$. The distinction between glass and lime particles is no longer clear. The smooth edged solid is presumed to be the calcium silicate product coating what used to be unreacted glass.

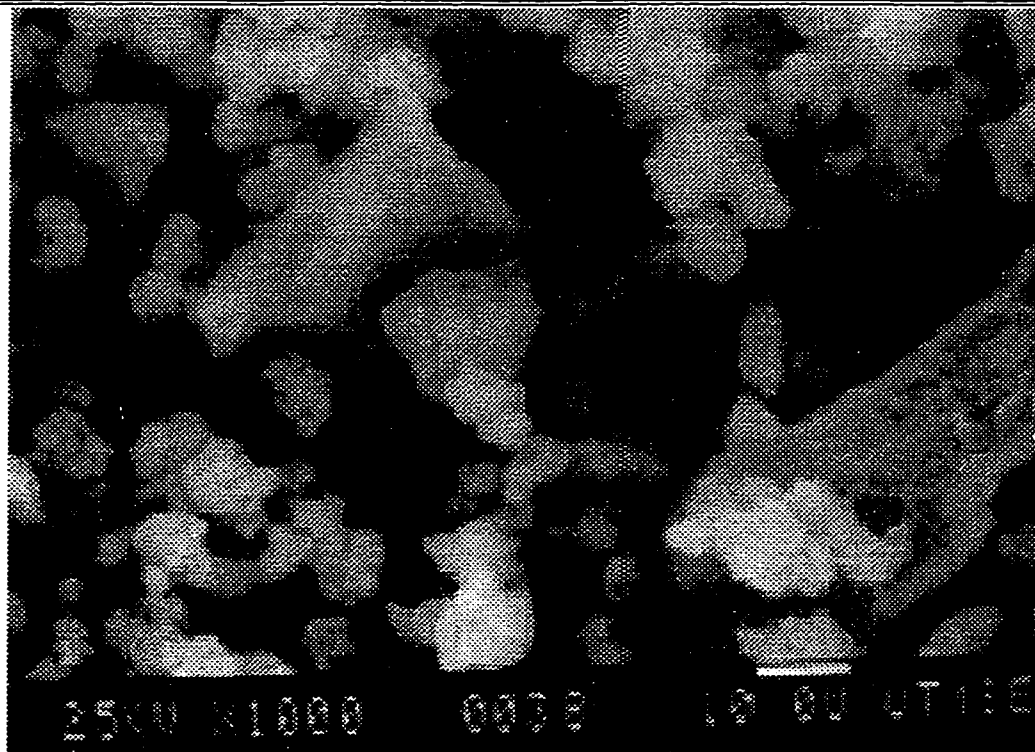


Figure 4.22: SEM: Reaction Product after 10 Hours

11/28/94-10

agitated; 92°C

1/1/0.5 lime/glass/gypsum - 20% solids

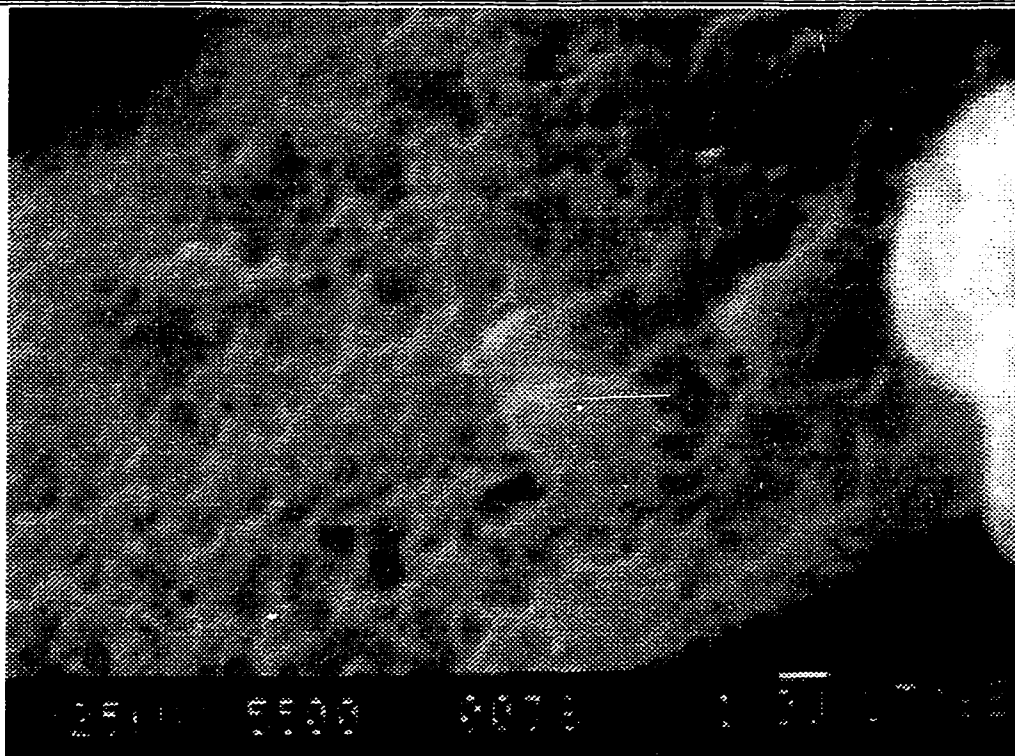


Figure 4.23: SEM: Reaction Product after 10 Hours - zoom

11/28/94-10

agitated; 92°C

1/1/0.5 lime/glass/gypsum - 20% solids

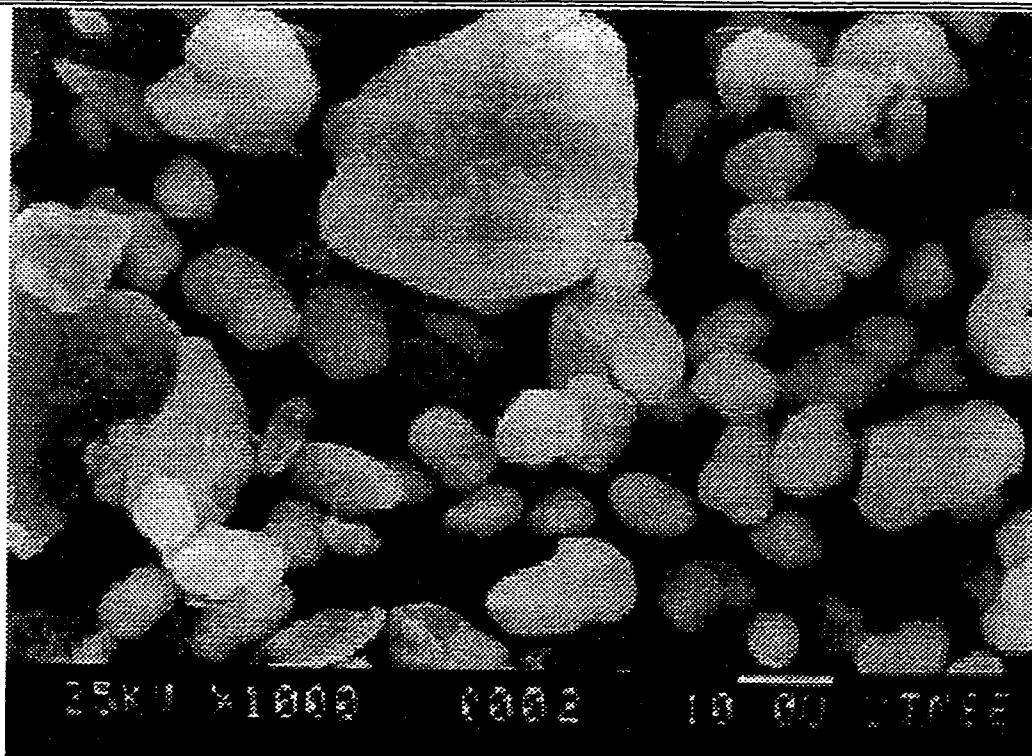


Figure 4.24: SEM: Reaction Product after 50 Hours

4/4/94-50
agitated; 92°C
1/1/0.5 lime/glass/gypsum - 20% solids

4.3.3 Surface Area Degradation

It has been known informally that the surface area of calcium silicates will degrade over time. This was not completely surprising, given the high surface areas of the solids. It was expected that the solids would degrade for a few months immediately after preparation before reaching a pseudo-steady state surface area that was more thermodynamically stable. Further degradation would probably occur at a slower rate.

Surface degradation was investigated in an effort to gain a better understanding of the feasible shelf-life of silicate sorbents. Figure 4.25 shows the degradation of the surface area for a selected sorbent. The sorbent studied for

degradation was also used for many of the experiments with SO_2 presented in Chapter 6. It is evident from Figure 4.25 that the surface area degraded consistently over the 16 month time period observed.

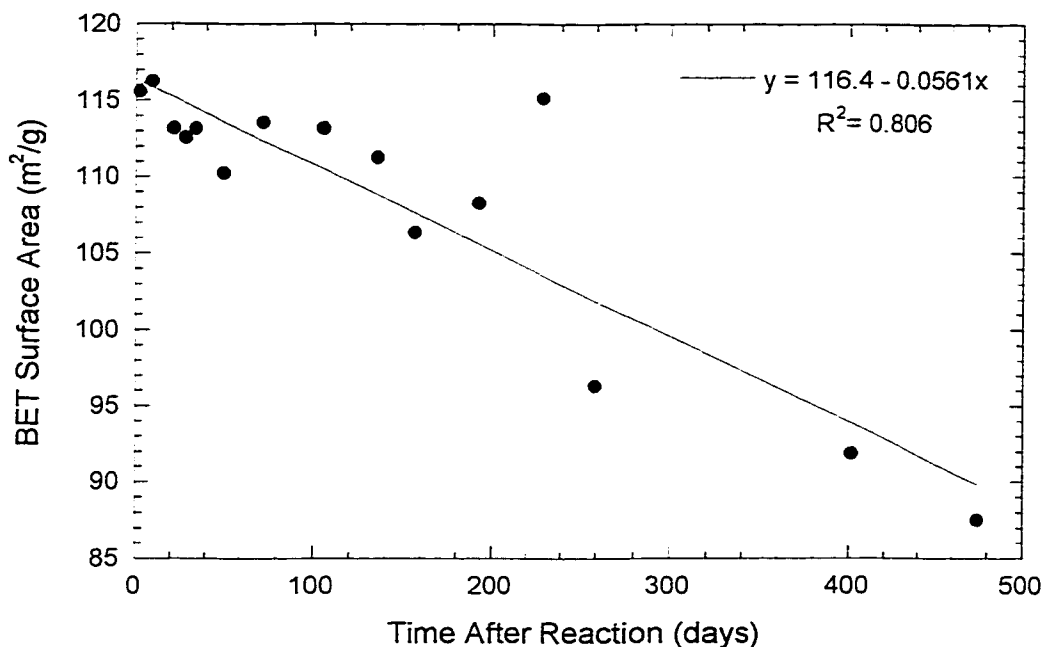


Figure 4.25: Surface Area Degradation

sample: 4/28/97-50

Other singular points were also observed for surface area degradation over the course of this work. Table 4.2 summarizes the results. The rate of degradation in Figure 4.25 is regressed at 1.68 % Area Change / month, which is fairly close to the average degradation rate of 1.60 % Area Change / month presented in Table 4.5. This rate of surface area degradation does demonstrate the need to limit shelf-life on the order of a few months.

It is hypothesized that the loss of surface area is caused by the slow transition of the solids into a more stable, more crystalline form. Figure 4.26 shows the X-ray diffraction patterns of two samples prepared by Kind (1994). The surface area details of these samples are listed in Table 4.2. While X-ray patterns

measured soon after the date of preparation were not available, it is likely that the sorbents resembled the common CSH patterns seen with glass, i.e. CSH humps with very little crystallinity. However, after 5-6 years of storage, the sorbents shown in Figure 4.26 have a significant amount of crystallinity.

Table 4.2: Surface Area Degradation of Sorbents

Sample ID	Original BET (m ² /g)	Second BET Date	Second BET (m ² /g)	%Change	%Change / months
8/18/92-4*	129	8/26/98	57.0	-55.8	-0.76
5/10/93-12*	120.8	8/26/98	30.8	-74.5	-1.16
4/4/94-50	129.6	9/4/98	51.8	-60.0	-1.13
11/21/94-5	21.0	2/2/98	17.8	-15.2	-0.40
11/21/94-25	62.4	10/31/97	58.2	-6.7	-0.19
12/6/94-15	72.4	3/11/98	41.0	-43.4	-1.11
9/25/96-23	82.8	5/19/98	67.5	-18.5	-0.92
1/22/97-43-20%	92.0	3/9/98	37.1	-59.7	-4.59
4/28/97-44	105.1	10/30/97	88.4	-15.9	-2.65
4/28/97-50	115.6	11/5/97	111.1	-3.89	-0.65
4/28/97-68	126.3	10/28/97	96.2	-23.8	-3.97
Average					-1.60

*Solids prepared by Kurt Kind from flyash and silica fume. (Kind, 1994)

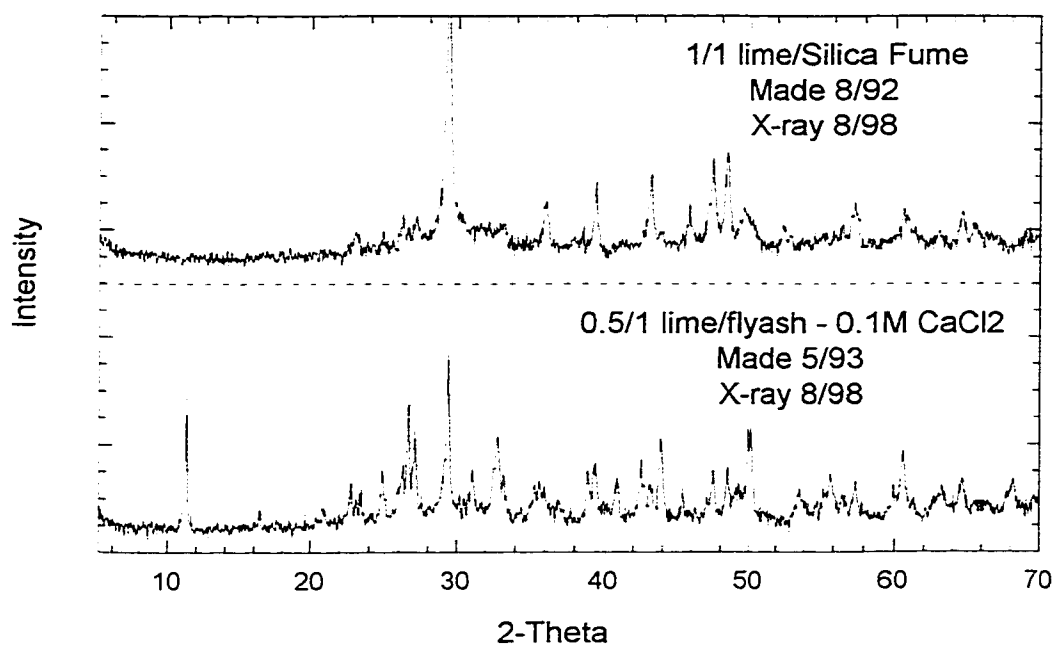


Figure 4.26: X-ray Pattern: Surface Area Degradation / Crystallinity

Samples prepared by Kind (1994).

1/1 lime/silica fume: 8/18/92-4

0.5/1 lime/flyash/0.1M CaCl₂: 5/10/93-12

Chapter 5: Calcium Silicate Production from Blast Furnace Slag

This chapter presents results from experiments to produce calcium silicate sorbent from lime and iron blast furnace slag. Iron blast furnace slag (slag) is similar to flyash and glass in that the silica of the solid is present as amorphous silica, and therefore available for reaction to form calcium silicates as described by Equations 4.1-3. The uniqueness of slag is in the high intrinsic calcium concentration, roughly equal parts calcium to silicon. This presents an interesting possibility: the activation of slag as an alkaline sorbent for desulfurization applications with a minimal amount of lime, thereby reducing the need to acquire (and ship) raw material.

Because the silica in slag is amorphous, just like flyash and glass, it was assumed that results pertaining to reaction conditions in those systems would also hold true with the lime/slag system. The composition of slag, however, is different than flyash and glass. Therefore, the experiments conducted with slag focused on the effects of the lime/slag recipe on the slurry and product, with the goal of creating a reactive sorbent with minimal lime.

Figure 5.1 shows the X-ray patterns for slag, glass, and silicate sorbents prepared from both. While the pattern for slag appeared slightly different than glass, it was clearly highly non-crystalline. The shift in the location of the amorphous hump was due to the different compositions of glass and slag. The silicate patterns also appeared to be very much the same, within the noise of an amorphous X-ray pattern. Again, in light of Figure 5.1 it was expected that except for some composition differences, the slag system would pattern itself after those of flyash and glass.

5.1 EFFECT OF REACTION RECIPE

This section presents the results and discussion concerning the effects of the reaction "recipe." Specifically, this means the lime/slag ratio and the addition of gypsum, CaCl_2 , H_2O_2 , FeSO_4 , or a $\text{NaSO}_3/\text{NaS}_2\text{O}_3$ mixture.

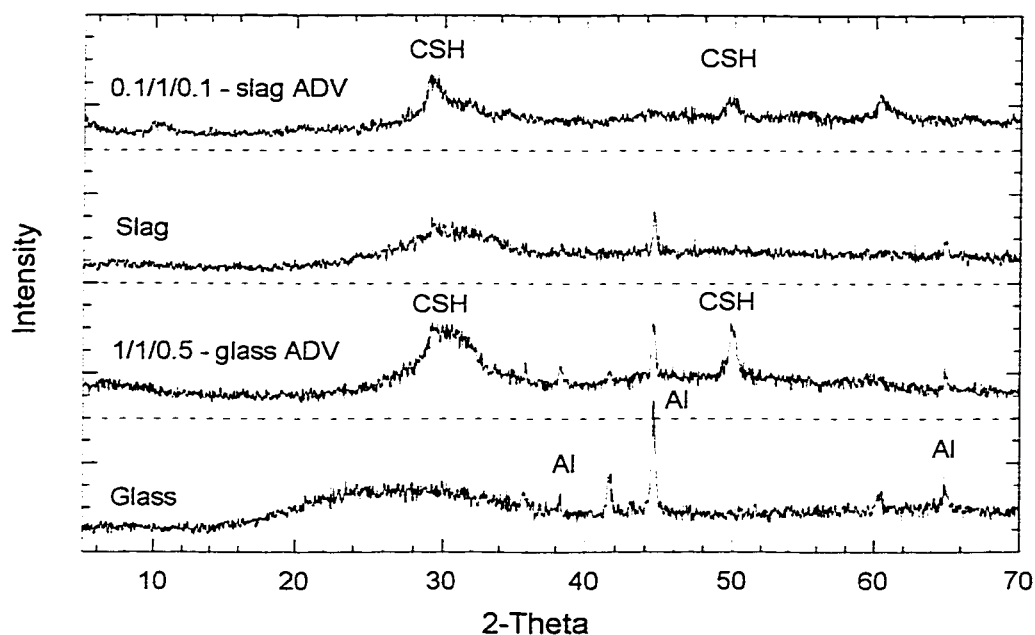


Figure 5.1: X-ray Pattern: Slag / Glass Comparison

glass: unreacted glass; SA=0.381 m²/g
 glass ADV: 4/28/97-68; SA=126 m²/g
 slag: unreacted slag; SA=3.6 m²/g
 slag ADV: 8/5/98-30; SA=139 m²/g

5.1.1 Sulfide Control

One of the more unique components in slag, as compared to flyash or glass, is sulfide. The nominal concentration of sulfide was expected to be 0-3.5 weight % (Table 3.2) of the slag. Gaseous hydrogen sulfide is a nuisance at 0.13 ppm, an irritant at 20 ppm, and dangerous at 150 ppm (Sigma-Aldrich, 1994). Therefore, it was decided that finding a suitable method of controlling the sulfide release during sorbent preparation would be useful for both bench scale and industrial applications.

Solution sulfide was measured by the potentiometric titration outlined in Section 3.1.4.3. Figures 5.2 and 5.3 show the effects of several different additives on the measured sulfide concentration and product surface area, respectively.

$\text{Na}_2\text{S}_2\text{O}_3$ and Na_2SO_3 were added with the expectation that the sulfide might convert to elemental sulfur or thiosulfate. The $\text{SO}_3^{2-}/\text{S}_2\text{O}_3^{2-}$ was added at a level of 0.1 M each at the start of the experiment. It is clear from Figure 5.2, however, that the $\text{SO}_3^{2-}/\text{S}_2\text{O}_3^{2-}$ mixture, in fact, increased the measured sulfide. Furthermore, Figure 5.3 shows a negative impact of these additives on surface area.

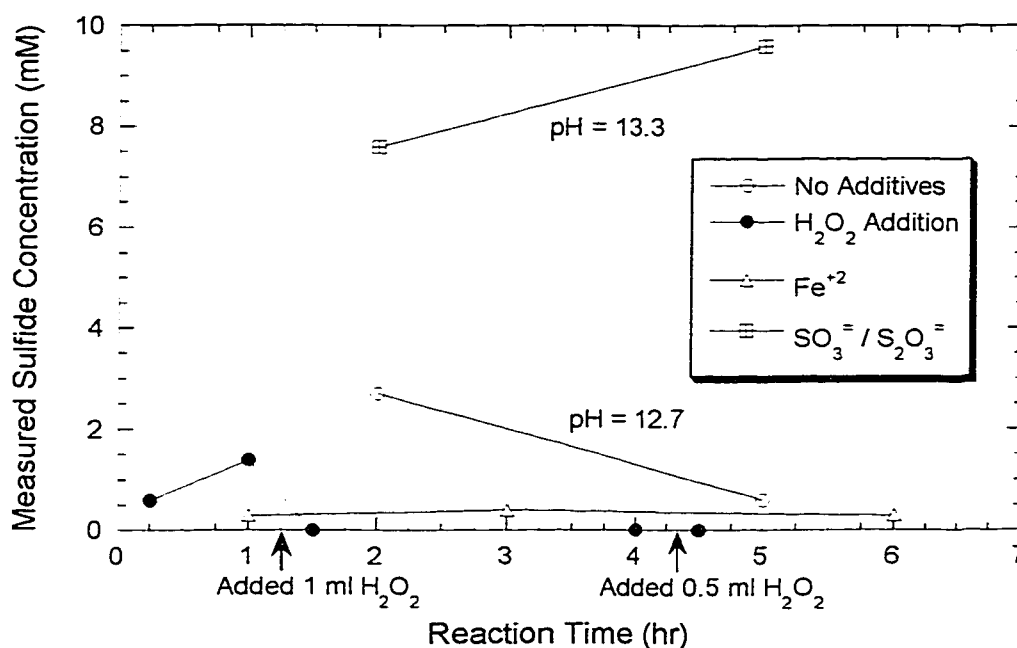


Figure 5.2: Effect of Additives on Sulfide Concentration

92°C; agitated; 400 mL water; 75 g lime; 25 g slag

H₂O₂ addition: Intermittent addition as shown on graph.

Fe²⁺: 0.13M FeSO₄•7H₂O added at start.

SO₃²⁻/S₂O₃²⁻: 0.1M Na₂SO₃ / 0.1M Na₂S₂O₃ added at start.

experiments: 5/15/98, 5/27/98, 5/29/98, 5/18/98

Figure 5.2 also shows the results from the addition of FeSO₄ at an initial level of 0.13M. It was hypothesized that the Fe²⁺ would precipitate the sulfide as FeS. While it was clear that Fe²⁺ reduced the amount of sulfide in solution, it appeared that there was an equilibrium limitation.

Hydrogen peroxide was added to the system in an attempt to oxidize the sulfide, as it was released from the slag, directly into SO_4^{2-} . The H_2O_2 was added intermittently as shown in Figure 5.2. The addition of H_2O_2 eliminated sulfide below detection, either by the electrode method or by lead acetate paper, which is claimed to have a detection limit of 25 ppm. The addition of Fe^{+2} or H_2O_2 did not significantly affect the rate of surface area formation shown in Figure 5.3.

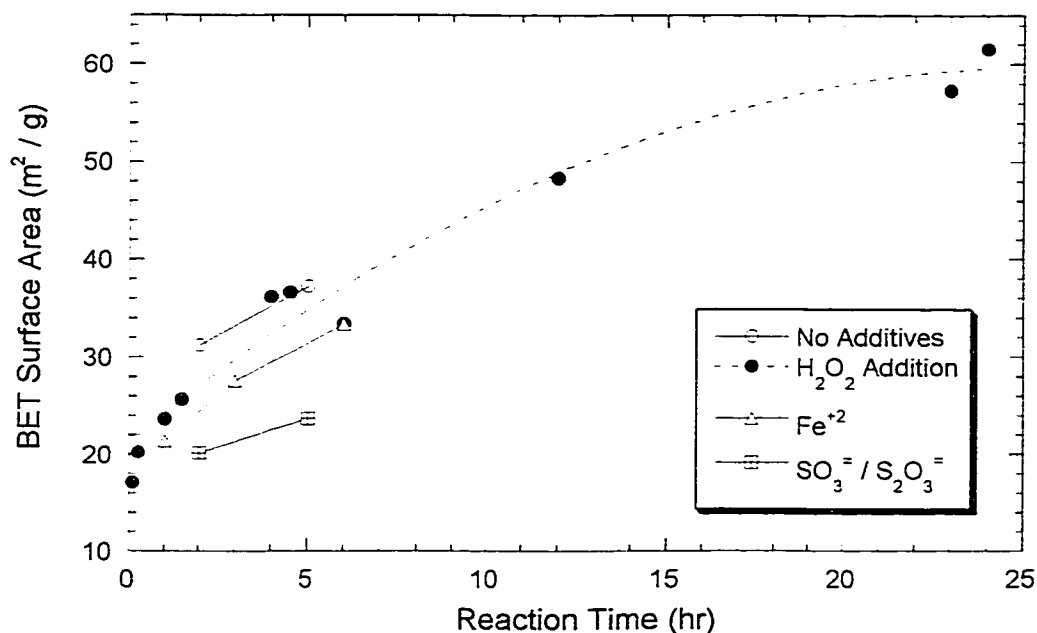


Figure 5.3: Effect of Additives on Surface Area

92°C; agitated; 400 mL water; 75 g lime; 25 g slag

H_2O_2 addition: Intermittent addition as shown on graph.

Fe^{+2} : 0.13M $\text{FeSO}_4 \cdot 7\text{H}_2\text{O}$ added at start.

$\text{SO}_3^{2-}/\text{S}_2\text{O}_3^{2-}$: 0.1M Na_2SO_3 / 0.1M $\text{Na}_2\text{S}_2\text{O}_3$ added at start.

It was decided to utilize the procedure of H_2O_2 addition for the bulk of experiments with slag. While the experiment presented in Figure 5.2 showed that 0.5-1 mL H_2O_2 was sufficient to oxidize the sulfide in solution, it was decided to use an excess of H_2O_2 during preparation experiments to ensure that the sulfide would not be evolved into the atmosphere. The reaction slurry was tested

periodically (every 1-2 hours) by lead acetate paper. If a positive reading was obtained, H_2O_2 was added in 3-5 mL increments until the lead acetate tested negative.

5.1.2 Effect of Lime/Slag Ratio

As mentioned previously, an interesting concept regarding silica sources with extremely high intrinsic alkalinity is the possibility of creating a reactive alkaline sorbent with a minimum of lime. An initial hydroxide level would be required to initiate the breakdown of the silica matrix as shown in Equation 4.2. This initial hydroxide concentration may come from added lime, sodium hydroxide, or perhaps from the dissolution of alkali from the silica itself, thereby creating a self-catalyzing effect. Once the silica matrix starts to dissolve, the intrinsic calcium, which is simultaneously dissolving, should fuel the formation of calcium silicates according to Equation 4.3.

Peterson (1987) and Peterson and Rochelle (1988) showed that high-calcium flyash could be activated for reaction without the addition of any lime. The addition of NaOH, however, increased the initial dissolution of glass, and thereby increased the SO_2 reactivity. The trade-off between the increased dissolution rates and the negative impacts of high NaOH concentrations on the calcium concentration was observed. Stroud (1991) also showed that a small amount of hydrated lime ($0.1\text{g Ca(OH)}_2 / \text{g flyash}$) would activate the high-calcium flyash.

The effect of lime/slag ratio on surface area formation was investigated in this research. Figure 5.4 shows that slag alone (0/1 lime/slag) increased in surface area from 3.6 to 25 m^2/g within the first four hours, but remained constant thereafter. The addition of lime increased the rate of surface area formation over reaction times up to 50 hours. Figure 5.4 shows that increasing the lime/slag ratio was beneficial up to a ratio of 3/1 lime/slag. Figure 5.5 shows the absolute (non-normalized) surface area data from the same experiments as Figure 5.4. It is clear from Figure 5.5 that the absolute surface area increased with lime addition up to 2/1 for reaction times below 10 hours. While it was hoped that a minimal amount

of lime would be sufficient, it is clear that low lime concentration limits the rate of surface area formation.

One hypothesis would be that at low calcium concentrations, the product precipitates on the surface of the lime, rather than on the surface of the slag. Therefore, the lime is essentially blinded, causing a drop in pH. Solids analysis was not performed to test this hypothesis.

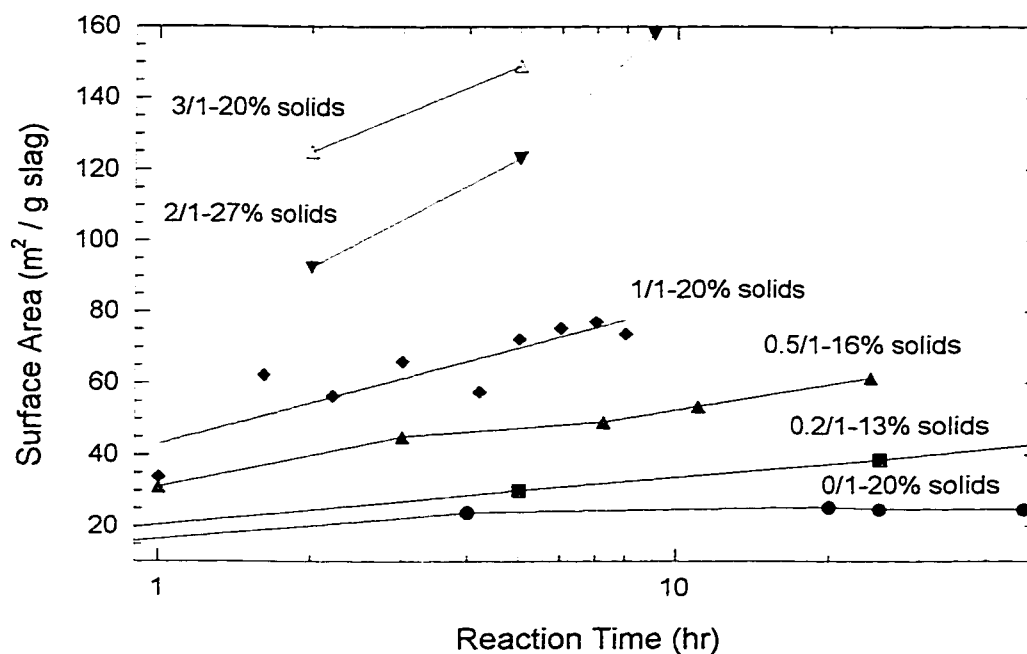


Figure 5.4: Effect of Lime/Slag Ratio on Agitated Solids

92°C; agitated; no additives

labels indicate: lime/slag ratio - wt.% solids of total.

0/1: 2/5/97; 0.2/1: 2/21/97; 0.5/1: 9/17/97

1/1: 1/31/96, 1/9/97; 2/1: 10/29/97; 3/1: 5/15/98

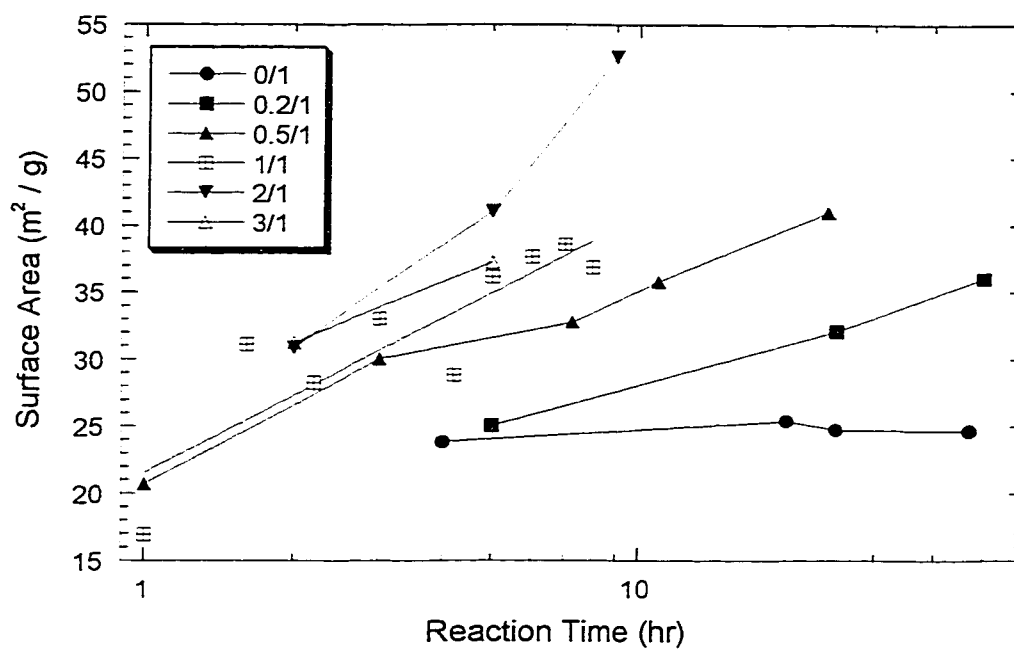


Figure 5.5: Effect of Lime/Slag on Un-normalized Surface Area

92°C; agitated; no additives

labels indicate: lime/slag ratio

0/1: 2/5/97; 0.2/1: 2/21/97; 0.5/1: 9/17/97

1/1: 1/31/96, 1/9/97; 2/1: 10/29/97; 3/1: 5/15/98

It was shown in Section 4.2.5 that agitation had a positive effect on the lime/glass/gypsum system only after a fairly high surface area was formed. Figure 5.6 shows results from agitated and non-agitated experiments to confirm whether agitation was indeed having a minimal effect. Within the experimental scatter, it appeared that agitation would not affect the lime/slag system for reaction times less than 50 hours.

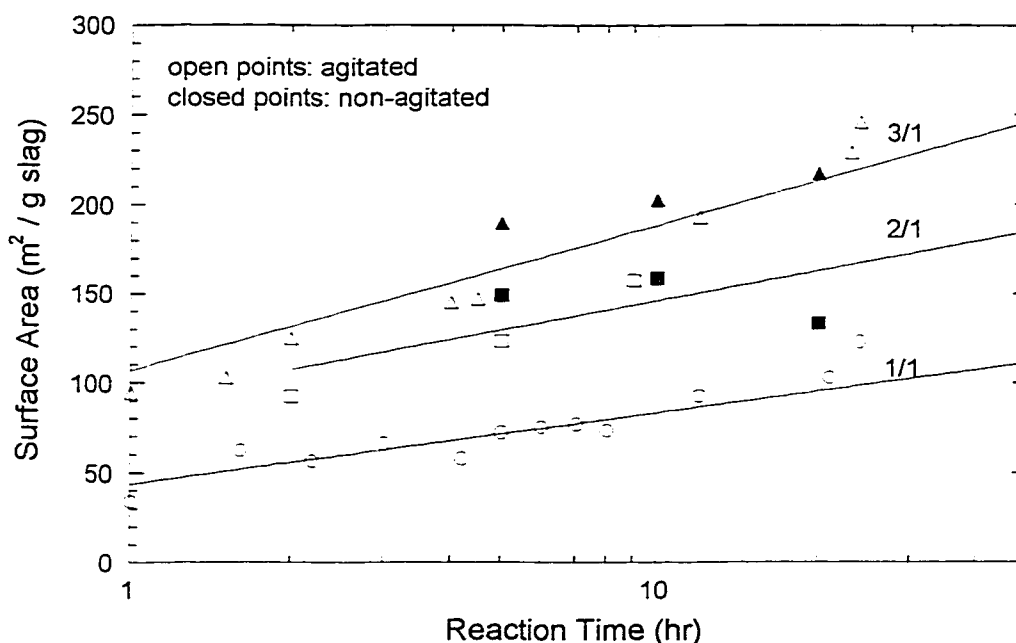


Figure 5.6: Effect of Agitation on Slag Sorbents

92°C; 20 wt.% solids

labels indicate: lime/slag wt. ratio

1/1: 1/31/96, 1/9/97, 6/17/98, 12/12/97

2/1: 10/29/97, 11/10/97, 12/2/97, 12/12/97

3/1: 5/15/98, 5/27/98, 6/3/98, 11/10/97, 12/2/97, 12/12/97

Because agitation was assumed to have a minimal effect on the system, non-agitated experiments were conducted to further elucidate the effect of lime/slag ratio. Figure 5.7 shows the absolute surface area formation as a function of lime/slag. Again, the surface area appeared to increase with lime/slag ratios up

to 2/1. With larger lime additions the surface area decreased, implying that excess lime was diluting the final solid.

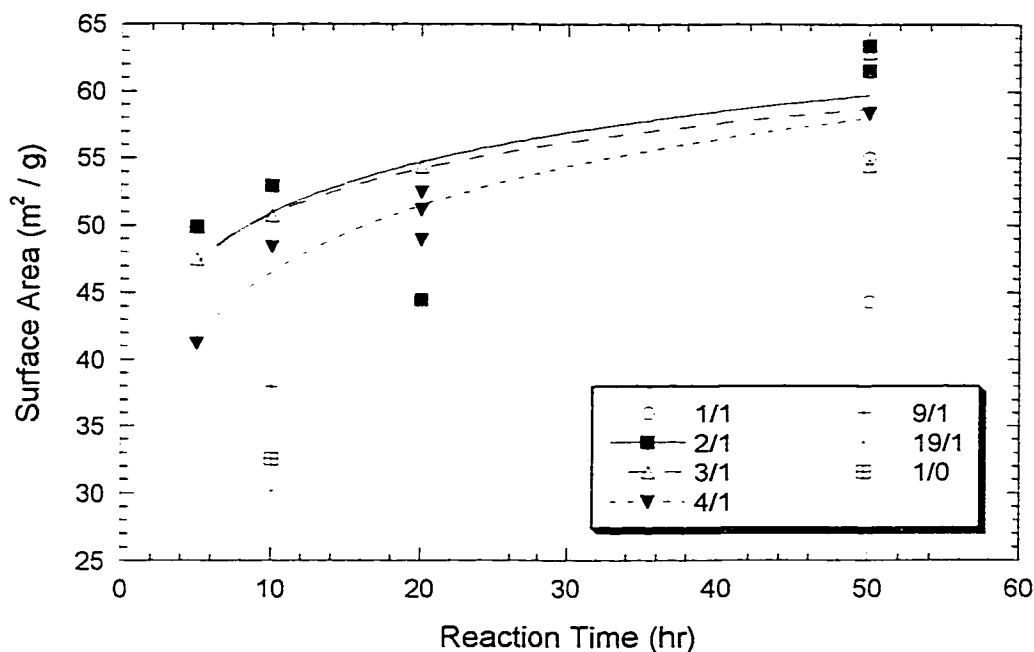


Figure 5.7: Effect of Lime/Slag Ratio on Non-agitated Solids

92°C; non-agitated; 20 wt.% solids

labels indicate: lime/slag wt. ratio

experiments: 11/10/97, 12/2/97, 12/12/97

5.1.3 Effect of Additives on Sorbent Formation

This section presents results from experiments in which additives, specifically gypsum and calcium chloride were added to the lime/slag system. All experiments discussed in this section were conducted at 92°C with agitation, in order that slurry solution analysis would be possible. The sulfide was controlled by the addition of H_2O_2 as mentioned in Section 5.1.1.

5.1.3.1 Effect of Gypsum

Because the addition of gypsum to flyash/lime and glass/lime systems increased surface area and SO_2 reactivity, it was decided to investigate whether there was a similar impact on the slag/lime system. Figure 5.8 shows that the

presence of gypsum increased surface area formation rather dramatically for lime/slag ratios of 0.5 and 1. In fact, the addition of a small amount of gypsum to the system at 0.5/1 lime/slag increased the surface area by almost threefold in the 30 hours of the experiment.

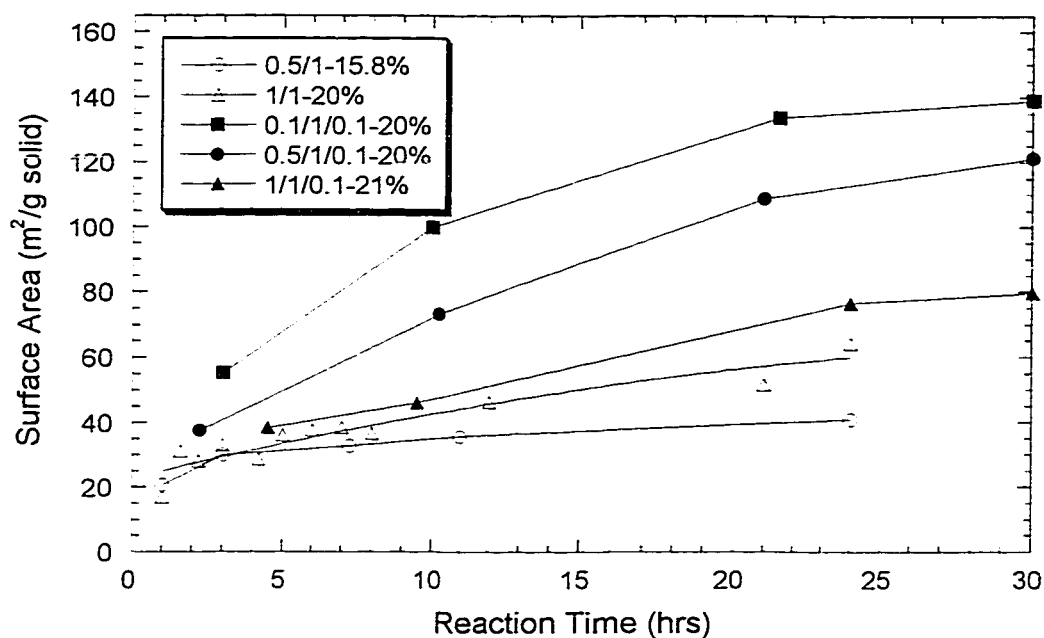


Figure 5.8: Effect of Gypsum on Slag Sorbent Surface Area

92°C; agitated

labels indicate: lime/slag wt. ratio - wt.% solids

0.5/1: 9/11/97; 1/1: 1/31/96, 1/9/97, 6/17/98;

0.1/1/0.1: 8/5/98; 0.5/1/0.1: 8/2/98; 1/1/0.1: 7/21/98

Figure 5.9 shows the calcium concentration in solution from experiments with and without gypsum. For the flyash and glass systems, it was shown that without gypsum present the calcium concentration would fall to ~1mM. For the slag system shown in Figure 5.9, the experiments without gypsum sustained a calcium concentration of ~5mM. This concentration was expected to be sufficient to maintain a reasonable rate of surface area formation. However, it is evident in Figure 5.8 that the reaction seems to slow significantly. While there was

significant scatter in the calcium data, the addition of gypsum did maintain a higher concentration of calcium overall.

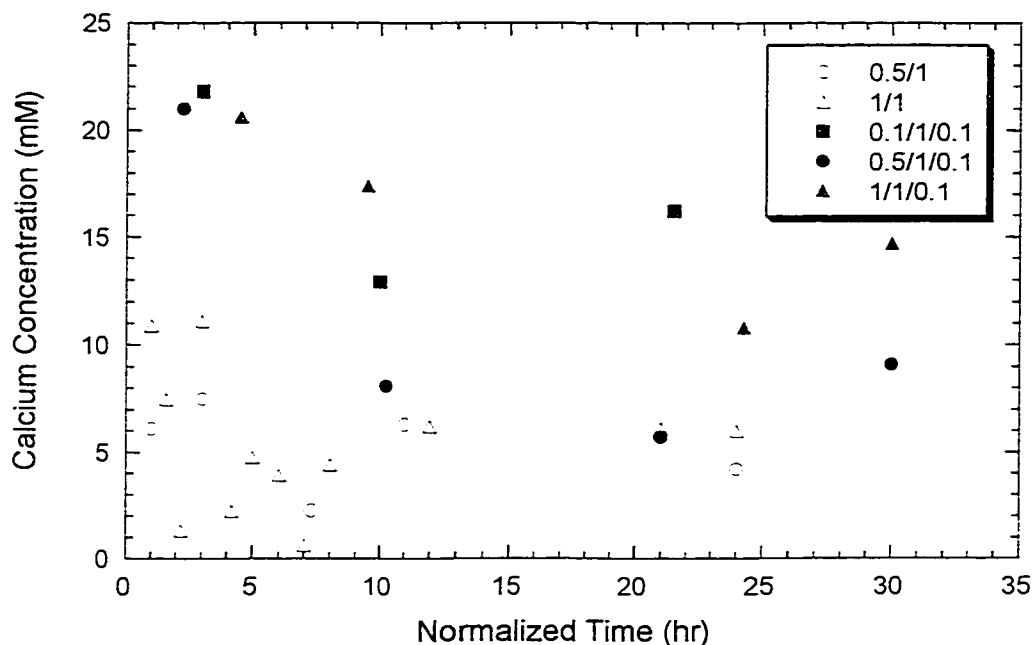


Figure 5.9: Effect of Gypsum on Calcium Concentration

92°C; agitated

labels indicate: lime/slag wt. ratio

0.5/1: 9/11/97; 1/1: 1/31/96, 1/9/97, 6/17/98;

0.1/1/0.1: 8/5/98; 0.5/1/0.1: 8/2/98; 1/1/0.1: 7/21/98

It appeared, however, that the calcium in solution might be from both the lime and gypsum, and that it was necessary for both lime and gypsum to be present in sufficient quantities. Figure 5.10 presents the normalized surface area results of the experiments also shown in Figure 5.8. It is clear that the experiment with 0.1/1/0.1 lime/glass/gypsum had a very high rate of surface formation, however, at longer reaction times, the rate decreased. It seemed that the 0.1 g lime/slag was depleted before the 30 hour maximum reaction time.

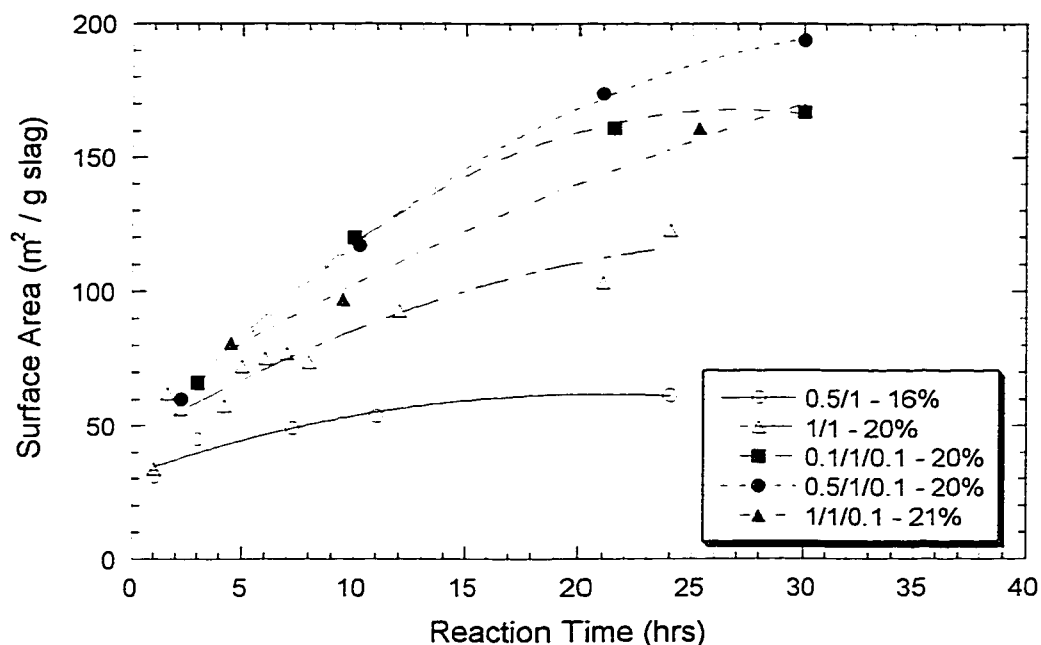


Figure 5.10: Effect of Gypsum on Normalized Slag Sorbent Surface Area

92°C; agitated

labels indicate: lime/slag wt. ratio - wt.% solids

0.5/1: 9/11/97; 1/1: 1/31/96, 1/9/97, 6/17/98;

0.1/1/0.1: 8/5/98; 0.5/1/0.1: 8/2/98; 1/1/0.1: 7/21/98

X-ray data supports this hypothesis. Figure 5.11 shows the diffraction patterns for the reaction with 1/1/0.1 lime/glass/gypsum. It is clear that excess lime is present until 30 hours and 80 m²/g have been formed. The reaction with 0.1/1/0.1 lime/glass/gypsum is represented by the patterns of Figure 5.12. While gypsum was still present in the pattern at 3 hours, no excess lime was visible as Ca(OH)₂ throughout the reaction. The results from the glass system showed that surface area would continue to form after X-ray no longer detected Ca(OH)₂. This was true in this system as well. However, it seemed that a higher amount of excess lime maintained the reaction for a longer time.

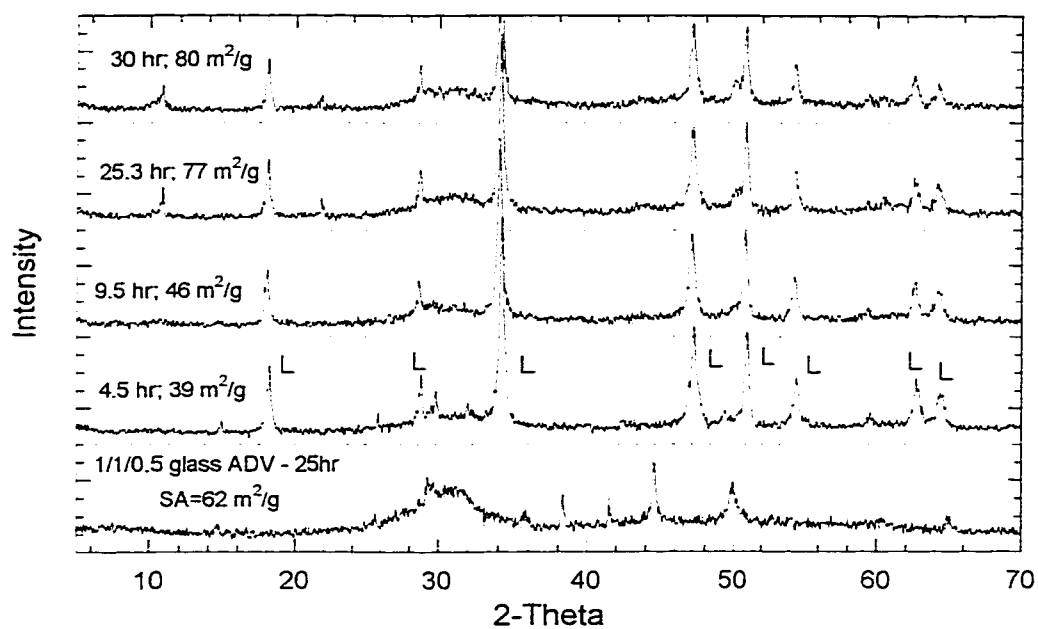


Figure 5.11: X-ray Pattern: Excess Lime in Slag Absorbents

92°C; agitated; 20 wt.% solids

all patterns except glass ADV: 7/21/98; 1/1/0.1 lime/slag/gypsum.

glass ADV: 11/21/94-25

L: Ca(OH)_2 peaks

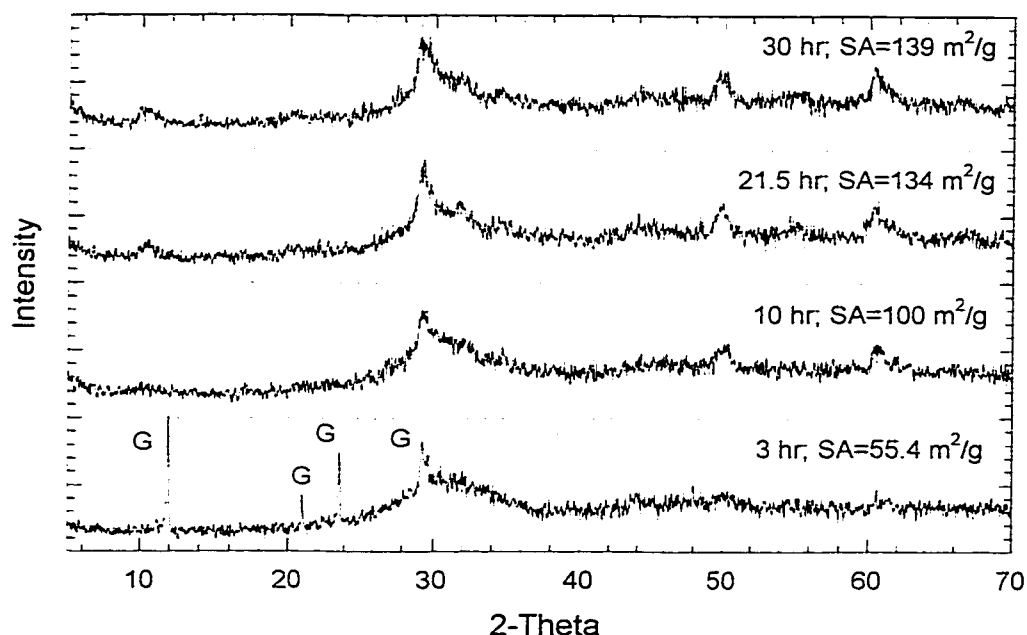


Figure 5.12: X-ray Pattern: Surface Area Formation Without Excess Lime

92°C; agitated; 20 wt.% solids

8/5/98; 0.1/1/0.1 lime/slag/gypsum.

G: gypsum peaks.

5.1.3.2 Effect of CaCl_2

Presuming that the results observed with the addition of gypsum were strictly a function of calcium concentration, it seemed obvious to observe the effects of boosting the calcium concentration with CaCl_2 . Figure 5.13 shows the formation of surface area from slag with 50 mM and 90 mM of CaCl_2 added. The addition of 50 mM CaCl_2 created a product with the same surface area behavior as that created with 0.1 g gypsum/g slag. The addition of 90 mM CaCl_2 caused an unexpected upward curvature in the formation of surface area curve. This is probably due to either experimental scatter, or the excessively high ionic strength of the solution slurry.

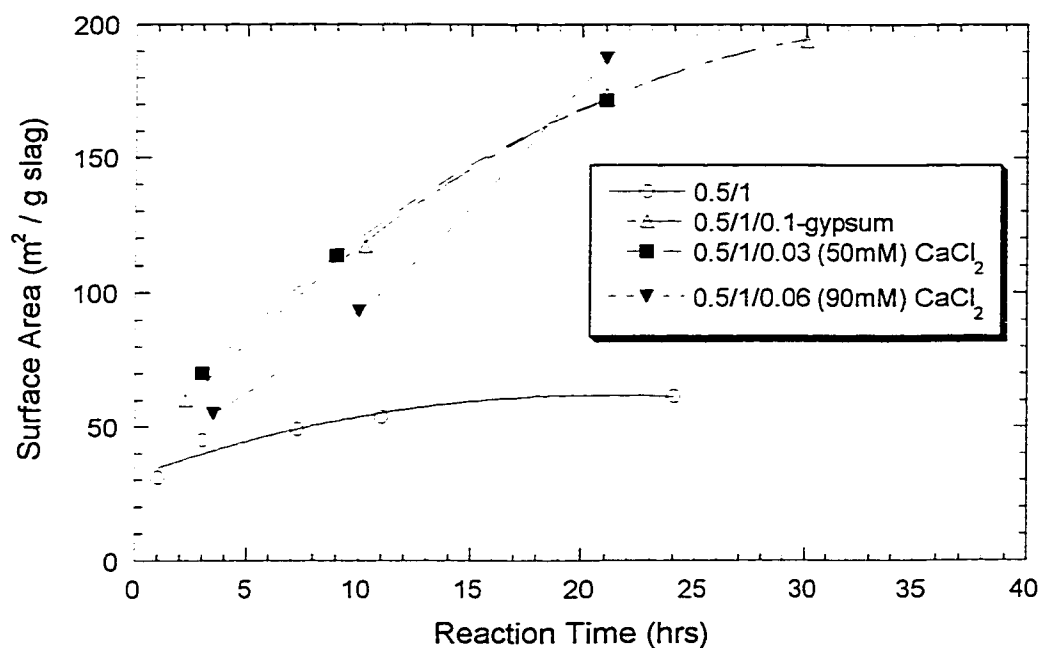


Figure 5.13: Effect of CaCl_2 on Surface Area

92°C; agitated

labels indicate: lime/slag/ CaCl_2 wt. ratio

0.5/1: 9/11/97; 0.5/1/0.1: 8/2/98

50 mM CaCl_2 : 8/17/98; 90 mM CaCl_2 : 8/25/98;

Figure 5.14 presents the calcium concentration data for the experiments with CaCl_2 added. The chloride experiments had a considerably larger concentration of calcium, however the surface area in Figure 5.13 did not increase likewise. Therefore, while a sufficient calcium concentration must be maintained, either by the addition of gypsum or calcium chloride, an extreme excess is not necessarily beneficial.

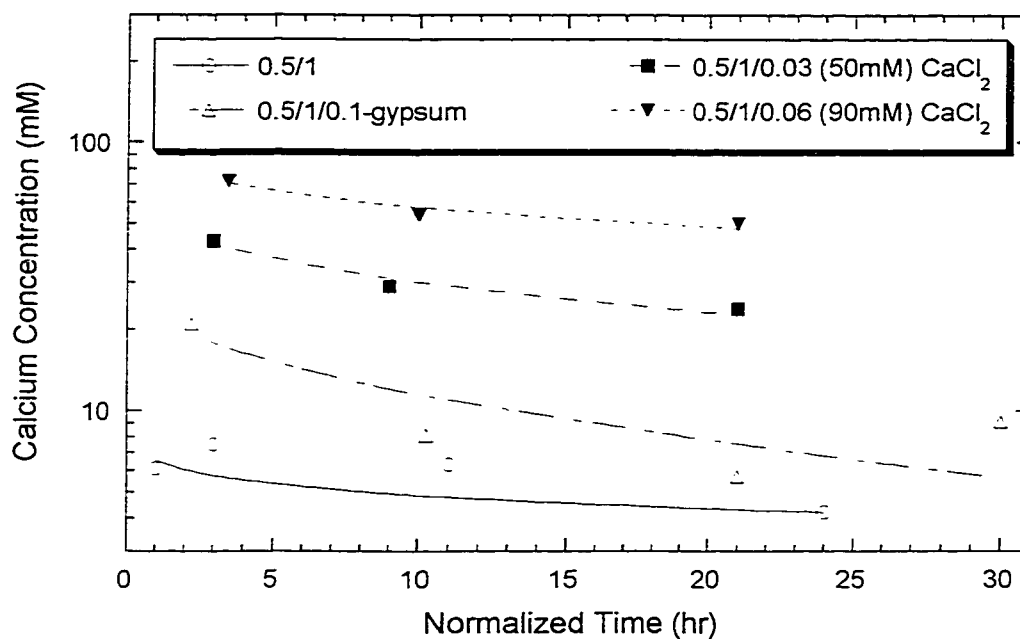


Figure 5.14: Effect of CaCl_2 on Calcium Concentration

92°C; agitated

labels indicate: lime/slag/ CaCl_2 wt. ratio

0.5/1: 9/11/97; 0.5/1/0.1: 8/2/98

50 mM CaCl_2 : 8/17/98; 90 mM CaCl_2 : 8/25/98

5.1.4 Release of Alkali from Slag

If the rate of surface area formation is proportional to the dissolution of the slag, it might follow that it is also proportional to the dissolution of individual components of the slag. This result was shown in Figure 4.13 for the dissolution from the lime/glass system.

Figure 5.15 shows the release of sodium from slag for several different reactant recipes. The experiments represented in Figure 5.15 include various lime/slag ratios, without additives, with gypsum, and with CaCl_2 . Except for a couple of outlying points (from the 90 mM CaCl_2 experiment) the release of sodium is quite linear with surface area. Figure 5.16 shows the release of potassium relative to sodium for experiments with gypsum or CaCl_2 present.

Again, excluding the two outliers, the behavior is strongly linear, implying that the potassium and sodium diffuse out from silica matrix at a proportional rate.

It is clear that the dissolution of alkali from the silica matrix is proportional to the formation of surface area. This does not imply that the dissolution of the silica matrix is rate limiting. Rather, the rate of both processes is probably controlled by diffusion through the calcium silicate product layer.

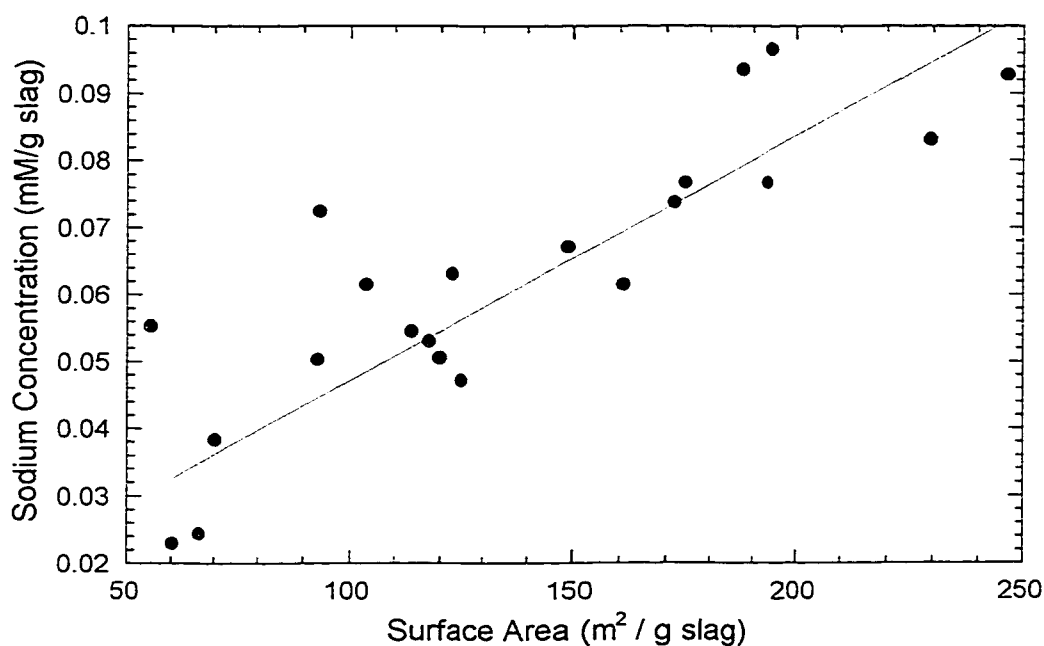


Figure 5.15: Release of Sodium from Slag During Preparation

92°C; agitated

experiments: 5/15/98, 6/3/98, 6/17/98,

8/2/98, 8/5/98, 8/17/98, 8/25/98

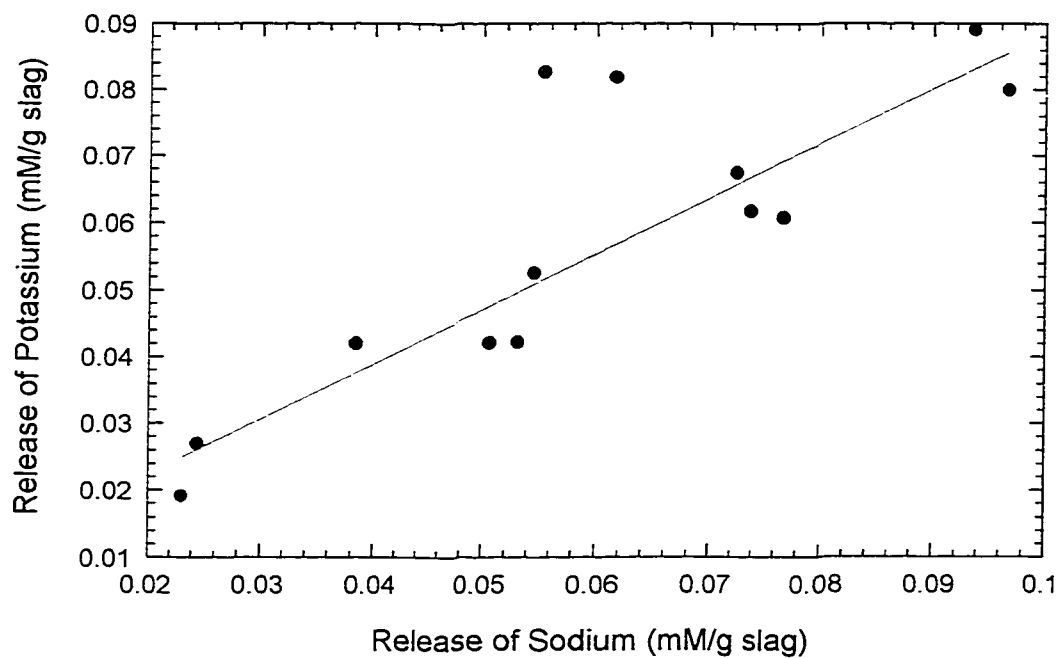


Figure 5.16: Ratio of Sodium to Potassium Dissolution from Slag

92°C; agitated

experiments: 8/2/98, 8/5/98, 8/17/98, 8/25/98.

5.2 SORBENT CHARACTERIZATION - SEM

Scanning electron microscopy was utilized to observe any differences that might occur with the slag sorbents. As stated previously, many aspects of the slag system were expected to be identical to those of the glass system. Therefore, in depth characterization of slag sorbents was not done.

Figure 5.17 shows the micrograph of unreacted slag. The particle size was significantly smaller than the glass shown in Figure 4.22. This was simply due to finer grinding, and was also evident in the larger surface area of $3.6 \text{ m}^2/\text{g}$ for slag as compared to $0.38 \text{ m}^2/\text{g}$ for glass.

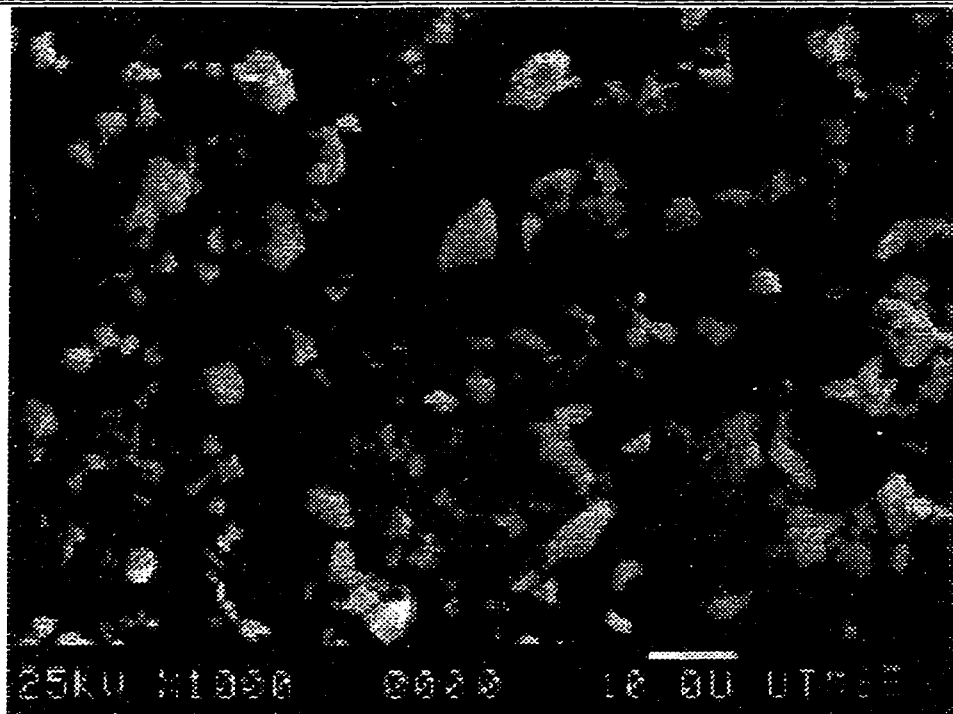


Figure 5.17: SEM: Unreacted Ground Iron Blast Furnace Slag

Figure 5.18 shows the sorbent created from lime, slag, and gypsum. In appearance, it was very similar to the product from glass. The particles, of course, appeared to be smaller, indicative of the smaller initial slag particles.

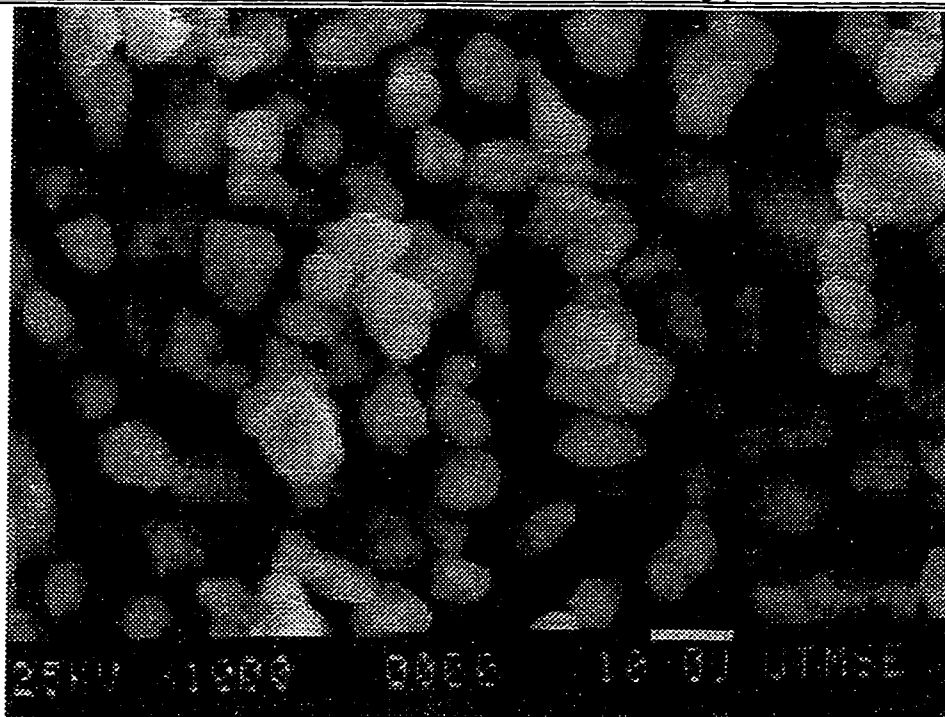


Figure 5.18: SEM: Calcium Silicate Sorbents from Slag

92°C; agitated
0.5/1/0.1 lime/slag/gypsum weight ratio
SA=121.5 m²/g; sample 8/2/98-30

Figure 5.19 shows solids prepared with 50 mM CaCl_2 in solution. While the author apologizes for any resolution lost in reproduction, it was quite clear that the solids appeared to have a different surface structure than that shown in Figure 5.18, even though the surface areas were essentially the same. X-ray patterns shown in Figure 5.20 failed to show any structural differences between the two solids, such as the presence of CaCl_2 precipitate. While both have excess lime present, the overall structures appeared to be that of CSH. Porosity measurements of the two solids indicated a difference in solid phase, however. The solid prepared with chloride had a porosity of $0.49 \text{ cm}^3/\text{g}$ compared to $0.66 \text{ cm}^3/\text{g}$ for the solids prepared with gypsum.

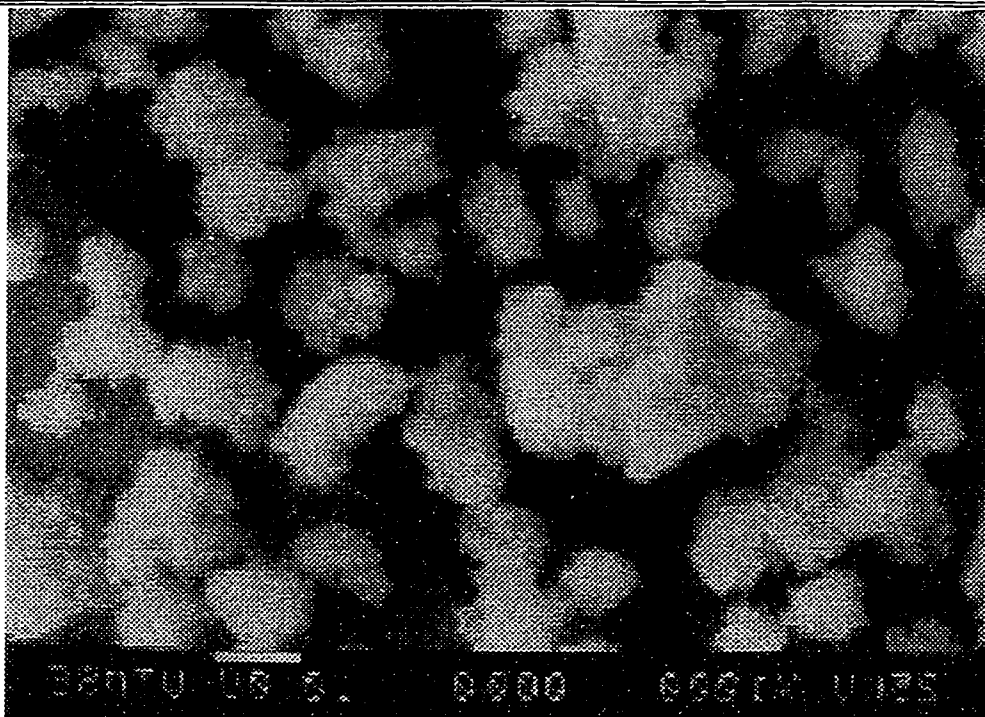


Figure 5.19: SEM: Slag Sorbent Prepared with CaCl_2

92°C; agitated; 50 mM CaCl_2

0.5/1 lime/slag weight ratio

SA=114.5 m^2/g ; sample 8/17/98-21

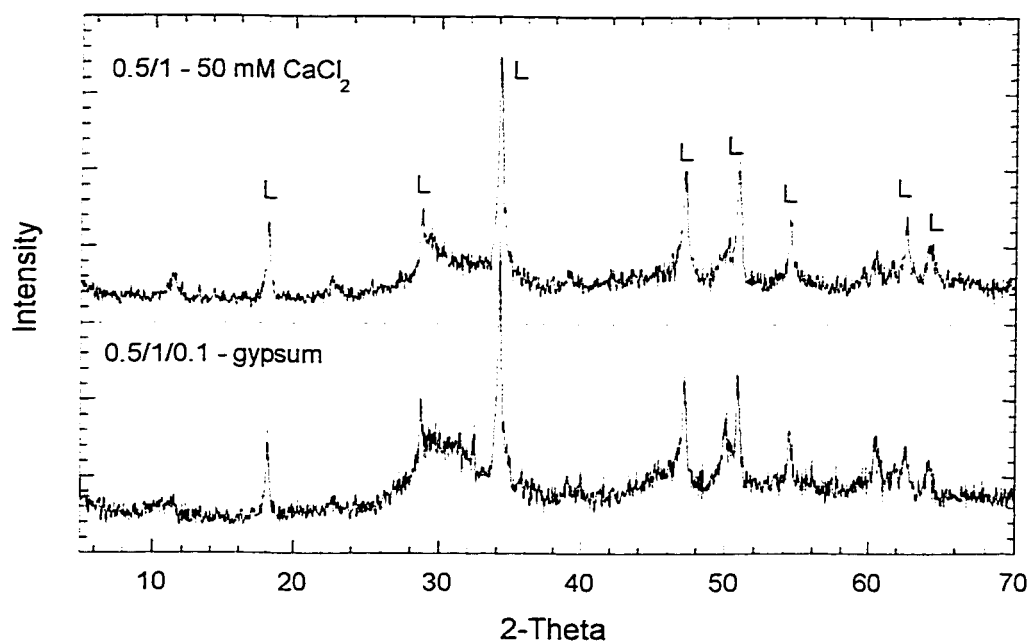


Figure 5.20: X-ray Pattern: Slag Sorbent Prepared with CaCl₂

0.5/1 - 50 mM CaCl₂: SA = 114.5 m²/g; 8/17/98-21

0.5/1/0.1 - gypsum: SA = 121.5 m²/g; 8/2/98-30

L: Ca(OH)₂ peaks

Chapter 6: Reaction of SO₂ with Glass and Slag Sorbents

This chapter presents the results from experiments studying the reaction between SO₂ and calcium silicate sorbents prepared from glass or slag. The scope of this research included investigating both the process variables of the system as well as comparing the reactivity of selected sorbents prepared in Chapters 4 and 5.

6.1 SANDBED GAS PHASE ANALYSIS

As described in Section 3.2, the SO₂ reaction was studied in a semi-batch, packed bed reactor. This experimental apparatus created a reaction system where the gas was continuously flowing and monitored and the solids were batch loaded. It was believed that the reaction rate was a strong function of solids conversion. This meant that as the reaction proceeded, and the solids were converted, the removal rate at each solid particle would change with time. Furthermore, a non-differential reactor, i.e. a large enough solids/gas ratio to affect the gas concentration, resulted in a concentration profile through the sorbent bed that changed with time. If the reaction was a function of SO₂ concentration, which it was expected to be at very low concentrations, then this represented a non-trivial reaction system.

An average conversion of the sorbent and total removal were utilized to observe gross effects of process conditions and sorbents. The evaluation of an exact point model of the SO₂ removal at any point in time and position in the sandbed, and therefore solids conversion and SO₂ concentration, is discussed in Section 6.5.

The effect of the analytical system timelag described in Appendix C was also neglected until the reactor system was modeled in Section 6.5. Therefore, for the results presented in Sections 6.2-3, the analytical timelag was obviously present at low solids conversion. Ideally, at time zero when the SO₂ flow was diverted from the bypass line into the fresh packed bed reactor, the concentration, and therefore the fraction removal, should have shown a step change to the maximum removal for that experiment. It is clear from the figures presented in Sections 6.2-3 that the timelag delayed the maximum removal for upwards of five minutes.

It should also be noted that experiments were conducted for a maximum of 60 minutes, unless SO₂ removal ceased at a much earlier time. For the bulk of experiments, the SO₂ removal at this time was small, but clearly greater than zero. This arbitrary time was chosen for experimental convenience.

6.1.1 Integration of SO₂ Removal Data

The raw data obtained from the analytical system described in Chapter 3 was recorded every 30 seconds as voltage output from the analyzer. This was converted to a measured outlet concentration by a two point calibration taken at 0 ppm and 1000 ppm (standardized calibration gas). This, of course, assumed that the relationship between voltage and concentration was linear over the range of the experiment.

Concentration (as a function of time) data was integrated to calculate SO₂ removal and cumulative solids conversion at each time step. The trapezoidal rule was used to integrate each 30 sec. time step, resulting in the moles of SO₂ removed in that time step. This was then converted to an average solids conversion by summing the total amount of SO₂ removed at that time and dividing by the total amount of alkalinity in the sandbed. Appendix D outlines the calculations described, which were normally done using an EXCEL spreadsheet. The results presented in Sections 6.2-3 are typically presented as fractional SO₂ removal (i.e. (inlet-outlet)/inlet) at time t as a function of cumulative solids conversion at time t. The bulk of experiments were conducted for one hour, unless SO₂ removal ceased much earlier. This means that in most cases SO₂ removal was greater than zero when the experiment was stopped.

The alkalinity used to normalize the SO₂ data to solids conversion was a measured value according to the procedure outlined in Section 3.1.3.4. This should include both the alkalinity of the original hydrated lime, as well as any alkalinity contributed from the glass or slag. Both the calcium and sodium concentrations in the silica were considered as alkalinity available for reaction according to Equations 6.1-2.



6.2 EFFECT OF PROCESS CONDITIONS ON SO₂ REACTION

As mentioned previously, there has been considerable work published regarding the effects of process conditions on the reaction of SO₂ with lime and calcium silicates. In general, it was expected that previous conclusions might hold true for this research as well. However, previous work utilized hydrated lime or flyash/lime sorbents which typically did not have the high surface area present in glass/lime sorbents. Therefore, as an extrapolation of previous investigations, this work measured the reactivity of a selected high surface area glass ADVACATE sorbent as a function of process conditions.

The particular sorbent used (Sample ID# 4/28/97-50) was prepared from a recipe of 1/1/0.5 lime/glass/gypsum (weight ratio) under agitated conditions for 50 hours at 92°C. It had a surface area of 96 m²/g, and a measured alkalinity of 6.60 mmol⁺² / g sorbent. It was chosen because of the high surface area as well as having a typical CSH X-ray pattern shown in Figure 6.9. In short, it was expected to be the best baseline sample to represent high surface area calcium silicates.

6.2.1 Effect of SO₂ Concentration

The effect of SO₂ concentration on the reactivity of the sorbents is of primary importance in any study or application. Regardless of the contacting system used, when high SO₂ removal is required, there will exist both high and low SO₂ concentration extremes. Therefore, any insight into this effect is beneficial.

Figure 6.1 presents the results from experiments conducted at 50°C and 58% RH, with SO₂ concentration ranging from 500 to 2000 ppm. The sorbent loading was 0.1 g solid for each experiment. An experiment at 500 ppm with 0.025 g sorbent is also included in the figure.

It is clear from the figure that fractional removal decreased with increasing SO₂ concentration. This means that the system, as a whole, was not first order in SO₂. If it were overall first order in concentration, as the concentration doubled, so would the removal, and the fractional removal would remain constant. Figure 6.1 shows that there was a significant difference between the three experiments.

The comparison between the 2000 ppm / 0.1 g and 500 ppm / 0.025 g might have elucidated a zero order SO₂ dependence of the overall system. If the

system were zero order in SO_2 concentration, than these two curves, with a constant solids / SO_2 ratio should have collapsed. Within the experimental scatter of the data, it was not clear whether these two curves collapsed.

This analysis of Figure 6.1 examined only the overall effect of SO_2 concentration. It should be emphasized that it was not expected to determine the exact concentration order without integrating a point model through the changing bed.

Figure 6.2 shows that the general trends seen at 58% RH also hold true at 28% RH. The crossing of the 500 and 1000 ppm lines are indicative of the experimental scatter in the sandbed reactor system.

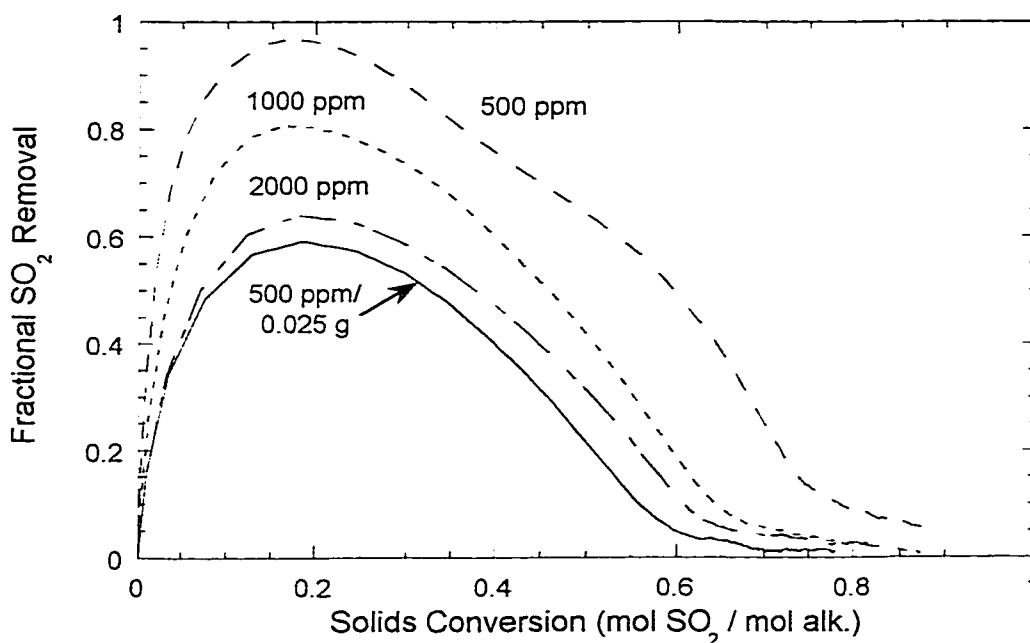


Figure 6.1: Effect of SO_2 Concentration

50°C; 58% RH; 1.521 slpm total
 0.1 g sorbent (except where noted); 4/28/97-50; SA=96 m²/g
 experiment #s: 51, 57, 60, 67

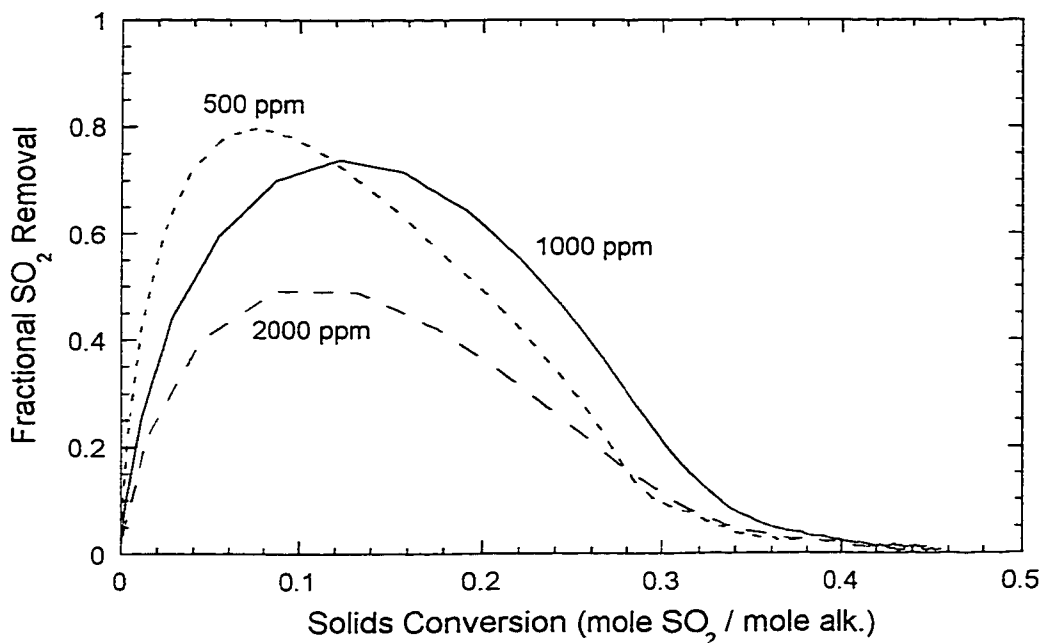


Figure 6.2: Effect of SO_2 Concentration at 29% RH

50°C; 29% RH; 1.521 slpm total
 0.1 g sorbent; 4/28/97-50; SA=96 m²/g
 experiment #s: 50, 78, 87

6.2.2 Effect of Temperature

As mentioned in Chapter 2, relative humidity has been shown to strongly influence the reaction between SO_2 and alkaline sorbents. The temperature in these studies, more often than not, was tied directly to the relative humidity by holding the absolute humidity constant. In this research, the relative humidity was held constant by varying the total water content of the gas stream.

Figure 6.3 shows the effect of changing the temperature at a constant relative humidity of 58%. There appeared to be a slight increase in removal rates with temperature, especially from 50°C to 69.5°C. The more significant effect, however, was the increase in maximum conversion with temperature.

The second "hump" seen in the results at 69.5°C was not expected, and was commonly indicative of experimental problems, probably poor dispersion of the sorbent on the sand.

The maximum rate of removal will greatly impact the contact time necessary for SO₂ removal in an industrial application. The maximum conversion, however, has a more profound economic impact. This characteristic will dictate the overall stoichiometric ratio needed between SO₂ and sorbent. If a solid will only achieve 50% conversion in a reasonable time, than twice as much sorbent or recycle will be required. Therefore, improvements in both the maximum removal rate as well as maximum solids conversion will be beneficial.

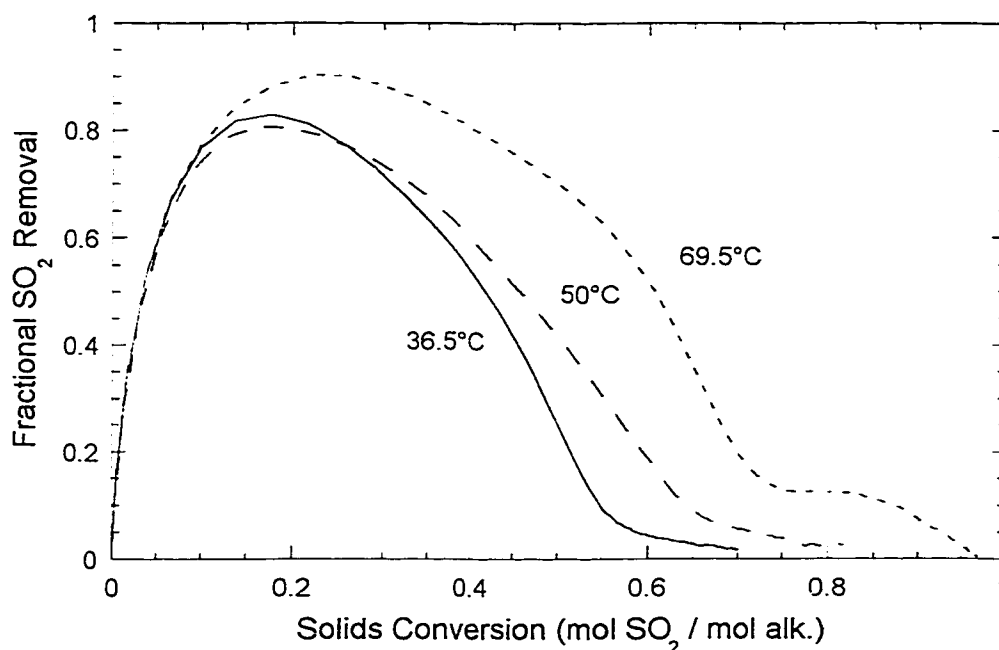


Figure 6.3: Effect of Temperature at Constant Relative Humidity

58-59% RH; ~1000 ppm SO₂; 1.521 slpm total
 0.1 g sorbent; 4/28/97-50; SA=96 m²/g
 experiment #s: 51, 54, 61

6.2.3 Effect of Relative Humidity

As previously mentioned, humidity in the gas has been known to have a dramatic effect on the reaction between SO_2 and alkaline sorbents. It was expected that the same trend would be seen with glass silicates. Figure 6.4 shows that at 50°C and 1000 ppm inlet SO_2 , relative humidity had a strongly positive effect on both the maximum SO_2 removal as well as the maximum conversion the solids reached within an hour.

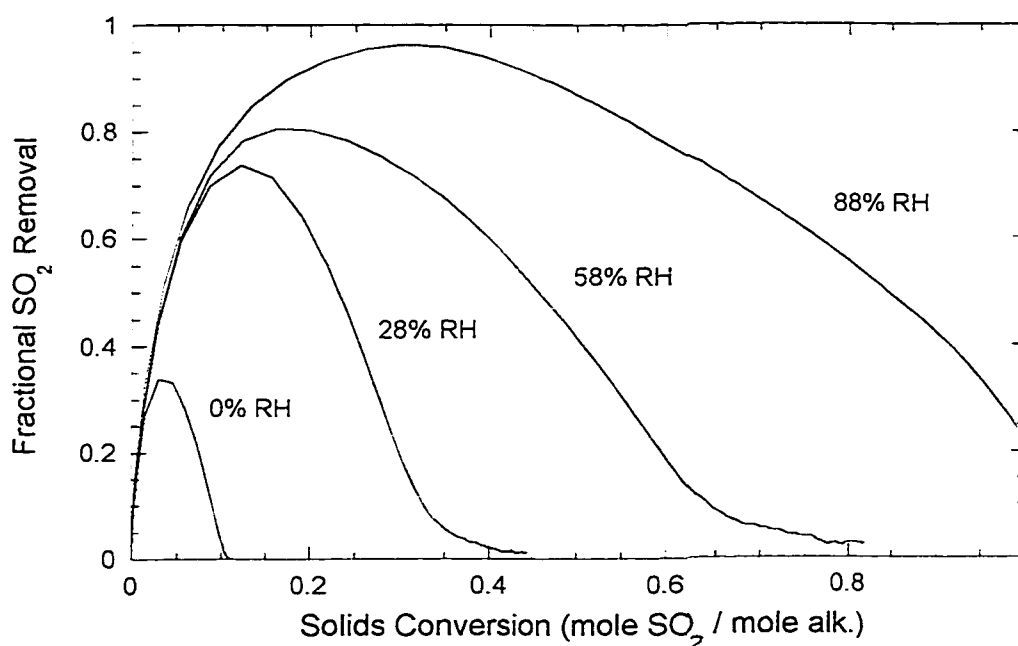


Figure 6.4: Effect of Relative Humidity at Constant Temperature

50°C ; ~ 1000 ppm SO_2 ; 1.521 slpm total
 0.1 g sorbent; 4/28/97-50; $\text{SA}=96 \text{ m}^2/\text{g}$
 experiment #s: 50, 51, 52, 53

It is also evident that the shapes of the curves at 0% and 88% RH were different than those at 29% and 58%. This was probably indicative of different physical systems. With a partial pressure of water in the gas, it is known that a certain amount of water will be adsorbed on the surface of the solids. Wasserman (1992) concluded that solids prepared without chloride exhibited a type II BET

isotherm for the adsorption of water. It has further been hypothesized by previous researchers that SO_2 dissolves into the adsorbed water layer to react with the lime or other alkalinity in the aqueous phase. At 0% relative humidity, this phenomena would not occur, and a direct gas/solid reaction must have been responsible for the feeble removal and conversions measured. At 88% relative humidity there was so much water present, that it is entirely feasible that small pores had completely filled with water, and the system no longer resembled a solid surface with adsorbed water.

Operationally, increasing the relative humidity beyond a certain point is unfeasible. This is simply due to the agglomeration that will eventually occur with the solids and equipment with excessive water in the gas stream. However, the experimental results reiterate the benefits of maximizing the water content within operational constraints.

6.2.4 Effect of Oxygen

Flue gas from most applications will normally have a nominal concentration of oxygen. Figure 6.5 shows the effect of 5 mol% oxygen in the gas stream on the removal of SO_2 with the sorbent prepared from glass.

It was expected that oxygen would have a beneficial effect on the removal of SO_2 . The hypothesis was that the oxidation of the reaction product from sulfite (SO_3^{-2}) to sulfate (SO_4^{-2}) would increase the reaction rate after a product layer was formed. The effect as shown in Figure 6.5, however, is not dramatic. Within the normal experimental scatter of the data, as shown in Section 6.1.2, oxygen does not seem to have had a significant effect.

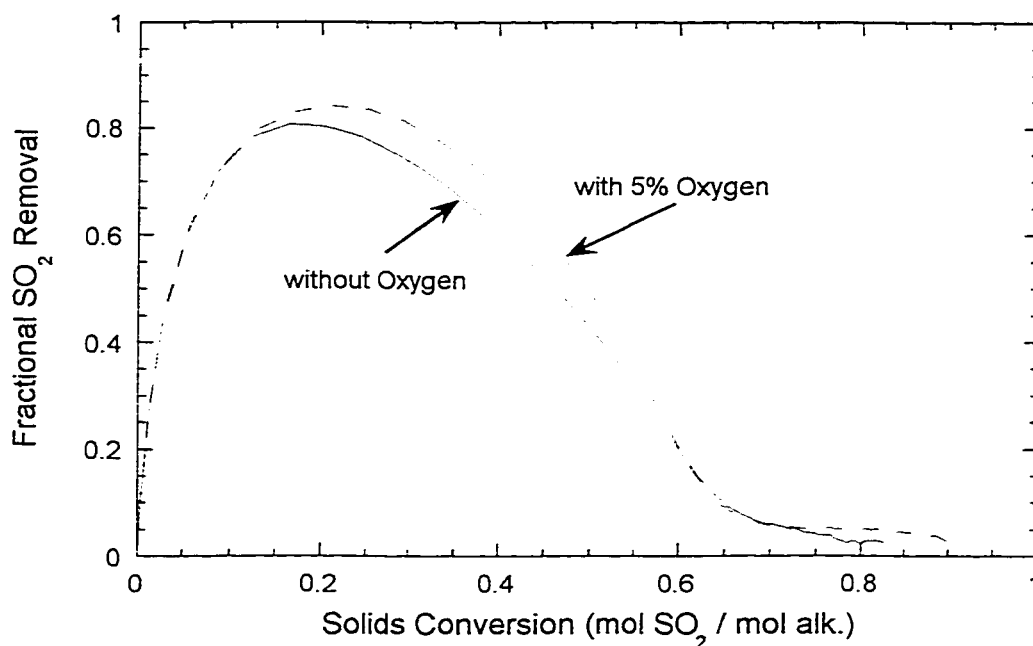


Figure 6.5: Effect of Oxygen on SO₂ Reactivity

50°C; 58% RH, ~1000 ppm SO₂; 1.521 slpm total
0.1 g sorbent; 4/28/97-50; SA=96 m²/g
experiment #s: 51, 69

6.3 EFFECT OF SORBENT CHARACTERISTICS ON SO₂ REACTION

The overriding goal of investigating the preparation of silicate sorbents in Chapters 4 and 5 was to maximize SO₂ reactivity. This section presents the results of experiments which measured the reactivity of selected sorbents prepared from glass or slag.

While surface area was used as the convenient measure of calcium silicate formation in Chapters 4 and 5, the correlation between surface area and SO₂ reactivity could only be expected to hold true for a constant solid phase. Therefore, solids that appeared to be different from the CSH phase seen in the baseline glass sorbent, regardless of surface area, were also tested.

6.3.1 Effect of Alkalinity / Surface Area

Because alkalinity was not only derived from the lime added to the solids, but also from the silica source, the alkalinity of the sorbents were a function of slurry preparation time. As surface area was also a direct function of reaction time, alkalinity and surface area were intrinsically inseparable for families of solids. If the effects of total alkalinity and surface area on SO_2 reactivity are separable, then Figure 6.6 shows the effect of surface area by normalizing the solids conversion by the actual measured alkalinity of each particular solid.

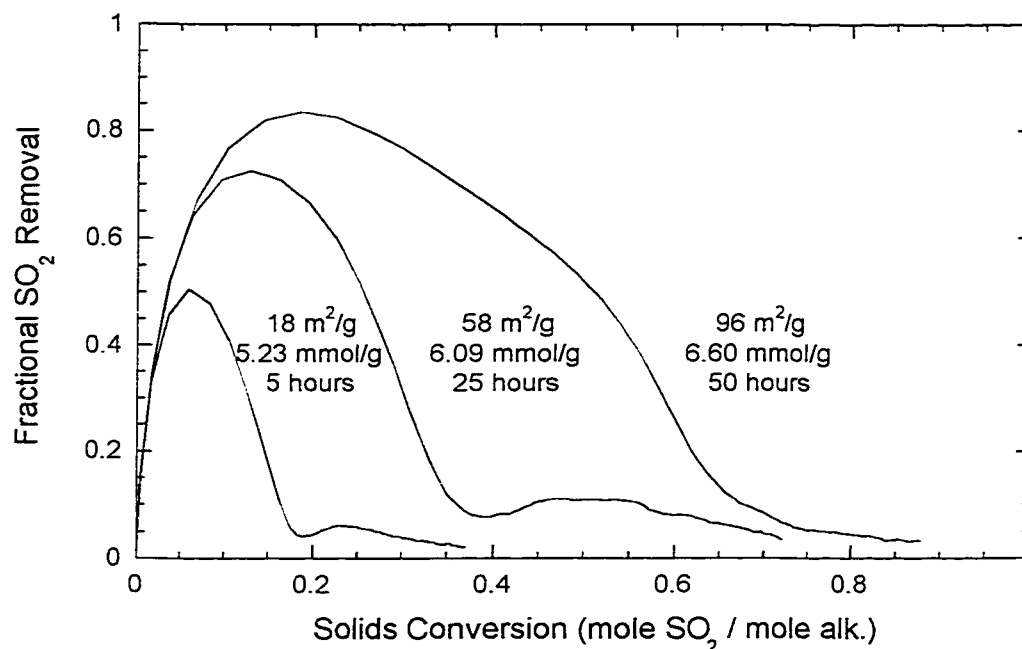


Figure 6.6: Effect of Surface Area / Alkalinity

50°C; 58% RH; ~1000 ppm SO_2

1.521 slpm total; 0.1 g sorbent

labels: surface area / divalent alkalinity / slurry reaction time

18 m^2/g : 11/21/94-5; 58 m^2/g : 11/21/94-25; 96 m^2/g : 4/28/97-50

experiment #: 51, 55, 58

Figure 6.6 shows clearly the dramatic impact increasing surface area had on the reactivity with SO_2 . Again, the benefit was noticed not only in the maximum rate of SO_2 removal, but in the final solids conversion.

The three sorbents used were all prepared under agitated conditions with gypsum present. The difference in samples was simply the reaction time in the slurry. As the reaction time increased, both the surface area and alkalinity of the solids increased, indicating a dissolution of alkali from the glass.

6.3.3 Reactivities of Other Silicate Sorbents

SO_2 reactivity of various sorbents prepared from glass and slag were tested at reactor conditions of 50°C , 58% RH, and ~ 1000 ppm SO_2 . The results presented in this section will be compared with the reactivity of the glass sorbent (4/28/97-50) used in Section 6.2.

The glass absorbent used in Section 6.2 was one of the highest surface area sorbents prepared, measuring in at $116 \text{ m}^2/\text{g}$ at the time of preparation. While other methods of solids preparation did not produce solids with such high surface area, the reactivity of a chosen few were tested. As mentioned previously, the correlation between surface area and SO_2 reactivity should hold constant only for a single solid phase. If it was likely the solid phase was different than the typical CSH seen in the glass sorbent used, the SO_2 reactivity was tested.

Obviously, a comparison between the glass sorbent used and unreacted hydrated lime was in order. Hydrated lime is the typical solid used industrially for low temperature dry sorbent injection. Figure 6.7 shows the SO_2 reactivity of the glass baseline sorbent compared with hydrated lime. It is clear that the silicate sorbent had a higher rate of reaction as well as a much higher maximum solids conversion. After an hour of contact time, the silicate was able to reach 80% alkalinity conversion, while the lime was still 70% unreacted.

A glass sorbent with a comparable surface to hydrated lime is also included on Figure 6.7. It is evident from the three experiments, that while CSH is more reactive than lime, it is only significantly different if substantial surface area is allowed to form. The primary benefit of CSH is clearly derived from the potential for large surface area solids.

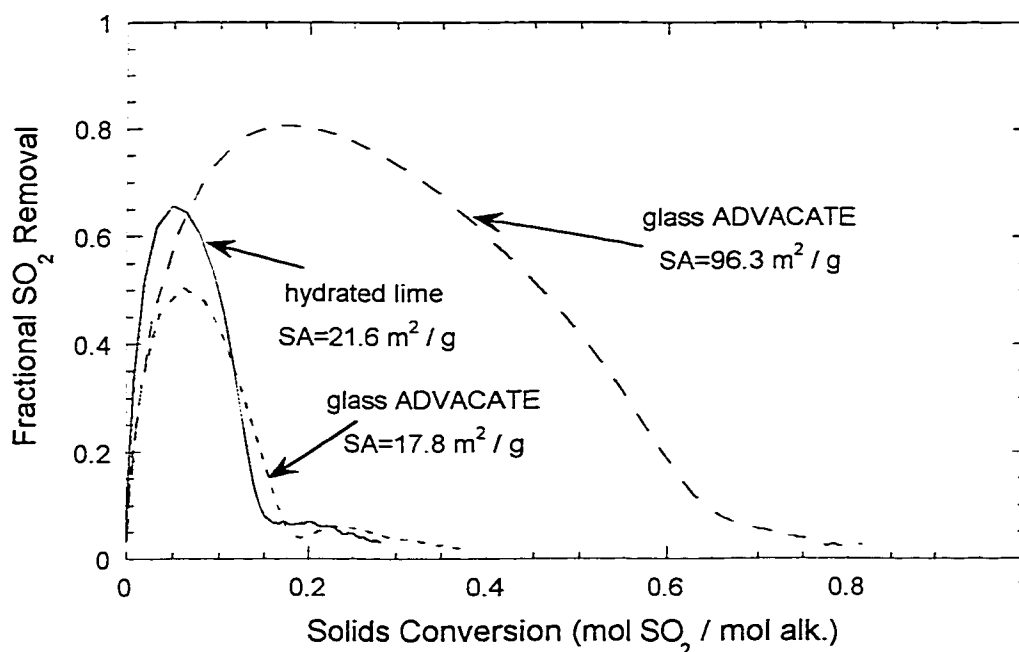


Figure 6.7: SO_2 Reactivity of Hydrated Lime and Glass ADVACATE

50°C; 58% RH; ~1000 ppm SO_2

1.521 slpm total; 0.1 g sorbent

hydrated lime: $\text{Ca}(\text{OH})_2$

Glass ADVACATE: 11/21/94-5; 4/28/97-50

experiment #s: 51, 55, 56

Figure 6.8 shows the SO_2 reactivity of two samples prepared at 120°C with and without gypsum present. As described in Section 4.2.4, sorbent prepared at 120°C had a lower ultimate surface area than sorbent prepared at 92°C. It was hypothesized that a different, more crystalline solid phase was being precipitated at 120°C. X-ray diffraction patterns in Figure 4.14 were somewhat more crystalline and supported this hypothesis. Figure 6.8 does not strongly suggest that the more crystalline solid had a significantly lower reactivity towards SO_2 . The reactivities of two sorbents prepared at 92°C are also plotted on the figure for comparison. Within the scatter of the experimental data, the 120°C and 92°C samples followed a rough trend which accounts for the differing surface areas. As mentioned

previously, the second hump at higher conversions and low removals was thought to be indicative of poor solids dispersion during the experiment.

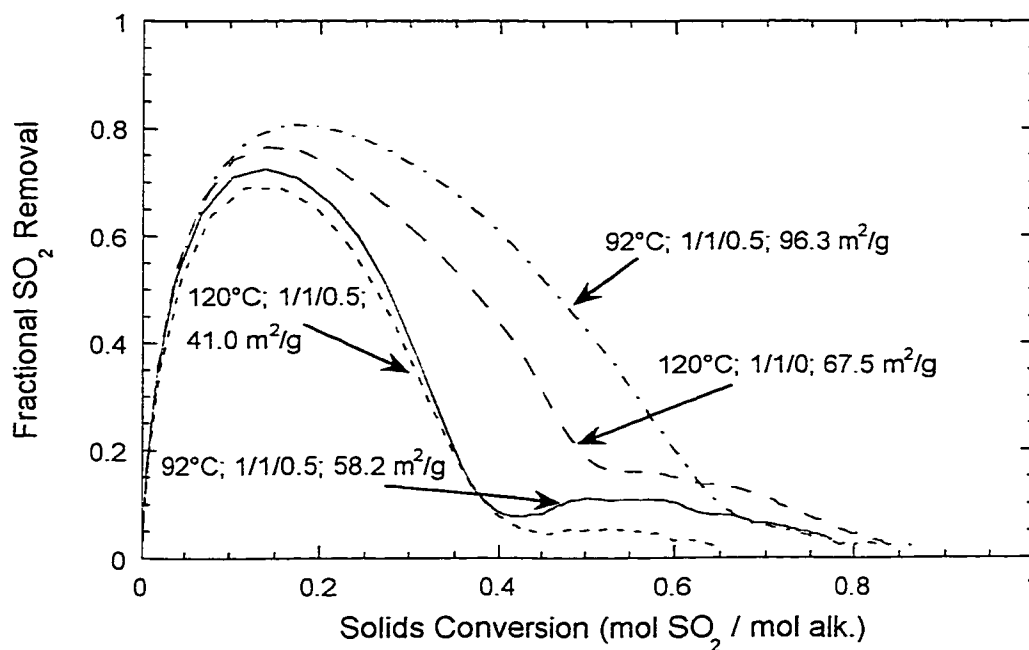


Figure 6.8: SO_2 Reactivity of Glass Sorbents Prepared at 120°C

50°C; 58% RH; ~1000 ppm SO_2

1.521 slpm total; 0.1 g sorbent

labels: slurry temp - lime/glass/gypsum wt ratio - surface area

120°C - 1/1/0: 9/25/96-23: 120°C - 1/1/0.5: 12/6/94-15

92°C - 58.2 m^2/g : 11/21/94-25: 92°C - 96 m^2/g : 4/28/97-50

experiment #s: 51, 58, 62, 63

Figure 6.9 shows the reactivity of a non-agitated sorbent compared with an agitated sorbent. While the rate of SO_2 removal is lower than the agitated sorbent, this was most likely due to the difference in surface areas, not preparation method.

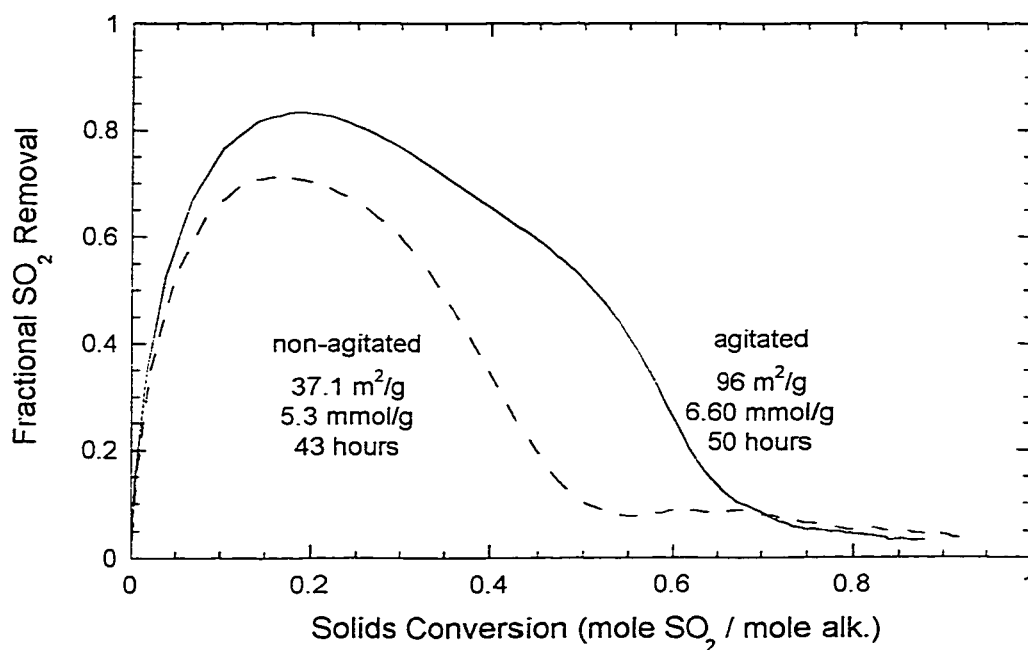


Figure 6.9: SO_2 Reactivity of Non-agitated Glass Sorbents

50°C; 58% RH; ~1000 ppm SO_2

1.521 slpm total; 0.1 g sorbent

labels: surface area - alkalinity - preparation reaction time

non-agitated: 1/22/97-43-20%; agitated: 4/28/97-50

experiment #s: 59, 64

Sorbents prepared from slag also appeared to form amorphous CSH as indicated by X-ray and SEM studies. Figure 6.10 shows the reactivities of two sorbents prepared from a 0.5/1/0.1 lime/slag/gypsum mixture. The SO_2 reactivity behavior of these samples appeared to be very similar to the sorbent prepared from glass. The sorbents prepared from slag exhibited a increase in reactivity with surface area, just like that seen in glass sorbents.

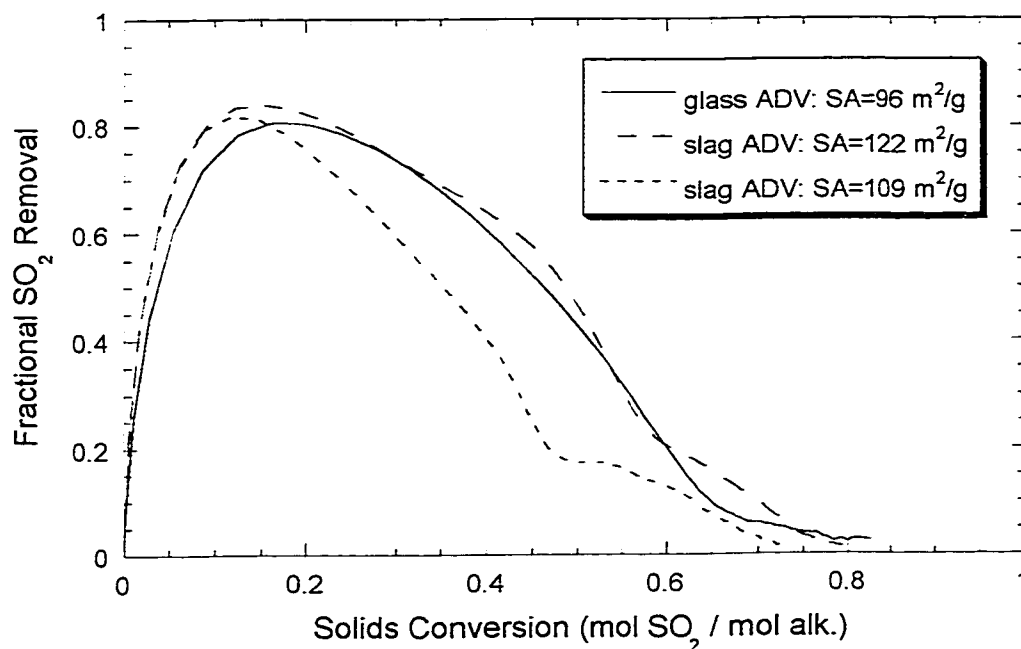


Figure 6.10: Reactivity of Slag Sorbents

50°C; 58% RH; ~1000 ppm SO₂

1.52l slpm total; 0.1 g sorbent

Glass ADV: 4/28/97-50; Slag ADV: 8/2/98-21 & -30

experiment #s: 51, 76, 81

The sorbent prepared from glass is included for general comparison. While it appeared that the glass sorbent outperformed the slag sorbents when surface area is considered, care should be taken when comparing the two sorbents directly. The slag sorbent was prepared from a mixture of 0.5/1/0.1 lime/slag/gypsum, while the glass sorbent was prepared from a 1/1/0.5 mixture. Even though the slag sorbent was prepared with less lime, the X-ray patterns shown in Figure 6.11 clearly indicate excess Ca(OH)₂. The bottom line is that while both solids were clearly amorphous CSH, the difference in recipes may account for the apparent difference in reactivities between the slag and glass absorbents.

It should also be noted that there was difficulty in measuring the alkalinity of the slag sorbents. It appeared that the slag partially, if not completely, dissolved

in 0.1M HCl used in the procedure outlined in Section 3.1.3.4. For one, the release of sulfide was noticed, which should not have been present in the precipitated calcium silicates under the conditions of H_2O_2 addition. Second, during titration to the phenolphthalein endpoint with NaOH, the solution would become cloudy and grey. This made endpoint determination very difficult. Therefore, since the sorbent alkalinity was uncertain, the solids conversion axis in Figure 6.10 was also uncertain.

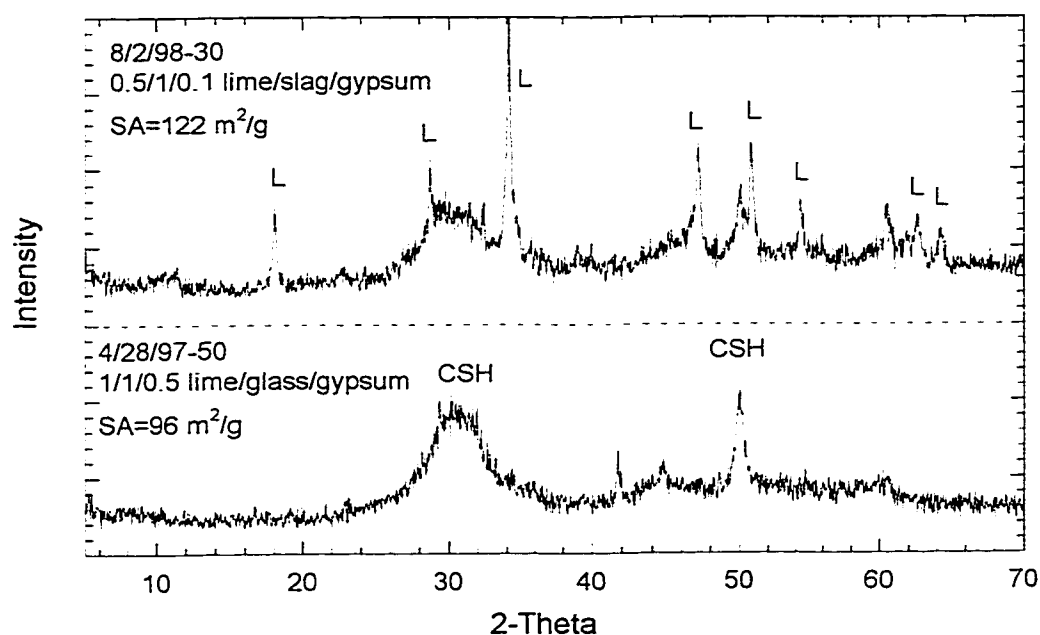


Figure 6.11: X-ray Pattern: Sorbents Prepared from Slag or Glass

92°C; agitated; 20 wt.% solids

Solids prepared from slag benefited greatly from the presence of a gypsum or calcium chloride solid phase during preparation. As seen in Section 5.1.3.2, the presence of CaCl_2 maintained a substantial calcium concentration in solution for the formation of high surface area solids. The SEM micrograph shown in Figure 5.19, however, suggested that the silicates prepared with CaCl_2 were different than those prepared with gypsum present. Figure 6.12 shows that the SO_2 reactivity of

sorbents prepared with CaCl_2 was substantially lower than that expected from the high surface area of the solids. It appeared that even though CaCl_2 was successful in producing a high surface area product, that surface area was not as reactive with SO_2 .

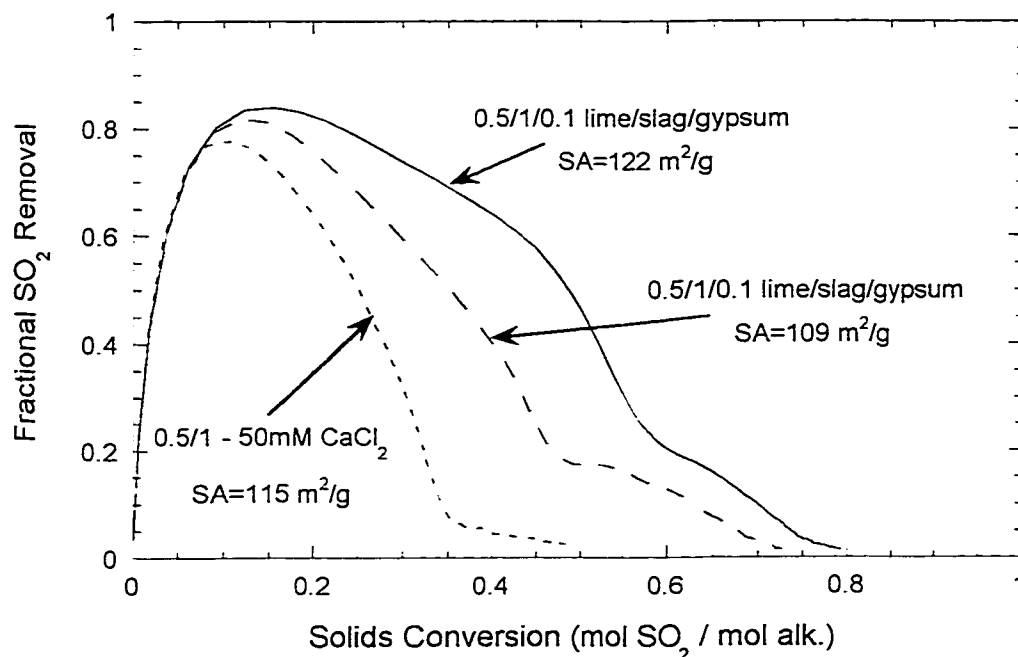


Figure 6.12: Reactivity of Slag Sorbents Prepared with CaCl_2

50°C; 58% RH; ~1000 ppm SO_2
 1.521 slpm total; 0.1 g sorbent
 Slag ADV w/ gypsum: 8/2/98-21 & -30
 Slag ADV w/ chloride: 8/17/98-21
 experiment #: 76, 81, 86

One hypothesis is that the CaCl_2 in the liquid solution remained in the pores of the solid after filtering, and precipitated during the drying process. This precipitate has a high surface area, but is not reactive towards SO_2 . The X-ray pattern of this sorbent shown in Figure 5.20, however, did not show any crystalline CaCl_2 which would be the expected precipitate.

Sorbents have been prepared by previous researchers from flyash and silica fume. Two of these sorbents prepared by Kurt Kind in a batch, agitated reactor at 92°C were tested for SO₂ reactivity. As shown in Section 4.3.3, the surface area of these solids degraded over several years of storage. Figure 6.13 shows the reactivity of these solids compared to glass sorbents of various surface areas. There was a good comparison between the silica fume sorbent and the glass sorbent having equal surface areas. This implied that even though these sorbents have partially crystallized, as shown in Figure 4.27, the correlation between surface area and reactivity held for the solid prepared from silica fume.

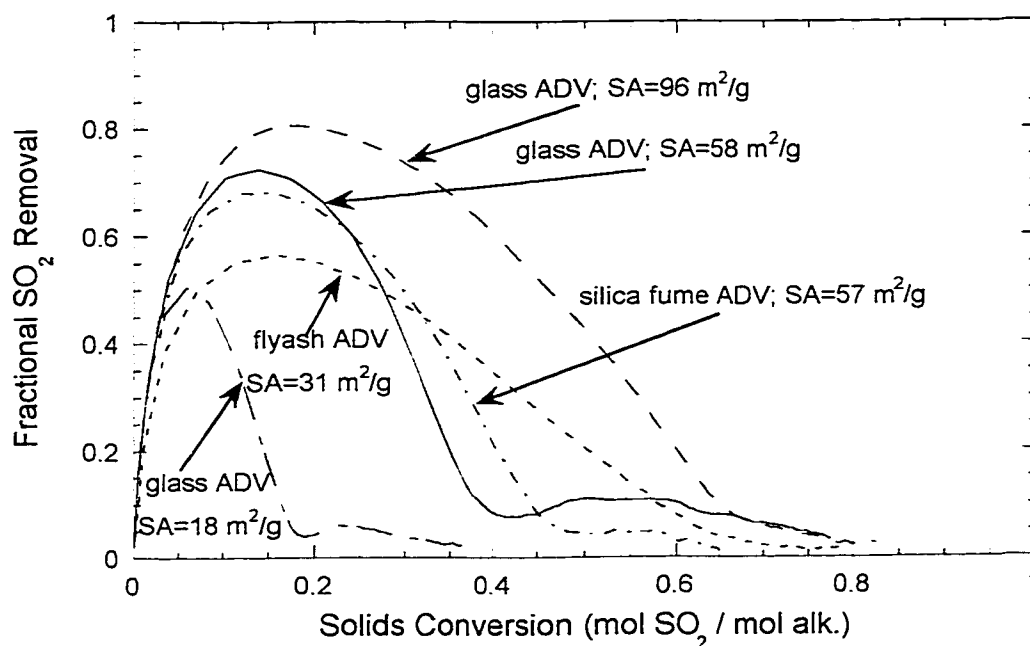


Figure 6.13: Reactivity of Sorbents Prepared from Flyash or Silica Fume

50°C; 58% RH; ~1000 ppm SO₂

1.521 slpm total; 0.1 g sorbent

Slag ADV w/ gypsum: 11/21/94-5 & -25; 4/28/97-50

Flyash ADV: 0.5/1 lime/flyash - 0.1M CaCl₂; 5/10/93-12*

Silica Fume ADV: 1/1 lime/fume; 8/18/92-4*

experiment #s: 51, 55, 58, 84, 85

*: prepared by Kind (1994)

The flyash sorbent was prepared with 0.2 N CaCl_2 in solution. As seen earlier, glass sorbent prepared with CaCl_2 exhibited lower reactivity than expected from surface area. The flyash / CaCl_2 sorbent reactivity appeared to fall within expected limits, considering the degraded surface area, though the shape of the curve was slightly abnormal. This unexpected curvature may be simply due to experimental scatter in the SO_2 reaction, or a real manifestation of the difference in solids composition. Figure 4.27 clearly shows that the flyash and silica fume sorbents were not made up solely of the amorphous CSH seen in the glass sorbents. However, the correlation between amorphous CSH and reactivity does not appear to be constant, as evidenced by the low reactivity of CSH prepared from slag with CaCl_2 .

6.4 CHARACTERIZATION OF SOLIDS AFTER REACTION WITH SO_2

Because the primary goal of this research was to optimize the preparation of sorbents from recycled glass or blast-furnace slag, and not a fundamental study of the SO_2 / alkaline solid reaction, indepth characterization of the reacted sorbents was not done. What measurements were taken to further the understanding of the system are presented in this section.

6.4.1 Verification of Final Conversions

The sorbents prepared from glass and slag showed extreme potential for higher SO_2 reactivity than hydrated lime. Many SO_2 experiments reached upwards of 80-90% solids conversion after an hour. Because of the extremely high conversions, and the potential economic benefit of maximizing this characteristic of the sorbent, the precision of that measurement was questioned.

Reacted solids from the sandbed, including the sand, were analyzed by the technique outlined in Section 3.1.3.4. Some difficulty was encountered by the presence of the sand which made the phenolphthalein endpoint difficult to determine. Table 6.1 shows the results of alkalinity titrations on sandbed runs with glass sorbent (4/28/97-50). The results assume a starting alkalinity of 6.6 mmol/g sorbent.

The results show that titration of the solids always resulted in lower solids conversions. Because of the difficulty in determining the endpoint, the gas phase conversion is the more trusted of the numbers.

Table 6.1: Alkalinity Titrations of Reacted Sandbed Solids

Sandbed Run ID	Solids Conversion via Alkalinity Titration	Solids Conversion via Gas Phase Analysis	% Difference
51	80	83	3.6
59	83	88	5.7
71	72	81	11
72	72	75	4.0

6.4.2 Surface Area and Porosity Degradation

It has been hypothesized that pore closure of the solids might occur as alkaline solids are reacted with SO_2 . The reaction product, CaSO_3 in this case, must have certainly precipitated somewhere on the solid. Given the high porosity of these sorbents, it was expected that a loss of porosity would be seen.

Full scale reacted solids characterization was difficult because of the sand used for dispersion. The sand is used specifically so that the sorbent will adhere to its surface. It was determined that separating the reacted solids from the sand would provide an unrepresentative sample and be unfruitful for the given scope of this project.

One sandbed experiment was conducted without sand, however, for the purpose of analyzing the reaction product. In this experiment, glass wool was placed in the reactor, resting on the glass frit. The sorbent was then placed in a heap on top of the glass wool. After exposure, the glass wool was removed carefully and the majority of the solids were recovered. Gas phase analysis of the reaction at 50°C , 58% RH, and ~ 1000 ppm showed 56% conversion. This was lower than the 80-90% normally seen, probably due to the poor contact between the SO_2 and undispersed solids.

Figure 6.14 shows the cumulative pore volume distributions for unreacted sorbent and the reacted solids from this particular experiment. The porosity decreased from 0.437 to 0.336 cm^3/g and the surface area from 96.3 to 66.4 m^2/g .

This indicates that there was indeed a degradation of the solid structure during the reaction, but not complete closure of a significant fraction of the porosity.

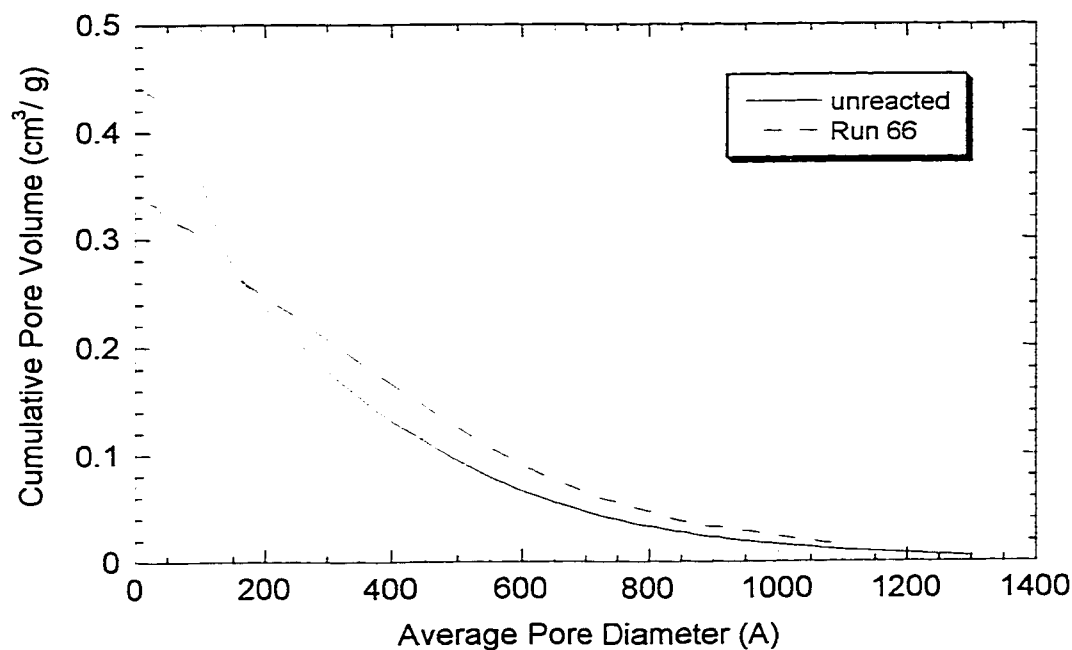


Figure 6.14: Porosity of Unreacted and Reacted Solids

58-59% RH; ~1000 ppm SO₂; 1.521 slpm total
 0.1 g sorbent; 4/28/97-50; SA=96 m²/g
 sorbent dispersed on 0.6 g glass wool
 experiment #: 66

6.4.3 X-ray Pattern of Reacted Solids

The X-ray diffraction pattern of the reacted sorbent was also measured as shown in Figure 6.15. The peaks at 2-Theta equal to 27.7, 28.8, and 48.7 correspond to calcium sulfite hemihydrate (PDF# 36-527, JCPDS, 1997). Another primary peak from this solid phase is expected at 26.1 2-Theta, but was not seen in Figure 6.15. The entire spectrum of peaks was not analyzed for all solid solution possibilities.

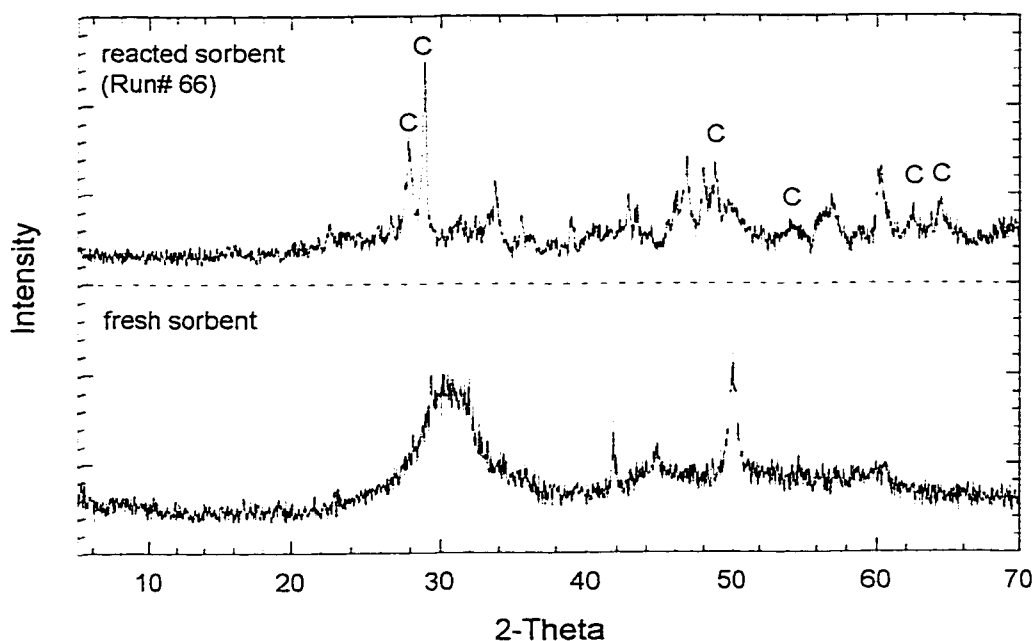


Figure 6.15: X-ray Pattern: Sorbent after SO₂ Reaction

58-59% RH; ~1000 ppm SO₂; 1.52l slpm total
0.1 g sorbent; 4/28/97-50; SA=96 m²/g
sorbent dispersed on 0.6 g glass wool
experiment #: 66
c: Calcium Sulfite Hemihydrate Peaks

6.5 REACTION MODELING

This section describes efforts to model the SO₂ reaction with high surface area silicates in a humid gas stream.

6.1.2 Experimental Reproducibility

Any model with regressed parameters is naturally limited by the limitations of the experimental data from which the parameters are regressed. Figure 6.16 presents the results from five sandbed experiments at nominally identical conditions.

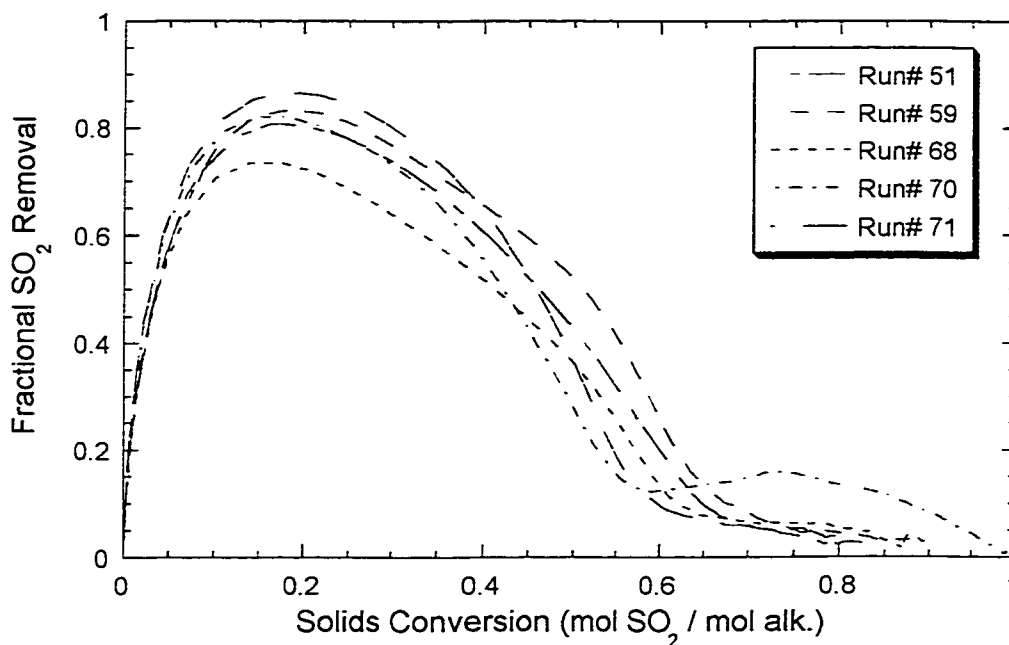


Figure 6.16: Precision of Sandbed Experimental Results

50°C; 58% RH; ~1000 ppm SO₂

1.521 slpm total; 0.1 g sorbent

Sorbent: 4/28/97-50 (glass ADVACATE)

It is clear from Figure 6.16 that the sandbed system had precision limitations. The most likely problem was poor dispersion of the sorbent on the sand. The procedure for dispersing the sorbent was to first weigh the powder into a beaker. The sand was then weighed into the same beaker, and the mixture stirred carefully by hand with a metal spatula. When the sorbent was no longer distinguishable from the sand, the entire mixture was poured into the reactor. If the sorbent was not dispersed evenly, it is possible that channeling, or uneven gas/solid contact occurred. This would explain the variations seen in Figure 6.16.

In light of the obvious deviation from one nominally identical experiment to another, care should be taken not to over-interpret modeling results. While one experiment may regress a certain set of parameters, many experiments were not

repeated, and therefore the regressed parameters for any singular experiment may not be entirely representative of those particular experimental conditions.

6.5.1 Reactor Integration Model

As mentioned previously, the sandbed reactor system utilized in this work was a semi-batch, un-steady state system. Therefore, to compare experimental measurements to any point model of the SO₂ removal rate, the SO₂ concentration must be calculated through the bed by integrating the model in both space and time. It was assumed that the SO₂ gas stream would behave in an ideal plug-flow manner and that the solids were uniformly distributed through the bed. The concentration change would therefore be defined by Equation 6.3.

$$\frac{QdC_{SO_2}}{Adz} = \frac{dC_{SO_2}}{dt} = -R_{SO_2} \quad (6.3)$$

By taking very small finite steps in both the time and space variables, this differential equation can be numerically integrated by Euler's method. This assumes that within small enough time and space steps the SO₂ concentration is constant. The sorbent bed was divided into 200 space steps and the concentration profile was calculated for 1 second time steps. The point model, calculated at each space and time step, was defined as a rate of SO₂ removal based on the solids conversion and SO₂ concentration at that time and place. The calculated SO₂ removal defined the SO₂ concentration in the gas stream heading to the next space step, and the conversion of the solids for that particular space step. This is described by the following equations.

$$\begin{aligned} [SO_2]_{i,t} &= [SO_2]_{i-1,t} - rate_{i-1,t} \\ rate_{i,t} &= f([SO_2]_{i,t}, conv_{i,t-1}) \end{aligned} \quad (6.4-6)$$

$$conv_{i,t} = \sum_{t=0}^t (rate_{i,t} / alk_i)$$

where $i \equiv$ space steps from 1 to 200.

alk_i = moles divalent alkalinity per space step.

Every two seconds, the timelag model described in Appendix C was applied to the outlet model concentration. Timelag coefficients were calculated only for two second time intervals due to experimental limitations during the timelag step change experiments. It should be noted that the timelag constants were not regressed during every experiment. Only the step change experiments described in Appendix C were used to calculate the coefficients used in the timelag correction.

Every 30 seconds the outlet concentration (ppm), corrected for the analytical timelag, was outputted for comparison with the apparent experimental SO₂ concentration indicated by the SO₂ analyzer. To more equally weight data at both high and low SO₂ concentrations, the logarithm of both the model concentration (ppm) and the experimental measurement indicated by the SO₂ analyzer (ppm) were compared.

The reactor integration model was coded in FORTRAN 77 and compiled on a local unix-based mainframe. The FORTRAN code is archived in Appendix E. Parameter estimation was achieved through the use of the Generalized Regression Package - Level 10 (Caracotsios, 1986). This non-linear parameter estimation package was designed to estimate the parameters of a user-defined model by minimizing the square of errors between arrays of data from the model estimation and measured observations.

As stated previously, the logarithm of the SO₂ concentration (ppm) values predicted by the model and measured experimentally were used for comparison. Therefore, the error in $\ln([SO_2])$, not $[SO_2]$, was minimized as defined in Equation 6.3. The number of observations per experiment was typically about 120, corresponding to 30 sec intervals for a one hour experiment.

$$\text{sumerr} = \sum_{\#obs} (\ln C_{\text{model}}(\text{ppm}) - \ln C_{\text{measured}}(\text{ppm}))^2 \quad (6.7)$$

6.5.2 Rate Model Derivation

A semi-empirical model was derived to fit the SO₂ concentration data. The hypothesized physical system shown in Figure 6.17 provided the functionality of

the model. However, it should be noted that considering the experimental limitations and the lack of physical evidence to support this hypothesized system, this model should be assumed to be unproven. The author recommends in Chapter 7 that further reacted solids characterization be conducted to test the physical validity of this model.

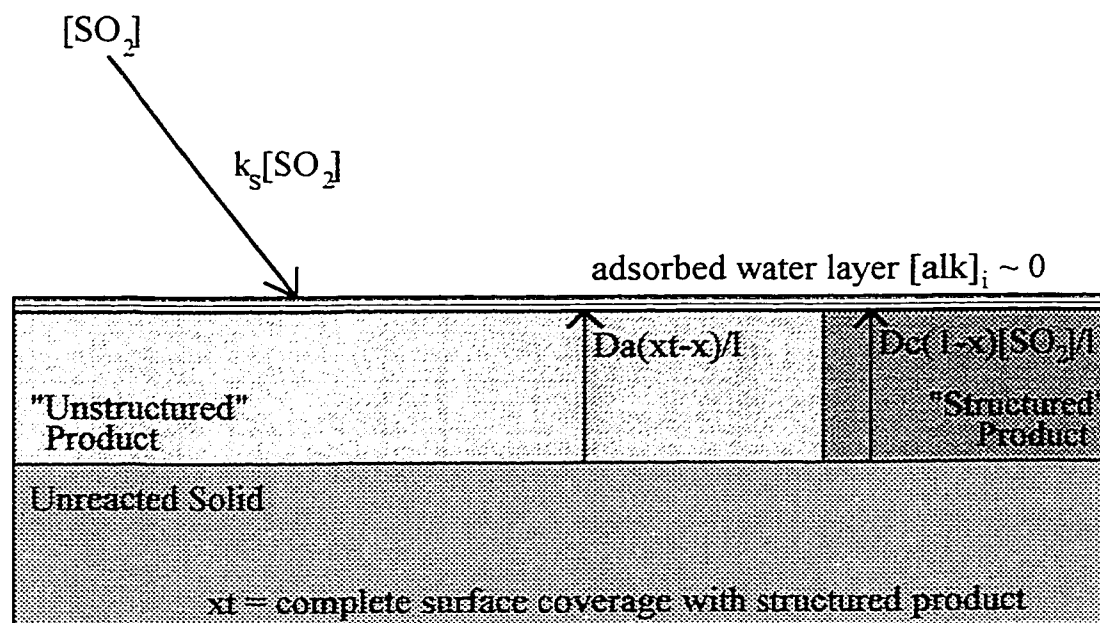


Figure 6.17: Physical System for SO_2 / Solid Reaction Model

Because of the very high surface area of the solid, the model was derived as a flat solid with processes occurring in one-dimension. This is in contrast to some previous models which used a 3-dimensional shrinking core model, for instance. The model was based on three primary phenomena occurring in the system. At the earliest of times, when no product was expected to exist, the rate was determined by the convective mass transfer of SO_2 to the water layer adsorbed on the surface of the solid as shown by Equation 6.8. Because the rate of reaction was assumed to be faster than mass transfer, the SO_2 interfacial concentration was assumed to be negligible.

$$\text{rate} = k_s([\text{SO}_2]_{\text{bulk}} - 0) \quad (6.8)$$

Almost immediately, however, a product layer consisting of CaSO_3 and silicic acid started to form. This first product formation was expected to be poorly structured, without time for the products to nucleate or crystallize. Equation 6.9 illustrates the rate of alkalinity diffusion through this product layer to the adsorbed water layer, where it reacts with SO_2 . It was assumed that the alkalinity was the diffusing component, in contrast to the SO_2 . Therefore, the driving force was related to the amount of alkalinity reacted, i.e. conversion. The parameter x_t is a transitional conversion which will be defined later in this description.

$$\text{rate} = \frac{K_{Da}(x_t - x)}{x} \quad (6.9)$$

Therefore, at moderate times, the rate was controlled by the two processes outlined in Equations 6.8-9. It was assumed that they would behave as resistances in series as shown in Equation 6.10.

$$\text{rate} = \frac{1}{\frac{1}{k_s[\text{SO}_2]_{\text{bulk}}} + \frac{x}{K_{Da}(x_t - x)}} \quad (6.10)$$

As time proceeded, however, the product layer had time to nucleate and crystallize, forming a more structured product layer with lower diffusivity. This rate was relatively much slower than the previous two phenomena, and it was assumed that at this slower rate, the SO_2 concentration may once again have a first order role as shown in Equation 6.11.

$$\text{rate} = \frac{K_{Dc}(1 - x)[\text{SO}_2]_{\text{bulk}}}{x} \quad (6.11)$$

It was assumed that the two diffusion processes would occur in parallel with each other as the surface of the product transformed from the unstructured product into the structured product. At the transition conversion, x_t , the surface of the solid was considered completely covered with the structured product. Assuming that this transformation was linear with conversion, a fraction (f_{xn}) related to the transition conversion x_t was defined. Therefore, the weighting of the

rate on the two processes was linearly transferred from Equation 6.10 to Equation 6.11 as conversion increased. At conversions greater than x_t , the rate was defined by Equation 6.11, because this rate was slower and now represented the rate-limiting step. This parallel system was represented by Equations 6.12-13.

$$\text{rate} = \frac{1 - \text{fxn}}{\frac{1}{k_s[\text{SO}_2]_{\text{bulk}}} + \frac{x}{K_{\text{Da}}(x_t - x)}} + \frac{\text{fxn} * K_{\text{Dc}}[\text{SO}_2]_{\text{bulk}}}{\frac{x}{1 - x}} \quad (6.12)$$

$$x < x_t: \text{fxn} \equiv \frac{x}{x_t} \quad (6.13)$$

$$x \geq x_t: \text{fxn} = 1.0$$

where: $x_t \equiv$ conversion with complete structured product layer coverage

$x =$ conversion (mole SO_2 removed / mol alkalinity⁺² in bed)

$[\text{SO}_2] =$ SO_2 concentration (mole fraction (m.f.))

$k_s [=]$ mol SO_2 / m.f. / sec / m^2

$K_{\text{Da}} [=]$ mol SO_2 / sec / m^2

$K_{\text{Dc}} [=]$ mol SO_2 / m.f. / sec / m^2

rate $[=]$ mol SO_2 / sec / m^2

Equations 6.12-13 represent the empirical model with four adjustable parameters, k_s , K_{Da} , K_{Dc} , and x_t , used to represent the rate of SO_2 removal in this work. Several other empirical models were tried, but with less success than the model presented here.

Figure 6.18 shows the results of the point model described above, integrated through the packed bed. Because the model results have been integrated through the bed, the solids conversion is representative of the average solids conversion throughout the bed, not the point conversion. Both the model results at the reactor outlet before and after the analytical timelag correction are shown.

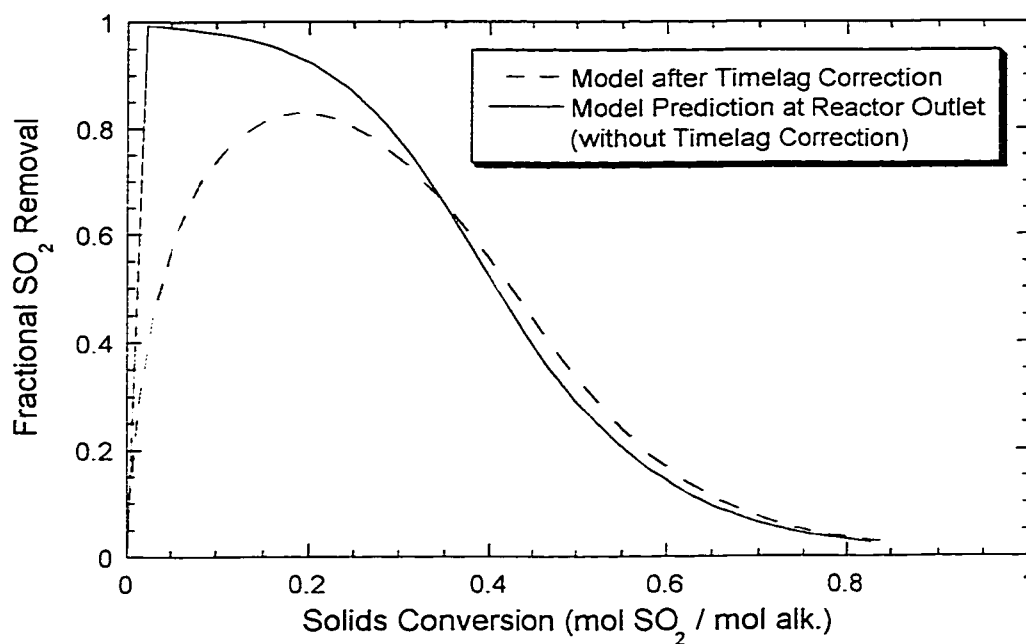


Figure 6.18: Effect of Timelag Correction on Model Prediction

Parameters regressed for Run#s: 51, 59, 68, 71
 Run Conditions: 50°C, 58% RH; ~1000 ppm SO₂
 Sorbent: 4/28/97-50 (glass ADVACATE)
 Regressed Model curve calculated at 1000 ppm

6.5.3 Model Fit and Parameters

Model parameters were regressed to fit experiments conducted with glass ADVACATE sorbents prepared from a 1/1/0.5 lime/glass/gypsum mixture. The model fit experimental data reasonably well from experiment to experiment. Figure 6.19 shows the regressed model fit for two experiments in which the model parameters were regressed separately for each. The parameters and confidence intervals for all individual regressions, including the two experiments shown in Figure 6.19, are presented in Table 6.2.

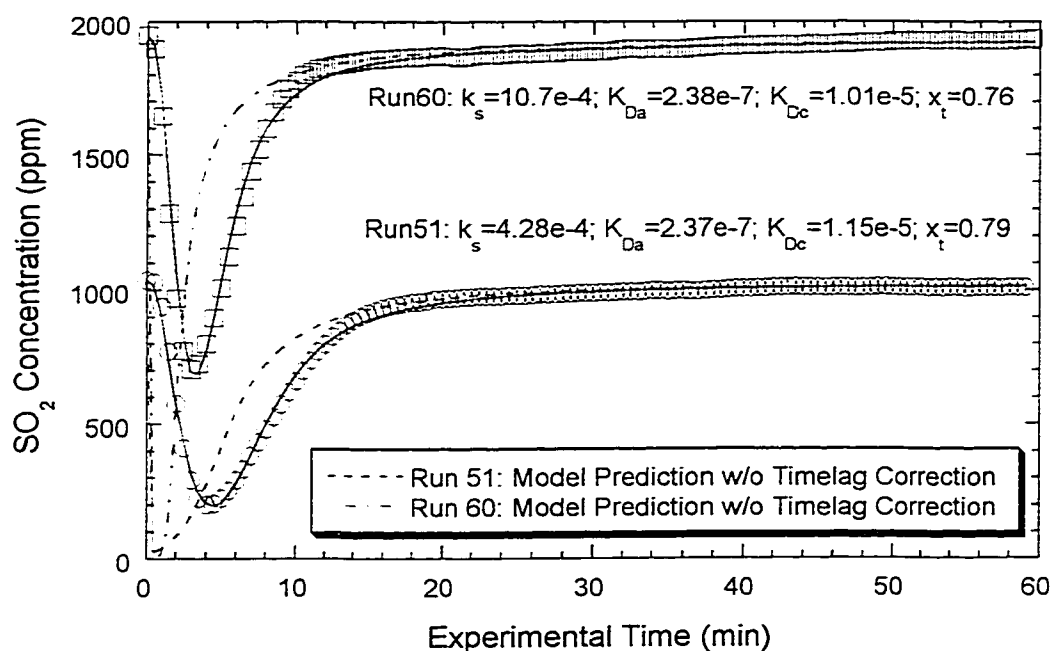


Figure 6.19: Model Fit for Individually Regressed Experiments

Run Conditions: 50°C, 58% RH; ~1000 ppm SO₂
 Sorbent: 4/28/97-50 (glass ADVACATE)

The parameters for five experiments, conducted at a solids loading of 0.025 g, were not regressed to the model (Run#s 67, 74, 80, 77, 79). In hindsight, the low solids loading coupled with the relatively high SO₂ concentration, placed these experiments outside of reasonable experimental limits. This is because the bulk of the reaction and solids conversion was occurring very quickly, and within the timelag period. While the timelag had been modeled separately, it was decided that data collected within a regime that was already highly dependent on a model with regressed parameters was perhaps less reliable. Furthermore, the remainder of the experimental data obtained after the initial reaction period represented very low SO₂ removal, and therefore a test of analytical precision. This is because removal was then the difference between two large measurements.

For many of the regressions, the parameter x_t naturally regressed to the conversion at which the rate decreased to a much slower rate. This 'knee' is

evident in Figure 6.16 at ~65%. For experiments which were difficult to converge due to experimental scatter, the parameter x_t was not regressed, and was fixed to the 'knee' indicated by the experimental data.

In light of the experimental deviations from one experiment to another, baseline regressions were established in which model parameters were regressed for several experimental runs simultaneously. The results from simultaneous regressions are presented in Table 6.3. Figure 6.20 shows the model results using parameters simultaneously regressed for four runs at nominally identical conditions of 50°C, 58% RH, and 1000 ppm SO₂. The results in Figure 6.20 have been integrated through the packed bed. Normally this integration tended to magnify errors in the model fit, since most of the error occurred at low conversions and was compounded throughout the integration. Figure 6.20, however, shows that the simultaneous regression fits the experimental data well.

A more global set of parameters presented in Table 6.3 was simultaneously regressed for seven experiments at 50°C and 58% RH. These included four of the experiments shown in Figure 6.20 as well as two experiments with a higher solids loading (0.2 g) and one with a higher SO₂ concentration. Using the global set of parameters, Figure 6.21 shows the best and worst fits of the model from the set of regressed experiments.

Table 6.2: Regressed Parameters for Individually Modeled Experiments
 Sorbent: 4/28/97-50; 1/1/0.5 lime/glass/gypsum; 92°C; agitated; surface area = 96m²/g; (except where noted)
 *Regression package unable to converge
 Confidence intervals represent 95% (2sigma) levels.

T	RH	Run#	Date	SO ₂ in	Solid	Notes	k _s * 10 ⁴	K _{Da} * 10 ⁷	K _{Dc} * 10 ⁵	X _t	sumerr	err/pt
(°C)	%			(ppm)	(g)		mol/mf/s/m ²	mol/s/m ²	mol/mf/s/m ²	mol/mol alk.		Eq. 6.14
50	58	57	2/2/98	500	0.1	Exp Prob.	*	*	*	*		36.1
50	58	51	1/20/98	1000	0.1		4.28±0.25	2.37±0.49	1.15±0.38	0.79±0.04	0.063	7.9
50	58	59	2/5/98	1000	0.1		5.39±0.83	1.71±0.77	1.64±0.11	0.83±0.10	0.319	11.6
50	58	68	6/1/98	1000	0.1		3.70±0.55	1.34±0.56	1.98±0.6	0.76±0.10	0.174	4.0
50	58	70	6/9/98	1000	0.1	2nd hump	92.2±57.8	10.6±11.7	26.8±7.6	0.65±0.23	0.684	43.7
50	58	71	6/10/98	1000	0.1		7.93±2.3	1.95±1.21	1.27±0.7	0.68±0.10	0.669	14.5
50	59	60	2/12/98	2000	0.1		10.7±4.6	2.38±0.72	1.01±0.30	0.76±0.05	0.0407	5.4
50	58	88	9/14/98	1000	0.2	2 hr. exp	4.12±0.47	0.774±0.441	2.35±0.45	0.734±0.15	1.348	10.2
50	58	89	9/15/98	1000	0.2	2 hr. exp	3.57±0.32	0.984±0.417	1.57±0.62	0.793±0.11	1.522	9.2
50	58	69	6/1/98	1000	0.1	5% O ₂	45.9±2.0	76.8±23.5	16.6±2.4	0.69±0.02	0.0465	48.1
50	58	72	6/10/98	1000	0.1	5% O ₂	16.2±10.7	2.38±1.7	0.838±0.6	0.63±0.10	1.04	23.7
50	29	73	8/17/98	500	0.1		4.95±0.90	2.29±0.68	0.242±0.09	0.286set	0.5196	
50	29	87	8/30/98	500	0.1		5.89±1.50	1.14±0.30	0.263±0.11	0.295set	0.672	
50	29	50	1/20/98	1000	0.1		15.0 ± 2.9	3.30 ± 0.46	0.138±.018	0.396 ± 0.01	0.0085	
50	29	78	8/20/98	2000	0.1		*	*	*	*		
36.5	59	54	1/28/98	1000	0.1		5.57±0.65	5.52±1.24	0.714±0.25	0.57set	0.274	
69.5	59	61	2/17/98	1000	0.1	Exp Prob.	5.82±1.01	3.13±2.8	5.29±1.76	0.81±0.15	0.402	
50	0	52	1/27/98	1000	0.1		169±41	3.70±6.42	0set	0.108set	0.0018	
50	88	53	1/27/98	1000	0.1		6.55±0.59	16.2±6.9	0set	1.0set	1.86	
Sorbent: 11/21/94-5 (Surface Area = 18 m ² /g)												
50	58	55	1/31/98	1000	0.1	Exp Prob.	1105±49	*11.4	1.03±0.14	0.236set	0.0298	
Sorbent: 11/21/94-2.5 (Surface Area = 58 m ² /g)												
50	58	58	2/2/98	1000	0.1	2nd hump	15.1±8.0	6.51±6.21	1.44±0.21	0.39±0.05	0.121	

The last column in Table 6.2 presents a measure of the relative fit of each individual experiment, whether parameters were regressed or not, with the global model at 50°C and 58% RH. Given the minimized sum of squares defined according to Equation 6.7, the error/point value in Table 6.2 is defined according to Equation 6.14. This error/point value was calculated to give an average relative measure of fit for experiments with different numbers of observations. Since this value represents essentially the square root of a sum of squares, it is not an indication of whether the model generally over- or under-predicted the experimental data. An error/point value of 0.00% indicates a perfect fit of model to experimental data.

$$\text{sumerr} = \sum_{\text{\#obs}} (\ln C_{\text{model}}(\text{ppm}) - \ln C_{\text{measured}}(\text{ppm}))^2 \quad (6.7)$$

$$\text{error / pt(\%)} = 100 \left[\left(\frac{\text{model}_t}{\text{meas}_t} \right) - 1 \right] = 100 \left[\exp \left(\sqrt{\frac{\text{sumerr}}{\text{\#observations}}} \right) - 1 \right] \quad (6.14)$$

Table 6.3: Simultaneous Model Regression Results

	$k_s \cdot 10^4$	$K_{Da} \cdot 10^7$	$K_{Dc} \cdot 10^5$	x_t	sumerr
Simultaneous Regression for 1000 ppm / 58% RH					
Run#s 51, 59, 68, 71	5.95±0.70	1.36±0.37	1.57±0.58	0.801±0.07	2.096
Simultaneous Regression for 58% RH					
Run#s 51, 59, 68, 71, 60, 88, 89	3.50±0.13	1.52±0.16	1.36±0.27	0.75 set	8.906
Simultaneous Regression for 29% RH					
Run#s 50 and 73	3.83±0.48	2.79±0.86	0.156±0.094	0.341set	1.570

Table 6.3 also presents the parameters regressed for two experiments conducted at 50°C and 29% relative humidity. It was expected that these parameters would differ from those regressed at 58% RH, because the qualitative experimental data was dramatically different. The results presented in Table 6.3 show that only the parameters K_{Dc} and x_t changed greatly. K_{Dc} dropped by about a factor of 9 and x_t decreased from 0.75 to 0.34 as shown in the experimental data.

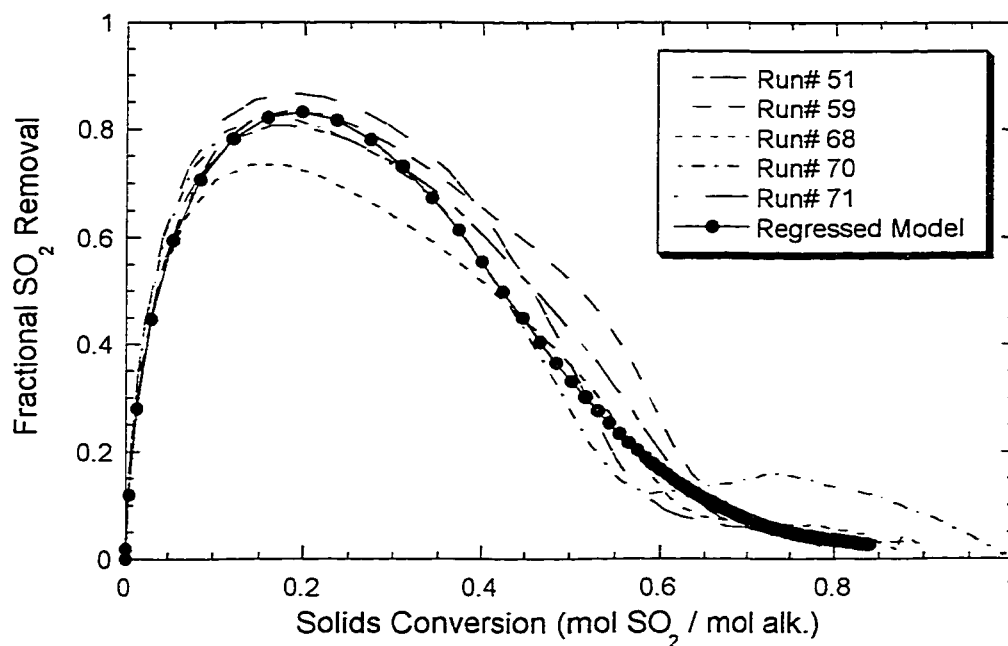


Figure 6.20: Regressed Model Compared to Experimental Precision

50°C; 58% RH; ~1000 ppm SO₂

1.521 slpm total; 0.1 g sorbent: 4/28/97-50 (glass ADVACATE)

Parameters simultaneously regressed Run#s: 51, 59, 68, 71 (not 70)

$k_s = 5.95e-4$; $K_{da} = 1.36e-7$; $K_{dc} = 1.57e-5$; $x_t = 0.80$

Regressed Model curve calculated at 1000 ppm

The value of the x_t parameter naturally converged to the experimentally measured 'knee' for many experiments. Therefore, it appeared that the model accurately predicted the functionality of this transition. The values for K_{Da} , however, regressed to $\sim 10^{-7}$ (mol SO₂ / s / m²). This converts to a diffusion coefficient (D_a) of $\sim 10^{-20}$ (m²/s), which is unreasonable even for solid diffusion. In light of this, and of the poor convergence of the model with sorbents of different surface areas shown in Table 6.2, it is believed that the model did not accurately represent the effects of surface area. Both the K_{Da} and K_{Dc} parameters were derived as strong functions of surface area.

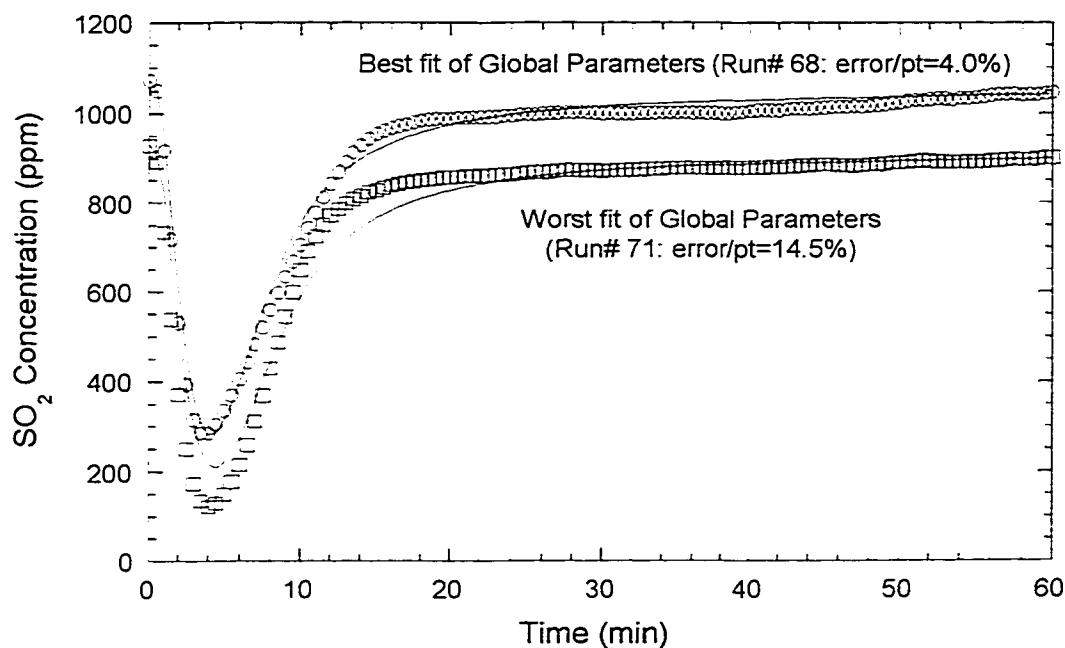


Figure 6.21: Best and Worst Fit of Global Parameters at 50°C / 58% RH

50°C; 58% RH; ~1000 ppm SO₂

1.521 lpm total; 0.1 g sorbent: 4/28/97-50 (glass ADVACATE)

Parameters simultaneously regressed for Run#s: 51, 59, 68, 71, 60, 88, and 89.

$k_s=3.50\text{e-}4$; $K_{Da}=1.52\text{e-}7$; $K_{Dc}=1.36\text{e-}5$; $x_t=0.75\text{set}$

6.5.4 Predicted Baghouse Behavior

The primary goal of developing a model for the SO₂ / sorbent reaction was to create a predictive tool to estimate the possible performance of a baghouse filter. This section presents the predictive results of the model developed above for a bagfilter.

The SO₂ point model developed here was integrated through a growing filter cake representative of a bagfilter operation. In contrast to the sandbed reactor, in which the entire sorbent bed is present at time zero, the filter cake in a bagfilter grows with time until the bag is cleaned by reverse pulsing or mechanical shaking. The amount of sorbent being added is defined by the stoichiometric ratio,

which equals the molar ratio of alkalinity added and SO_2 in the gas stream. The total time of accumulation between cleanings for one bag was defined as filter cake accumulation. This is also equal to the time to clean all of the bags in the system, and is defined here as cycle time. The difference arises when considering which concentration is being monitored, the flow from one bag, or the average flow from the entire system.

The FORTRAN code representing this system is presented in Appendix E. It used the same model developed above to represent SO_2 removal as a function of SO_2 concentration and solids conversion. In this case, a fresh layer of sorbent was considered applied to the front edge of the bed at each time step. The amount of sorbent added was determined by the stoichiometric ratio multiplied by the SO_2 inlet rate. The concentration profile of the bed was then calculated at each time step (sec). This is most easily represented by defining the origin of our space axis at the surface of the bagfilter. Therefore at each time step, the following relationships apply.

$$\begin{aligned} i_t &= i_{t-1} + 1 \\ [\text{SO}_2]_{i_t} &= [\text{SO}_2]_{\text{in}} \\ \text{conv}_{i_t} &= 0.0 \end{aligned} \tag{6.15}$$

where i_t represents the total # of space intervals at time t .

Figure 6.22 shows the model prediction for the bagfilter outlet at a stoichiometric ratios (mol alkalinity fed / mol SO_2) of 1.0 and 1.5. This instantaneous removal is indicative of the outlet concentration from a single bag, not of the entire baghouse.

Figure 6.23 presents the prediction for a bagfilter operation as a function of cycle time. The average removal indicated here is indicative of the average over the entire baghouse, as defined by Equation 6.16. The predicted removal (White, 1989) using hydrated lime as the sorbent is also shown in Figure 6.23. It is clear that the calcium silicate solid is a strong improvement over hydrated lime, which only provides 33% removal at a stoichiometry of 1.5 with a 60 minute cycle time.

$$\text{avg. removal} = \frac{\sum_{t=0}^t 100 * \frac{[\text{SO}_2]_{\text{in}} - [\text{SO}_2]_{\text{out},t}}{[\text{SO}_2]_{\text{in}}}}{t} \quad (6.16)$$

where: $[\text{SO}_2]$ [=] ppm

It is clear from the Figures 6.22-23 that increasing relative humidity increases SO_2 removal. It should also be noted that Nelli (1997) showed that the presence of NO_2 in the gas stream would increase the SO_2 removal.

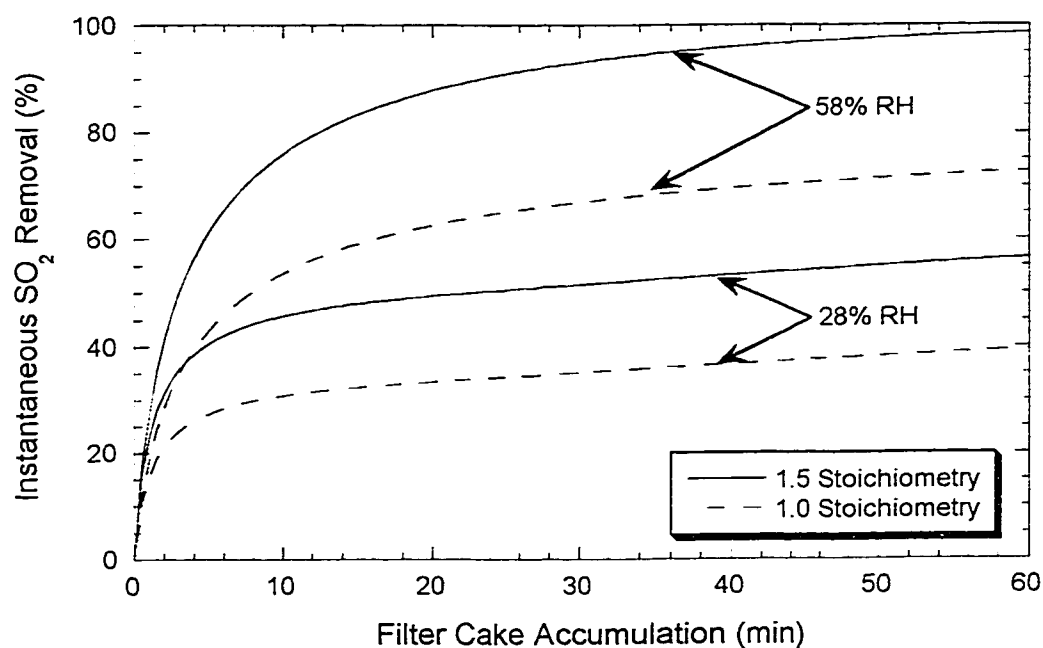


Figure 6.22: Individual Bagfilter Performance

1000 ppm SO_2 ; 50°C

Using Glass ADVACATE; 4/28/97-50; 96 m²/g

Model Parameters Used:

58%: $k_s=3.50\text{e-}4$; $K_{Da}=1.52\text{e-}7$; $K_{Dc}=1.36\text{e-}5$; $x_t=0.75$

28%: $k_s=3.83\text{e-}4$; $K_{Da}=2.79\text{e-}7$; $K_{Dc}=0.156\text{e-}5$; $x_t=0.341$

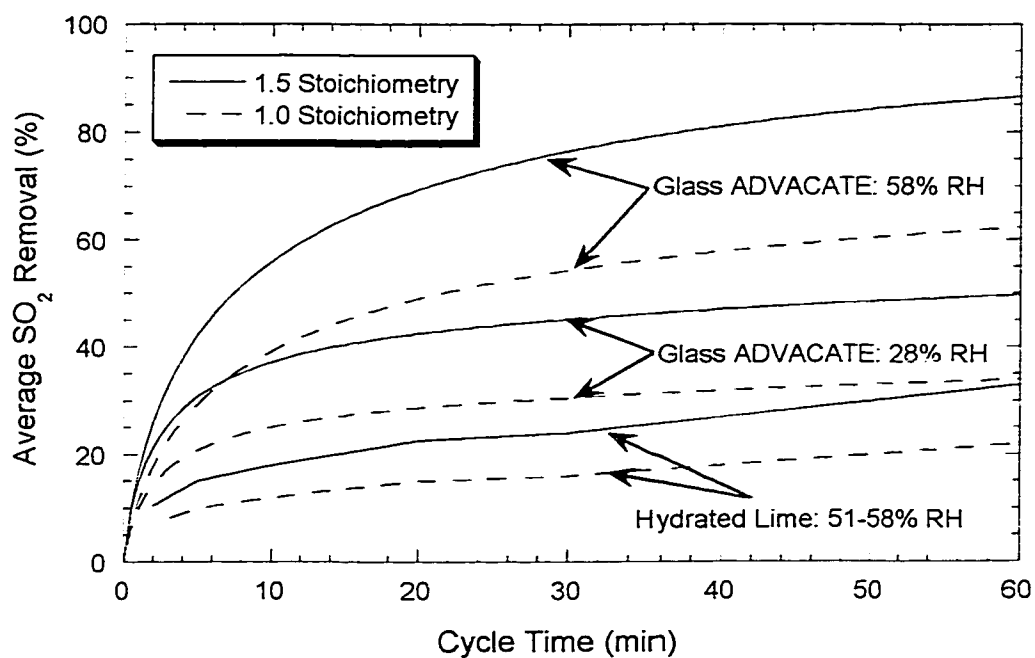


Figure 6.23: Overall Baghouse Filter Performance

1000 ppm SO₂; 50°C

Using Glass ADVACATE; 4/28/97-50; 96 m²/g

Model Parameters Used:

58%: $k_s=3.50\text{e-}4$; $K_{Da}=1.52\text{e-}7$; $K_{Dc}=1.36\text{e-}5$; $x_t=0.75\text{set}$

28%: $k_s=3.83\text{e-}4$; $K_{Da}=2.79\text{e-}7$; $K_{Dc}=0.156\text{e-}5$; $x_t=0.341\text{set}$

Figure 6.24 shows the effect of the stoichiometric ratio for a given relative humidity of 58%. Utilization is a normalized stoichiometric ratio, equal to the moles of SO_2 removed / moles alkalinity fed to the system. It appears from the graph that the SO_2 removal decreases rapidly as utilization increases past a certain point. This range of utilization with rapid changes in SO_2 removal corresponds to stoichiometric ratios of about 2. At lower utilization, i.e. higher stoichiometric ratio, the removal approaches 100%.

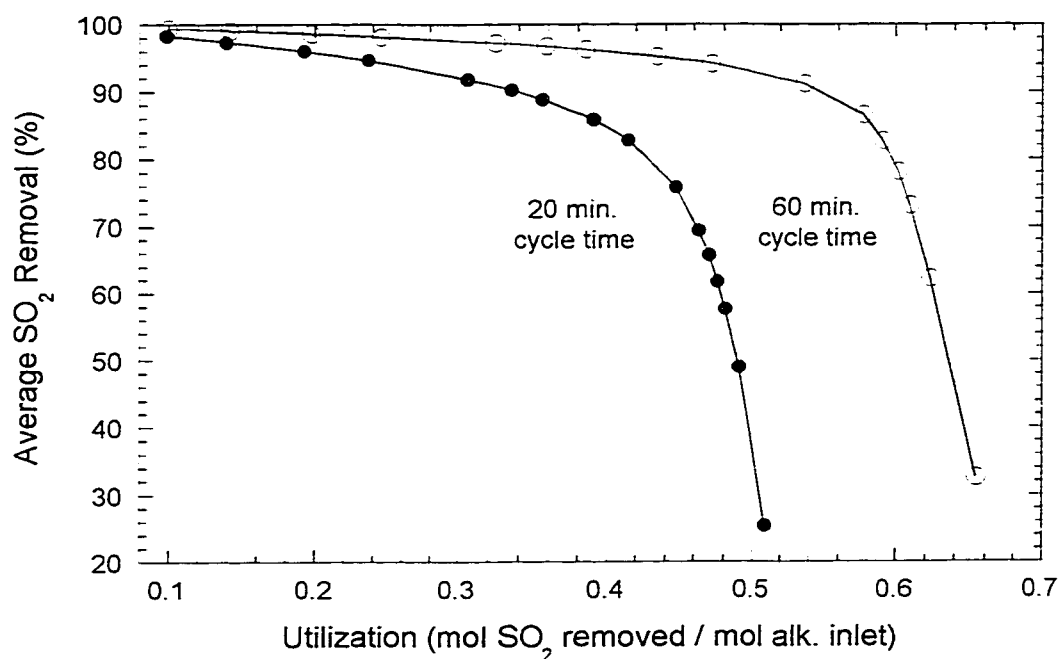


Figure 6.24: Effect of Alkalinity Utilization

1000 ppm SO_2 ; 50°C; 58% RH

Using Glass ADVACATE; 4/28/97-50; 96 m^2/g

Model Parameters Used:

$k_s=3.50\text{e-}4$; $K_{Da}=1.52\text{e-}7$; $K_{Dc}=1.36\text{e-}5$; $x_t=0.75\text{set}$

The average removal as a function of SO_2 concentration is presented in Figure 6.25 for a 60 minute cycle time. It is clear from the graph that increasing inlet SO_2 concentration results in higher average SO_2 removal. It should be noted

that this range of SO_2 concentration represents a broad extrapolation from the experimental data range of 500-2000 ppm.

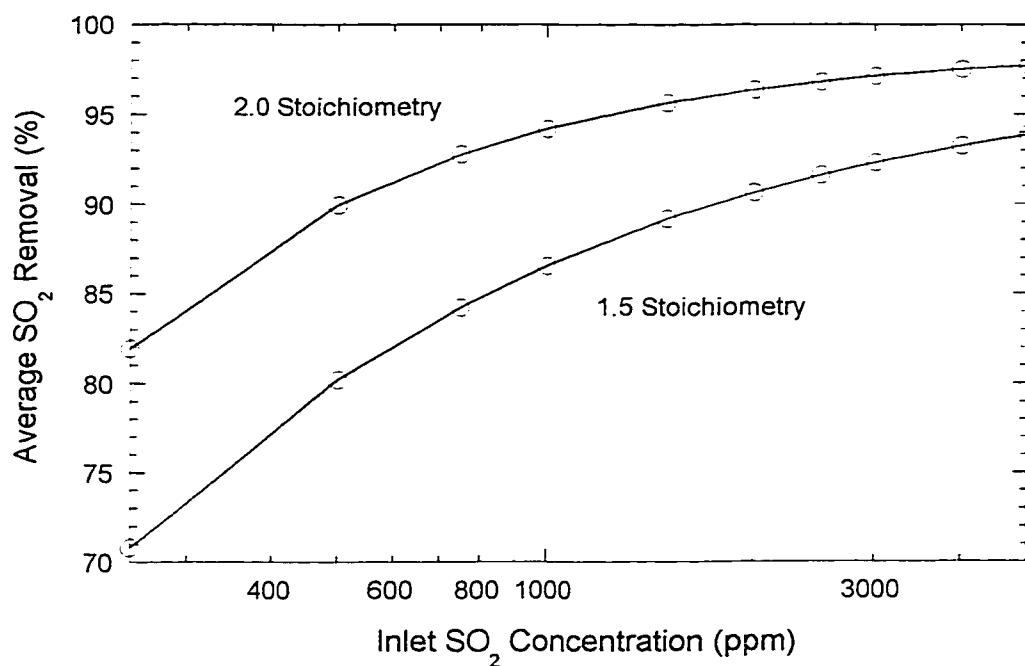


Figure 6.25: Effect of SO_2 Concentration

1 hour cycle time

50°C; 58% RH

Using Glass ADVACATE; 4/28/97-50; 96 m^2/g

Model Parameters Used:

$k_s=3.50\text{e-}4$; $K_{Da}=1.52\text{e-}7$; $K_{Dc}=1.36\text{e-}5$; $x_t=0.75\text{set}$

Table 6.4 presents predictions of average SO_2 removal for a baghouse operating at 58% relative humidity and a range of SO_2 concentration and stoichiometric ratio.

Table 6.4: Baghouse Predictions of Average SO_2 Removal
 50°C; 58% RH
 Using Glass ADVACATE; 4/28/97-50; 96 m²/g
 Model Parameters Used:
 $k_s=3.50\text{e-}4$; $K_{Da}=1.52\text{e-}7$; $K_{Dc}=1.36\text{e-}5$; $x_t=0.75\text{set}$

Stoichiometry = 1.0			
	250 ppm	1000 ppm	5000 ppm
5 min	14.66	29.32	40.72
60 min	51.68	62.34	73.37
300 min	69.02	77.36	88.52
Stoichiometry = 2.0			
	250 ppm	1000 ppm	5000 ppm
5 min	27.12	53.32	74.31
60 min	81.96	94.20	97.76
300 min	96.29	98.84	99.55
Stoichiometry = 3.0			
	250 ppm	1000 ppm	5000 ppm
5 min	37.54	69.69	89.61
60 min	90.44	97.28	99.13
300 min	98.09	99.45	99.83

The ultimate operating parameter in a baghouse, however, is not cycle time as much as pressure drop. Therefore, for a given operating system, the limiting factor to SO_2 removal will be the amount of solids the bags can hold before cleaning. Assuming a constant gas flow rate of F/A (mol gas / min / m²) and a cycle time of 60 min, a bagfilter operating at a stoichiometric ratio of 2.0 and SO_2 concentration of 1000 ppm will deposit solids equal to 0.12 F/A (mol alk / m²). Table 6.5 presents the average SO_2 removal at extreme ranges of operating conditions, i.e. 250 ppm / 1.0 stoic. and 5000 ppm / 3.0 stoic., in which the total

amount of solids collected remains constant. The total amount of solids in Table 6.5 is also varied to extreme conditions of 0.015F/A and 0.5F/A (mol alk / m²), compared to a typical value of 0.12F/A (mol alk / m²).

Table 6.5: Baghouse Predictions Holding Solids Loading Constant
 50°C; 58% RH
 Using Glass ADVACATE; 4/28/97-50; 96 m²/g
 Model Parameters Used:
 $k_s=3.50e-4$; $K_{Da}=1.52e-7$; $K_{Dc}=1.36e-5$; $x_t=0.75$ set

Cycle Time (min) / SO ₂ Removal (%)			
Solids=0.015F/A	250 ppm	1000 ppm	5000 ppm
1.0 Stoic. Ratio	60 min / 51.68%	15 min / 45.05%	3 min / 33.89%
2.0	30 min / 68.24%	7.5 min / 62.80%	1.5 min / 48.55%
3.0	20 min / 72.93%	5 min / 69.69%	1 min / 57.84%
Solids=0.12F/A	250 ppm	1000 ppm	5000 ppm
1.0	480 min / 72.58%	120 min / 69.10%	24 min / 62.07%
2.0	240 min / 95.37%	60 min / 94.20%	12 min / 88.79%
3.0	160 min / 96.42%	40 min / 95.92%	8 min / 93.51%
Solids=0.50F/A	250 ppm	1000 ppm	5000 ppm
1.0	2000 min / 83.09%	500 min / 81.70%	100 min / 78.98%
2.0	1000 min / 98.89%	250 min / 98.61%	50 min / 97.31%
3.0	667 min / 99.14%	167 min / 99.02%	33 min / 99.21%

Chapter 7: Conclusions and Recommendations

This work investigated the preparation of silicate sorbents using recycled container glass or iron blast furnace slag as an amorphous silica source. The reaction between these solids and SO_2 was also studied. This chapter summarizes the main conclusions from this work. A more detailed discussion of these conclusions is located in Chapters 4-6. The chapter concludes with the author's recommendations for further work.

7.1 SORBENT PREPARATION FROM GLASS

The addition of gypsum to the lime/glass system formed solids with much higher surface area at 92°C . The gypsum solid phase quickly converted into either the hemihydrated or anhydrous form upon the start of the reaction. The presence of the CaSO_4 solid, however, was able to maintain a sufficient calcium concentration in solution to allow the silicate hydration reaction to continue for very long times. When the calcium concentration was allowed to drop below 1 mM, i.e. if gypsum was not added, then the formation of surface area slowed drastically.

Increasing the temperature of the slurry to 120°C increased the surface area of solids formed at short reaction times. The rate of surface area formation slowed remarkable after $170 \text{ m}^2/\text{g}$ glass of surface area formed, however, ultimately forming lower surface area solids than were prepared at 92°C . The addition of gypsum at 120°C increased the calcium concentration, and therefore surface area, only marginally. This is probably due to the very low solubility of CaSO_4 at 120°C . The addition of CaCl_2 maintained a higher calcium concentration, yet the rate of surface area formation also slowed after $170 \text{ m}^2/\text{g}$ glass. X-ray diffraction patterns of sorbents prepared at 120°C indicated that a more crystalline solid phase was being formed. This crystalline solid phase was most like responsible for the lower surface area formed at 120°C .

Agitation showed no effect on the surface area below $70 \text{ m}^2/\text{g}$ when solids were prepared with gypsum. Varying the solids content between 20% and 50% during non-agitated preparation also had no effect for solids up to $70 \text{ m}^2/\text{g}$. Above

this surface area, agitation positively affected the surface area, though solids content was not overly important.

The rate of surface area formation was directly proportional to the initial surface area of the glass. This will have a direct impact on the economics of the process. An economic analysis between the amount of grinding and the reaction time will be necessary to determine the optimum initial glass size.

The rate of surface area degradation of the glass sorbent was measured and indicated that while the sorbent is fairly stable, shelf-life should be limited to a few months. Within some scatter, a value of 1.6 %change/time ($\text{m}^2/\text{g}/\text{month}$) was determined.

The rate of silica dissolution from glass was faster when calcium silicates were not precipitating. This indicated that while the dissolution of the glass may be the initial chemical rate-limiting step, it was not the rate limiting step during sorbent preparation. Most likely, a diffusion process through the calcium silicate product layer was rate-limiting.

The lime/glass/gypsum reaction mixture formed CSH and surface area up to $130 \text{ m}^2/\text{g}$, even when the lime or CaSO_4 solids phase was no longer visible by X-ray diffraction. Solids prepared with gypsum at various reaction times were analyzed. The gypsum solid phase very quickly converted into the anhydrous or hemihydrate form of CaSO_4 . Both the CaSO_4 and lime were visible until the solid reached $\sim 60 \text{ m}^2/\text{g}$. After this, neither crystalline phase was evident, only the more amorphous pattern of calcium silicate hydrate (CSH).

7.2 SORBENT PREPARATION FROM SLAG

Sulfide is one of the unique constituents found in slag which is released as the silica matrix dissolves. The addition of H_2O_2 eliminated sulfide in solution beyond detection. The addition of $\text{SO}_3^{=}/\text{S}_2\text{O}_3^{=}$ not only decreased the rate of surface area formation, it increased the sulfide in solution. The addition of FeSO_4 decreased the amount of sulfide to a finite, but measurable, concentration in solution.

Considering the extremely high concentration of lime naturally in slag, it was desired to prepare high surface area solids using a minimal amount of

additional lime. However, a substantial amount of additional lime was needed to maintain the high pH necessary to facilitate the reaction. In fact, X-ray diffraction shows that excess lime was present as $\text{Ca}(\text{OH})_2$ in most of the slag sorbents, even those conducted at a 0.5/1 lime/slag ratio. This indicated that the lime was being used to maintain a pH, and that the intrinsic lime in the slag was, indeed, being consumed to form calcium silicates.

The addition of gypsum was extremely helpful by increasing the calcium concentration in solution and forming higher surface area solids. Reactions without any additives maintained a calcium concentration at ~ 5 mM, which should have been sufficient according to the results seen in the experiments conducted with glass. It was clear, however, that the addition of gypsum was beneficial.

The addition of CaCl_2 also increased the solution calcium substantially as well as the rate of surface area formation. The SEM of the CaCl_2 sorbent, however, indicated that this solid was different from those prepared from glass or slag, with or without gypsum. While the SEM of those solids appeared to be smoothly amorphous, the SEM of the slag/ CaCl_2 solid appeared textured, or "fluffy". The X-ray pattern of this solid showed excess lime and the typical CSH pattern. It was expected that perhaps CaCl_2 had precipitated on the surface, but this was not visible from X-ray. The porosity of this solid was also lower than a solid prepared from gypsum with the same surface area. The SO_2 reactivity of this solid was studied and is commented on in Section 7.3.

7.3 SORBENT REACTION WITH SO_2

Varying relative humidity, at a constant temperature of 50°C , had a remarkable effect on both the rate of SO_2 removal as well as the maximum solids conversion. At zero relative humidity, a small amount of SO_2 was removed, and only 11% of the alkalinity reacted after an hour. The rate of SO_2 removal and maximum solids conversion increased with increasing relative humidity up to 87%, though the reaction at 87% appeared to be of a different functionality than those at 29% and 58% RH. Realistically, 87% RH is not feasible in an industrial application due to problems caused by condensation and subsequent agglomeration of the solids.

The rate of reaction with SO_2 was strongly dependent on the surface area of the sorbent. Increasing surface area dramatically increased both the rate of SO_2 removal and the maximum conversion of the solids. This result seemed independent of the method of preparation, except in the case of slag sorbents prepared with CaCl_2 . In this instance the SO_2 reactivity was significantly lower than expected from the surface area. This led to the conclusion that while high surface area was necessary for high SO_2 reactivity, it was not sufficient.

Solids after reaction with SO_2 had X-ray patterns indicative of calcium sulfite hemihydrate. The porosity of the solids decreased during the SO_2 reaction.

The addition of oxygen did not have a significant effect on the removal of SO_2 as was expected. Previous researchers have hypothesized that the oxidation of sulfite to sulfate increased the diffusion limited rate of SO_2 reaction with sorbent. It is thought that the solids used in this work may have been too reactive for the oxygen effect to be pronounced.

Varying temperature, with relative humidity held constant, had a small effect on the rate of SO_2 removal and a notable positive effect on the maximum solids conversion.

The precisional limitations of this particular packed bed reactor system was investigated. It was shown that while qualitative comparisons between one reaction and another are feasible, one should be careful not to over interpret a single, unreproduced experiment. The most likely problem in this system was thought to be poor dispersion of the sorbent.

A semi-empirical model for the SO_2 / glass sorbent system showed that for a baghouse filter cycle time of one hour at 58% relative humidity, a stoichiometric ratio of 1.5 will achieve 87% removal from a 1000 ppm SO_2 gas stream. Increasing the stoichiometry to 2.0 and the gas concentration to 2000 ppm increased the removal efficiency to 94%. The calcium silicate prepared in this work represents an immense improvement over hydrated lime, which White (1989) predicted would achieve 33% average removal in a baghouse with a cycle time of 60 min, at a stoichiometric ratio of 1.5.

7.4 RECOMMENDATIONS

While both the sorbent preparation and SO_2 reaction systems have been studied extensively, the following areas may warrant further research.

Investigate the preparation of sorbent with gypsum present under low-temperature, non-agitated conditions, high solids loading. This would represent the minimum in production costs.

Investigate the SO_2 / sorbent reaction in conjunction with detailed reacted sorbent characterization. Determine the physical system, the rate-limiting processes, and the exact reaction products. Determine the fundamental impact of relative humidity on the system.

Investigate the impact of chloride on the sorbent preparation and SO_2 / sorbent systems. Previous research, as well as this work, showed contradictory effects of chloride. Analyze how this will impact systems with chloride in the flue gas or flyash.

Considering the slurry chemistry results shown with high alkalinity silica sources, investigate the preparation of sorbent from high-calcium flyash or portland cement.

It is hypothesized that at high or low calcium concentrations the product precipitates on the surface of the silica source or the lime, respectively. Attempt to make calcium silicates by dissolving amorphous silica with NaOH , and then adding CaCl_2 slowly. The goal is to precipitate product in the bulk solution, not on either surface.

Appendix A: Analytical Procedures

This appendix outlines the operating procedures for the main analytical equipment used during the course of this research. These procedures are derived both from equipment operating manuals and personal experience. In some instances, these procedures and rules-of-thumb are specific to modifications made to these particular apparatus.

A.1 ATOMIC ABSORPTION STANDARD OPERATING INSTRUCTIONS

A.1.1 Initial Preparations.

- Connect Back-up Battery.
- Plug AA in, and turn on.
- Install correct lamp, and set current. (lamp needs 0-30 minutes to warm up)
- Rinse and refill water trap. Be sure to re-connect drainage tubing!!!
- Clean and install correct burner, using card to align correctly.
- Set slit width and detector wavelength. Maximize signal on analog meter, using "SB Auto Gain" to recalibrate when the signal is too strong.
- Open cylinder valves in utility corridor. Regulators should be set at 8-10 psig for Acetylene, and 60 psig for N₂O (if used).

A.1.2 Start-up.

- Set instrument to "SB Auto Gain", "Internal Repeat", "ABS"
- Select burning type.
- Turn on hood.
- Press "flame on" to light flame. (This sometimes takes several tries. If process does not reach point of ignition, try increasing fuel supply. If ignitor tries, but doesn't succeed in lighting flame, turn off hood while lighting to decrease breeze through area. If using acet/N₂O burner, you can also light using acet/air setting, and then switch to acet/N₂O setting. This sometimes helps.)
- Adjust fuel and oxidant flows to suggested settings.

A.1.3 Aligning it all.

- Let AA run blank solution to clear system out.
- Aspirate calibration standard and compare absorbance reading to value in manual. If too low, try adjusting vertical and horizontal position of burner, or burner ratio. You should be able to get 50%-100% of literature absorbance.
- Set AA to "CONC", "RUN MEAN", "DB".
- Input standard values: "Value Std. 1" and entering standard one, etc. note: only use as many decimal places as your largest standard will have.

A.1.4 Calibrating.

- Place aspiration tube into zero solution; press "READ"; wait for signal to stabilize; press "CAL Zero"
- Place aspiration tube into lower standard solution; press "READ"; wait for signal to stabilize; press "CAL STD1"
- Place aspiration tube into higher standard solution; press "READ"; wait for signal to stabilize; press "CAL STD2"
- Place aspiration tube into zero solution; press "READ"; wait for signal to stabilize; press "CAL Zero"

note: You can recalibrate the zero point of the curve without redoing the entire curve.

A.1.5 Running Samples.

- Test each sample.
- Recalibrate as needed. This instrument's calibration will drift!

A.2 BET SURFACE AREA STANDARD OPERATING INSTRUCTIONS

These procedures apply specifically to analyzing calcium silicate solids on the Micromeritics ASAP 2010.

A.2.1 Preparing Samples

- Weigh sample bomb, filler rod, and valve plug cap. (Make sure they are clean and dry!)
- Place ~1 g sample into bomb using funnel.

- Use tissue to clean any residual powder inside the tube above the fill line (typically where the bomb label is located). The sample must be below the top of the liquid nitrogen (LN2) wicking system.
- Carefully place (do not drop!) filler rod into bomb, and cover with valve plug.

A.2.2 Degassing Samples

note: Always use Manual control for degassing powders. The Automatic protocol is too harsh and will boil the powder into the degas manifold.

- Load sample onto a degas (or analysis) port, being sure that rubber gasket is correctly placed around tube of sample bomb, and finger tighten locking nut.
- Pressurize the manifold to atmospheric pressure with nitrogen. DO NOT OVERPRESSURE! The nitrogen tank is typically at ~5psig, which the manifold cannot withstand. Be alert to close valve when atm pressure light comes on.
- Open valve from manifold to sample.
- Evacuate manifold and sample with slowing restriction (open slow degas valve) until a pressure reading is registered on manifold pressure gauge. (three decimal points indicates a reading out of range)
- When pressure is substantially lower (i.e. a pressure reading is registered on gauge), open the unrestricted valve to the vacuum pump.
- For most calcium silicates, overnight degassing at ambient temperatures is normally sufficient. If the surface area is particularly high ($>100 \text{ m}^2/\text{g}$) a longer degassing time may be necessary.
- To check sample outgassing rate, close valves to vacuum pump, leaving sample open to manifold. Observe the increase in manifold pressure. Recommended maximum outgassing rate is $0.1 \text{ } \mu\text{m Hg} / \text{sec}$.
- When sample is outgassed, close valves to vacuum pump. Pressurize manifold and sample to atmospheric pressure. Close valve to sample and remove sample from port. Weigh sample bomb, etc. with sample.

A.2.2 Preparing for Analysis

- Fill cold trap and analysis dewars with liquid nitrogen (LN2) to where the liquid level is between the hole and the end of the dipstick tool. Hang cold

trap dewar on metal lip and cover with foam insulator. Place analysis dewar in dewar elevator.

- Create a new sample information file for each sample. There is space for sample identification as well as all analysis procedures. For normal BET surface area measurements of calcium silicates, adsorption pressure readings below $0.1 P/P_{\text{sat}}$ are used. For pore size distributions, BJH desorption measurements are taken. **DO NOT USE FAST EVACUATION WITH POWDERS!** Report options may be changed after analysis, but analysis points and details may not, so choose carefully.

A.2.3 Analyzing

- Load sample onto analysis port, again being careful that the rubber gasket is in place, and finger tighten the locking nut.
- Choose analyze on computer interface. It will prompt you for the sample information file pertaining to your sample.

A.2.4 Reports

- Choose Start Report on computer interface. It will prompt you for the sample information file pertaining to your sample. In the sample information file, you can alter which reports are generated, the formatting of those reports, and which data points are used for which calculations.

Appendix B: Experimental Data

This appendix serves to archive the raw data collected during the course of this research. While most of the data is referred to in the previous dissertation text, no discussion is present in this section. There is also some data archived in this section that is not referred to previously.

B.1 RAW MATERIALS

Table B.1: Ground Recycled Glass

Mesh Size	Mesh Diameter (μm)	Measured BET Surface Area (m^2/g)	Average BET Surface Area (m^2/g)
80-100	149-177	0.14	0.12
		0.16	
		0.06	
100-120	125-149	0.18	0.11
		0.07	
		0.07	
270-325	44-53	0.29	0.27
		0.27	
		0.26	
<325	<44	0.55	0.52
		0.51	
		0.51	
Second Batch			
30-80	177-590	0.04	0.04
		0.04	
80-200	74-177	0.08	0.10
		0.12	
<325	<44	0.39	0.38
		0.37	
		0.41	
		0.39	
		0.35	

B.2 ABSORBENT PREPARATION FROM GLASS EXPERIMENTS

Table B.2: Absorbent Preparation from Glass Experimental Results

Sample ID: Date experiment started.
 Time: Reaction time for particular sample.
 Norm Time: Reaction time * SA_0 / SA_{0ref} ; $SA_{0ref} = 0.381 \text{ m}^2/\text{g}$.
 % Solids: 100 * g initial solids / g (solids + water)
 Initial Area: Initial Glass Surface Area
 SA: Surface area of solid sample (m^2/g).
 Norm SA: SA * wt. total initial solids (g) / wt. initial glass (g)
 pH: ambient pH of liquid filtrate
 Ca / Na: calcium / sodium concentration of liquid filtrate.
 Dival. Alk.: Divalent Alkalinity determined by pH titration (See Section 3.1.3.4)
 - : not measured
 x: X-ray data available, See Table B.4.

B.2.1 Agitated Experiments

1/1 lime/glass - 92°C

Sample ID	Time	Norm	Solids	Initial	SA	Norm SA	pH	Ca	Na	Dival.
(date)	(hr)	(hr)	%	Area	m^2/g	m^2/g glass		mM	mM	Alk. mMol/g
1/19/94	3	4.12	20	0.523	21.69	43.38	12.87	0.98	80.80	-
1/19/94	6	8.24	20	0.523	32.12	64.24	13.03	0.46	116.10	-
1/19/94	9	12.35	20	0.523	35.41	70.82	13.07	1.03	127.90	-
1/19/94	11.5	15.79	20	0.523	37.27	74.54	13.11	1.02	131.00	-

1/31/94	0	0.00	20	0.523	10.34	20.68	12.33	12.91	6.95	-
1/31/94	0.25	0.34	20	0.523	9.50	19.00	12.34	8.37	9.53	-
1/31/94	0.5	0.69	20	0.523	8.58	17.16	12.48	9.49	14.40	-
1/31/94	1	1.37	20	0.523	11.62	23.24	12.60	7.38	27.30	-
1/31/94	3	4.12	20	0.523	25.39	50.78	12.86	1.00	42.40	-
1/31/94	6	8.24	20	0.523	32.80	65.60	12.98	0.92	122.70	-
11/28/94	10	10.00	20	0.381	47.88	95.76	13.04	1.48	-	-
11/28/94	20	20.00	20	0.381	53.97	107.93	13.08	1.50	-	-
11/28/94-x	32	32.00	20	0.381	64.24	128.47	13.15	1.16	-	-
11/28/94-x	40	40.00	20	0.381	69.49	138.98	13.17	1.46	-	-

1/1 lime/glass - 120°C

9/25/96	1	1.00	16.7	0.381	40.78	81.56	-	2.46	81.40	-
9/25/96	5	5.00	16.7	0.381	64.70	129.40	-	1.37	126.60	-
9/25/96-x	10	10.00	16.7	0.381	69.82	139.64	-	1.09	156.70	-
9/25/96-x	23	23.00	16.7	0.381	82.75	165.50	-	1.04	185.50	6.82
9/25/96	33	33.00	16.7	0.381	90.90	181.80	-	1.07	-	-

1/1/0.5 lime/glass/gypsum - 92°C

3/2/94	2	2.75	20	0.523	15.04	37.60	12.23	20.60	25.12	-
3/2/94	4	5.49	20	0.523	23.56	58.90	12.39	17.25	59.06	-
3/2/94	6	8.24	20	0.523	30.86	77.15	12.04	12.30	77.97	-
3/2/94	8	10.98	20	0.523	21.07	52.69	12.42	14.53	118.50	-
3/2/94	10	13.73	20	0.523	29.97	74.92	12.50	12.74	146.14	-
3/5/94-x	10	13.73	20	0.523	37.95	94.88	12.23	15.40	122.44	-

3/5/94	14	19.22	20	0.523	51.88	129.70	12.30	12.40	163.48	-
3/5/94	17	23.34	20	0.523	62.51	156.26	12.46	12.15	215.98	-
3/5/94	20	27.45	20	0.523	70.05	175.12	12.55	14.10	255.50	-
4/4/94	30	41.18	20	0.523	87.51	218.79	12.11	10.40	330.40	-
4/4/94	34	46.67	20	0.523	102.57	256.42	8.95	9.22	312.30	-
4/4/94	45	61.77	20	0.523	119.92	299.81	8.69	8.10	382.30	-
4/4/94	50	68.64	20	0.523	129.59	323.98	8.45	8.87	433.90	6.5
8/22/94-x	10	7.17	20	0.273	23.97	59.93	12.38	14.73	75.13	-
8/22/94	27	19.35	20	0.273	54.37	135.93	12.58	18.84	210.87	-
8/22/94	46	32.96	20	0.273	84.27	210.67	12.52	14.95	340.47	-
8/22/94	54	38.69	20	0.273	90.86	227.15	12.20	10.08	414.85	-
11/21/94-x	5	5.00	20	0.381	20.98	52.45	-	-	-	5.23
11/21/94	21	21.00	20	0.381	69.08	172.71	-	-	-	-
11/21/94-x	25	25.00	20	0.381	62.40	156.00	-	-	-	6.09
11/21/94	33	33.00	20	0.381	82.05	205.13	-	-	-	-
11/21/94	42	42.00	20	0.381	116.59	291.48	-	96.76	241.89	-
11/21/94	50	50.00	20	0.381	128.63	321.57	-	113.38	283.46	-
4/28/97-x	44.65	44.65	20	0.381	105.1	262.75	-	-	-	6.61
4/28/97	50	50.00	20	0.381	115.6	289.00	-	-	-	6.60
4/28/97	55	55.00	20	0.381	119.1	297.75	-	-	-	-
4/28/97-x	68	68.00	20	0.381	126.3	315.75	-	-	-	6.54

1/1/0.5 lime/glass/gypsum - 120°C

7/21/94	3	4.12	20	0.523	31.67	79.18	12.74	3.98	156.50	-
7/21/94	5.5	7.55	20	0.523	69.20	172.99	12.94	1.04	220.30	-
7/21/94	9	12.35	20	0.523	74.43	186.09	12.97	1.02	255.20	-
7/21/94	23	31.57	20	0.523	75.58	188.96	12.98	0.52	248.90	-
12/6/94	4	4.00	20	0.381	45.95	114.88	13.00	6.03	-	-
12/6/94	8	8.00	20	0.381	65.95	164.88	13.09	2.48	-	-
12/6/94-x	15	15.00	20	0.381	72.43	181.08	13.28	1.11	-	5.73

3/1/0.5 lime/glass/gypsum - 92°C

6/16/98	5	5	22	0.381	28.70	129.15	12.45	20.60	-	-
6/16/98	10	10	22	0.381	44.23	199.04	12.48	18.10	-	-
6/16/98	24	24	22	0.381	68.70	309.15	12.55	18.80	-	-
6/19/98	39	39	22	0.381	82.32	370.44	12.64	10.50	-	-
6/19/98	48	48	22	0.381	85.36	384.12	12.69	6.70	-	-

1/1/0.3 lime/glass/chloride - 120°C

9/19/96	1	1	18.7	0.381	40.37	92.85	-	196.50	84.60	-
9/19/96	5	5	18.7	0.381	73.46	168.96	-	144.90	178.20	-
9/19/96	11	11	18.7	0.381	84.45	194.24	-	131.40	205.80	-
9/19/96-x	24	24	18.7	0.381	90.02	207.05	-	119.00	268.40	-
9/19/96	35	35	18.7	0.381	98.26	226.00	-	117.10	304.20	-

B.2.2 Non-agitated Experiments

1/1/0.5 lime/glass/gypsum - 92°C

Sample ID	Time (hr)	Norm Time (hr)	% Solids	Initial Area m ² /g	SA m ² /g	Norm SA m ² /g glass	DiValent Alk. mMol/g
(date)							
3/6/95	1	1.00	20	0.381	6.84	17.11	-
3/6/95	3	3.00	20	0.381	12.38	30.95	-
3/6/95	5	5.00	20	0.381	15.26	38.16	-
3/6/95	20	20.00	20	0.381	35.20	87.99	-
3/25/95	10	10	20	0.381	20.14	50.34	-
3/25/95	48	48	20	0.381	56.14	140.35	-
3/25/95	53	53	20	0.381	61.85	154.63	-
1/22/97	2	2	20	0.381	15.51	38.78	-
1/22/97	6	6	20	0.381	33.65	84.13	-
1/22/97	19.08	19.08	20	0.381	63.58	158.95	-
1/22/97	25.75	25.75	20	0.381	67.04	167.60	-
1/22/97-x	43	43	20	0.381	91.97	229.93	5.3
1/22/97	50	50	20	0.381	96.44	241.10	-
4/7/97-x	66.75	66.75	20	0.381	96.46	241.15	-
4/7/97	66.75	66.75	20	0.381	95.76	239.40	-
4/7/97-x	90	90	20	0.381	78.68	196.70	-
4/7/97	90	90	20	0.381	82.61	206.53	-
8/7/97	50	50	20	0.381	81.7	204.25	-
9/17/97	72.25a	72.25	20	0.381	103.7	259.25	-

9/17/97	72.25c	72.25	20	0.381	102.7	256.75	-
10/3/97	66a	66	20	0.381	106.2	265.50	-
10/3/97	66c	66	20	0.381	102	255.00	-
12/20/95	3.2	3.2	33	0.381	13.79	34.48	-
12/20/95	7	7	33	0.381	28.21	70.53	-
12/20/95	10.2	10.2	33	0.381	36.10	90.25	-
12/20/95	25	25	33	0.381	58.18	145.45	-
1/16/96	19	19	33	0.381	56.81	142.03	-
1/16/96	30.5	30.5	33	0.381	66.07	165.18	-
1/16/96	42.5	42.5	33	0.381	83.10	207.75	-
1/16/96	51	51	33	0.381	83.13	207.83	-
3/1/96	2	2	50	0.381	12.80	32.00	-
3/1/96	4	4	50	0.381	18.00	45.00	-
3/1/96	6	6	50	0.381	20.30	50.75	-
3/1/96	8	8	50	0.381	24.50	61.25	-
3/20/96	17	17	50	0.381	39.70	99.25	-
3/20/96	20	20	50	0.381	46.00	115.00	-
3/20/96	26	26	50	0.381	55.00	137.50	-
3/20/96	45	45	50	0.381	62.10	155.25	-
3/20/96	69	69	50	0.381	69.30	173.25	-
1/22/97-x	43	43	50	0.381	82.04	205.10	-
8/3/96	50	50	23	0.381	79.03	197.58	-

8/3/96	50	50	30	0.381	84.97	212.43	-
8/3/96	50	50	40	0.381	72.07	180.18	-
8/3/96	50	50	50	0.381	79.13	197.83	-
8/3/96	50	50	20	0.381	87.45	218.63	-
8/18/96	25	25	20	0.381	62.65	156.63	-
8/18/96	25	25	30	0.381	55.00	137.50	-
8/18/96	25	25	40	0.381	56.89	142.23	-
8/18/96	25	25	50	0.381	55.70	139.25	-
<i>1/1/0.5 lime/glass/gypsum - 25°C</i>							
5/11/95	22 days	22	50	0.381	10.76	26.90	-
5/11/95	33 days	33	50	0.381	14.64	36.60	-
5/11/95	43 days	43	50	0.381	15.14	37.85	-
5/11/95	60 days	60	50	0.381	19.97	49.93	-

B.3 ABSORBENT PREPARATION FROM SLAG EXPERIMENTS

Table B.3: Absorbent Preparation from Slag Experimental Results

Recipe: lime/glass/gypsum weight ratio.
Sample ID: Date experiment started.
Time: Reaction time for particular sample.
% Solids: 100 * g initial solids / g (solids + water)
H₂O₂: Periodic hydrogen peroxide addition to control S⁻² release.
SA: Surface area of solid sample (m²/g).
Norm SA: SA * wt. total initial solids (g) / wt. initial slag (g)
pH: ambient pH of liquid filtrate
Ca / Na / K: calcium / sodium / potassium concentration of liquid filtrate.
Dival. Alk.: Divalent Alkalinity determined by pH titration (See Section 3.1.3.4)
- : not measured
x: X-ray Diffraction data available; See Table B.4.

B.3.1 Agitated Slag Preparation Experiments at 92°C

Recipe	Sample	Time	Solids	H ₂ O ₂	SA	Norm	pH	Ca	Na	K	Dival.
	(date)	(hr)	(%)		(m ² /g)	SA (m ² /g)		mM	mM	mM	Alk mM/g
0/1/0	2/5/97	4	20	no	23.84	23.84	11.68	2.54	-	-	-
	2/5/97	20	20	no	25.43	25.43	11.75	2.51	-	-	-
	2/5/97	25	20	no	24.77	24.77	11.74	2.1	-	-	-
	2/5/97	47	20	no	24.7	24.7	11.91	0.904	-	-	-

0.2/1/0	2/21/97	5	13	no	25.08	30.10	12.08	-	-	-	-
	2/21/97	25	13	no	32.1	38.52	12.16	-	-	-	-
	2/21/97	50	13	no	36.03	43.24	12.15	-	-	-	-
0.5/1/0	9/11/97	1	15.8	no	20.76	31.14	12.27	6.1	-	-	-
	9/11/97	3	15.8	no	30.06	45.09	12.26	7.5	-	-	-
	9/11/97	7.25	15.8	no	32.8	49.2	12.26	2.25	-	-	-
	9/11/97	11	15.8	no	35.8	53.7	12.32	6.3	-	-	-
	9/11/97	24	15.8	no	41	61.5	12.35	4.2	-	-	-
0.05 M CaCl2											
0.5/1/0	8/17/98	3	20	yes	46.8	70.2	12.39	42.6	6.4	7.02	-
	8/17/98	9	20	yes	75.7	113.55	12.18	29.3	9.1	8.77	-
	8/17/98-x	21	20	yes	114.5	171.75	12.35	23.7	12.3	10.30	8.9
0.09 M CaCl2											
0.5/1/0	8/25/98	3.5	20	yes	36.81	55.22	11.94	71.94	9.23	13.79	-
	8/25/98	9	20	yes	62.2	93.3	12.02	53.96	12.08	11.25	-
	8/25/98	21	20	yes	125	187.5	12.12	49.71	15.6	14.86	-
1/1/0	1/31/96	1	20	no	16.99	33.98	-	10.9	-	-	-
	1/31/96	2.2	20	no	28.27	56.54	-	1.32	-	-	-
	1/31/96	4.2	20	no	28.84	57.68	-	2.23	-	-	-
	1/31/96	6	20	no	37.68	75.36	-	3.91	-	-	-
	1/31/96	8	20	no	36.87	73.74	-	4.4	-	-	-

3/1/0	5/27/98	0.25	20	yes	20.24	80.96	12.33	12.6	-	-	-
	5/27/98	1	20	yes	23.66	94.64	12.26	11.5	-	-	-
	5/27/98	1.5	20	yes	25.71	102.84	12.30	11.6	-	-	-
	5/27/98	4	20	yes	36.21	144.84	12.38	12.8	-	-	-
	5/27/98	4.5	20	yes	36.63	146.52	12.43	14.8	-	-	-
	6/3/98	12	20	yes	48.37	193.48	12.48	13.2	4.8	-	-
	6/3/98	23	20	yes	57.34	229.36	12.22	4.5	5.2	-	-
	6/3/98	24	20	yes	61.61	246.44	12.30	7.7	5.8	-	-
0.1/1/0.1	8/5/98-x	3	20	yes	55.41	66.49	12.20	21.8	5.09	5.62	7.9
	8/5/98-x	10	20	yes	99.94	119.93	11.80	12.9	10.55	8.78	-
	8/5/98-x	21.5	20	yes	133.9	160.68	11.80	16.2	12.83	17.07	7.2
	8/5/98-x	30	20	yes	139.3	167.16	not enough liquid				7.1
0.5/1/0.1	8/2/98	2.25	20	yes	37.62	60.19	12.16	21	3.6	3.00	-
	8/2/98	10.25	20	yes	73.43	117.49	12.26	8.1	8.3	6.60	8.4
	8/2/98	21	20	yes	108.9	174.24	12.32	5.7	12	9.50	8.4
	8/2/98-x	30	20	yes	121.5	194.40	12.48	9.1	15.1	12.50	8.3
1/1/0.1	7/21/98-x	4.5	21	yes	38.56	80.98	12.19	-	-	-	-
	7/21/98-x	9.5	21	yes	46.2	97.02	12.08	-	-	-	-
	7/21/98-x	24	21	yes	76.66	160.99	12.36	-	-	-	-
	7/21/98-x	30	21	yes	79.87	167.73	12.49	-	-	-	-

B.3.2 Non-agitated Slag Preparation Experiments at 92°C

Recipe lime/glass	Sample (date)	Time (hr)	%sol	SA (m ² /g)	Norm SA (m ² /g)	Dival. Alk mM/g
2/1	11/10/97	5	20	49.86	149.58	
2/1	11/10/97	20	20	44.49	133.47	
3/1	11/10/97	5	20	47.48	189.92	
3/1	11/10/97	20	20	54.36	217.44	
4/1	11/10/97	5	20	41.16	205.8	
4/1	11/10/97	20	20	48.91	244.55	
4/1	11/10/97	20	30	51.14	255.7	
4/1	11/10/97	20	50	52.44	262.2	
2/1	12/2/97	10	20	52.96	158.88	
3/1	12/2/97	10	20	50.72	202.88	
4/1	12/2/97	10	20	48.4	242	
9/1	12/2/97	10	20	38	380	
19/1	12/2/97	10	20	30.17	603.4	
1/0	12/2/97	10	20	32.57	0	
1/1	12/12/97	50	20	55.02	110.04	
1/1	12/12/97	50	20	44.34	88.68	
2/1	12/12/97	50	20	61.57	184.71	
2/1	12/12/97	50	20	63.44	190.32	
3/1	12/12/97	50	20	62.93	251.72	
3/1	12/12/97	50	20	54.45	217.8	
4/1	12/12/97	50	20	58.33	291.65	
4/1	12/12/97	50	20	58.41	292.05	11.08

B.4 X-RAY DIFFRACTION PATTERNS FOR SOLID SORBENTS

Table B.4: Cross-Reference for X-ray Diffraction Patterns

Sample ID#	Location in Text
11/28/94-32	Fig. 4.19
11/28/94-40	Fig. 4.19
9/25/96-10	Fig. 4.19
9/25/96-23	Fig. 4.19
3/5/94-10	Fig. 4.17
8/22/94-10	Fig. 4.17
11/21/94-5	Fig. 4.17
11/21/94-25	Figs. 4.12, 4.17, 4.19
4/28/97-44.65	Figs. 4.17, 4.18
4/28/97-68	Figs. 4.17, 5.1
12/6/94-15	Fig. 4.12
1/22/97-43-20%	Fig. 4.18
4/7/97-66.75a	Fig. 4.15
4/7/97-90a	Fig. 4.15
1/22/97-43-50%	Fig. 4.18
9/19/96-24	Fig. 4.12
8/17/98-21	Fig. 5.20
8/5/98-3	Fig. 5.12
8/5/98-10	Fig. 5.12
8/5/98-21.5	Fig. 5.12
8/5/98-30	Figs. 5.1, 5.12
8/2/98-30	Fig. 5.20
7/21/98-4.5	Fig. 5.11
7/21/98-9.5	Fig. 5.11
7/21/98-24	Fig. 5.11
7/21/98-30	Fig. 5.11

B.5 SANDBED EXPERIMENTAL DATA

This section archives the raw data from the SO₂ packed bed experiments. Most experiments typically were conducted for an hour, with measurements recorded every 30 sec. In order to conserve space, longer time data, when the SO₂ concentration changed very little, is reported at longer time intervals.

An overall key to all sandbed runs is located at the end of the section in Table B.6.

Table B.5: Sandbed Experimental Data

Run#50: 1/20/98; 50°C; 29% RH

0.1 g Sorb: 4/28/97-50; 96.3 m²/g; 0.437 cm³/g

min	ppm	min	ppm	min	ppm	min	ppm	min	ppm
0	1049.0	7.5	855.7	15	1002.5	23	1021.8	38	1034.5
0.5	1043.6	8	890.1	15.5	1004.9	24	1022.4	39	1034.5
1	954.8	8.5	915.5	16	1007.3	25	1023.0	40	1036.3
1.5	783.1	9	935.4	16.5	1007.3	26	1026.1	41	1035.1
2	588.0	9.5	950.5	17	1007.9	27	1026.7	42	1033.9
2.5	423.0	10	961.4	17.5	1009.1	28	1027.9	43	1034.5
3	314.8	10.5	968.7	18	1011.6	29	1028.5	44	1030.3
3.5	275.0	11	974.7	18.5	1014.0	30	1029.7	46	1035.7
4	300.3	11.5	980.1	19	1014.6	31	1030.3	48	1037.5
4.5	375.3	12	986.2	19.5	1015.8	32	1031.5	50	1036.9
5	475.0	12.5	991.0	20	1017.0	33	1032.1	52	1036.9
5.5	577.7	13	993.4	20.5	1016.4	34	1032.7	54	1035.7
6	670.1	13.5	996.4	21	1017.0	35	1034.5	56	1037.5
6.5	748.1	14	998.9	21.5	1016.4	36	1035.1	58	1036.9
7	809.1	14.5	1000.7	22	1018.2	37	1035.1	59	1036.3

Run#51: 1/20/98; 50°C; 58% RH

0.1 g Sorb: 4/28/97-50; 96.3 m²/g; 0.437 cm³/g

min.	ppm	min.	ppm	min.	ppm	min.	ppm	min.	ppm
0	1036.6	7.5	430.7	15	913.8	23	974.6	38	998.1
0.5	1028.8	8	480.1	15.5	922.2	24	975.8	39	1002.9
1	939.7	8.5	526.5	16	930.6	25	978.8	40	1004.7
1.5	768.6	9	571.0	16.5	938.4	26	980.6	41	1006.5
2	574.6	9.5	616.2	17	944.5	27	983.6	42	1008.9
2.5	410.2	10	657.8	17.5	948.7	28	984.2	43	1010.7
3	290.9	10.5	698.1	18	953.5	29	986.0	44	1009.5
3.5	224.1	11	734.9	18.5	957.1	30	989.0	46	1007.7
4	200.0	11.5	769.2	19	959.5	31	991.5	48	1010.1
4.5	204.2	12	797.5	19.5	963.7	32	992.7	50	1010.7
5	224.1	12.5	824.0	20	965.6	33	992.7	52	1007.7
5.5	253.6	13	846.9	20.5	969.2	34	995.7	54	1007.7
6	290.9	13.5	867.4	21	971.6	35	995.1	56	1007.7
6.5	333.1	14	886.0	21.5	973.4	36	996.3	58	1008.9
7	381.3	14.5	900.5	22	973.4	37	995.1	59	1010.1

Run#52: 1/27/98; 50°C; 0% RH

0.1 g Sorb: 4/28/97-50; 96.3 m²/g; 0.437 cm³/g

min	ppm	min	ppm	min	ppm	min	ppm	min	ppm
0	1008.7	7.5	989.2	15	1006.4	23	1009.9	38	1013.3
0.5	986.3	8	992.6	15.5	1005.9	24	1012.2	39	1013.3
1	867.9	8.5	995.5	16	1006.4	25	1012.2	40	1014.5
1.5	735.7	9	997.2	16.5	1006.4	26	1012.2	41	1015.6
2	667.3	9.5	999.0	17	1005.3	27	1012.2	42	1014.5
2.5	674.2	10	999.5	17.5	1005.9	28	1012.2	43	1013.3
3	724.8	10.5	1001.3	18	1005.9	29	1012.7	44	1013.9
3.5	787.4	11	1003.0	18.5	1006.4	30	1012.2	46	1011.6
4	843.2	11.5	1003.6	19	1007.6	31	1013.3	48	1011.6
4.5	889.2	12	1004.1	19.5	1008.7	32	1013.3	50	1013.9
5	923.1	12.5	1004.7	20	1008.1	33	1014.5	52	1013.9
5.5	947.2	13	1004.7	20.5	1009.3	34	1013.9	54	1013.9
6	962.7	13.5	1005.3	21	1009.9	35	1015.0	56	1017.3
6.5	974.8	14	1005.3	21.5	1009.9	36	1012.7		
7	982.9	14.5	1007.0	22	1010.4	37	1013.3		

Run#53: 1/27/98; 50°C; 88% RH

0.1 g Sorb: 4/28/97-50; 96.3 m²/g; 0.437 cm³/g

min	ppm	min	ppm	min	ppm	min	ppm	min	ppm
0	998.4	7.5	110.4	15	598.3	23	953.5	38	990.9
0.5	975.4	8	143.7	15.5	628.2	24	963.9	39	990.3
1	847.2	8.5	178.2	16	659.8	25	972.5	40	990.3
1.5	660.4	9	215.5	16.5	688.6	26	978.3	41	989.8
2	479.9	9.5	250.6	17	717.9	27	984.0	42	989.2
2.5	333.4	10	286.8	17.5	748.9	28	984.6	43	989.8
3	224.2	10.5	320.7	18	781.7	29	986.3	44	989.2
3.5	150.0	11	354.1	18.5	813.3	30	985.7	46	988.0
4	99.4	11.5	386.3	19	840.9	31	988.0	48	988.6
4.5	66.7	12	418.4	19.5	866.8	32	988.6	50	990.9
5	44.8	12.5	448.9	20	888.0	33	988.6	52	987.5
5.5	35.6	13	479.9	20.5	907.0	34	989.2	54	986.9
6	40.8	13.5	510.4	21	921.4	35	990.9	56	984.6
6.5	58.1	14	538.6	21.5	932.9	36	990.9	58	986.3
7	82.8	14.5	569.0	22	943.2	37	991.5	60	986.9

Run#54: 1/28/98; 36.5°C; 59% RH

0.1 g Sorb: 4/28/97-50; 96.3 m²/g; 0.437 cm³/g

min	ppm	min	ppm	min	ppm	min	ppm	min	ppm
0	1008.3	7.5	481.4	15	932.7	23	966.2	38	980.0
0.5	984.1	8	537.9	15.5	939.6	24	967.3	39	982.9
1	850.2	8.5	594.5	16	940.8	25	969.1	40	982.3
1.5	660.3	9	651.6	16.5	944.2	26	969.6	41	982.9
2	476.7	9.5	705.3	17	947.1	27	970.8	42	982.9
2.5	331.3	10	752.6	17.5	949.4	28	970.8	43	980.6
3	233.2	10.5	792.5	18	950.6	29	973.7	44	982.3
3.5	183.5	11	824.2	18.5	954.1	30	974.3	46	982.9
4	172.6	11.5	850.2	19	955.8	31	975.4	48	986.4
4.5	189.9	12	871.5	19.5	958.7	32	976.6	50	986.4
5	225.7	12.5	887.7	20	959.3	33	977.7	52	988.7
5.5	272.4	13	902.7	20.5	961.6	34	977.7	54	989.3
6	322.6	13.5	913.7	21	962.1	35	977.7	56	987.5
6.5	375.2	14	922.3	21.5	961.6	36	978.9	58	989.3
7	427.7	14.5	927.5	22	964.4	37	978.9	60	989.8

Run#55: 1/31/98; 50°C; 58% RH

0.1 g Sorb: 11/21/94-5; 17.8 m²/g; 0.134 cm³/g

min	ppm	min	ppm	min	ppm	min	ppm	min	ppm
0	1031.8	7.5	969.9	15	979.4	23	973.5	38	998.4
0.5	1006.2	8	976.4	15.5	977.6	24	975.8	39	998.4
1	870.5	8.5	981.2	16	976.4	25	976.4	40	996.7
1.5	690.2	9	986.0	16.5	974.1	26	978.8	41	999.6
2	559.9	9.5	987.7	17	973.5	27	981.2	42	1000.2
2.5	510.5	10	988.9	17.5	971.7	28	983.6	43	1001.4
3	537.9	10.5	990.7	18	969.9	29	986.0	44	1001.4
3.5	612.3	11	989.5	18.5	968.7	30	987.7	46	1005.0
4	699.2	11.5	988.3	19	968.1	31	990.1	48	1005.6
4.5	775.9	12	988.3	19.5	969.9	32	990.7	50	1003.8
5	839.0	12.5	988.3	20	970.5	33	990.7	52	1007.4
5.5	883.6	13	987.1	20.5	969.9	34	993.1	54	1008.0
6	917.5	13.5	986.0	21	971.1	35	993.7	56	1009.2
6.5	940.7	14	983.6	21.5	971.7	36	994.3	58	1009.8
7	957.4	14.5	982.4	22	971.1	37	996.1		

Run#56: 2/2/98; 50°C; 58% RH

0.1 g Sorb: Ca(OH)₂; 22.1 m²/g; 0.112 cm³/g

min	ppm	min	ppm	min	ppm	min	ppm	min	ppm
0	1022.3	7.5	874.4	15	953.3	23	954.5	38	973.8
0.5	997.8	8	896.6	15.5	951.0	24	951.0	39	974.4
1	861.0	8.5	914.8	16	950.4	25	950.4	40	973.2
1.5	666.3	9	925.9	16.5	951.6	26	952.2	41	971.5
2	493.9	9.5	933.5	17	951.6	27	954.5	42	972.6
2.5	389.3	10	939.3	17.5	954.5	28	959.2	43	972.0
3	351.3	10.5	942.8	18	955.1	29	959.2	44	974.4
3.5	363.6	11	945.7	18.5	957.4	30	960.9	46	979.6
4	406.8	11.5	947.5	19	957.4	31	959.2	48	980.2
4.5	474.0	12	951.0	19.5	956.3	32	959.2	50	980.2
5	557.0	12.5	952.2	20	955.1	33	959.8	52	985.5
5.5	647.1	13	953.9	20.5	954.5	34	961.5	54	987.8
6	727.7	13.5	952.8	21	955.7	35	965.6	56	987.8
6.5	792.6	14	953.3	21.5	954.5	36	967.4	58	987.8
7	840.5	14.5	954.5	22	954.5	37	969.1	60	989.6

Run#57: 2/2/98; 50°C; 58% RH

0.1 g Sorb: 4/28/97-50; 96.3 m²/g; 0.437 cm³/g

min	ppm	min	ppm	min	ppm	min	ppm	min	ppm
0	536.0	7.5	43.8	15	222.7	23	412.7	38	489.8
0.5	522.6	8	57.3	15.5	233.2	24	427.3	39	489.2
1	450.7	8.5	71.3	16	245.5	25	440.7	40	491.6
1.5	346.6	9	85.9	16.5	258.9	26	453.0	41	492.2
2	248.4	9.5	100.5	17	271.8	27	460.0	42	493.9
2.5	170.1	10	114.0	17.5	285.8	28	464.7	43	495.7
3	114.0	10.5	125.7	18	298.1	29	468.8	44	497.4
3.5	74.8	11	138.5	18.5	310.4	30	470.5	46	498.0
4	48.5	11.5	149.6	19	322.7	31	473.5	48	498.0
4.5	32.7	12	160.8	19.5	335.5	32	476.4	50	500.3
5	21.6	12.5	171.3	20	347.8	33	480.5	52	501.5
5.5	17.0	13	181.2	20.5	360.7	34	482.8	54	503.9
6	18.7	13.5	191.7	21	373.5	35	485.7	56	505.0
6.5	24.0	14	201.7	21.5	384.6	36	487.5	58	507.9
7	32.7	14.5	212.8	22	394.0	37	487.5	60	507.9

Run#58: 2/2/98; 50°C; 58% RH

0.1 g Sorb: 11/21/94-25; 58.2 m²/g; 0.420 cm³/g

min	ppm	min	ppm	min	ppm	min	ppm	min	ppm
0	991.3	7.5	765.7	15	917.7	23	885.5	38	917.7
0.5	969.7	8	806.6	15.5	916.5	24	886.1	39	918.9
1	838.8	8.5	836.4	16	914.2	25	887.9	40	921.8
1.5	650.6	9	857.5	16.5	913.0	26	888.5	41	925.9
2	476.4	9.5	875.0	17	913.6	27	887.3	42	930.5
2.5	354.2	10	883.8	17.5	913.0	28	888.5	43	934.6
3	289.3	10.5	892.6	18	912.4	29	887.9	44	934.1
3.5	273.6	11	899.6	18.5	908.9	30	889.0	46	938.1
4	291.1	11.5	906.0	19	905.4	31	889.6	48	942.2
4.5	334.9	12	910.1	19.5	902.5	32	893.1	50	946.9
5	397.5	12.5	914.2	20	898.4	33	901.3	52	952.2
5.5	477.6	13	914.2	20.5	896.6	34	907.7	54	956.3
6	564.1	13.5	915.9	21	892.6	35	913.6	56	958.6
6.5	643.6	14	917.1	21.5	889.0	36	915.9	58	963.9
7	711.9	14.5	916.5	22	887.9	37	918.3	59	968.0

Run#59: 2/5/98; 50°C; 58% RH
 0.1 g Sorb: 4/28/97-50; 96.3 m²/g; 0.437 cm³/g

min	ppm	min	ppm	min	ppm	min	ppm	min	ppm
0	1035.3	7.5	405.2	15	915.7	23	970.5	38	989.5
0.5	1009.2	8	444.5	15.5	922.3	24	975.8	39	990.1
1	874.1	8.5	485.5	16	929.4	25	977.0	40	991.9
1.5	676.5	9	533.1	16.5	933.0	26	978.8	41	993.1
2	488.5	9.5	583.7	17	935.4	27	981.2	42	993.1
2.5	341.6	10	639.1	17.5	938.9	28	980.6	43	993.7
3	241.6	10.5	694.4	18	942.5	29	981.2	44	995.5
3.5	188.0	11	746.8	18.5	946.1	30	983.6	46	997.3
4	171.4	11.5	790.2	19	948.5	31	984.2	48	1000.8
4.5	181.5	12	824.1	19.5	953.2	32	986.0	50	1000.2
5	208.9	12.5	849.7	20	957.4	33	984.2	52	1000.2
5.5	244.6	13	869.9	20.5	960.4	34	985.4	54	1002.6
6	285.6	13.5	884.2	21	962.7	35	986.5	56	1003.2
6.5	326.7	14	896.7	21.5	965.7	36	987.7	58	1002.0
7	365.9	14.5	907.4	22	967.5	37	989.5	59	1001.4

Run#60: 2/12/98; 50°C; 59% RH
 0.1 g Sorb: 4/28/97-50; 96.3 m²/g; 0.437 cm³/g

min	ppm	min	ppm	min	ppm	min	ppm	min	ppm
0	1949.2	7.5	1521.3	15	1857.7	23	1877.7	38	1906.1
0.5	1900.8	8	1598.0	15.5	1857.7	24	1876.6	39	1906.1
1	1645.3	8.5	1657.9	16	1860.9	25	1880.8	40	1909.2
1.5	1283.7	9	1707.4	16.5	1861.9	26	1879.8	41	1910.3
2	969.3	9.5	1746.3	17	1864.0	27	1881.9	42	1912.4
2.5	772.7	10	1777.8	17.5	1864.0	28	1885.0	43	1914.5
3	703.4	10.5	1798.8	18	1865.1	29	1888.2	44	1914.5
3.5	724.4	11	1811.4	18.5	1868.2	30	1889.2	46	1915.5
4	798.0	11.5	1822.0	19	1870.3	31	1890.3	48	1922.9
4.5	896.8	12	1828.3	19.5	1871.4	32	1895.5	50	1926.0
5	1006.1	12.5	1835.6	20	1869.3	33	1896.6	52	1929.2
5.5	1123.9	13	1838.8	20.5	1869.3	34	1896.6	54	1931.3
6	1237.4	13.5	1845.1	21	1865.1	35	1897.7	56	1929.2
6.5	1342.6	14	1848.2	21.5	1868.2	36	1896.6	58	1931.3
7	1436.1	14.5	1852.4	22	1869.3	37	1901.9	59	1935.5

Run#61: 2/17/98; 69.5°C; 59% RH

0.1 g Sorb: 4/28/97-50; 96.3 m²/g; 0.437 cm³/g

min	ppm	min	ppm	min	ppm	min	ppm	min	ppm
0	999.0	7.5	250.0	15	851.8	23	871.7	38	950.7
0.5	975.7	8	289.3	15.5	857.5	24	875.7	39	955.8
1	846.2	8.5	331.3	16	862.1	25	880.8	40	957.5
1.5	657.5	9	379.0	16.5	866.6	26	884.8	41	962.1
2	473.4	9.5	437.0	17	868.9	27	891.6	42	964.4
2.5	328.5	10	498.4	17.5	869.5	28	895.6	43	966.1
3	225.6	10.5	565.4	18	870.6	29	903.0	44	968.9
3.5	155.7	11	630.2	18.5	869.5	30	910.9	46	970.6
4	116.5	11.5	686.5	19	870.0	31	918.9	48	976.3
4.5	97.8	12	732.5	19.5	870.0	32	925.7	50	977.4
5	100.0	12.5	767.7	20	869.5	33	930.8	52	978.6
5.5	118.8	13	796.2	20.5	871.2	34	936.0	54	976.9
6	146.1	13.5	816.6	21	870.0	35	939.4	56	979.7
6.5	179.6	14	831.4	21.5	871.2	36	944.5	58	981.4
7	214.2	14.5	843.3	22	871.2	37	947.3	60	980.8

Run#62: 2/25/98; 50°C; 58% RH

0.1 g Sorb: 12/6/94-15; 41.0 m²/g; 0.397 cm³/g

min	ppm	min	ppm	min	ppm	min	ppm	min	ppm
0	1065.4	7.5	874.6	15	1007.8	23	1011.5	38	1013.9
0.5	1037.5	8	905.5	15.5	1008.5	24	1009.7	39	1013.9
1	894.0	8.5	927.9	16	1010.3	25	1010.3	40	1016.9
1.5	691.7	9	944.3	16.5	1012.1	26	1012.1	41	1016.3
2	508.8	9.5	957.6	17	1012.7	27	1012.1	42	1019.4
2.5	384.6	10	967.9	17.5	1013.9	28	1010.3	43	1022.4
3	330.7	10.5	976.4	18	1013.9	29	1010.9	44	1024.8
3.5	333.1	11	981.8	18.5	1015.1	30	1010.3	46	1029.7
4	372.5	11.5	986.7	19	1016.9	31	1008.5	48	1030.9
4.5	445.2	12	992.1	19.5	1018.1	32	1007.8	50	1030.3
5	534.8	12.5	995.7	20	1017.5	33	1009.1	52	1031.5
5.5	626.9	13	1000.0	20.5	1016.9	34	1010.9	54	1033.3
6	710.5	13.5	1001.8	21	1014.5	35	1011.5	56	1038.7
6.5	780.7	14	1006.0	21.5	1012.7	36	1013.9	58	1041.8
7	834.6	14.5	1007.2	22	1011.5	37	1012.7	60	1043.6

Run#63: 2/25/98; 50°C; 58% RH

0.1 g Sorb: 9/25/96-23; 67.5 m²/g; 0.335 cm³/g

min	ppm	min	ppm	min	ppm	min	ppm	min	ppm
0	1081.1	7.5	588.1	15	907.9	23	945.5	38	1029.7
0.5	1051.5	8	639.0	15.5	908.5	24	952.1	39	1032.7
1	903.7	8.5	688.7	16	909.1	25	960.0	40	1030.9
1.5	695.3	9	737.7	16.5	912.8	26	967.3	41	1033.9
2	501.5	9.5	782.5	17	917.0	27	977.6	42	1039.3
2.5	359.2	10	821.3	17.5	920.0	28	981.8	43	1041.8
3	278.6	10.5	850.4	18	925.5	29	989.7	44	1045.4
3.5	252.6	11	872.2	18.5	926.7	30	995.1	46	1045.4
4	262.3	11.5	887.3	19	929.7	31	1001.2	48	1047.8
4.5	296.2	12	897.0	19.5	934.0	32	1003.6	50	1053.9
5	338.6	12.5	903.1	20	934.6	33	1007.2	52	1053.9
5.5	386.4	13	906.1	20.5	934.6	34	1014.5	54	1052.1
6	437.3	13.5	907.3	21	936.4	35	1018.8	56	1053.9
6.5	487.0	14	907.9	21.5	937.6	36	1024.2	58	1055.7
7	537.2	14.5	908.5	22	939.4	37	1026.6	60	1056.3

Run#64: 2/26/98; 50°C; 58% RH

0.1 g Sorb: 1/22/97-43-20%; 37.1 m²/g; 0.238 cm³/g

min	ppm	min	ppm	min	ppm	min	ppm	min	ppm
0	1052.2	7.5	778.8	15	968.2	23	961.0	38	988.6
0.5	1024.0	8	824.3	15.5	971.8	24	962.2	39	992.2
1	880.7	8.5	858.5	16	971.2	25	964.0	40	994.0
1.5	679.3	9	884.9	16.5	970.6	26	962.8	41	996.4
2	495.8	9.5	903.5	17	971.2	27	961.6	42	998.2
2.5	371.7	10	919.1	17.5	971.2	28	959.2	43	998.2
3	311.8	10.5	929.9	18	969.4	29	962.8	44	997.0
3.5	301.0	11	939.5	18.5	967.0	30	966.4	46	994.6
4	321.4	11.5	946.7	19	966.4	31	970.0	48	998.2
4.5	359.7	12	950.8	19.5	965.2	32	971.8	50	1001.2
5	413.1	12.5	955.0	20	964.0	33	977.2	52	999.4
5.5	486.2	13	958.6	20.5	960.4	34	979.6	54	1004.2
6	569.6	13.5	961.0	21	958.6	35	981.4	56	1006.6
6.5	649.3	14	964.0	21.5	958.6	36	985.6	58	1008.4
7	721.8	14.5	966.4	22	960.4	37	985.0	60	1007.8

Run#65: 2/26/98; 50°C; 58% RH

0.1 g Sorb: 12/12/97-4/1-B; 48.1 m²/g; 0.228 cm³/g

min	ppm	min	ppm	min	ppm	min	ppm	min	ppm
0	1070.8	7.5	644.5	15	926.9	23	1006.4	38	1030.5
0.5	1045.0	8	693.6	15.5	936.4	24	1007.6	39	1031.7
1	902.8	8.5	730.2	16	945.3	25	1011.3	40	1035.1
1.5	696.5	9	760.1	16.5	952.6	26	1011.3	41	1034.2
2	502.3	9.5	784.2	17	958.5	27	1014.3	42	1035.1
2.5	355.4	10	803.8	17.5	964.4	28	1017.2	43	1034.2
3	261.4	10.5	820.5	18	971.1	29	1019.2	44	1034.2
3.5	215.2	11	836.7	18.5	976.0	30	1020.9	46	1034.7
4	211.0	11.5	851.2	19	977.7	31	1023.4	48	1034.2
4.5	237.8	12	864.5	19.5	983.1	32	1026.8	50	1035.1
5	285.9	12.5	877.5	20	988.5	33	1028.0	52	1038.3
5.5	351.3	13	887.8	20.5	993.4	34	1028.8	54	1038.3
6	426.6	13.5	896.6	21	995.1	35	1030.5	56	1041.8
6.5	506.4	14	908.7	21.5	999.3	36	1030.5	58	1040.5
7	581.3	14.5	917.8	22	1002.2	37	1030.5	60	1038.3

Run#66: 3/9/98; 50°C; 58% RH - on 0.609 g glass wool

0.1 g Sorb: 4/28/97-50; 96.3 m²/g; 0.437 cm³/g

min	ppm	min	ppm	min	ppm	min	ppm	min	ppm
0	1013.0	7.5	898.9	15	927.2	23	939.5	38	950.1
0.5	991.2	8	902.5	15.5	928.9	24	940.1	39	951.8
1	918.9	8.5	903.6	16	929.5	25	939.5	40	953.0
1.5	864.2	9	907.8	16.5	928.3	26	938.9	41	951.8
2	840.7	9.5	910.7	17	930.7	27	940.1	42	952.4
2.5	834.9	10	913.0	17.5	931.9	28	943.0	43	954.2
3	839.0	10.5	915.4	18	931.9	29	944.8	44	952.4
3.5	847.2	11	916.6	18.5	931.9	30	944.2	46	953.0
4	856.0	11.5	917.2	19	931.9	31	943.6	48	953.6
4.5	862.5	12	920.1	19.5	933.0	32	947.1	50	951.8
5	871.3	12.5	921.9	20	933.0	33	948.3	52	953.0
5.5	877.8	13	922.5	20.5	933.0	34	946.6	54	953.6
6	885.4	13.5	922.5	21	935.4	35	947.1	56	953.6
6.5	890.7	14	924.2	21.5	938.3	36	948.9	58	954.8
7	894.2	14.5	925.4	22	938.9	37	949.5	60	955.4

Run#67: 3/30/98; 50°C; 58% RH

0.025 g Sorb: 4/28/97-50; 96.3 m²/g; 0.437 cm³/g

min	ppm	min	ppm	min	ppm	min	ppm	min	ppm
0	525.4	7.5	439.3	15	503.6	23	507.7	38	511.2
0.5	512.4	8	454.0	15.5	504.2	24	508.3	39	508.3
1	441.1	8.5	465.8	16	503.6	25	509.5	40	508.3
1.5	345.5	9	474.1	16.5	503.6	26	510.6	41	507.1
2	270.1	9.5	480.0	17	503.0	27	510.6	42	508.9
2.5	227.0	10	485.9	17.5	503.6	28	510.1	43	507.1
3	214.1	10.5	490.0	18	504.2	29	509.5	44	508.3
3.5	224.1	11	492.4	18.5	504.7	30	509.5	46	508.3
4	245.3	11.5	496.5	19	504.7	31	511.8	48	506.5
4.5	274.8	12	497.7	19.5	504.2	32	510.6	50	506.5
5	307.2	12.5	498.9	20	504.7	33	511.2	52	505.9
5.5	340.2	13	500.0	20.5	505.9	34	511.2	54	504.7
6	370.3	13.5	501.2	21	505.9	35	510.1	56	504.2
6.5	398.0	14	502.4	21.5	505.9	36	510.1	58	504.2
7	420.4	14.5	503.6	22	507.1	37	509.5	60	504.7

Run#68: 6/1/98; 50°C; 58% RH

0.1 g Sorb: 4/28/97-50; 96.3 m²/g; 0.437 cm³/g

min	ppm	min	ppm	min	ppm	min	ppm	min	ppm
0	1072.6	7.5	521.2	15	954.3	23	993.1	38	999.3
0.5	1050.4	8	559.4	15.5	962.3	24	995.6	39	1001.8
1	918.0	8.5	597.6	16	967.9	25	997.4	40	1004.8
1.5	719.0	9	633.3	16.5	972.2	26	999.9	41	1006.7
2	531.7	9.5	667.8	17	975.9	27	1001.1	42	1007.3
2.5	393.7	10	705.4	17.5	980.8	28	1002.4	43	1010.4
3	316.1	10.5	743.0	18	984.5	29	1001.8	44	1011.0
3.5	285.9	11	778.1	18.5	987.0	30	999.9	46	1015.3
4	285.9	11.5	812.6	19	987.6	31	999.3	48	1016.5
4.5	305.6	12	843.4	19.5	988.8	32	999.9	50	1023.9
5	335.8	12.5	869.9	20	988.8	33	1000.5	52	1031.9
5.5	369.7	13	892.1	20.5	990.0	34	1001.8	54	1033.8
6	405.4	13.5	913.0	21	990.7	35	1002.4	56	1040.0
6.5	443.0	14	930.3	21.5	991.9	36	1001.1	58	1041.2
7	482.4	14.5	944.5	22	992.5	37	1000.5	60	1046.7

Run#69: 6/1/98; 50°C; 58% RH; 5% Oxygen
 0.1 g Sorb: 4/28/97-50; 96.3 m²/g; 0.437 cm³/g

min	ppm	min	ppm	min	ppm	min	ppm	min	ppm
0	1046.1	7.5	393.7	15	946.3	23	987.6	38	995.0
0.5	1041.8	8	452.8	15.5	951.9	24	989.4	39	995.0
1	946.3	8.5	514.4	16	958.0	25	986.4	40	993.7
1.5	760.9	9	576.0	16.5	961.1	26	988.8	41	991.9
2	563.7	9.5	635.2	17	965.4	27	990.7	42	993.1
2.5	399.2	10	691.3	17.5	967.9	28	990.7	43	992.5
3	284.6	10.5	742.4	18	970.3	29	992.5	44	995.0
3.5	213.8	11	786.1	18.5	971.6	30	992.5	46	993.7
4	176.8	11.5	823.7	19	973.4	31	992.5	48	996.2
4.5	165.7	12	853.3	19.5	975.3	32	993.7	50	997.4
5	172.5	12.5	878.5	20	977.1	33	991.9	52	999.3
5.5	196.5	13	897.0	20.5	979.6	34	991.3	54	1000.5
6	234.1	13.5	916.1	21	981.4	35	990.1	56	1004.2
6.5	282.2	14	929.1	21.5	984.5	36	993.1	58	1004.8
7	335.2	14.5	938.3	22	985.1	37	992.5	60	1007.3

Run#70: 6/9/98; 50°C; 58% RH
 0.1 g Sorb: 4/28/97-50; 96.3 m²/g; 0.437 cm³/g

min	ppm	min	ppm	min	ppm	min	ppm	min	ppm
0	960.5	7.5	451.6	15	840.3	23	826.2	38	858.2
0.5	920.4	8	506.4	15.5	842.8	24	822.5	39	863.8
1	751.0	8.5	558.8	16	844.0	25	817.5	40	871.8
1.5	548.3	9	608.1	16.5	841.6	26	812.0	41	875.5
2	377.1	9.5	652.4	17	841.0	27	808.3	42	880.4
2.5	262.5	10	693.7	17.5	839.7	28	808.9	43	883.5
3	197.8	10.5	727.6	18	839.1	29	813.9	44	889.0
3.5	173.7	11	755.9	18.5	838.5	30	818.8	46	900.1
4	173.7	11.5	775.7	19	836.6	31	824.9	48	908.7
4.5	192.2	12	793.5	19.5	836.0	32	829.9	50	914.9
5	217.5	12.5	808.9	20	834.2	33	833.6	52	921.7
5.5	250.8	13	818.2	20.5	832.3	34	836.0	54	928.4
6	289.0	13.5	826.2	21	830.5	35	841.6	56	936.5
6.5	337.0	14	832.3	21.5	830.5	36	845.9	58	937.1
7	393.7	14.5	836.0	22	829.3	37	851.4	60	941.4

Run#71: 6/10/98; 50°C; 58% RH

0.1 g Sorb: 4/28/97-50; 96.3 m²/g; 0.437 cm³/g

min	ppm	min	ppm	min	ppm	min	ppm	min	ppm
0	928.6	7.5	369.2	15	829.3	23	863.6	38	878.9
0.5	891.9	8	429.4	15.5	834.6	24	864.8	39	880.1
1	734.2	8.5	487.3	16	840.0	25	868.3	40	880.1
1.5	538.7	9	544.6	16.5	843.5	26	868.9	41	880.1
2	371.0	9.5	600.1	17	847.0	27	872.4	42	881.3
2.5	249.9	10	648.6	17.5	849.4	28	873.6	43	881.9
3	173.7	10.5	691.1	18	851.2	29	873.6	44	884.9
3.5	135.3	11	724.8	18.5	853.0	30	871.9	46	884.9
4	122.9	11.5	750.8	19	854.7	31	874.2	48	886.0
4.5	130.0	12	772.0	19.5	857.1	32	875.4	50	890.8
5	149.5	12.5	786.8	20	857.7	33	876.6	52	894.3
5.5	178.4	13	799.2	20.5	858.9	34	877.8	54	892.5
6	214.4	13.5	808.7	21	859.5	35	879.5	56	894.9
6.5	258.7	14	816.3	21.5	859.5	36	878.9	58	897.8
7	311.9	14.5	824.0	22	861.8	37	879.5	60	902.0

Run#72: 6/10/98; 50°C; 58% RH; 5% Oxygen

0.1 g Sorb: 4/28/97-50; 96.3 m²/g; 0.437 cm³/g

min	ppm	min	ppm	min	ppm	min	ppm	min	ppm
0	917.3	7.5	374.5	15	848.2	23	871.9	38	874.8
0.5	880.1	8	450.1	15.5	851.2	24	873.6	39	878.4
1	721.8	8.5	523.9	16	854.7	25	873.6	40	876.6
1.5	526.3	9	590.7	16.5	857.1	26	873.6	41	876.6
2	361.5	9.5	648.0	17	859.5	27	873.6	42	877.8
2.5	242.2	10	694.7	17.5	862.4	28	873.0	43	876.6
3	158.3	10.5	732.5	18	863.0	29	874.2	44	876.6
3.5	105.2	11	760.8	18.5	863.0	30	876.6	46	879.5
4	76.2	11.5	783.3	19	864.2	31	876.6	48	878.9
4.5	73.3	12	799.8	19.5	864.8	32	875.4	50	879.5
5	92.2	12.5	813.4	20	864.2	33	874.8	52	881.3
5.5	127.6	13	822.2	20.5	864.8	34	873.6	54	883.1
6	174.9	13.5	831.7	21	866.5	35	874.2	56	886.0
6.5	233.9	14	838.8	21.5	867.1	36	874.2	58	886.0
7	301.3	14.5	843.5	22	868.9	37	874.8	60	886.0

Run#73: 8/17/98; 50°C; 29% RH;
0.1 g Sorb: 4/28/97-50; 96.3 m²/g; 0.437 cm³/g

min	ppm	min	ppm	min	ppm	min	ppm	min	ppm
0	534.4	7.5	277.6	15	487.7	23	506.0	38	517.9
0.5	512.0	8	305.0	15.5	490.1	24	507.2	39	518.5
1	420.9	8.5	333.4	16	492.4	25	509.0	40	518.8
1.5	308.3	9	360.3	16.5	494.2	26	509.3	41	519.0
2	215.2	9.5	385.4	17	495.7	27	510.2	42	519.6
2.5	154.9	10	407.3	17.5	497.2	28	510.8	43	519.9
3	125.3	10.5	425.3	18	498.1	29	512.0	44	519.6
3.5	116.8	11	439.2	18.5	498.9	30	513.1	46	521.1
4	122.4	11.5	450.5	19	500.7	31	513.1	48	521.4
4.5	136.6	12	459.9	19.5	501.3	32	513.1	50	522.3
5	155.5	12.5	467.3	20	502.5	33	513.4	52	523.2
5.5	177.9	13	472.9	20.5	503.4	34	514.9	54	523.8
6	201.0	13.5	478.3	21	504.3	35	516.1	56	524.1
6.5	225.8	14	481.8	21.5	504.9	36	516.7	58	523.8
7	250.7	14.5	485.4	22	505.2	37	517.9	60	525.6

Run#74: 8/17/98; 50°C; 58% RH;
0.025 g Sorb: 4/28/97-50; 96.3 m²/g; 0.437 cm³/g

min	ppm	min	ppm	min	ppm	min	ppm	min	ppm
0	967.8	7.5	917.6	15	939.1	23	936.7	38	947.5
0.5	927.8	8	923.0	15.5	939.1	24	936.7	39	948.7
1	766.0	8.5	926.6	16	939.1	25	936.1	40	951.1
1.5	606.6	9	930.8	16.5	938.5	26	936.1	41	951.1
2	536.7	9.5	931.4	17	939.1	27	937.9	42	952.2
2.5	557.0	10	933.1	17.5	939.1	28	939.1	43	952.8
3	623.9	10.5	934.3	18	937.9	29	941.5	44	952.2
3.5	697.3	11	935.5	18.5	936.7	30	941.5	46	955.2
4	761.8	11.5	935.5	19	936.1	31	942.1	48	958.2
4.5	811.3	12	936.1	19.5	936.1	32	941.5	50	957.0
5	847.2	12.5	937.9	20	937.9	33	942.1	52	957.0
5.5	872.2	13	939.1	20.5	936.7	34	945.1	54	958.2
6	890.2	13.5	940.3	21	936.1	35	945.7	56	960.0
6.5	903.3	14	940.3	21.5	935.5	36	945.7	58	958.2
7	912.2	14.5	939.7	22	936.1	37	945.7	60	960.0

Run#75: 8/19/98; 50°C; 58% RH;
0.1 g Sorb: slag; 3.62 m²/g

min	ppm	min	ppm	min	ppm	min	ppm
0	1000.1	7.5	984.5	15	992.6	23	994.1
0.5	998.6	8	988.2	15.5	992.6	24	993.4
1	998.6	8.5	989.7	16	993.4	25	993.4
1.5	954.8	9	991.2	16.5	993.4	26	995.6
2	856.1	9.5	991.9	17	994.1	27	994.1
2.5	830.2	10	992.6	17.5	994.1	28	995.6
3	850.9	10.5	991.2	18	994.1	29	995.6
3.5	884.3	11	991.9	18.5	994.1	30	993.4
4	913.3	11.5	992.6	19	994.1	31	992.6
4.5	936.3	12	992.6	19.5	994.1		
5	952.6	12.5	991.2	20	994.1		
5.5	964.4	13	991.2	20.5	992.6		
6	972.6	13.5	991.2	21	991.2		
6.5	977.1	14	991.2	21.5	992.6		
7	982.3	14.5	991.2	22	993.4		

Run#76: 8/19/98; 50°C; 58% RH;
0.1 g Sorb: 8/2/98-30; 121.5 m²/g; 0.663 cm³/g

min	ppm	min	ppm	min	ppm	min	ppm	min	ppm
0	998.6	7.5	315.2	15	789.9	23	887.5	38	966.5
0.5	953.9	8	339.8	15.5	798.8	24	897.2	39	968.8
1	774.3	8.5	365.1	16	805.6	25	906.9	40	971.0
1.5	563.3	9	392.7	16.5	812.3	26	917.3	41	973.2
2	387.5	9.5	424.0	17	816.7	27	924.0	42	973.2
2.5	268.2	10	463.5	17.5	821.9	28	929.3	43	974.0
3	198.2	10.5	506.7	18	828.7	29	936.7	44	973.2
3.5	166.1	11	554.4	18.5	834.6	30	943.4	46	977.0
4	160.2	11.5	604.3	19	840.6	31	947.9	48	977.0
4.5	168.4	12	651.3	19.5	848.0	32	952.4	50	977.7
5	186.2	12.5	690.8	20	853.2	33	956.8	52	980.7
5.5	210.1	13	723.6	20.5	860.0	34	959.8	54	980.7
6	236.2	13.5	748.2	21	865.9	35	962.8	56	982.9
6.5	263.7	14	766.1	21.5	871.1	36	965.8	58	983.7
7	289.1	14.5	779.5	22	877.8	37	965.8	60	983.7

Run#77: 8/20/98; 50°C; 58% RH;

0.025 g Sorb: 4/28/97-50; 96.3 m²/g; 0.437 cm³/g

min	ppm	min	ppm	min	ppm	min	ppm	min	ppm
0	2006.4	7.5	1956.9	15	1942.3	23	1959.1	38	1983.9
0.5	1924.3	8	1959.1	15.5	1942.3	24	1961.4	39	1983.9
1	1617.2	8.5	1961.4	16	1942.3	25	1965.9	40	1987.3
1.5	1408.0	9	1961.4	16.5	1943.4	26	1963.6	41	1988.4
2	1405.8	9.5	1961.4	17	1943.4	27	1965.9	42	1985.0
2.5	1507.0	10	1961.4	17.5	1943.4	28	1971.5	43	1981.6
3	1624.0	10.5	1961.4	18	1945.6	29	1974.9	44	1983.9
3.5	1723.0	11	1959.1	18.5	1947.9	30	1974.9	46	1988.4
4	1799.4	11.5	1955.8	19	1946.8	31	1978.3	48	1983.9
4.5	1852.3	12	1954.6	19.5	1947.9	32	1981.6	50	1987.3
5	1890.5	12.5	1952.4	20	1949.0	33	1983.9	52	1987.3
5.5	1917.5	13	1951.3	20.5	1951.3	34	1982.8	54	1988.4
6	1935.5	13.5	1947.9	21	1952.4	35	1981.6	56	1989.5
6.5	1947.9	14	1947.9	21.5	1952.4	36	1981.6	58	1987.3
7	1954.6	14.5	1945.6	22	1954.6	37	1983.9	60	1987.3

Run#78: 8/20/98; 50°C; 29% RH;

0.1 g Sorb: 4/28/97-50; 96.3 m²/g; 0.437 cm³/g

min	ppm	min	ppm	min	ppm	min	ppm	min	ppm
0	2006.2	7.5	1879.6	15	1958.4	23	1980.7	38	1995.1
0.5	1921.8	8	1896.2	15.5	1959.5	24	1980.7	39	1995.1
1	1571.8	8.5	1906.2	16	1959.5	25	1984.0	40	1989.5
1.5	1207.5	9	1915.1	16.5	1959.5	26	1981.8	41	1992.9
2	1020.8	9.5	1921.8	17	1960.7	27	1982.9	42	1995.1
2.5	1026.4	10	1928.4	17.5	1964.0	28	1986.2	43	1990.6
3	1163.0	10.5	1930.7	18	1964.0	29	1989.5	44	1989.5
3.5	1333.0	11	1936.2	18.5	1962.9	30	1988.4	46	1989.5
4	1484.1	11.5	1941.8	19	1962.9	31	1986.2	48	1998.4
4.5	1601.8	12	1945.1	19.5	1964.0	32	1988.4	50	1992.9
5	1690.7	12.5	1950.7	20	1964.0	33	1989.5	52	1996.2
5.5	1751.8	13	1950.7	20.5	1966.2	34	1992.9	54	1996.2
6	1801.8	13.5	1954.0	21	1970.7	35	1997.3	56	1998.4
6.5	1837.3	14	1954.0	21.5	1977.3	36	1998.4	58	1995.1
7	1860.7	14.5	1954.0	22	1977.3	37	1996.2	60	1996.2

Run#79: 8/21/98; 50°C; 58% RH;
0.025 g Sorb: 4/28/97-50; 96.3 m²/g; 0.437 cm³/g

min	ppm	min	ppm	min	ppm	min	ppm	min	ppm
0	2004.1	7.5	1950.1	15	1944.4	23	1961.3	38	1986.1
0.5	1918.5	8	1953.4	15.5	1947.8	24	1962.5	39	1990.6
1	1589.8	8.5	1954.6	16	1950.1	25	1968.1	40	1992.9
1.5	1355.6	9	1956.8	16.5	1947.8	26	1970.3	41	1989.5
2	1355.6	9.5	1956.8	17	1947.8	27	1972.6	42	1990.6
2.5	1468.2	10	1956.8	17.5	1950.1	28	1971.5	43	1990.6
3	1596.5	10.5	1956.8	18	1951.2	29	1974.8	44	1991.7
3.5	1704.6	11	1951.2	18.5	1951.2	30	1974.8	46	1990.6
4	1782.3	11.5	1950.1	19	1953.4	31	1977.1	48	1992.9
4.5	1839.7	12	1950.1	19.5	1952.3	32	1980.5	50	1989.5
5	1878.0	12.5	1948.9	20	1950.1	33	1983.9	52	1989.5
5.5	1905.0	13	1947.8	20.5	1953.4	34	1983.9	54	1986.1
6	1925.3	13.5	1945.6	21	1953.4	35	1983.9	56	1987.2
6.5	1937.7	14	1945.6	21.5	1954.6	36	1986.1	58	1990.6
7	1944.4	14.5	1945.6	22	1954.6	37	1987.2	60	1987.2

Run#80: 8/21/98; 50°C; 58% RH;
0.025 g Sorb: 4/28/97-50; 96.3 m²/g; 0.437 cm³/g

min	ppm	min	ppm	min	ppm	min	ppm	min	ppm
0	998.6	7.5	947.2	15	959.7	23	950.7	38	980.0
0.5	957.3	8	952.5	15.5	959.1	24	950.7	39	981.8
1	786.9	8.5	956.7	16	957.9	25	953.1	40	984.2
1.5	614.7	9	959.1	16.5	957.3	26	956.7	41	985.4
2	532.2	9.5	960.3	17	956.7	27	960.3	42	987.8
2.5	552.5	10	962.7	17.5	955.5	28	962.7	43	987.8
3	627.2	10.5	963.3	18	955.5	29	965.1	44	990.8
3.5	708.6	11	962.7	18.5	953.7	30	967.5	46	990.2
4	778.5	11.5	965.1	19	951.9	31	971.7	48	991.4
4.5	832.3	12	966.9	19.5	951.9	32	974.1	50	990.8
5	870.6	12.5	965.1	20	950.7	33	975.9	52	990.8
5.5	896.9	13	962.7	20.5	950.7	34	978.2	54	990.2
6	916.7	13.5	962.7	21	950.7	35	978.8	56	992.6
6.5	931.6	14	962.1	21.5	950.7	36	978.8	58	993.2
7	940.0	14.5	960.3	22	951.9	37	979.4	60	992.6

Run#81: 8/25/98; 50°C; 58% RH;
0.1 g Sorb: 8/2/98-21; 108.9 m²/g

min	ppm	min	ppm	min	ppm	min	ppm	min	ppm
0	998.0	7.5	450.1	15	825.3	23	864.8	38	955.5
0.5	957.9	8	485.0	15.5	825.8	24	870.0	39	959.6
1	784.0	8.5	519.9	16	825.8	25	878.8	40	960.8
1.5	578.1	9	553.7	16.5	825.3	26	885.7	41	962.5
2	402.5	9.5	588.0	17	825.8	27	893.3	42	964.3
2.5	278.6	10	621.1	17.5	827.6	28	904.9	43	965.4
3	207.1	10.5	658.4	18	828.8	29	913.1	44	965.4
3.5	181.5	11	699.1	18.5	832.2	30	918.9	46	972.4
4	188.4	11.5	736.3	19	835.2	31	923.6	48	973.0
4.5	214.0	12	765.4	19.5	839.8	32	928.2	50	976.5
5	250.7	12.5	788.0	20	843.9	33	933.4	52	974.7
5.5	290.8	13	804.3	20.5	849.1	34	937.5	54	976.5
6	331.5	13.5	813.6	21	853.8	35	939.3	56	980.5
6.5	372.2	14	819.4	21.5	858.4	36	943.9	58	981.1
7	411.8	14.5	823.5	22	859.6	37	952.0	60	980.5

Run#82: 8/25/98; 50°C; 58% RH;
0.1 g Sorb: 8/17/98-21; 114.5 m²/g; 0.490 cm³/g

min	ppm	min	ppm	min	ppm	min	ppm	min	ppm
0	998.6	7.5	424.5	15	868.0	23	849.0	38	896.2
0.5	999.7	8	480.8	15.5	866.3	24	836.9	39	904.2
1	998.0	8.5	539.5	16	866.3	25	832.9	40	910.0
1.5	958.3	9	597.0	16.5	865.1	26	839.8	41	919.8
2	792.6	9.5	649.4	17	865.1	27	847.9	42	925.5
2.5	586.7	10	695.4	17.5	864.0	28	857.1	43	929.5
3	415.3	10.5	733.4	18	862.8	29	865.1	44	931.8
3.5	303.1	11	766.2	18.5	859.9	30	872.0		
4	247.3	11.5	795.5	19	857.6	31	881.2		
4.5	229.5	12	820.2	19.5	855.9	32	888.1		
5	234.6	12.5	837.5	20	854.8	33	895.6		
5.5	256.5	13	849.0	20.5	853.6	34	885.8		
6	288.7	13.5	858.2	21	852.5	35	876.6		
6.5	327.8	14	864.5	21.5	852.5	36	876.0		
7	372.7	14.5	867.4	22	850.7	37	885.8		

Run#83: 8/26/98; 50°C; 58% RH;
0.1 g Sorb: 8/17/98-21; 114.5 m²/g; 0.490 cm³/g

min	ppm	min	ppm	min	ppm	min	ppm	min	ppm
0	999.7	7.5	581.4	15	908.9	23	918.1	38	940.0
0.5	960.7	8	660.7	15.5	908.9	24	917.6	39	940.0
1	792.9	8.5	729.7	16	910.7	25	918.1	40	942.3
1.5	586.6	9	782.0	16.5	910.1	26	918.7	41	944.6
2	410.2	9.5	820.5	17	916.4	27	920.4	42	948.0
2.5	282.6	10	848.6	17.5	919.3	28	921.6	43	948.0
3	206.2	10.5	867.0	18	919.9	29	920.4	44	951.5
3.5	174.6	11	878.5	18.5	919.3	30	921.6	46	956.1
4	175.8	11.5	887.1	19	917.6	31	923.9	48	960.1
4.5	201.6	12	894.0	19.5	917.0	32	925.6	50	961.8
5	243.0	12.5	898.6	20	917.6	33	928.5	52	965.2
5.5	294.1	13	903.2	20.5	917.0	34	930.2	54	967.5
6	351.6	13.5	906.1	21	916.4	35	929.6	56	970.4
6.5	420.0	14	907.8	21.5	914.1	36	935.4	58	971.6
7	498.1	14.5	908.9	22	915.8	37	939.4	60	975.6

Run#84: 8/26/98; 50°C; 58% RH;
0.1 g Sorb: 5/10/93-12; 30.8 m²/g; sample prepared by Kind

min	ppm	min	ppm	min	ppm	min	ppm	min	ppm
0	1000.3	7.5	739.2	15	939.4	23	968.4	38	983.8
0.5	959.9	8	767.1	15.5	943.4	24	971.3	39	983.8
1	791.6	8.5	792.7	16	948.0	25	971.3	40	982.1
1.5	614.7	9	813.2	16.5	950.2	26	973.0	41	982.1
2	501.5	9.5	830.8	17	952.5	27	974.7	42	982.1
2.5	448.6	10	849.0	17.5	955.9	28	975.8	43	983.8
3	435.0	10.5	865.5	18	957.6	29	977.0	44	983.8
3.5	448.1	11	875.7	18.5	959.9	30	978.7	46	986.6
4	475.9	11.5	887.7	19	961.0	31	978.1	48	986.6
4.5	512.3	12	900.2	19.5	962.2	32	980.4	50	984.9
5	552.7	12.5	907.6	20	963.9	33	978.7	52	982.1
5.5	594.2	13	914.4	20.5	963.9	34	980.4	54	986.6
6	634.0	13.5	921.8	21	963.9	35	982.1	56	984.4
6.5	672.7	14	927.5	21.5	963.9	36	982.1	58	983.8
7	708.0	14.5	934.9	22	965.0	37	981.5	60	983.8

Run#85: 8/26/98; 50°C; 58% RH;
0.1 g Sorb: 8/18/92-4; 57.0 m²/g; sample prepared by Kind

min	ppm	min	ppm	min	ppm	min	ppm	min	ppm
0	998.6	7.5	712.4	15	945.1	23	955.5	38	962.5
0.5	960.2	8	756.6	15.5	946.2	24	953.8	39	966.0
1	788.0	8.5	793.9	16	947.4	25	952.0	40	967.2
1.5	589.1	9	822.4	16.5	949.1	26	948.6	41	969.5
2	440.3	9.5	846.2	17	950.9	27	947.4	42	967.8
2.5	354.2	10	866.0	17.5	950.9	28	947.4	43	966.0
3	319.3	10.5	882.3	18	952.0	29	950.9	44	966.0
3.5	318.7	11	898.0	18.5	952.0	30	952.0	46	972.4
4	340.2	11.5	910.2	19	953.8	31	950.9	48	971.8
4.5	377.4	12	919.5	19.5	954.4	32	949.7	50	975.3
5	427.5	12.5	926.5	20	954.4	33	950.9	52	980.0
5.5	482.1	13	930.5	20.5	955.0	34	949.1	54	981.1
6	542.6	13.5	934.0	21	955.0	35	953.8	56	980.0
6.5	603.1	14	939.3	21.5	954.4	36	952.0	58	981.1
7	660.7	14.5	942.7	22	956.7	37	955.5	60	985.8

Run#86: 8/30/98; 50°C; 58% RH;
0.1 g Sorb: 8/17/98-21; 114.5 m²/g; 0.490 cm³/g

min	ppm	min	ppm	min	ppm	min	ppm	min	ppm
0	998.6	7.5	596.0	15	933.7	23	944.7	38	960.3
0.5	960.9	8	648.2	15.5	933.7	24	947.6	39	961.5
1	790.1	8.5	697.4	16	935.4	25	952.2	40	960.9
1.5	580.4	9	745.5	16.5	938.9	26	954.0	41	963.2
2	402.6	9.5	790.1	17	941.2	27	954.6	42	963.2
2.5	286.1	10	828.3	17.5	942.4	28	954.0	43	965.0
3	230.0	10.5	857.2	18	943.0	29	951.1	44	963.2
3.5	221.8	11	880.4	18.5	944.1	30	953.4	46	966.1
4	243.9	11.5	895.5	19	944.1	31	954.6	48	967.9
4.5	282.7	12	907.6	19.5	944.7	32	956.9	50	970.2
5	330.7	12.5	916.3	20	944.1	33	959.2	52	973.1
5.5	379.4	13	924.4	20.5	943.0	34	958.6	54	971.9
6	432.1	13.5	929.6	21	941.2	35	959.2	56	972.5
6.5	487.1	14	932.5	21.5	941.8	36	961.5	58	972.5
7	542.7	14.5	932.0	22	944.7	37	961.5	60	973.1

Run#87: 8/30/98; 50°C; 29% RH;

0.1 g Sorb: 4/28/97-50; 96.3 m²/g; 0.437 cm³/g

min	ppm	min	ppm	min	ppm	min	ppm	min	ppm
0	500.4	7.5	256.0	15	445.4	23	470.9	38	485.7
0.5	478.8	8	275.4	15.5	449.4	24	472.4	39	486.0
1	392.2	8.5	294.8	16	450.4	25	474.5	40	485.7
1.5	287.2	9	312.8	16.5	452.2	26	476.0	41	485.7
2	198.4	9.5	330.0	17	454.0	27	476.0	42	486.4
2.5	138.8	10	346.2	17.5	455.8	28	476.7	43	486.0
3	108.9	10.5	361.7	18	457.3	29	479.6	44	486.0
3.5	101.4	11	375.3	18.5	458.4	30	481.4	46	488.6
4	108.9	11.5	389.3	19	459.8	31	481.7	48	487.5
4.5	125.1	12	402.6	19.5	461.6	32	481.7	50	488.6
5	146.7	12.5	413.8	20	461.6	33	481.7	52	488.6
5.5	168.6	13	423.1	20.5	463.4	34	482.8	54	487.5
6	191.3	13.5	430.7	21	465.2	35	483.9	56	490.4
6.5	214.3	14	436.4	21.5	465.9	36	485.0	58	490.4
7	235.5	14.5	441.1	22	467.3	37	485.0	60	491.8

Run#88: 9/14/98; 50°C; 58% RH;

0.2 g Sorb: 4/28/97-50; 96.3 m²/g; 0.437 cm³/g

min	ppm	min	ppm	min	ppm	min	ppm	min	ppm
0	998.6	15	514.3	30	818.1	45	845.2	75	945.1
0.5	959.8	15.5	550.2	30.5	818.1	46	849.9	76	948.6
1	788.8	16	583.1	31	817.6	47	855.8	78	952.7
1.5	580.7	16.5	613.0	31.5	818.1	48	860.5	80	959.2
2	403.2	17	640.7	32	818.1	49	866.3	82	965.7
2.5	273.9	17.5	665.3	32.5	819.9	50	868.7	84	972.1
3	184.6	18	688.9	33	820.5	51	872.2	86	971.0
3.5	124.7	18.5	711.2	33.5	819.9	52	874.0	88	975.1
4	86.5	19	730.6	34	819.3	53	878.1	90	975.7
4.5	61.2	19.5	747.6	34.5	818.1	54	879.3	92	974.5
5	44.1	20	764.7	35	817.0	55	882.8	94	975.1
5.5	34.7	20.5	780.5	35.5	818.1	56	887.5	96	975.7
6	30.6	21	794.1	36	819.3	57	891.0	98	975.7
6.5	33.0	21.5	804.0	36.5	819.9	58	895.1	100	980.9
7	41.2	22	814.0	37	822.9	59	896.9	104	979.2
7.5	54.1	22.5	822.9	37.5	825.2	60	901.6	108	977.4
8	70.6	23	829.3	38	827.0	61	906.3	112	981.5
8.5	92.9	23.5	834.6	38.5	829.9	62	909.2	116	982.7
9	117.0	24	837.0	39	832.3	63	911.0	120	982.1
9.5	144.1	24.5	838.7	39.5	833.4	64	916.3		
10	171.1	25	838.1	40	835.2	65	921.6		
10.5	199.3	25.5	836.4	40.5	837.0	66	923.3		
11	230.4	26	835.8	41	838.7	67	926.3		
11.5	259.8	26.5	834.0	41.5	840.5	68	928.6		
12	291.6	27	831.7	42	841.1	69	929.8		
12.5	324.5	27.5	829.3	42.5	841.1	70	932.8		
13	357.4	28	826.4	43	841.1	71	935.7		
13.5	395.0	28.5	822.9	43.5	841.7	72	936.3		
14	434.4	29	820.5	44	841.7	73	940.4		
14.5	473.8	29.5	819.3	44.5	842.8	74	943.3		

Run#89: 9/14/98; 50°C; 58% RH;
0.2 g Sorb: 4/28/97-50; 96.3 m²/g; 0.437 cm³/g

min	ppm	min	ppm	min	ppm	min	ppm	min	ppm
0	998.0	15	454.9	30	876.3	45	902.2	75	945.1
0.5	956.8	15.5	491.4	30.5	876.3	46	900.4	76	942.7
1	785.2	16	530.8	31	879.3	47	901.6	78	948.6
1.5	575.4	16.5	569.0	31.5	879.3	48	902.8	80	952.1
2	398.5	17	604.2	32	881.0	49	906.3	82	956.3
2.5	269.2	17.5	639.5	32.5	883.4	50	907.5	84	956.8
3	181.1	18	672.4	33	885.7	51	909.8	86	959.2
3.5	122.3	18.5	702.4	33.5	888.1	52	910.4	88	959.2
4	84.1	19	727.6	34	889.8	53	912.2	90	959.2
4.5	58.8	19.5	747.6	34.5	892.2	54	912.2	92	961.0
5	42.4	20	764.7	35	892.2	55	913.9	94	963.3
5.5	34.7	20.5	778.2	35.5	893.4	56	916.3	96	963.9
6	33.0	21	789.9	36	894.6	57	920.4	98	966.3
6.5	37.1	21.5	800.5	36.5	895.1	58	920.4	100	971.0
7	44.7	22	811.1	37	895.1	59	923.3	104	970.4
7.5	56.5	22.5	820.5	37.5	895.7	60	925.1	108	975.1
8	71.8	23	828.7	38	894.6	61	926.3	112	979.8
8.5	88.2	23.5	834.6	38.5	894.6	62	929.2	116	978.0
9	109.4	24	841.7	39	895.1	63	928.6		
9.5	132.9	24.5	848.1	39.5	895.1	64	930.4		
10	158.2	25	854.0	40	895.1	65	932.2		
10.5	184.6	25.5	859.3	40.5	895.1	66	934.5		
11	211.6	26	864.0	41	895.7	67	937.5		
11.5	239.3	26.5	866.9	41.5	896.9	68	941.0		
12	266.9	27	868.7	42	899.8	69	939.8		
12.5	296.3	27.5	869.9	42.5	899.8	70	939.2		
13	325.1	28	871.0	43	901.6	71	938.6		
13.5	355.6	28.5	874.0	43.5	902.8	72	939.8		
14	386.8	29	875.7	44	904.0	73	939.2		
14.5	420.3	29.5	874.6	44.5	904.5	74	940.4		

Table B.6: Summary of Sandbed Experiments

RUN#	Date	Temp °C	RH %	SO ₂ ppm	Solid g	Sorbent	Notes
50	1/20/98	50	29	1000	0.1	4/28/97-50	10 g sand +20g sand w/ sorbent
51	1/20/98	50	58	1000	0.1	4/28/97-50	10 g sand +20g sand w/ sorbent
52	1/27/98	50	0	1000	0.1	4/28/97-50	10 g sand +20g sand w/ sorbent
53	1/27/98	50	88	1000	0.1	4/28/97-50	
54	1/28/98	36.5	59	1000	0.1	4/28/97-50	
55	1/31/98	50	58	1000	0.1	11/21/94-5	Very noisy
56	2/2/98	50	58	1000	0.1	hydrated lime	Lime
57	2/2/98	50	58	500	0.1	4/28/97-50	
58	2/2/98	50	58	1000	0.1	11/21/94-25	Double hump
59	2/5/98	50	58	1000	0.1	4/28/97-50	
60	2/12/98	50	59	2000	0.1	4/28/97-50	
61	2/17/98	69.5	59	1000	0.1	4/28/97-50	Exp problems
62	2/25/98	50	58	1000	0.1	12/6/94-15	1/1/0.5-120C
63	2/25/98	50	58	1000	0.1	9/25/96-23	1/1/0-120C
64	2/26/98	50	58	1000	0.1	1/22/97-43-20%	Non-agitated sample
65	2/26/98	50	58	1000	0.1	12/12/97-4/1-B	NA-4/1-lime/slag
66	3/9/98	50	58	1000	0.1	4/28/97-50	On .609g glass wool
67	3/30/98	50	58	500	0.025	4/28/97-50	
68	6/1/98	50	58	1000	0.1	4/28/97-50	
69	6/1/98	50	58	1000	0.1	4/28/97-50	5% Oxygen
70	6/9/98	50	58	1000	0.1	4/28/97-50	Double hump
71	6/10/98	50	58	1000	0.1	4/28/97-50	
72	6/10/98	50	58	1000	0.1	4/28/97-50	5% Oxygen
73	8/17/98	50	29	500	0.1	4/28/97-50	
74	8/17/98	50	58	1000	0.025	4/28/97-50	
75	8/19/98	50	58	1000	0.1	slag	slag
76	8/19/98	50	58	1000	0.1	8/2/98-30	0.5/1/0.1 lime/slag/gyp
77	8/20/98	50	58	2000	0.025	4/28/97-50	
78	8/20/98	50	29	2000	0.1	4/28/97-50	
79	8/21/98	50	58	2000	0.025	4/28/97-50	
80	8/21/98	50	58	1000	0.025	4/28/97-50	
81	8/25/98	50	58	1000	0.1	8/2/98-21	0.5/1/0.1 lime/slag/gyp
82	8/25/98	50	58	1000	0.1	8/17/98-21	exp problems
83	8/26/98	50	58	1000	0.1	8/17/98-21	0.5/1 - 0.05M CaCl ₂
84	8/26/98	50	58	1000	0.1	5/10/93-12	Flyash Sorbent
85	8/26/98	50	58	1000	0.1	8/18/92-4	Silica Fume Sorbent
86	8/30/98	50	58	1000	0.1	8/17/98-21	0.5/1 - 0.05M CaCl ₂
87	8/30/98	50	29	500	0.1	4/28/97-50	
88	9/14/98	50	58	1000	0.2	4/28/97-50	
89	9/14/98	50	58	1000	0.2	4/28/97-50	

Appendix C: Timelag Analysis of SO₂ Analytical Train

The purpose of the SO₂ analyzer is to measure the concentration at the outlet of the sandbed reactor. This concentration is subject to drastic and rapid changes over the course of an experiment. This is especially true at time zero, when a constant flow at the inlet SO₂ concentration is diverted from bypass to the reactor, and the outlet concentration makes an instantaneous step-change drop. The concentration is also expected to change rapidly during the course of reaction as the sorbent is reacted. The analyzer, however, does not manage to execute these sharp concentration changes. In part, this timelag may be due to the physical tubing connecting the reactor to the analyzer, but it is probably also due to the analyzer itself. Unfortunately, the analyzer used in this work was designed for steady-state measurements, not time-dependent analysis. This appendix will present what was found regarding the timelag, as well as an empirical model to estimate the relationship between the concentration at the outlet of the reactor and the measured concentration.

C.1 SUSPECTED SOURCES OF TIMELAG

Figure C.1 shows the equipment between the sandbed reactor and the analyzer. The outlet concentration from the reactor, C_{exp} , is the variable of interest. However, the concentration that is measured and recorded is C_{meas} .

A physical timelag would be expected in the system from the lines and analyzer reaction chamber. The flowrate through the analyzer is approximately 15.7 ml/s and the chamber has a volume of ~500 ml. Therefore, one would expect a physical timelag on the order of 30 sec. Figure 3.4 shows that the measured data takes around four minutes to reach the maximum removal, which theoretically should occur at time zero.

Also, the analyzer electronics has an electronic signal dampening routine installed to smooth the signal. Unfortunately, the actual algorithm was not available, so this was treated as a black box.

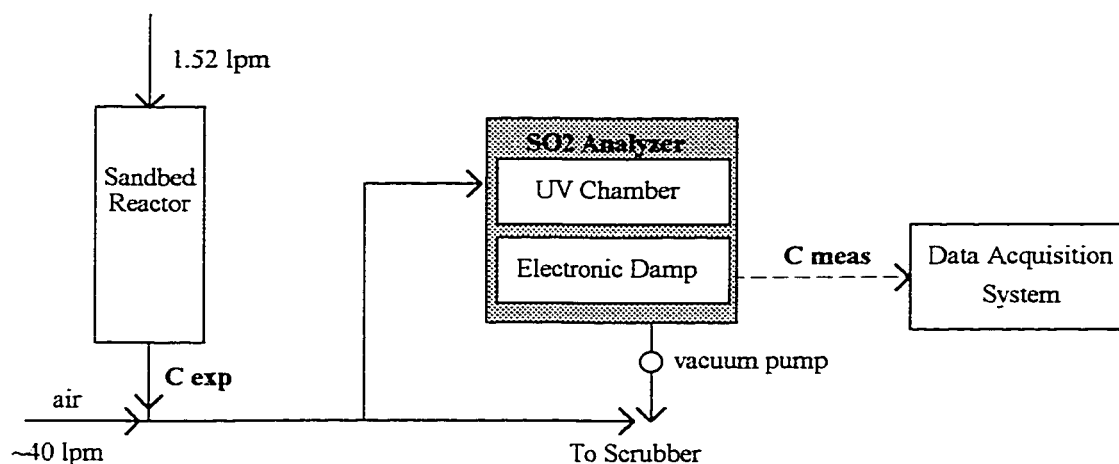


Figure C.1: SO_2 Analytical System

C.2 TIMELAG MODEL

A series of step change experiments was performed to gather information regarding the system without the sandbed reactor in place. The synthesized flue gas was run through the bypass line around the reactor. At specified times, the concentration was changed. It usually took ~ 20 seconds for the actual concentration change to take place due to the response of the flow controllers. The time when the change was completed was used as the nominal time of the step change. Figure C.2 shows two experiments conducted at 0%RH and 58%RH respectively. For these experiments, the SO_2 concentration was measured and recorded every two seconds. For both experiments the concentration was originally at ~ 1000 ppm, changed to 500 ppm, changed to 0 ppm, and returned to the original ~ 1000 ppm. An example of the analyzer drift over the course of the entire day is evident in that the first experiment started at 1005 ppm and the second at 983 ppm.

The timelag was modeled by Equations C.1-3. These two experiments, and two others in which the SO_2 concentration was recorded only every 30 sec, were fit with this model. Parameters were regressed using the EXCEL non-linear regression SOLVER routine, minimizing the square of the normalized differences

as shown in Equation C.4. The results of these independent regressions are shown in Table C.1. Relative humidity was not expected to affect the SO₂ measurement, because the flue gas is so heavily diluted prior to analysis. As neither the measurement interval nor the relative humidity in the flue gas seemed to affect the parameters greatly, the two experiments shown in Figure C.2 were regressed together. The parameters from the regression shown in Figure C.2 ($\Theta=23.77$ (sec/2), $k=7.93\text{e-}5$ (sec/2)⁻¹) were regressed at 2 sec intervals ($dt = 2$ sec) and incorporated as such into the sandbed reactor model to correct for the timelag.

$$\frac{dC_1}{dt} = \frac{C_{\text{exp}} - C_1}{\Theta} \quad (\text{C.1})$$

$$\frac{dC_2}{dt} = \frac{C_1 - C_2}{\Theta} - k(C_2 - C_0) \quad (\text{C.2})$$

$$\frac{dC_3}{dt} = \frac{C_2 - C_3}{\Theta} - k(C_3 - C_0) \quad (\text{C.3})$$

where C_0 = initial SO₂ concentration (~1000 ppm)

$$\text{regress parameters minimizing: } \sum \left(\frac{C_{\text{meas}} - C_3}{C_{\text{meas}}} \right)^2 \quad (\text{C.4})$$

Table C.1: Timelag Regression Results

Experiment	Θ (sec)	k (sec) ⁻¹
2 sec. measurements, 0%RH	11.898	3.35e-5
2 sec. measurements, 58%RH	11.670	6.0e-5
30 sec. measurements, 0%RH	12.090	3.33e-5
30 sec. measurements, 58%RH	12.416	1.86e-5
2 sec. measurements, 0 & 58%RH	11.886	3.97e-5

It should be emphasized that the model outlined in Equations C.1-3 is an empirical model. It began as a series of three CSTR's which would represent some middle ground between CSTR and PFR behavior. An adsorption term was then added to the second and third CSTR with the expectation that some of the timelag was due to surface adsorption of SO₂ on the lines of the equipment. However, this model didn't provide an adequate fit and the adsorption terms were altered by

changing the driving force from $(C_{\text{gas}} - C_{\text{equil}}^*)$ to $(C_{\text{gas}} - C_0)$. Therefore, while the model originated from a theoretical basis, the final model can only be called empirical. It should also be noted that the modeled residence time of 35.7 sec. (3CSTR's at $\Theta = 11.89$ s) is of the same magnitude as the expected residence time through the analytical train.

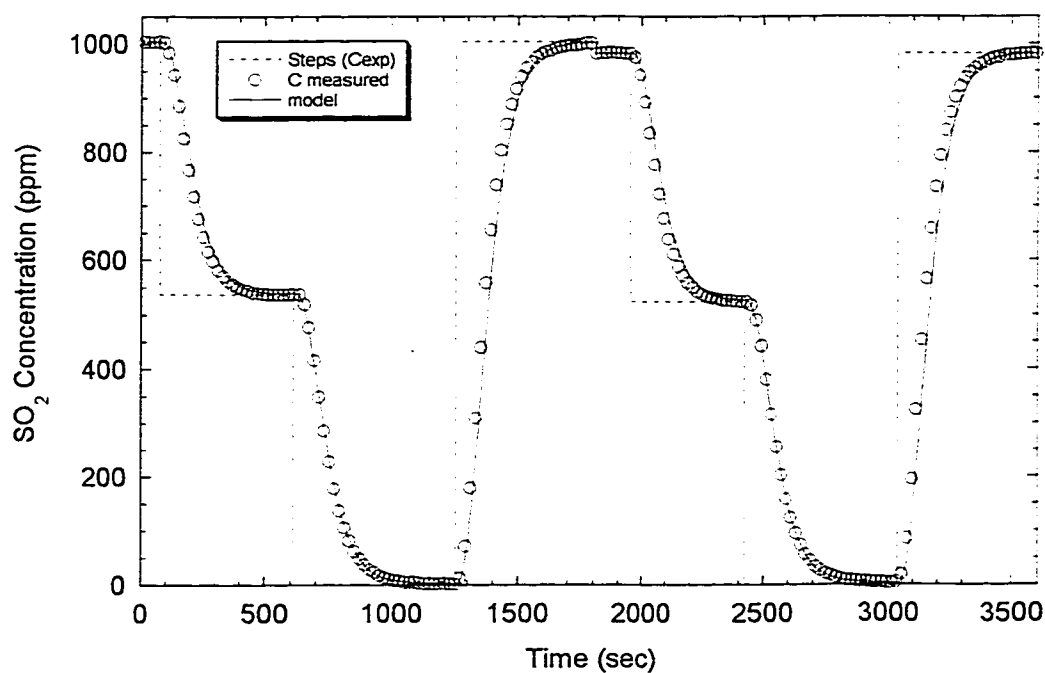


Figure C.2: Timelag Model: Step Change Regression

Two separate experiments shown. C_{meas} recorded at 2 sec intervals;. Every 10th C_{meas} shown for clarity.

Regressed parameters: $\Theta = 23.77 \text{ (sec/2)}$; $k = 7.93\text{e-}5 \text{ (sec/2)}^{-1}$.

Appendix D: Sample SO₂ Removal Calculations

This appendix outlines the calculations used to find average SO₂ removal and solids conversion values. These calculations were conducted using an EXCEL spreadsheet.

Table D.1 shows an example of raw data for Experiment# 51. This experiment used 0.1 g of glass ADVACATE, which had a divalent alkalinity of 0.0066 mmol/g. The total gas flow rate was 1.521 slpm. Calculations will be demonstrated for the data at 1.5 minutes.

Table D.1 Experimental Raw Data for Sample Calculations

Time (min)	C _{in} (ppm)	C _{exp} (ppm)	fxn conv	fxn rem
0	1036.63	1036.63	0	0
0.5	1036.63	1028.80	0.000184	0.007554
1	1036.63	939.65	0.00265	0.093549
1.5	1036.63	768.59	0.0112	0.258568

Fractional SO₂ removal (fxn rem) is an instantaneous measurement defined by the following.

$$\text{fxn_rem} = \frac{C_{\text{in}} - C_{\text{out}}}{C_{\text{in}}} = \frac{1036.63 - 768.59}{1036.63} = 0.2585$$

Fractional solids conversion (fxn conv) is a cumulative measurement of the extent of reaction normalized to the original amount of alkalinity.

$$\text{flow}\left(\frac{\text{mol}}{\text{s}}\right) = 1.521\left(\frac{\text{l}}{\text{min}}\right) * \frac{\text{min}}{60\text{s}} * \frac{1\text{atm}}{0.08206 \frac{\text{latm}}{\text{molK}} 298.15\text{K}} = 1.036\text{e}-3 \frac{\text{mol}}{\text{s}}$$

$$\text{rem}_{0.5} = \left(1036.63 - \frac{1036.63 + 1028.8}{2}\right) \text{ppm} * \frac{1.036\text{e}-3(\text{mol} / \text{s})}{10^6} * 30\text{sec} = 1.22\text{e}-7 \text{mol}$$

$$\text{rem}_{1.0} = \left(1036.63 - \frac{1028.8 + 939.65}{2}\right) \text{ppm} * \frac{1.036\text{e}-3(\text{mol} / \text{s})}{10^6} * 30\text{sec} = 1.63\text{e}-6 \text{mol}$$

$$\text{rem}_{1.5} = (1036.63 - \frac{768.59 + 939.65}{2}) \text{ppm} * \frac{1.036\text{e}-3(\text{mol} / \text{s})}{10^6} * 30 \text{sec} = 5.67\text{e}-6 \text{mol}$$

$$\sum \text{sumrem} = 1.22\text{e}-7 + 1.63\text{e}-6 + 5.67\text{e}-6 = 7.42\text{e}-6 \text{mol}$$

$$\text{fxn_conv} = \frac{7.42\text{e}-6 \text{molSO}_2}{0.0066 \frac{\text{molalk}}{\text{g}} * 0.1 \text{g}} = 0.0112$$

Appendix E: Fortran Code for Packed Bed and Baghouse Systems

This appendix includes the fortran code routines for the sandbed reactor system as well as the baghouse prediction model.

E.1 SANDBED REACTOR MODEL

The sandbed model code archived here is formatted as a subroutine. This was for the purpose of parameter regression with GREG which calls the user-defined model in subroutine format.

```
c      model.f
c      theoretical model for engine.f
c      2 Diffusion Layers in parallel
c
      subroutine model (par,f,nob,npar,ider,deriv,minfo)
      implicit double precision (a-h,o-z)
      integer nobs
      character*30 runid,solid
      dimension par(4),f(201),z(201),sobs(300),error(300),slobs(300)
      dimension time(130),so2del(201),conv(201),alkleft(201),so2(201)
      dimension so2flow(201),fxn(201)
c
c      so2con=inletso2(ppm);nobs=#observations;alk=mmol alk in bed
c      z=so2ppm;so2flow=molso2/s
c      so2flow=molso2/s;so2=m.f.so2
c      vr=area/step;flow=slpm;gasflow=moltot/s
c      a,b,c=intermediate rate calculations (dummies)
c
c      read information from data file
c
      open(unit=12,file='input.dat',status='unknown')
      read(12,*) so2con,nobs,runid,solid
      read(12,*) solwt,alk,temp,rh
c
      do 5 k=1,nobs
          read(12,*)sobs(k)
          slobs(k)=log(sobs(k))
5      continue
```

```

close(12)
c
sumerr=0
c
c
general definitions
c
vr=96*solwt/200
flow=1.521
gasflo=flow/0.08206*1/297/60
c
c
initial reactor conditions (needed to zero values for greg iterations)
a=0.0
b=0.0
c=0.0
do 7, ci=1,201
    conv(ci)=0.0
    alkleft(ci)=alk/200
    fxn(ci)=0.0
    so2(ci)=0.0
    z(ci)=0.0
    so2flow(ci)=0.0
7
continue
c
c
initial conditions and parameters for analyzer correction
m=1
cin=so2con
c0=so2con
c1=so2con
c2=so2con
c3=so2con
theta=23.77088
ck=7.93e-5
c
c
initial conditions for Greg Output
c
i=observation#
c
i=1
time(1)=0
f(1)=log(so2con)

```

```

c
c   inlet so2 flows
c
  so2flow(1)=gasflo*so2con/1.0e6
  so2(1)=so2con/1e6
c
c   so2rate is a function of so2(mf) from previous space step (same t)
c   and conversion from previous time step (same z)
c
c   Dance through time t(j) in 30 second blocks.
100 do 200 j=1,30
c
c   Dance through space. z(k)
  do 100 k=2,201
    a=1/so2(k-1)/par(1)
    b=conv(k)/par(2)/(par(4)-conv(k))
    c=so2(k-1)*par(3)/conv(k)*(1.0-conv(k))
    if (conv(k).le.0.0) c=0.0
    so2del(k)=vr*(fxn(k)*c+(1-fxn(k))/(a+b))
    if (so2del(k).ge.alkleft(k)) so2del(k)=alkleft(k)
    if (so2del(k).ge.so2flow(k-1)) so2del(k)=so2flow(k-1)
    conv(k)=conv(k)+so2del(k)/alk*200
    fxn(k)=conv(k)/par(4)
    if (fxn(k).ge.1.0) fxn(k)=1.0
    alkleft(k)=(1-conv(k))*alk/200
    so2flow(k)=so2flow(k-1)-so2del(k)
    so2(k)=so2flow(k)/gasflo
    z(k)=so2flow(k)/gasflo*1e6
100  continue
c
c   Analyzer Correction on z(last) every 2 seconds. (n=toggle)
c
  n=n+1
  if (n.eq.2) then
    c3=c3+(c2-c3)/theta-ck*(c3-c0)
    c2=c2+(c1-c2)/theta-ck*(c2-c0)
    c1=c1+(cin-c1)/theta
    cin=z(201)
    n=0

```



```

endif
200 continue
c
c Setting Greg output (f(i)) at 30 second intervals.
c
i=i+1
time(i)=time(i-1)+30
f(i) = log(c3)
error(i)=f(i)-slobs(i)
sumerr=sumerr+error(i)**2
c
if (i.lt.nobs) goto 10
c
write (*,*) par(1),par(2),par(3),par(4),sumerr
return
end

```

E.2 BAGHOUSE PREDICTION MODEL

```

c baghouse.f
c bagfilter prediction model
c 2 Diffusion Layers in parallel
c
program baghouse
implicit double precision (a-h,o-z)
dimension time(130),so2del(3601),conv(3601),alkleft(3601)
dimension so2flow(3601),fxn(3601),z(3601),par(4),so2(3601)
c
c time=min;so2del=molso2/s;so2=m.f.so2;so2flow=molso2/s;z=ppm
c flow=slpm;gasflo=moltotal/s;alk=molalk added each sec
c so2fin=molso2/s inlet;so2cin=mfso2 conc inlet
c
read (*,*) so2con,stoic
c
c initial reactor conditions
flow=1.521
gasflo=flow/0.08206*1/297/60
so2fin=gasflo*so2con/1.0e6
so2cin=so2con/1e6
alk=so2fin*stoic

```

```

solalk=0.0066
sa=96
vr=alk*sa/solalk
c
c   initial time settings: i=counter of 30 sec intervals
min=60
i=1
time(1)=0
iend=min*2+1
c
c   model parameters
c
par(1)=5.95e-4
par(2)=1.36e-7
par(3)=1.57e-5
par(4)=0.801
c
c   Dance through time t(j) in 30 second blocks.
10 do 200 j=1,30
c
c   Add sorbent to bed each time loop
m=m+1
conv(m)=0
alkleft(m)=alk
so2(m+1)=so2cin
so2flow(m+1)=so2fin
c
c   Dance through space. z(k) for each time and growing bed
do 100 k=m,1,-1
    a=1/so2(k+1)/par(1)
    b=conv(k)/par(2)/(par(4)-conv(k))
    c=so2(k+1)*par(3)/conv(k)*(1.0-conv(k))
    if (conv(k).le.0.0) c=0.0
    so2del(k)=vr*(fxn(k)*c+(1-fxn(k))/(a+b))
    if (so2del(k).ge.alkleft(k)) so2del(k)=alkleft(k)
    if (so2del(k).ge.so2flow(k+1)) so2del(k)=so2flow(k+1)
    conv(k)=conv(k)+so2del(k)/alk
    fxn(k)=conv(k)/par(4)
    if (fxn(k).ge.1.0) fxn(k)=1.0

```

```

        alyleft(k)=(1-conv(k))*alk
        so2flow(k)=so2flow(k+1)-so2del(k)
        so2(k)=so2flow(k)/gasflo
        z(k)=so2flow(k)/gasflo*1e6
100    continue
c
c    calculate average removal for this cycle time
c
        so2rem=100*(so2con-z(1))/so2con
        totrem=totrem+so2rem
        avgrem=totrem/m
c
200    continue
c
c    Output (f(i)) at 30 second intervals.
c
        i=i+1
        time(i)=time(i-1)+0.5
c
c
        write(*,*) so2rem,avgrem
        if (i.lt.iend) goto 10
c
c
        stop
        end

```

References

- Acurex Environmental, X-ray Fluorescence Analysis on Amber Glass Sample, 1996.
- Boyd, D., D. Thompson, Corning Glass Works, "Glass," Kirk-Othmer, Encyclopedia of Chemical Technology, 3rd edition. Vol. 11. John Wiley and Sons, 1980.
- Brunauer, S., P. H. Emmett, E. Teller, "Adsorption of Gases in Multimolecular Layers," *Journal of the American Chemical Society*, **60**, pp. 309-319, 1938.
- Caracotsios, M., "Model Parametric Sensitivity Analysis and Nonlinear Parameter Estimation: Theory and Applications," Ph.D. Dissertation, The University of Wisconsin, Madison, 1986.
- Chisholm, P. N., G. T. Rochelle, "Simultaneous Dry Absorption of HCl and SO₂ with Hydrated Lime from Humidified Flue Gas," submitted to *Industrial Engineering and Chemistry Research*, September 1998.
- Chu, P., G. T. Rochelle, "Removal of SO₂ and NO_x from Stack Gas by Reaction with Calcium Hydroxide Solids," *JAPCA*, **39**, 175-179, 1989.
- El-Shamy, T. M., J. Lewins, R. W. Douglas, "The Dependence on the pH of the Decomposition of Glasses by Aqueous Solutions," *Glass Technology*, **13**, No. 3, June 1972.
- Garea A., J. R. Viguri, A. Irabien, "Kinetics of Flue Gas Desulphurization at Low Temperatures: Fly Ash/Calcium (3/1) Sorbent Behaviour," *Chemical Engineering Science*, **52**, No. 5, pp. 715-732, 1997.
- Hill, A., "The Transition Temperature of Gypsum to Anhydrite," *Journal of the American Chemical Society*, **59**, pp. 2242-2244 (1937).
- Holzman, M. I., R. S. Atkins, "Retrofitting Acid Gas Controls: A Comparison of Technologies," *Solid Waste & Power*, **2**, No. 5, October 1988.
- Iler, R., The Chemistry of Silica, John Wiley & Sons, 1979.

- Irabien, A., F. Cortabitarte, M. I. Ortiz, "Kinetics of Flue Gas Desulfurization at Low Temperatures: Nonideal Surface Adsorption Model," *Chemical Engineering Science*, **47**, No. 7, pp. 1533-1543, 1992.
- Izquierdo, J. F., F. Cunill, J. C. Martinez, J. Tejero, A. Garcia, "Fly Ash Reactivation for the Desulfurization of Coal-Fired Utility Station's Flue Gas," *Separation Science and Technology*, **27**, No.1, pp. 61-72, 1992.
- JCPDS, International Centre for Diffraction Data, "Alphabetical Index - Inorganic Phases," 1997.
- Jozewicz, W., G. T. Rochelle, "Dry Scrubbing: Flyash Recycle," Final Draft Report for EPA Cooperative Agreement CR 81 1531, Washington, D.C., 1986a.
- Jozewicz, W., G. T. Rochelle, "Fly Ash Recycle in Dry Scrubbing," *Environmental Progress*, **5**(4), 219-224, November, 1986b.
- Jozewicz, W., J. C. S. Chang, C.B. Sedman, T.G. Brna, "Characterization of Advanced Sorbents for Dry SO₂ Control," presented at the AIChE Spring National Meeting, Houston, Texas, March 29-April 2, 1987.
- Jozewicz, W., J. C. S. Chang, C.B. Sedman, T.G. Brna, "Silica-Enhanced Sorbents for Dry Injection Removal of SO₂ from Flue Gas," *JAPCA*, **38**, 1027-1034, 1988a.
- Jozewicz, W., C. Jorgensen, J. S. Chang, C. B. Sedman, T. G. Brna, "Development and Pilot Plant Evaluation of Silica-Enhanced Lime Sorbents for Dry Flue Gas Desulfurization," *JAPCA*, **38**, pp. 796-805, 1988b.
- Jozewicz, W., J. Chang, ACUREX Corporation, "Evaluation of FGD Dry Injection Sorbents and Additives," Vol 1: Development of High Reactivity Sorbents. US EPA Contract # 68-02-3988. EPA-600/7-89-0006a, 1989.
- Jozewicz, W., J. C. S. Chang, C. B. Sedman, "Bench-scale Evaluation of Calcium Sorbents for Acid Gas Emission Control," *Environmental Progress*, **9**, No. 3, August, 1990.

- Jozewicz, W., B. K. Gullett, S. C. Tseng, "A Novel Calcium-Based Sorbent for the Removal of Flue Gas HCl by Dry Injection," presented at the Second International Conference on Municipal Waste Combustion, Tampa, Florida, April 16-19, 1991a.
- Jozewicz, W., G. T. Rochelle, D. E. Stroud, "Reaction of Moist Calcium Silicate Reagents with Sulfur Dioxide in Humidified Flue Gas," Paper 7-12, presented at the 1991 SO₂ Control Symposium, Washington DC, EPRI TR-101054, December, 1991b.
- JTM Industries, "Report of Flyash: W. A. Parish Unit #8," analysis conducted by JTM Industries, Inc., Stafford, Texas, February 13, 1996.
- Kind, K. K., "Hydrothermal Preparation of High Surface Area Calcium Silicate from Lime and Fly Ash in a Flow Reactor," Ph.D. Dissertation, The University of Texas at Austin, 1994.
- Kind, K. K., P. D. Wasserman, G. T. Rochelle, "Effects of Salts on Preparation and Use of Calcium Silicates for Flue Gas Desulfurization," *Environmental Science and Technology*, **28**, 277-283, 1994.
- Klingspor, J., H. T. Karlsson, I. Bjerle, "A Kinetic Study of the Dry SO₂-Limestone Reaction at Low Temperature," *Chemical Engineering Communication*, **22**, pp. 81-103, 1983.
- Koch, "Material Safety Data Sheet: Ground Granulated Blast-Furnace Slag," National Fire Protection Association, 1980.
- Kuehn, S. E., "Utility Plans Take Shape for Title IV Compliance," *Power Engineering*, pp. 19-26, August 1993.
- Ma, W., C. Liu, P. W. Brown, S. Komarneni, "Pore Structures of Fly Ashes Activated by Ca(OH)₂ and CaSO₄•2H₂O," *Cement and Concrete Research*, **25**, No. 2, pp. 417-425, 1995.
- Martinez, J. C., J. F. Izquierdo, F. Cunill, J. Tejero, J. Querol, "Reactivation of Fly Ash and Ca(OH)₂ Mixtures for SO₂ Removal of Flue Gas," *Industrial Engineering and Chemistry Research*, **30**, pp. 2143-2147, 1991.
- Micromeritics, "Operator's Manual; Accelerated Surface Area and Porosimetry System," Micromeritics Corp., July 1995.

- Nelli, C. H., "Nitrogen Dioxide Removal by Calcium Silicate Solids," Ph.D. Dissertation, The University of Texas at Austin, 1997.
- O'Connor, T. L., S. A. Greenberg, "The Kinetics for the Solution of Silica in Aqueous Solutions," *Journal of Physical Chemistry*, **62**, 1195-1198, 1958.
- Peacey, J. G., W. G. Davenport, The Iron Blast Furnace: Theory and Practice, International Series on Materials Science and Technology, Volume 31, 1979.
- Peterson, J. R., "Aqueous Reaction of Fly Ash and $\text{Ca}(\text{OH})_2$ to Produce Calcium Silicate Absorbent for Flue Gas Desulfurization," M.S. Thesis, The University of Texas at Austin, 1987.
- Peterson, J. R., G. T. Rochelle, "Aqueous Reaction of Fly Ash and $\text{Ca}(\text{OH})_2$ to Produce Calcium Silicate Absorbent for Flue Gas Desulfurization," *Environmental Science and Technology*, **22**(11), 1299-1304, 1988.
- Peterson, J. R., "Hydrothermal Reaction of Lime with Fly Ash to Produce Calcium Silicates for Dry Flue Gas Desulfurization," Ph.D. Dissertation, The University of Texas at Austin, 1990.
- Peterson, J. R., G. T. Rochelle, "Lime/Fly Ash Materials for Flue Gas Desulfurization: Effects of Aluminum and Recycle Materials," presented at the 1990 SO_2 Control Symposium, New Orleans, Louisiana, May 8-11, 1990.
- Platt, J., " SO_2 Compliance After 2000: Slam Dunk or Something Else Altogether?," presented at The Mega Symposium, Washington, DC, EPRI TR-108683/V2, August 25-29, 1997.
- Regourd, M., "Microstructure of Cement Blends Containing Fly Ash, Silica Fume, Slag, and Fillers," *Materials Research Society Symposium Proceedings: Microstructural Development During Hydration of Cement*, Struble and Brown, eds., December, 1986.
- Rochelle, G. T., "Acid Rain Reduction," *Discovery*, **13**(1), 33-37, 1993.
- Rochelle, G. T., W. Jozewicz, "Process for Removing Sulfur from Sulfur-containing Gases," U.S. Patent Number: 4,804,521, February 14, 1989.

- Rochelle, G. T., W. G. White, W. Jozewicz, J. C. S. Chang, "Reaction of Hydrated Lime with SO₂ in Humidified Flue Gas," presented at the 1990 SO₂ Control Symposium, New Orleans, Louisiana, May 8-11, 1990.
- Rochelle, G. T., W. Jozewicz, "Process for Removing Sulfur from Sulfur-containing Gases," U.S. Patent Number: 4,931,264, February 14, 1990.
- Ruiz-Alsop, R., "Effect of Relative Humidity and Additives on the Reaction of Sulfur Dioxide with Calcium Hydroxide," Ph.D. Dissertation, The University of Texas at Austin, 1986.
- Sedman, C., M. Maxwell, B. Hall, "Pilot Plant Support for ADVACATE/MDI Commercialization," Paper 4B-5, presented at the 1991 SO₂ Control Symposium, Washington DC, EPRI TR-101054/V2, December, 1991.
- Shen, C. H., "Nitrogen Dioxide Absorption in Aqueous Sodium Sulfite," Ph.D. Dissertation, The University of Texas at Austin, 1997.
- Sigma-Aldrich, H₂S Material Safety Data Sheet, 1994.
- Stroud, D. E., "Agglomeration of Damp Calcium Silicate Sorbents for Flue Gas Desulfurization," M.S. Thesis, The University of Texas at Austin, 1991.
- Tamele, M. W., L. B. Ryland, R. N. McCoy, "Simultaneous Determination of Hydrogen Sulfide and Mercaptans by Potentiometric Titration," *Analytical Chemistry*, **32**, No. 8, pp. 1007-1011, July 1960.
- Taylor, H., The Chemistry of Cements, Volume 1, Academic Press, New York, 1964.
- Tsuchiai, H., T. Ishizuka, T. Ueno, H. Hattori, H. Kita, "Highly Active Absorbent for SO₂ Removal Prepared from Coal Fly Ash," *Industrial Engineering and Chemistry Research*, **34**, pp. 1404-1411, 1995.
- Varian, "Analytical Methods for Flame Spectroscopy," Varian Techtron Pty. Ltd., 1979.
- Virgalitte, S. J., et al., "Ground Granulated Blast-Furnace Slag as a Cementitious Constituent in Concrete," ACI Manual of Concrete Practice, Part 1 - 1997, Beavers, H., et al., editors, American Concrete Institute, 1997.

- Wasserman, P. D., "Effects of Inorganic Salts on Calcium Silicate Sorbents for Flue Gas Desulfurization," M.S. Thesis, The University of Texas at Austin, August 1992.
- White, W. G., "Differential Reaction of SO_2 in Flue Gas with Lime-based Sorbents at 66°C for 10 to 7200 Seconds," M.S. Thesis, The University of Texas at Austin, December, 1989.

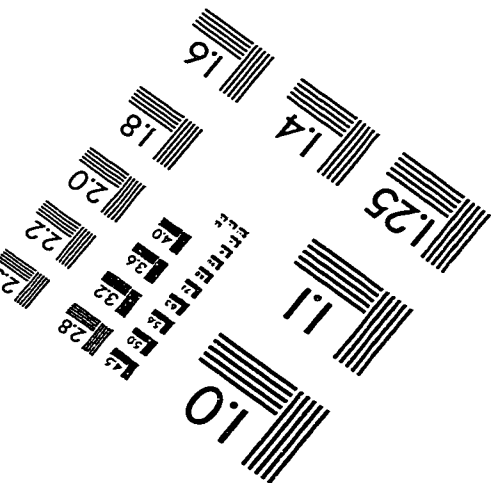
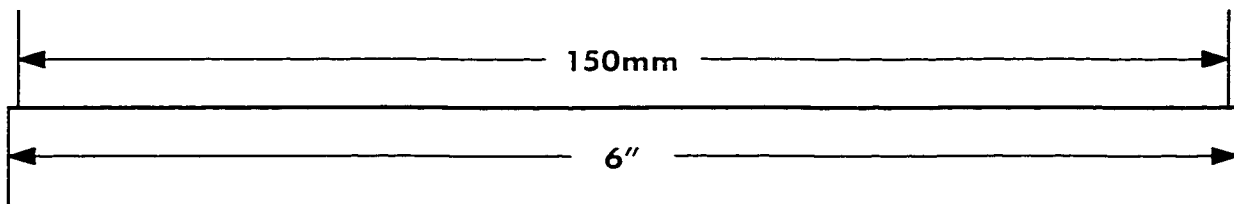
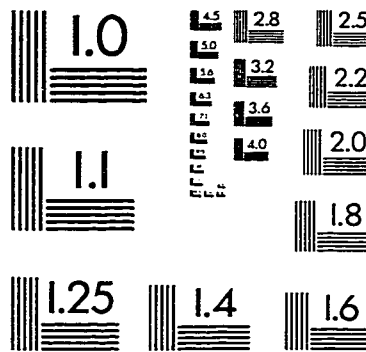
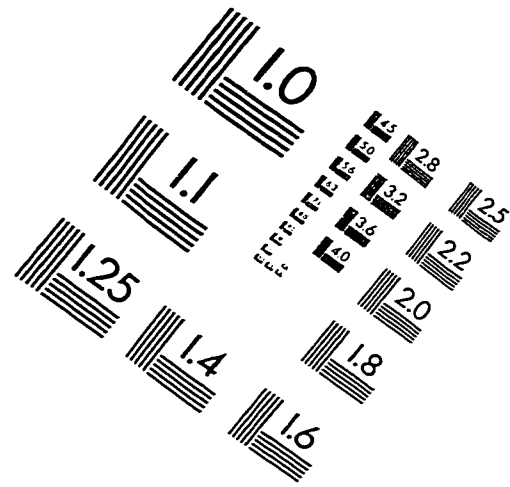
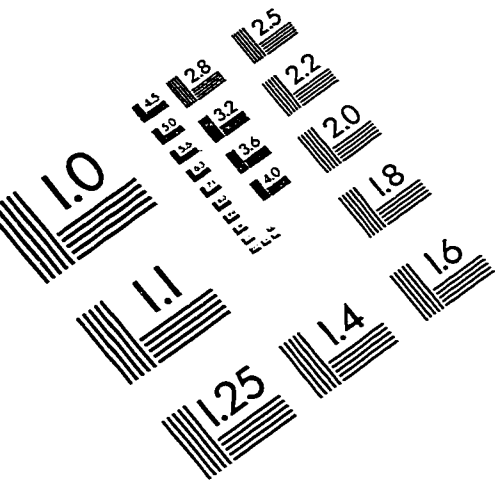
Vita

Lia Frieda Arthur was born June 29, 1972 in Las Cruces, New Mexico, the second child of Paul K. and Joy L. Arthur. After graduating valedictorian from Mayfield High School in May 1988, she entered New Mexico State University. She received her Bachelor of Science in Chemical Engineering in May 1992. During the summers of 1990 and 1991, she was employed by Phillips Petroleum Company, R&D, in Bartlesville, Oklahoma. After graduating from NMSU, she completed two internships with Dow Chemical USA, Texas Operations, in Freeport, Texas. In January 1993, she entered the graduate program at The University of Texas at Austin under the supervision of Dr. Gary Rochelle. On May 9, 1998, she married Edward R. Brodnax. Upon completion of the requirements to obtain her Ph.D. in Chemical Engineering, she has accepted employment with Radian International, LLC, in Walnut Creek, California.

Permanent address: 2050 San Acacio
Las Cruces, NM 88001

This dissertation was typed by the author.

IMAGE EVALUATION TEST TARGET (QA-3)



APPLIED IMAGE, Inc.
1653 East Main Street
Rochester, NY 14609 USA
Phone: 716/482-0300
Fax: 716/288-5989

© 1993, Applied Image, Inc., All Rights Reserved

